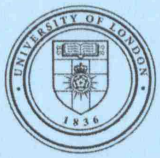



# UNIVERSITY OF LONDON THESIS

Degree PhD Year 2007 Name of Author LESLIE, Jonathan Dale

# STUDIES ON THE FUNCTIONS OF DELTA PROTEINS IN THE ZEBRAFISH

**Jonathan Dale Leslie**

University College London

and

Cancer Research UK London Research Institute

Ph.D. supervisor: Dr. Julian H. Lewis

A thesis submitted for the degree of Doctor of Philosophy

University College London

July, 2007





ProQuest LLC
789 East Eisenhower Parkway
P.O. Box 1346
Ann Arbor, MI 48106-1346

I, Jonathan Dale Leslie, confirm that the work presented in this thesis is my own. Where information has been derived from other sources, I confirm that this has been indicated in the thesis.

# Abstract

The Notch cell-cell signalling pathway plays a key role both in development and in adult life, controlling cell fate decisions in a wide variety of animal tissues. At its core lie the Notch receptors and their ligands, the proteins of the Delta and Jagged/Serrate family. Both ligand and receptor are transmembrane proteins that interact via their extracellular domains, yet the intracellular domains of the Notch ligands are also important for the activation of Notch receptors on neighbouring cells. In all vertebrates we find a conserved subset of Deltas ending in the C-terminal motif ATEV*, a potential PDZ-binding sequence. This motif mediates the interaction between Delta and the members of the MAGI family of scaffolding proteins. Surprisingly, blocking this interaction has no effect on Delta-mediated processes, indicating that it is not essential for normal Delta function. However, in embryos in which the interaction between Magi and DeltaD is blocked, we find that primary motor neurons are misplaced, a phenotype not seen in the DeltaD loss of function mutant *after eight*. These data suggest that MAGI proteins may somehow function to restrict Delta function.

Recent updates to the zebrafish genome database have revealed a novel ATEV-Delta that is orthologous to mammalian Delta-like 4 (Dll4), a Notch ligand essential for normal vascular development. Zebrafish *dll4*, like *dll4* in the mouse, is expressed in arterial endothelial cells. Embryos lacking Dll4 initially develop normally, but at later stages exhibit an overproduction of arterial endothelial cells and excessive angiogenic sprouting. A similar phenotype is seen in embryos lacking the receptor Notch1b and in embryos in which all Notch signalling is blocked with the gamma-secretase inhibitor DAPT. Over-activation of the Notch pathway produces an opposite effect. The excessive angiogenesis observed in embryos lacking Dll4 is blocked by inhibition of the vascular endothelial growth factor (VEGF) signalling pathway. Thus, Dll4-Notch signalling acts as an angiogenic "off" switch, making endothelial cells deaf to VEGF.

# Note on nomenclature

Conventions for naming proteins vary in different species. When referring to a protein in humans, the convention is to use all capital letters. In the mouse and zebrafish, the convention is to capitalise only the first letter, unless the name is an acronym, in which case it sometimes appears in all capital letters and sometimes does not. The result is a typographical chaos that is not only confusing, but also unsustainable when the name of a protein might refer to that protein in a particular species, or in general.

To have some consistency in this thesis, I have used the following rules for proteins whose names are acronyms, such as MAGI (Membrane Associated Guanylate Kinase with Inverted domain arrangement) or VEGF (Vascular Endothelial Growth Factor): when referring to the protein in general, I have written the name in all capital letters (MAGI, VEGF), but when referring to the protein in the zebrafish or the mouse specifically, I have capitalised only the first letter (Magi, Vegf).

# Acknowledgements

I thank Cancer Research UK for generously funding my Ph.D. and the many people who have contributed in one way or another to my four years in London. I am largely a product of those contributions:

I first thank my parents, Lenore Peloso and Philip Leslie, and my sister, Stephanie Kahn.

I thank my previous mentors who each taught me many valuable lessons along the way: Richard Cyr, Jerry Kaplan, Diane McVey-Ward, Mark Leppert, Nanda Singh and Frank Gertler.

I thank the members of the Vertebrate Development Laboratory (past and present): Gavin Wright, Neil Vargesson, Rachael Brooker, Francois Giudicelli, Nico Daudet, Ertugrul Ozbudak, Cecile Crosnier, Linda Ariza-McNaughton, Adam Bermange, Russel Collins, Anja Hanisch, Christine Hodgetts, Claudia Linker, Emre Ozturk, Despina Stamataki, Phil Taylor and Christian Tendeng: it has been a privilege to work beside you.

I thank Holger Gerhardt, who has been an incredibly supportive, enthusiastic and helpful colleague; Gavin Wright, who left me his project; Steve Johnson, my collaborator; Mike Mitchell, for his help with bioinformatics; Jenny Corrigan, for her expertise in sectioning; and Peter Jordan, for his help with live-cell imaging. I thank the members of the Developmental Biology Supergroup and especially David Ish-Horowicz, Helen McNeill, Sally Leevers and Nick Tapon.

I am most grateful to Adam Bermange, Cecile Crosnier, Phil Taylor and Michele Weber for their many helpful comments on this thesis, and to my second and third supervisors, Caroline Hill and Ralf Adams.

I thank Jonathan Tobin, Adam Bermange and Linda Ariza-McNaughton for their contributions to the MAGI and the Delta 4 projects.

I must extend a very special thank-you to Phil Taylor for his expertise in fish care, for his patience in working with me and for his many hours of tireless help.

I thank Linda Ariza-McNaugton: my mother would be very grateful if she knew I had you looking after me.

I thank my flatmates: Ditte, for her patience and her friendship; Stringer and Scotia, for their loyalty and companionship; and most recently, Rachel, Vic and Darren for helping to create a very nice home.

I thank many friends who have made this a wonderful chapter in my life: Anne, Steffi, Sara G, Gerry, Tan, Christian, Grant, Mary, Cherryl, Megan, Per, Andrea, Inbal, Liz, Jordan, Lena, Rhian, Seamus, Matthias and others I have surely forgotten.

Three people have been exceptionally important to me over these years. I am indebted to Katrin Layer: without you, this never would have happened; thank you. Rubiana Souza: you are as precious as your name suggests. And Mariam Orme: thank you for many good moments.

I am indebted to Julian Lewis for his seemingly endless supply of advice, support and encouragement. Thank you, Julian.

# Table of Contents

# List of Figures

# List of Tables

# List of Movies

# Chapter 1: Introduction

## 1.1 Cell-cell communication and the Notch signalling pathway

Any multicellular organism can be thought of as a community of individual cells, with each cell unselfishly working, living and dying for the benefit of the society as a whole. Both throughout development and in adult life, the behaviour of each individual cell must be strictly controlled in time and space. This is achieved through various mechanisms of cell-cell communication, which enable cells to coordinate their patterns of movement, growth, division, differentiation and apoptosis. One such mechanism for cell-cell communication is the Notch signalling pathway, which controls cell fate decisions in a wide variety of tissues throughout development and in the adult (Artavanis-Tsakonas et al., 1999; Lewis, 1998). At its core lie the Notch receptors and their ligands, the proteins of the Delta and Jagged (Serrate) families. Both receptor and ligand are single-pass type I transmembrane glycoproteins, which interact at sites of cell-cell contact. At the most basic level, signalling occurs when the ligand on one cell binds the receptor on a neighbouring cell, thereby triggering a series of proteolytic cleavages that release the intracellular domain of Notch (NICD; Fig. 1.1B). This then translocates to the nucleus where it acts as a transcriptional co-activator for target genes (reviewed in (Artavanis-Tsakonas et al., 1999)). The Notch pathway is somewhat unusual in this regard: the receptor itself is its own downstream effector. Notch signalling may, therefore, seem relatively simple and straightforward compared to other signal transduction pathways. Yet there are additional components that add many levels of complexity, and the ways in which many of these affect Notch signalling are still poorly understood.

When considering Notch signalling, we typically think of the two cells involved as the "signal-sending" cell and the "signal-receiving" cell. In this context, communication is unidirectional, with the signal-sending cell expressing the ligand while the signal-receiving cell expresses the receptor. In

reality, both cells often express both the ligand and the receptor, and the outcome of the Notch signalling is based on the relative amount of activation exchanged between the two and the way in which signal reception influences ligand production.

It should also be noted that growing evidence indicates that Notch ligands, like the receptors themselves, may undergo proteolytic cleavage at the membrane, releasing intracellular fragments which may, in turn, have a role in transcriptional regulation (Kiyota and Kinoshita, 2004; LaVoie and Selkoe, 2003; Six et al., 2003). Thus, there are reasons to believe that Notch signalling may in fact be bi-directional, although evidence of this still remains very scanty.

During my graduate studies, I pursued two major projects investigating the function of Delta proteins. The first, which is covered in Chapter 3 and the Appendix, analyzed an interaction between the intracellular domain of Delta and the MAGI family of scaffolding proteins. The second, covered in Chapters 4 and 5, focussed on the role of Delta-Notch signalling in the control of angiogenesis. Each chapter contains a fairly detailed introduction to the particular questions I tried to answer. Consequently, I have left a lot of that information out of this introductory chapter. Instead, I use this introduction to review the molecular details of the Notch pathway and some ways in which Notch signalling affects cell fate decisions and tissue patterning.

### 1.1.1 Notch protein is processed by cleavage and glycosylation on its way to the cell surface

At the centre of the Notch pathway lie the Notch receptors themselves, which will, in the course of their lifetimes, interact with a myriad of other pathway components. For this reason, and because the Notch pathway plays such a vital role in development and adult life, great efforts have been made to understand its structure and the specific functions of its constituent domains. It is appropriate, therefore, for me to give a short overview of what we know about the structure of the Notch protein itself. Although I often refer to Notch in the generic sense, which is indeed accurate when referring to the single

*notch* gene found in *Drosophila*, it should be borne in mind that higher vertebrates have several *notch* genes; mammals, for example, have four. For the purpose of this discussion, I will continue to refer to Notch in the generic sense. In Chapter 5, however, I explore different effects from loss of different Notch proteins in vascular patterning, reflecting the fact that they often have different roles in different tissues.

Notch is a large (300 kDa), single-pass transmembrane protein, composed of a long, heterodimeric extracellular domain ($N^{EC}$) that mediates interactions with its ligand (any one of the so-called DSL (Delta/Serrate/Lag-2) proteins), and an intracellular domain ($N^{ICD}$) that functions as the downstream effector (Fig. 1.1; reviewed in (Lubman et al., 2004)). The majority of the extracellular domain is composed of 36 EGF-like (Epidermal Growth Factor) repeats (Wharton et al., 1985). Interestingly, only the $11^{th}$ and $12^{th}$ EGF repeats mediate the interaction between receptor and ligand (Rebay et al., 1991). However, it has recently been shown that many of the other EGF repeats also play a role by helping to optimize Notch-ligand interaction (Xu et al., 2005). C-terminal to the EGF repeats are three LNR (Lin-Notch repeats; Fig. 1.1A) repeats, which appear to play a role in maintaining the receptor in its resting conformation when not bound to ligand (Greenwald and Seydoux, 1990; Rand et al., 2000). $N^{EC}$ also contains the heterodimerization domain that maintains the interaction between the two monomeric subunits (discussed below).

The intracellular domain of Notch, which can be thought of as the effector region of the molecule, contains a number of different domains involved in nuclear localization and transcriptional activation. The RAM (RBP-Jκ-associated molecule) domain mediates the interaction between $N^{ICD}$ and the transcription factor CSL (C promoter binding factor 1/Su(H)/Lag-1; also known as RBP-Jκ; see below; Fig. 1.1) (Tamura et al., 1995). The RAM domain has also been shown to contain a sequence through which Notch can interact with NFκB (Nuclear Factor kappa B) in a non-canonical pathway, discussed later in this chapter (Wang et al., 2001). The RAM domain is followed by a series of seven ankyrin repeats (ANK), which mediate protein-protein interactions and are essential for the interaction between the RAM

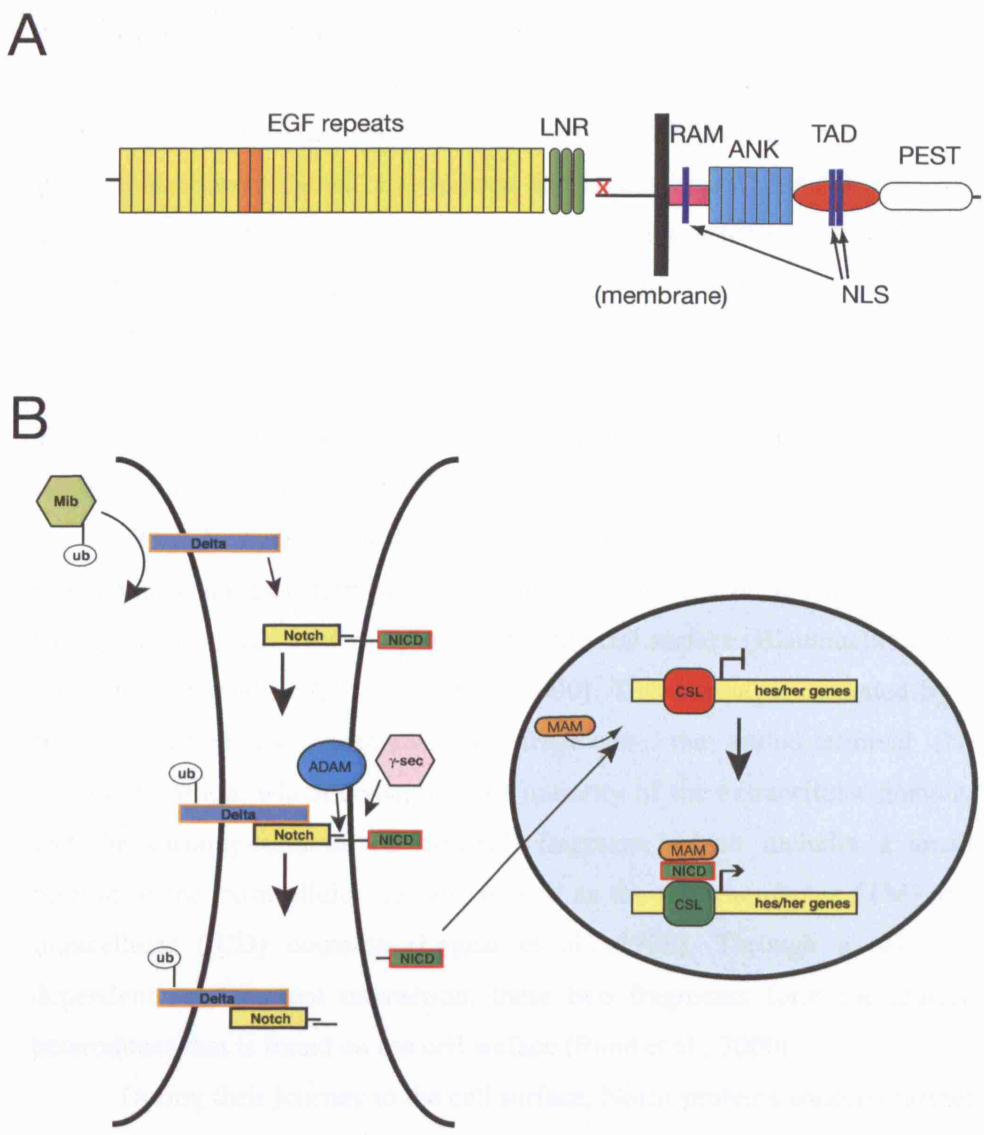


**Figure 1.1. Structure of Notch and the core of the Notch signalling pathway.** (**A**) Schematic representation of the Notch protein. Yellow boxes: EGF repeats; orange boxes: EGF repeats 11 and 12; green boxes: LNR repeats; red X: heterodimerization domain; pink box: RAM domain; light blue boxes: ankryn repeats; red oval: transcriptional activation domain; white box: PEST domain; dark blue bars: nuclear localisation signals. The large black bar represents the plasma membrane. (**B**) Depiction of the core events of the Notch signalling pathway. Many steps and components have been omitted for the sake of simplicity. See text for a more detailed description.

domain and CSL (Jarriault et al., 1995; Kato et al., 1997; Kodoyianni et al., 1992; Matsuno et al., 1997; Tani et al., 2001). C-terminal to the ANK domain is the transcriptional activation domain (TAD), which plays a role in the interaction between Notch and histone acetyltransferases (HATs) (Kurooka and Honjo, 2000) and is essential for transcriptional activation (Fryer et al., 2002; Kurooka and Honjo, 2000; Oswald et al., 2001; Wallberg et al., 2002). The PEST (proline (P), glutamate (E), serine (S), threonine (T)-rich), which mediates protein turnover (Rechsteiner, 1988), is located near the C-terminus. The intracellular domain of Notch also contains three nuclear localisation signals (NLS; (Kopan et al., 1994)).

The life cycle of a Notch receptor molecule includes a series of proteolytic cleavages, termed S1, S2 and S3. The first occurs in the trans-Golgi network, before the receptor reaches the cell surface (Blaumueller et al., 1997; Logeat et al., 1998; Rand et al., 2000). This cleavage, mediated by a furin-like convertase, generates two fragments: the amino-terminal (N-terminal) portion, which constitutes the majority of the extracellular domain, and the carboxy-terminal (C-terminal) fragment, which includes a small portion of the extracellular domain as well as the transmembrane (TM) and intracellular (ICD) domains (Logeat et al., 1998). Through a calcium-dependent non-covalent interaction, these two fragments form the mature heterodimer that is found on the cell surface (Rand et al., 2000).

During their journey to the cell surface, Notch proteins undergo further posttranslational modifications in the form of N-linked and O-linked glycosylation. N-linked glycosylation is a common feature among eukaryotes and is especially prevalent in proteins found at the cell surface (reviewed in (Parodi, 2000)). O-linked glycosylation of the EGF-like repeats in the extracellular domain of the Notch receptor appears to have an important role in modulating its affinity for different ligands in certain contexts.

Notch is targeted for two unusual types of O-linked glycosylation: O-glucosylation and O-fucosylation (Moloney et al., 2000b). The addition of the O-linked fucose monosaccharide appears to be critical for Notch signalling; *Drosophila* lacking Ofut1 (the fucosyltransferase responsible for O-fucosylation of EGF domains) have phenotypes similar to, and often as severe as, those seen when all Notch signalling is blocked (Okajima and Irvine, 2002;

Okajima et al., 2003; Sasamura et al., 2003). Similarly, mice carrying a targeted mutation of the mammalian ortholog, *Pofut1*, have defects in many Notch-dependent processes (Shi and Stanley, 2003).

O-glucose and O-fucose can be further modified to produce trisaccharide and tetrasaccharide modifications, respectively. The first step in the elongation of O-fucose side groups is catalyzed by the β1,3-*N*-acetylglucose aminyltransferase Fringe (Moloney et al., 2000a), which, in *Drosophila*, enhances Delta-mediated Notch activation while inhibiting Notch activation by Serrate (Fleming et al., 1997; Klein and Arias, 1998; Panin et al., 1997). The situation is somewhat more complicated in mammals, which have 3 *fringe* paralogs (*lunatic fringe, manic fringe* and *radical fringe*) that appear to have different effects on different Notch receptors (Chen et al., 2001; Hicks et al., 2000; Moloney et al., 2000a; Shimizu et al., 2001).

### 1.1.2 Ligand binding triggers activating cleavages

When Notch encounters its ligand, it undergoes a conformational change that exposes the second cleavage site (S2), which is located in the extracellular region of the $N^{TM}$ fragment, thus allowing for cleavage by the ADAM family (A Disintegrin And Metalloproteinase) proteinases: ADAM10 (or Kuzbanian) in *Drosophila* and ADAM17 (or TACE; TNF-α converting enzyme) in mammals (Fig. 1.1B) (Brou et al., 2000; Mumm et al., 2000). ADAM cleavage is a prerequisite for the final, S3 cleavage to occur. This event, which is mediated by presenilin-1/gamma-secretase, occurs within the TM domain and releases the NICD into the cytoplasm (De Strooper et al., 1999; Ray et al., 1999; Song et al., 1999; Struhl and Greenwald, 1999; Ye et al., 1999). The liberated $N^{ICD}$ (termed activated Notch) can now translocate to the nucleus (Fig. 1.1B).

The exact way in which ligand binding permits S2 cleavage by ADAM has only recently been elucidated. Clues had initially come from studies of T-acute lymphoblastic leukaemia/lymphoma (T-ALL), an aggressive neoplasm of immature T-cells (Aster et al., 2000; Ellisen et al., 1991; Pear et al., 1996).

Using Notch pathway inhibitors in a screen of human T-ALL cell lines and primary tumours, Weng et al found that T-ALL is frequently associated with gain-of-function mutations in *NOTCH1* (Weng et al., 2004). Malecki et al went on to show that many of these mutations produced excessive Notch activation in the absence of ligand but were dependent upon S2 and S3 cleavages (Malecki et al., 2006). Furthermore, the authors showed that the majority of these mutations were in the heterodomain of Notch, the region in which $N^{EC}$ and $N^{TM}$ bind one another via non-covalent interactions (Malecki et al., 2006). These findings indicate that in the absence of ligand, the S2 cleavage site is normally hidden from ADAM by the interaction of the two fragments; these mutant forms of Notch, by contrast, fail to properly protect their S2 sites, allowing for inappropriate ADAM cleavage and hyper-activation of the Notch pathway. The implication, therefore, is that upon binding to its ligand, a conformational change in the receptor unmasks the S2 site and the cascade of proteolytic cleavages is allowed to proceed.

While these studies significantly added to our understanding of how Notch activation is controlled in the absence of ligand, they did little to explain exactly how ligand binding exposes the S2 site. Recently, Nichols et al filled this gap through a series of experiments in culture (Nichols et al., 2007). Using endocytosis-defective DSL ligands, the authors showed that the binding of ligand by Notch alone is insufficient to trigger ADAM proteolysis; receptor-bound ligand can only activate Notch when it is targeted for endocytosis in the signal-sending cell. The strong suggestion, therefore, is that internalization of the bound ligand in the signal-sending cell produces a mechanical force that physically dissociates $N^{EC}$ and $N^{TM}$, thereby exposing the S2 site and allowing for ADAM cleavage (Nichols et al., 2007).

After S2 and S3 cleavages, the intracellular domain of Notch is free to move to the nucleus, where it exerts its effects by activating the transcription factor CSL (Fig. 1.1B) (Fortini and Artavanis-Tsakonas, 1994; Struhl and Adachi, 1998). In the absence of NICD, CSL functions as a transcriptional repressor, acting with the co-repressors SMRT, NcoR, CIR, SHARP, KyoT2 and Skip to block the transcription of Notch targets, such as the HES (Hairy/Enhancer of Split) genes (Hsieh et al., 1999; Kao et al., 1998; Oswald et al., 2002; Taniguchi et al., 1998; Zhou et al., 2000b). When CSL binds

NICD, the interaction between CSL and the co-repressor complex is antagonized, thereby allowing CSL to switch activity and activate transcription (Kato et al., 1997; Tamura et al., 1995; Tani et al., 2001; Zhou et al., 2000a; Zhou et al., 2000b). The CSL-NICD complex recruits the transcriptional co-activator Mastermind (MAM), which recruits histone acetyltransferases (Fryer et al., 2002; Kao et al., 1998; Oswald et al., 2001; Wallberg et al., 2002) and appears to be critical for transcription (Jeffries et al., 2002; Kitagawa et al., 2001; Wu et al., 2000). MAM also promotes the phosphorylation of NICD by CyclinC and Cyclin-dependent kinase 8 (CycC, CDK8), thereby facilitating NICD degradation mediated by the proteosome (Schweisguth, 1999) or the E3-ubiquitin ligases Sel-10 (Fryer et al., 2002; Fryer et al., 2004; Hubbard et al., 1997) or Su(Dx) (Supresssor of Deltex) (Cornell et al., 1999; Fostier et al., 1998).

### 1.1.3 Ubiquitination, endocytosis and non-canonical Notch signalling

The above description of Notch signalling represents a canonical, CSL-dependent view of the pathway. Growing evidence, however, indicates that Notch signalling may also follow an alternative, non-canonical pathway that operates independently of CSL and may, in some cases, operate independently of DSL ligands.

This notion began with the finding that the E3 ubiquitin ligase Deltex (Dx) positively regulates Notch signalling (Busseau et al., 1994; Diederich et al., 1994; Matsuno et al., 1995; Xu and Artavanis-Tsakonas, 1990). The way in which ubiquitination affects the activity of the Notch receptor was somewhat clarified by Gupta-Rossi et al, who showed that ubiquitination of the intracellular domain of Notch targets the protein to endocytic vesicles and is required for cleavage by gamma-secretase and for Notch activation (Gupta-Rossi et al., 2004). Hori et al linked these observations by demonstrating that overexpressing Dx promotes Notch endocytosis and that the delivery of Notch to the late endosome is required for Dx-mediated Notch activation (Hori et al., 2004). The authors further demonstrated that some Notch signalling events

occur independently of CSL but require Dx, and that these non-canonical CSL-independent Notch signalling events do not require the receptor's interaction with DSL ligands. Thus, Notch ubiquitination and endocytosis appear to be essential aspects of the signalling pathway.

To make matters even more complicated, ubiquitination also appears to play another role in the life of the Notch receptor, that of receptor degradation. In the absence of DSL-mediated Notch stimulation, the E3 ubiquitin ligases Nedd4 and Su(Dx) have been shown to direct the endocytosis of the receptor for either degradation or recycling (Sakata et al., 2004; Wilkin et al., 2004). Moreover, these studies show that Nedd4 and Su(Dx) antagonize Deltex by targeting Notch (Wilkin et al., 2004), or Deltex itself (Chastagner et al., 2006; Sakata et al., 2004), for degradation. This may help to protect against sporadic, incorrect Notch activation in the absence of DSL ligands (Sakata et al., 2004). Thus, it appears that the endocytic pathway may play an important role in regulating the balance between Notch activation, mediated by Deltex, and Notch down-regulation, mediated by Nedd4 and Su(Dx).

Evidence for another, DSL-dependent but non-canonical activity of Notch has come from studies of T-cell differentiation. Notch1 has been shown to antagonize NFκB signalling by binding the p50 subunit of NFκB, thereby blocking its ability to bind its recognition sequence on target genes (Guan et al., 1996). This finding opens the possibility of cross-talk between the Notch and NFκB pathways, an idea that has been bolstered by the finding that NFκB can activate Jagged1 expression (Bash et al., 1999). Moreover, Oswald et al have shown that NFκB2 (p52 NFκB subunit) is a direct transcriptional target of Notch1 through the canonical, CSL-dependent, pathway (Oswald et al., 1998). Together, these findings set the stage for a form of lateral inhibition mediated by cross-talk between NFκB and Notch (Wang et al., 2001). This idea is supported by more recent studies that have shown that the p65 subunit of NFκB plays a role in sequestering the CSL corepressor SMRT out of the nucleus and away from target genes (Espinosa et al., 2003).

Although my own research did not investigate non-canonical Notch signalling as such, I have included this brief description to underscore the fact that the consequences of Notch signalling may be much more far-reaching than might be initially predicted. As we learn more about the way that Notch

feeds into other signalling pathways, it becomes increasingly important to bear in mind that the downstream effects resulting from perturbations of Notch signalling may actually be seen in seemingly unrelated pathways. Indeed, we are now often faced with having to consider how one pathway affects another, not just how one member of a pathway affects another member of the same pathway. This idea will be revisited in Chapter 5, where I investigate ways in which Notch signalling affects the VEGF pathway.

## 1.2 Notch ligands

In the preceding section I introduced the structure and molecular biology of Notch and discussed the way in which the receptor exerts its downstream effects. However, both of my PhD projects have been largely focused on upstream events in the pathway, specifically, the biology of Delta ligands. In the following section I will describe Notch ligands in more detail, including their structure, the cellular processes that enable them to activate Notch receptors in trans and possible ways that they might affect a cell's behaviour in cis. It should be noted that DSL ligands, in addition to their role in activating Notch in trans, also appear to inhibit Notch activation in cis (de Celis and Bray, 1997; Klein et al., 1997; Li and Baker, 2004; Micchelli et al., 1997; Sakamoto et al., 2002). The functional consequences of cis-inhibition remain to be determined.

### 1.2.1 The extracellular domains of Notch ligands have structural similarities to each other and to Notch receptors

Notch ligands fall into two major families, the Delta proteins and the Serrate/Jagged proteins, both of which are single-pass transmembrane proteins. *Drosophila* has only one member representing each family, whereas vertebrates have several; mammals, for example have three *Delta* and two *Jagged* (or *Serrate* in *Drosophila*) genes. The general structure of Delta and

Jagged proteins are similar (Fig. 1.2A), although there are some differences between the two, and the size of each domain can vary both within and among species (reviewed in (Fleming, 1998)).

As in Notch, the extracellular domains of Delta and Jagged proteins are dominated by a series of EGF-like repeats. The exact role of the EGF repeats is not entirely understood, but they are thought to somehow stabilize or modify receptor-ligand interactions (Fleming, 1998). The N-terminal region of the extracellular domain contains a region that has been termed the EBD (EGF-motif binding domain) for its role in binding to the EGF-like repeats of Notch (Muskavitch, 1994). This is composed of the NT (N-terminal) domain, which contains a region termed the MNNL domain found in many Notch ligands (Marchler-Bauer et al., 2007), and the DSL domain (Delta/Serrate/Lag-2), which is so-named due to its high conservation among Notch ligands (Muskavitch, 1994). Mutations in the DSL domain block the ligand's ability for both trans-activation and cis-inhibition of Notch (Glittenberg et al., 2006), underscoring its necessity for ligand-receptor binding. The EBD domain also appears to be important for Fringe's role in directing the differential capacity for Delta or Serrate to bind Notch: if the EBD domain of Serrate is replaced with that of Delta, Fringe is no longer able to block Notch activation by the chimeric molecule (Fleming et al., 1997).

Between the EGF repeats and the transmembrane domain lies a cysteine-rich region (CR) that is found in Jagged, but not Delta, proteins. Again, the precise function of this domain is unclear, although it may serve to select the specific Notch receptor for Jagged binding and it appears to be required for Notch activation by Jagged in some contexts (Kiyota and Kinoshita, 2002).

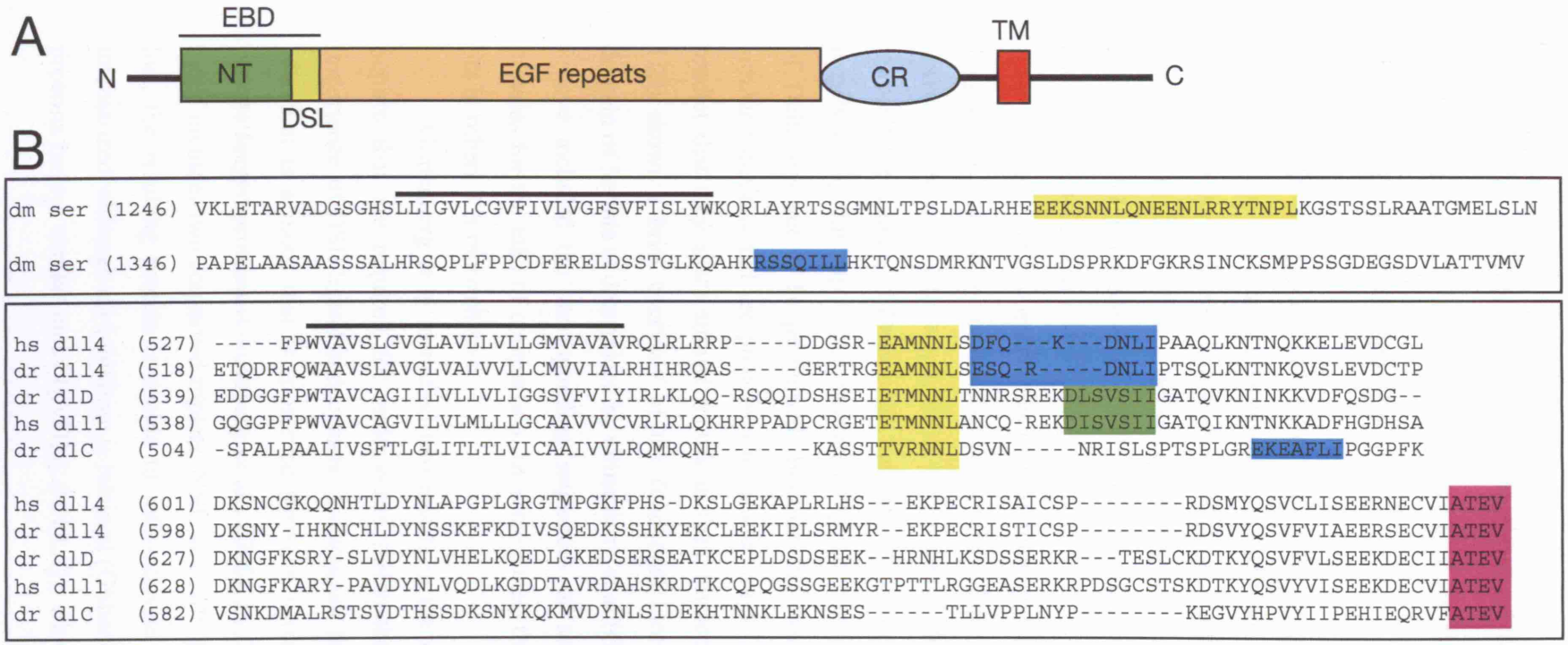


**Figure 1.2. Structural elements of Notch ligands (DSL proteins).** (**A**) Domain structure of DSL ligands. N: amino terminus; C: carboxy terminus; NT: N-terminal domain (green); DSL: DSL domain (yellow); EBD: EGF motif-binding domain (black bar); EGF repeats (beige); CR: cysteine-rich region, found only in Serrate/Jagged poteins (blue); TM: transmembrane domain (red). (**B**) Transmembrane domain (black bar) and intracellular domains of *Drosophila* Serrate (top panel) and several vertebrate Delta proteins. Yellow box: the domain containing the NNL and NPL triplets in Serrate and the corresponding motif in Delta. Blue box: the dileucine motif in Serrate and a candidate region in some Deltas. (The green box corresponds to a possible dileucine motif in Dll1 and Dld.) Purple box: C-terminal ATEV motif. (A) is adapted from Glittenberg et al (2006). Motifs in *Drosophila* Serrate in (B) are based on Glittenberg et al (2006). hs: *Homo sapiens*, dm: *Drosophila melanogaster*, dr: *Danio rerio*.

## 1.2.2 The intracellular domains of Notch ligands are functionally important and have conserved motifs

Although DSL ligands bind Notch via their extracellular domains, the transmembrane and intracellular domains of Delta and Jagged are also crucial for Notch activation and ligand processing, as I shall discuss in detail in Chapter 3 (Chitnis et al., 1995; Glittenberg et al., 2006; Hukriede and Fleming, 1997; Hukriede et al., 1997; Sun and Artavanis-Tsakonas, 1996; Sun and Artavanis-Tsakonas, 1997).

Despite the important roles that the intracellular domains of Delta and Jagged play, the specific motifs that govern these functions have not been well defined. Recently, Glittenberg et al performed a detailed analysis of the intracellular domain of *Drosophila* Serrate (Glittenberg et al., 2006), thereby largely filling this gap in our understanding, although, a similar investigation of Delta has yet to be performed. Because the two proteins have largely similar functions and are processed in similar ways (see below), one would predict that they share similar motifs in their intracellular domains. Figure 1.2B shows a brief overview of the functional motifs of the intracellular domain of Serrate as determined by Glittenberg et al (Glittenberg et al., 2006). I have included the corresponding sequences of several vertebrate Delta proteins for the sake of comparison. In some cases, the similarity is striking, but in others it is more elusive.

Glittenberg et al identified two motifs in the intracellular domain of Serrate that are required for endocytosis (Glittenberg et al., 2006) (the importance of DSL ligand endocytosis is discussed in greater detail below). The first is a motif that is conserved between invertebrate and vertebrate Serrate/Jagged proteins (Glittenberg et al., 2006). In *Drosophila* Serrate, this motif includes two conserved triplets, NNL and NPL (Fig. 1.2B); if these are lost, the resulting protein is unable to trans-activate Notch and fails to be internalized, although cis-inhibition is retained (Glittenberg et al., 2006). Delta proteins have a similar motif ([E/D]$x_{2-4}$NN[L/I]), which appears in a similar

location with respect to the transmembrane domain ((Glittenberg et al., 2006); Fig. 1.2B).

The other motif identified by Glittenberg et al is a dileucine motif that appears to be essential for endocytosis, but, somewhat surprisingly, is dispensible for trans-activation and cis-inhibition (Glittenberg et al., 2006). This motif ([D/E/R]$x_{3-5}$L[L/I]) is involved with intracellular sorting and protein internalization (Bonifacino and Traub, 2003; Sandoval et al., 2000). Both human and zebrafish Delta-like 4 (Dll4) and DeltaC have a motif that fits this consensus, although the location is somewhat different than in *Drosophila* Serrate (Fig. 1.2B). However, this motif is less conspicuous in other vertebrate Deltas (Fig. 1.2B). Whether it performs a similar function in these Delta proteins remains to be determined.

A third feature that is prevalent among vertebrate Deltas is the motif ATEV* at the C-terminus of a subset of Delta proteins (Wright et al., 2004). At the molecular level, this motif mediates interactions with PDZ domains, as will be discussed in detail below and in Chapter 3. However, the functional importance of this motif in terms of the Notch pathway remains somewhat of a mystery. Although Jagged proteins do not seem to share this motif, many Serrate/Jagged proteins end with a C-terminal valine residue which could potentially mediate a similar interaction (reviewed in (Nourry et al., 2003)).

Thus, while we know a considerable amount about the molecular biology of Notch ligands, there are many questions that still remain unanswered. During my PhD, one of my projects was aimed at dissecting some of these functions on a molecular level. The details of this project will be covered in Chapter 3.

### 1.2.3 Upstream events: DSL ligands, endocytosis and ubiquitination

While ubiquitination and endocytosis appear to be important in regulating the activity of the Notch receptor in the signal-receiving cell, these processes also play an essential role in the signal-sending cell (Seugnet et al., 1997). DSL ligand endocytosis, mediated by the E3 ubiquitin ligases Mind bomb and

Neuralized (Fig. 1.1B), is required for activation of the Notch receptor in trans (Itoh et al., 2003; Lai et al., 2005; Le Borgne et al., 2005; Wang and Struhl, 2005). The ubiquitination of DSL ligands is thought to promote their internalization via the action of Epsin endocytic adaptor proteins, such as Liquid facet (Lqf) in *Drosophila* (Overstreet et al., 2004; Tian et al., 2004; Wang and Struhl, 2004; Wang and Struhl, 2005; Yeh et al., 2001).

Yet the exact way in which DSL ubiquitination and internalization affect Notch signalling remains unknown. One possibility is that Epsin targets ubiquitinated DSL ligands to a special subset of endocytic vesicles that are specialized for Notch activation (Wang and Struhl, 2004; Wang and Struhl, 2005). Another model predicts that internalization is required to prime DSL ligands for signalling. In this way, ligands initially reach the plasma membrane in an inactive state. Upon ubiquitination, they are internalized into a recycling endocytic pathway that somehow makes them able to activate Notch and targets them back to the cell surface (Wang and Struhl, 2004; Wang and Struhl, 2005), presumably for a second round of endocytosis. In either case, it is thought that the forces driving internalization of the receptor-bound ligand create tension within the Notch molecule, thereby inducing a conformational change in Notch that leads to detachment of the $N^{EC}$ fragment and thus exposes the S2 cleavage site and allows for ADAM-mediated proteolysis. Evidence in support of this has come from the observation that, upon cleavage of Notch by ADAM protease, the extracellular domain of Notch is found in the signal-sending cell (Nichols et al., 2007; Parks et al., 2000).

This brief review of the Notch pathway is by no means exhaustive, and while we understand some aspects of the Notch pathway well, there are still significant gaps in our knowledge. While relatively direct and simple compared to other signal transduction pathways, the Notch pathway includes a large cast of molecules that can modulate signalling in many ways in both the signal-sending and the signal-receiving cell. In the following section I will step away from the molecular details of the pathway and focus on the role it plays in cell fate decisions and tissue patterning.

## 1.3 The effects of Notch signalling in cell fate decisions and tissue patterning

The Notch signalling pathway enables cells to communicate with their immediate neighbours, and, thereby, to coordinate their cell fate decisions. The Notch pathway lies at the core of several fundamental developmental processes, such as lateral inhibition, cell lineage decisions and tissue boundary formation, and the result can be seen at the level of tissues, organs and even organ systems.

### 1.3.1 Notch-mediated lateral inhibition produces fine-grained patterning

Close examination of many animal tissues reveals fine-grained patterning, where different types of cells are interspersed with one another, sometimes in a regular, highly ordered mosaic. One striking example of this is in the mechanosensory epithelium of the vertebrate inner ear, which has an alternating pattern of hair cells and supporting cells, with each hair cell surrounded on all sides by supporting cells such that no two hair cells are in direct contact with one another (Fig. 1.3A). This epithelium is generated from a prosensory patch composed of precursor cells, each having the potential to differentiate into either a supporting cell or a hair cell (Adam et al., 1998; Haddon et al., 1999). How, then, do the cells in this population coordinate their differentiation to produce the fine-grained pattern found in the mature tissue?

The answer lies in lateral inhibition, a process mediated by the Notch pathway (Fig. 1.3B). In lateral inhibition, a differentiating cell inhibits its neighbours from embarking down the same path of differentiation, either by driving them towards an alternative cell fate or by maintaining them in an undifferentiated state (reviewed in (Lewis, 1996)). A key ingredient of Notch-mediated lateral inhibition is the repression of DSL ligand expression, creating a feedback loop that makes levels of ligand expression in neighbouring cells

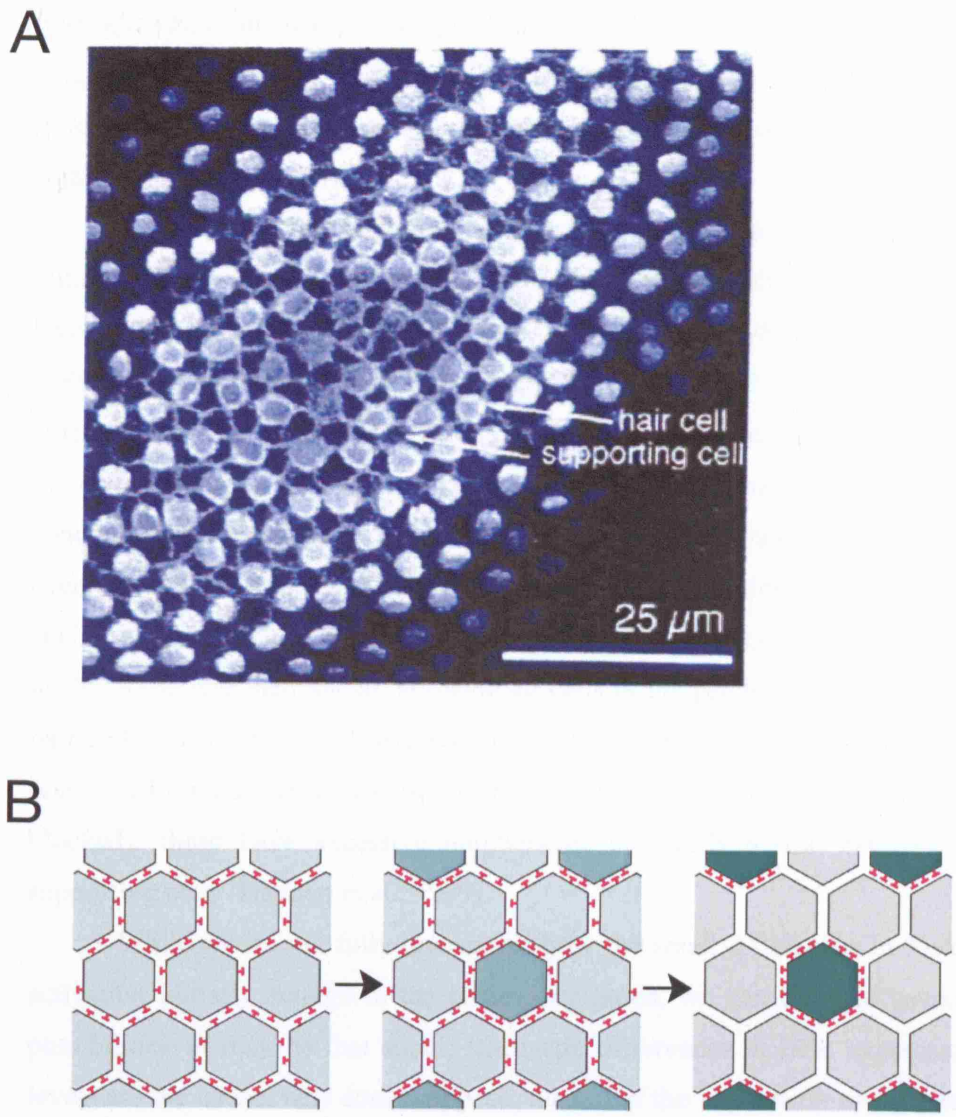


**Figure 1.3. Lateral inhibition and the control of cell fate decisions.** (**A**) Optical section (confocal image) of the basilar papilla in the inner ear of a chick embryo. Note the mosaic of hair cells (stained with anti-hair cell antibody, white blobs) and supporting cells (outlined by their cortical actin, stained with fluorescent phalloidin. (Reproduced from Adam et al (1998)). (**B**) Diagram depicting the way in which lateral inhibition creates fine-grained patterns, such as that shown in (A). In this case, all cells are initially in an undifferentiated state (light green, left panel) and deliver a basal level of inhibition to one another (red "Ts"). As some cells begin to differentiate (darker green, middle panel), they deliver more of an inhibitory signal than they receive. The result is a pattern in which cells that have differentiated (dark green, right panel) are surrounded by cells which are either maintained in an undifferentiated state or take on a different developmental fate (grey, right panel). In the case of the ear, hair cells (green, right panel) prevent their neighbours (grey, right panel) from taking on a hair cell fate. These cells then differentiate into supporting cells.

interdependent: an increase of ligand in one cell will drive a decrease in its neighbours. The result is that small differences in Notch signalling can, in time, be self-amplifying so as to produce an all-or-nothing difference between adjacent cells (Fig. 1.3B).

In the case of the auditory epithelium, all cells in the prosensory patch initially express both ligand and receptor and, consequently, deliver a basal level of Notch signalling to one another (Adam et al., 1998; Morrison et al., 1999). At some point, small differences in the level of Notch activation emerge, allowing some cells to escape lateral inhibition and embark on a path of differentiation towards a hair cell fate. These nascent hair cells concomitantly block hair cell differentiation in their neighbours, which eventually differentiate into supporting cells (Fig. 1.3) (Eddison et al., 2000; Haddon et al., 1999). When Notch signalling fails, nascent hair cells are unable to deliver their signal, allowing all cells in the patch to differentiate as hair cells. This effect is clearly seen in the mechanosensory patches of *mind bomb* (*mib*) mutant embryos (in which all Notch signalling is believed to be blocked): these have excessive numbers of hair cells at the expense of supporting cells (Haddon et al., 1999).

While we do not fully understand how the small differences in Notch activation initially emerge in the prosensory patch, we can think of several possibilities. It may be that small, stochastic differences in DSL expression levels are the cause. One could suppose, then, that the conversion to a pattern of contrasting cell states could start with a small group of cells. Once the cells in this group begin differentiating, the wave of lateral inhibition could easily spread across the patch. Another possibility is that asymmetric cell division in progenitors produces daughter cells that are not equivalent in their ability to send or to receive Notch activation. For example, one might suppose that one daughter cell could inherit more Mind bomb or Neuralized than the other, thereby ensuring that that cell will be better equipped to deliver Notch signalling than its neighbours. In a similar way, one daughter cell might inherit more of the Notch antagonist Numb, thereby making that cell deaf to Notch activation. This latter case appears to be the driving force behind lineage decisions that generate the *Drosophila* mechanosensory bristle (Frise

et al., 1996; Spana and Doe, 1996; Spana et al., 1995) and will be the subject of the next section.

### 1.3.2 Notch signalling drives cell lineage decisions: one example

As discussed above, lateral inhibition, mediated by Notch signalling, can drive seemingly equivalent neighbouring cells towards different developmental fates. In a similar way, Notch signalling can function to consolidate a pre-existing bias between two neighbouring cells, and thereby direct lineage decisions within a cluster of cells. The cells that give rise to the *Drosophila* mechanosensory bristles provide a good example of this process. Each sensory bristle organ is composed of four cells, all derived from a single sensory organ precursor (SOP) (Hartenstein and Posakony, 1989). Each SOP undergoes an asymmetric cell division to produce two daughter cells, the pIIa and the pIIb. These, in turn, divide asymmetrically to produce the hair (or shaft) and socket cells and the neuron and sheath cells, respectively. As with the sensory epithelium of the inner ear, blockade of Notch signalling results in excessive numbers of one cell type at the expense of the other. For example, if the Notch pathway is blocked during the first SOP division, both daughter cells take on the pIIb fate, and the resulting organ lacks all pIIa-derived cell types (Hartenstein and Posakony, 1990).

The asymmetric cell fates of the daughter cells of the SOP result from asymmetric inheritance of Notch pathway components. In all of the cell divisions between the SOP and the mature organ, the E3 ubiquitin ligase Neuralized and the Notch antagonist Numb are asymmetrically distributed to one of the two daughter cells (Frise et al., 1996; Guo et al., 1996; Le Borgne and Schweisguth, 2003; Rhyu et al., 1994; Spana and Doe, 1996; Spana et al., 1995). The effect is two-fold: in the same daughter cell, DSL ligands are primed to deliver a signal (through the activity of Neuralized) and Notch activation is blocked (through the activity of Numb).

In addition to asymmetric distribution of Neuralized and Numb, more recent studies have indicated that the endosomal GTPase Rab11 and its

effector, Sec15, are asymmetrically distributed to the pIIb daughter cell (Emery et al., 2005; Jafar-Nejad et al., 2005). These molecules have been shown to play a role in the endocytosis of Delta, a process that is essential for the ligand's ability to activate Notch in the pIIa cell. Moreover, Emery et al have also shown that after pIIb/pIIa cytokinesis, Delta moves through a recycling endosomal pathway in the pIIb cell that allows it to interact with Notch on the surface of the pIIa. By contrast, the authors show that in the pIIa cell, Delta may be targeted to a degradative compartment (Emery et al., 2005). Thus, while differences in cell composition underlie the specification of daughter cell lineages during SOP divisions, the Notch pathway is indispensable for the communication between the daughter cells that ensures that the cells follow the correct path of differentiation.

### 1.3.3 Notch signalling controls the formation of tissue boundaries

During development, boundaries between non-equivalent populations of cells are established that help to give organs and tissues their characteristic shapes and functions. These boundaries are not merely interfaces or edges, but also can function as secondary signalling, or organizing, centres (reviewed in (Lewis, 1998; Takahashi, 2005)). At the interface, Notch signalling exchanged between the border cells of each group can have an inductive role on the band of cells at the boundary, giving them a distinct character and, in so doing, helping to reinforce the differences between the two flanking populations.

Boundary formation is characterised by specific and often mutually exclusive gene regulation between the two groups of cells. The dorsal-ventral boundary of the *Drosophila* wing imaginal disc provides a good example of this. At the wing margin, ventral cells expressing *notch* and *delta* oppose dorsal cells expressing *notch*, *serrate* and *fringe* (reviewed in (Bray, 1998; Irvine, 1999)). Fringe functions cell-autonomously to shift Notch's specificity for its ligands, causing increased affinity for Delta at the expense of Serrate (Fleming et al., 1997; Klein and Arias, 1998; Panin et al., 1997). Thus, dorsal boundary cells are preferentially activated by Delta expressed in the adjacent

ventral boundary cells, and are unresponsive to activation by Serrate in the neighbouring dorsal boundary cells (de Celis et al., 1996; Doherty et al., 1996; Fleming et al., 1997; Kim et al., 1995; Panin et al., 1997). The result is an induction of the downstream targets *cut* and *wingless* and the subsequent organization of wing outgrowth (de Celis and Bray, 1997).

This situation differs from lateral inhibition in an important way: while Notch activation causes a repression of DSL ligand expression in lateral inhibition, boundary cells that receive Notch activation must maintain expression of DSL ligands in order to maintain signalling to the boundary cells in the adjacent compartment. In other words, dorsal boundary cells, which receive Notch activation from the opposing Delta-expressing cells, maintain high levels of Serrate expression through a positive-feedback loop (de Celis and Bray, 1997).

This role for the Notch pathway is a recurrent theme in animal development. Indeed, Notch signalling has been shown to play an important role in forming boundaries in other developmental contexts, such as in the *Drosophila* eye (Papayannopoulos et al., 1998), in the limb buds of *Drosophila* (de Celis et al., 1998) and vertebrates (Laufer et al., 1997; Rodriguez-Esteban et al., 1997) and in vertebrate somite segmentation (Conlon et al., 1995; Dunwoodie et al., 1997; Evrard et al., 1998; Jen et al., 1997; Kusumi et al., 1998; McGrew et al., 1998; Morimoto et al., 2005; Palmeirim et al., 1997; Takahashi et al., 2000; Zhang and Gridley, 1998).

### 1.3.4 Notch signalling can also govern the behaviour of fully differentiated cells

In the preceding sections I discussed three situations in which Notch signalling controls cell fate determination: lateral inhibition, cell lineage decisions and tissue boundary formation. In these processes, the signal-sending cell embarks on a path towards terminal differentiation, as, for example, in the case of the hair cells of the inner ear. Similarly, the signal-receiving cell is either driven towards an alternative developmental fate or maintained in an undifferentiated state. However, Notch signalling has also been shown to occur between fully

differentiated cells, suggesting that it also plays some role in controlling behaviour in cells whose fate has already been decided with regard to the basic choices of cell type (for example, see (Ahmad et al., 1995)). In Chapter 5 I show in vivo evidence in support of this notion: Notch signalling between endothelial cells acts as a switch, controlling when and where cell motility and proliferation are turned on and off. Thus, Notch signalling appears to not only be responsible for determining terminal cell fate, but may also regulate changes in the behaviour of cells that are already differentiated.

### 1.3.5 The Notch pathway plays a role in cell motility

Another role of the Notch pathway that is especially relevant to my PhD involves the control of cell motility, although the molecular mechanisms governing these effects are still poorly understood. Disrupting Notch signalling in *Drosophila* impairs cell movements involved in the formation of the proventriculus (Fuss et al., 2004) and in dorsal closure (Zecchini et al., 1999). More recent work in *Drosophila* has shown that the Notch pathway also plays an important role in the migration of border cells (Wang et al., 2007) and peripheral glia (Edenfeld et al., 2007), underscoring its importance as a general pathway controlling cell motility.

Similar findings have been reported in higher vertebrates: mice lacking Dll1 seem to have impaired neural crest cell migration, leading to misformed dorsal root ganglia and sympathetic ganglia (De Bellard et al., 2002). Notch signalling also influences neurite outgrowth (Berezovska et al., 1999; Franklin et al., 1999; Levy et al., 2002). There are several conceivable ways in which such effects might occur. Given that Notch signalling governs cell fate decisions, compromised cell migration might simply reflect abnormal cell fate choices rather than any direct effect on motility. However, Notch signalling seems to regulate the morphology and the motility of post-mitotic cells (Berezovska et al., 1999; Franklin et al., 1999), somewhat arguing against this explanation, at least in some cases.

Interestingly, Notch ligands also seem to influence cell motility and the cytoskeleton, not only by activating Notch in trans (Franklin et al., 1999), but also in a cell-autonomous manner (De Joussineau et al., 2003; Lowell and Watt, 2001; Wright et al., 2004). Overexpressing full-length Delta induces the formation of filopodia (see Chapter 3; (De Joussineau et al., 2003) and promotes cohesiveness (Lowell and Watt, 2001), while forms of Delta lacking portions of their intracellular domains appear to have the opposite effect (De Joussineau et al., 2003; Lowell and Watt, 2001).

There is some evidence, as I shall elaborate in Chapter 5, that Delta's effect on cell motility, when acting through the Notch pathway in trans, is mediated by cross-talk between the Notch pathway and other signalling pathways, such as the c-Jun N-terminal kinase (JNK) (Zecchini et al., 1999) or the VEGF (Leslie et al., 2007; Siekmann and Lawson, 2007; Suchting et al., 2007) signalling pathways. However, the fact that Delta can affect cell motility cell-autonomously (De Joussineau et al., 2003; Lowell and Watt, 2001) suggests that there may be other mechanisms responsible for its effect. The way in which Delta affects cell motility became, unexpectedly, one of the central themes for my PhD work and will be a subject that is revisited repeatedly in the chapters that follow.

# Chapter 2: Materials and Methods

## 2.1 Fish

### 2.1.1 General care

Zebrafish were maintained at 27.5°C in dechlorinated London tap water on a 14/10 hour light/dark cycle and embryos were collected from spontaneous spawnings. Staging was according to Kimmel et al (Kimmel et al., 1995).

### 2.1.2 Mutants and transgenics

*mind bomb*$^{-/-}$ (*mib*$^{-/-}$, *mib*$^{ta52b/ta52b}$) embryos were obtained by crossing heterozygous *mib*$^{ta52b/+}$ adults. Homozygous mutant offspring were identified by the presence of somite defects (Jiang et al., 1996). *after eight* (*aei*; *dld*$^{tr233/tr233}$) and *beamter* (*bea; dlc*$^{tw12b/tw12b}$) embryos were obtained by crossing homozygous mutant adults and confirmed by the presence of somite defects (van Eeden et al., 1996a).

*delta-like 4* (*dll4*; *dll4*$^{j16e1/j16e1}$) embryos were obtained by crossing heterozygous *dll4*$^{j16e1/+}$ adults (identified by genotyping, see below). The chromosome carrying *dll4*$^{j16e1}$ also contained the recessive mutant allele *sparse* (*spa*; *kita*$^{b5}$), thus *dll4*$^{j16e1/j16e1}$ could be identified by the pigment defect associated with *kita*$^{b5/b5}$ (Parichy et al., 1999).

*Tg(fli1:EGFP)y1* (Lawson and Weinstein, 2002b) embryos were obtained by crossing GFP-positive (either heterozygous or homozygous) adults.

### 2.1.3 Generation of the *dll4*$^{j16e1/j16e1}$ mutant

The *j16e1* mutant allele was discovered by my collaborator, Stephen Johnson (Washington University Medical School, St. Louis, MO), through a mutagenesis screen for suppressors of the *long fin* (*lof*) mutation, which is

characterised by fin overgrowth (van Eeden et al., 1996b). Dr. Johnson and colleagues mutangenized *lof*$^{-/-}$ males by standard spermatagonial mutagenesis (Driever et al., 1996) and crossed them to wild-type females. The screen produced five mutations at the *lof* locus and one second site suppressor. This was mapped to a minimal critical region containing only the *dll4* gene (SL Johnson, personal communication).

# 2.2 Genetic techniques

## 2.2.1 Morpholino and mRNA injections

Injected reagents were diluted in Danieau buffer (58 mM NaCl, 0.7 mM KCl, 0.4 mM $MgSO_4$, 0.6 mM $Ca(NO_3)$, 5.0 mM HEPES, pH 7.1-7.3; (Nasevicius and Ekker, 2000)) containing 0.2% phenol red and 2 to 4 nL were injected into the yolk of 1 to 4 cell stage embryos.

### 2.2.1.1 Morpholinos

Morpholino sequences (GeneTools) are:

| target | sequence (5' to 3') |
|---|---|
| *deltaD* splice modifying (MO[dlD-V]) | GGTTTTGGACTTACCTCGGTTGCAA |
| MO[dlD-V] mismatch control (mismatched bases in lowercase) | GcTTTTcGACTTAgCTCGcTTcCAA |
| *magi1* translation blocking (MO[MAGI1]) | CACAGAAACAGGTGGCTCCGCTGAC |
| *dll4* translational blocking (JLMO2) | GTGAGCCAAGCTGCCATGCTTTTCG |
| *dll4* exon 3/intron 3 splice modifying (JLMO5) | GATAAAATCGAATCTTACCTACAGG |
| *dll4* exon 6/intron 6 splice modifying (used for knock-down; MO[Dll4]) | TAGGGTTTAGTCTTACCTTGGTCAC |
| MO[Dll4] mismatch control (mismatched bases in lowercase) | TAcGGTTTAcTCTTAgCTTcGTgAC |
| *sox32* (*casanova*) (MO[cas]) (Sakaguchi et al., 2001) | GCATCCGGTCGAGATACATGCTGTT |
| *notch1a* (Lorent et al., 2004) | GAAACGGTTCATAACTCCGCCTCGG |
| *notch1b* (Milan et al., 2006) | AATCTCAAACTGACCTCAAACCGAC |
| *notch2* (Lorent et al., 2004) | AGGTGAACACTTACTTCATGCCAAA |
| *notch3* (Lorent et al., 2004) | ATATCCAAAGGCTGTAATTCCCCAT |

**Table 2.1. Morpholino sequences.** The concentrations used are included in the text, with the exceptions of the morpholinos targeted against *notch1a, notch1b, notch2 and notch3*, which were used at 0.8 pMol (7 ng) per embryos according to the authors' procedures.

### 2.2.1.2 mRNA

Plasmids containing the gene of interest were linearized and de-salted by ethanol precipitation. mRNA was synthesized using the mMessage mMachine kit (Ambion) according to the manufacturer's instructions, de-salted by LiCl precipitation and dissolved in water. The integrity of mRNAs was confirmed by agarose gel electrophoresis.

### 2.2.2 Conditional transgene expression

For misexpression of $N^{ICD}$, we used fish carrying *hsp70:Gal4* and *UAS:*$N^{ICD}$ (*UAS:myc-notch1a-intra*) constructs as described (Scheer et al., 2001). Heat-shock was performed at 37°C by transferring embryos into tubes containing pre-warmed aquarium water. After a 30 minute incubation, the embryos and the aquarium water were transferred back into 10 cm Petri dishes, moved to room temperature and allowed to cool slowly to 27.5°C. Samples were maintained at 27.5°C for the remainder of the experiment.

## 2.3 Drug treatments

N-[N-(3,5-difluorophenacetyl)-L-alanyl]-S-phenylglycine t-butyl ester (DAPT; Merck) or SU5416 (Merck) was dissolved in DMSO, stored at -20°C and added to aquarium water to give a final concentration of 100 μM DAPT or 2 μM SU5416 plus 0.2% or 0.01% DMSO, respectively. Aquarium water containing 0.2% or 0.01% DMSO alone was used as a control. All samples were kept in the dark during the course of the treatment.

## 2.4 Molecular techniques

### 2.4.1 Genotyping

Adult zebrafish heterozygous for the *dll4* mutation were identified by PCR-based genotyping on tail fin genomic DNA. Fish were anaesthetized in 160 μg/ml Tricaine and a 2-4 mm piece of tail was removed. Each sample was digested in 150 μl genomic DNA extraction buffer (10 mM Tris (pH 8.0), 100 mM EDTA (pH 8.0), 0.5% SDS, 200 μg/ml Proteinase K (Roche); (Westerfield, 2000) for 3 hours at 60°C. Samples were then moved to 99°C for five minutes to inactivate the Proteinase K and centrifuged at 16,000xG for one minute. Supernatants were removed and stored at -20°C. 3 μl of each supernatant was used for each of two 25 μl PCR reactions, one (positive control) specific for the wild-type allele and the other specific for the mutant

allele. The forward primer for both reactions was 5'-GGAGGGATGCAGTGAGG-3', the wild-type reverse primer was 5'-GTCACAGAACAGTCCACC-3' and the mutant reverse primer was 5'-GTCACAGAACAGTCCACT-3'. The PCR was performed using 0.4 μM of each primer, 0.2 mM of each dATP, dGTP, dCTP and dTTP (Roche) and adjusted to 50 mM KCl, 10 mM tris-HCl (pH 8.0-8.3) and 1.5 mM $MgCl_2$. Amplification was performed using recombinant *taq* (*Thermus aquaticus*) DNA polymerase with the following cycling conditions: 4 minutes at 94°C; 30 cycles of 30 seconds at 94°C, 30 seconds at 64°C, 35 seconds at 72°C; 10 minutes at 72°C. The entire reaction volume was analyzed by agarose gel electrophoresis.

## 2.4.2 Gene sequencing, bioinformatics, and cloning

### 2.4.2.1 Sequencing

DNA sequencing was performed on an Applied Biosystems 3730 DNA Analyzer using the ABI BigDye Terminator v3.1 chemistry. A list of primers and the corresponding genes is provided in Table 2.1 below.

| name | primer sequence (5' to 3') | target |
|---|---|---|
| SP6 | CATACGATTTAGGTGACACTATAG | universal |
| T7 | AATACGACTCACTATAG | universal |
| T3 | ATTAACCCTCACTAAAG | universal |
| JLP23 | ATGGCTTGTGTTTGATCCTGG | *dll4* |
| JLP24 | ATGACTTGATTTGTCCTCTTGG | *dll4* |
| JLP25 | GGAAAAGCCAGAGTGTAGG | *dll4* |
| JLP26 | GGATGTTGCCTTTACTTCTA | pME18S-FL3 plasmid |
| JLP27 | CGACCTGCAGCTCGAGCACA | pME18S-FL3 plasmid |
| JLP28 | CATTGATTATTGAGGCCTGG | *dll4* |
| JLP29 | AGAGGAGAGCGAACAGTC | *dll4* |

**Table 2.2. Sequencing primers.**

### 2.4.2.2 Cloning

The full length zebrafish *magi1* cDNA was cloned by Dr. Gavin Wright (see appendix) by both 5' and 3' RACE using SMART RACE kit (Clontech) following the manufacturer's protocols using 24 hour zebrafish cDNA and oligonucleotides based on a zebrafish EST sequence (GenBank Accession Number AW078333) from the Zebrafish Washington University MPIMG EST library. C-terminally tagged Magi1-EGFP was created by cloning full length *magi1* cDNA into the KpnI site of the pCS2+ vector (Turner and Weintraub, 1994) by Dr. Wright.

Plasmids encoding DeltaD and DeltaD-TE* were also made by Dr. Wright by cloning the cDNAs of each into the XbaI/EcoRI sites of the pCS2+ vector (Turner and Weintraub, 1994).

The zebrafish *dll4* was identified as a predicted transcript in the Ensembl zebrafish genome database (Ensembl Gene ENSDARG00000053401). An EST clone (IMAGE:7418341) was identified by BLAST that contained end sequences 5' and 3' to the Ensembl predicted transcript, corresponding to the first and last exons, respectively. This cDNA has subsequently been identified as the full-length zebrafish *dll4* cDNA in GenBank (Accession Number BC117624).

For the *dll4* in situ hybridization probe, a 480 nucleotide fragment was amplified using the primers: 5'-atatactcgagGTGCCTTAACGCCAGTGCTG-3' (forward; non-annealing tail in lowercase; XhoI restriction site is underlined) and 5'-atataactagtCACACTCTCCAGGTTTGGAGC-3' (reverse; non-annealing tail in lowercase; SpeI restriction site is underlined). The resulting product was cloned into the XhoI/SpeI sites of the pBS ks(+) vector. For the anti-sense probe, the plasmid was linearized with XhoI and the RNA was made using T7 RNA polymerase. For the sense control probe, the plasmid was linearized with SpeI and the RNA was made using T3 RNA polymerase.

The plasmid encoding Myc-tagged Mind bomb was a generous gift of Ajay Chitnis (NIH, USA) and is described in Itoh et al (Itoh et al., 2003).

## 2.4.3 RT-PCR

Embryos were dechorionated with 1 mg/ml pronase in E3 buffer (5 mM NaCl, 0.17 mM KCl, 0.33 mM $CaCl_2$, 0.33 mM $MgSO_4$) at room temperature for 5 minutes and transferred to 1.5 ml microfuge tubes. The medium was removed with a pipette and the tubes were then placed on dry ice. The tissue was allowed to thaw and was immediately ground up using a small pestle. RNA was purified from the samples using the SV Total RNA Isolation kit (Promega) according to the manufacturer's instructions. Reverse transcription was performed using the RETROscript kit (Ambion) with random primers on 2 μg of RNA according to the manufacturer's instructions.

For *EF-1α*, PCR was performed using 1 µl of reverse transcription product in 25 µl total reaction volume and the following primers: 5'-GCCAGGCTCGTTTTGAGGAA-3' (forward) and 5'-CAGTGTGGCAATCCAGCACT-3' (reverse).

For *dll4*, PCR was performed in two rounds using hemi-nested primers. The first PCR was performed on 5 µl of reverse transcription product in 25 µl total reaction volume using the primers 5'-CATTGATTATTGAGGCCTGG-3' (forward) and 5'-CTGTCACACTCTCGCACCTG-3' (reverse). 1 µl of this product was then used for a second round of amplification, also in 25 µl total volume, using the same reverse primer with a different forward primer: 5'-GTTTCGGCCACTACACCTGC-3'.

All PCR reactions were performed using 0.4 µM of each primer, 0.2 mM of each dATP, dGTP, dCTP and dTTP (Roche) and adjusted to 50 mM KCl, 10 mM tris-HCl (pH 8.0-8.3) and 1.5 mM $MgCl_2$. Amplification was performed using recombinant *taq* (*Thermus aquaticus*) DNA polymerase with the following cycling conditions: 4 minutes at 94°C; 30 cycles of 30 seconds at 94°C, 30 seconds at 54°C, 1 minute at 72°C; and 10 minutes at 72°C. Products were resolved by agarose gel electrophoresis.

# 2.5 Molecular analysis

## 2.5.1 Cell culture, transfections, immunocytochemistry and live imaging

### 2.5.1.1 Cell culture, transfections and immunocytochemistry

HEK293T cells or L-cells were grown at 37°C under 5% $CO_2$ in Eagle's medium with Dulbecco's modifications containing 5% heat-inactivated foetal calf serum. On the day before an experiment, the cells were plated on glass coverslips. Cells were transiently transfected with 1µg of plasmid DNA per well in a 24-well plate using Superfect Transfection Reagent (Qiagen). 24 hours after transfection, cells were rinsed in PBS and fixed in 4%

paraformaldehyde in PBS for 15 minutes at room temperature. Fixed cells were permeabilized in 0.2% Triton X-100 in PBS for 15 minutes at room temperature, rinsed in PBS, and incubated in blocking solution (1% BSA in PBS) for 30 minutes at room temperature. Cells were then stained with the appropriate antibodies (see below) and coverslips were mounted on slides in Citifluor (Citifluor, Ltd.) and examined with a Zeiss LSM510 confocal microscope.

### 2.5.1.2 Whole-mount immunohistochemistry

For examination of blood vessels, *fli1:EGFP* embryos were fixed in 4% paraformaldehyde in PBS overnight at 4°C and washed in PBS at room temperature. In most cases, embryos were permeabilized in antibody solution (PBS containing 10% goat serum, 2% BSA, 0.5% Triton X-100 and 10 mM $NaN_3$) for several hours at room temperature, washed in PBS containing 1% Triton X-100 and mounted in SlowFade Gold (Invitrogen) containing 0.2 μg/ml DAPI (Sigma). In some cases (when amplification of the GFP signal was required, embryos were permeabilized as above and stained with rabbit-anti-GFP primary antibody (Molecular Probes; diluted 1:500 in antibody solution) for several hours at room temperature or overnight at 4°C, washed as above, stained with Alexa-fluor 488 goat-anti-rabbit secondary antibody (Molecular Probes) for several hours at room temperature, washed and mounted as above. Specimens were examined with a Zeiss LSM510 confocal microscope.

### 2.5.1.3 Antibodies

All antibodies were diluted in antibody solution. Mouse-anti-DeltaD antibody (zdd2) was used at 1:100 as in Itoh et al. (Itoh et al., 2003). Rabbit-anti-GFP primary antibody (Molecular Probes) was used at 1:500. Rabbit-anti-Magi1, -Magi2 and -Magi3 antibodies (Sigma-Aldrich) were used at 1:100. Chicken-anti-Myc (IgY fraction; Molecular probes) was used at 1:1000. Mouse-anti-HNK-1/N-CAM (Sigma) was used at 1:50. Mouse-anti-acetylated-Tubulin (Sigma) was used at 1:100.

For secondary detection, Cy3-conjugated donkey-anti-chicken IgY (Jackson) was used at 1:500. Alexa Fluor 488, 546 or 633 goat-anti-Mouse

IgG or -anti-Rabbit IgG (Sigma) were used at 1:500. Phalloidin (Molecular Probes) was used at a 1:100 dilution in the secondary antibody solution.

#### 2.5.1.4 Endothelial cell counts

Endothelial cells were counted from projections of Z-series of optical sections. The region counted in each specimen spanned two somites (three intersegmental vessels (ISVs) and the intervening segments of the dorsal aorta (DA) and the dorsal longitudinal anastomotic vessel (DLAV).

#### 2.5.1.5 Live imaging

Living *fli1:EGFP* embryos were anaesthetized in aquarium water containing 320 μg/ml Tricaine (Sigma) and mounted on a glass-bottom dish (MatTek) in a drop of 37°C aquarium water containing 0.2% agarose. The droplet was allowed to solidify at room temperature. Images were captured with a Zeiss LSM 510 inverted confocal microscope equipped with a 63x 1.2 NA water immersion objective. Embryos were maintained at 28°C in an environmental chamber during the course of the experiment. Frames for movies were collected every 30 seconds for 20 minutes. Each frame is the projection of a Z-series of optical sections.

To film circulation, embryos were anaesthetized in aquarium water containing 320 μg/ml Tricaine and mounted on a microscope slide in 3% methyl cellulose. Movies were collected in real time on a Lietz Diaplan microscope using a Panasonic F15 CCD video camera and iMovie HD software.

### 2.5.2 In situ hybridization

Wholemount in situ hybridisation followed the protocol of Thisse (Westerfield, 2000) or of Ariza-McNaughton and Krumlauf (Ariza-McNaughton and Krumlauf, 2002).

### 2.5.2.1 Tissue preparation

Embryos were manually dechorionated and fixed in fresh 4% paraformaldehyde in PBS (4% paraformaldehyde/PBS) for either 3-5 hours at room temperature or overnight at 4°C. Embryos were washed in several changes of PBS at room temperature over 3 hours, incubated in 50% methanol/PBS for 5 minutes, and stored in 100% methanol at -20°C. For hybridisation, embryos stored in methanol were brought to room temperature and rehydrated step-wise through 5-minute incubations in 75% methanol/PBS, 50% methanol/PBS and 25% methanol/PBS followed by several changes of PBS containing 0.1% Tween-20 (PBST) over 2-4 hours. Embryos were treated with 10 µg/ml Proteinase K (Promega) in PBST at room temperature for different times depending on their age (e.g. 5 minutes for 24 hours-post-fertilization (hpf), 10 minutes for 36 hpf, 15-20 minutes for 48 hpf). Embryos were then rinsed in PBST and re-fixed in 4% paraformaldehyde/PBS for 20 minutes at room temperature followed by changes of PBST over several hours at room temperature.

### 2.5.2.2 Probe synthesis

Probes for *islet1* (Inoue et al., 1994), *col2a1* (Yan et al., 1995), *myod* (Weinberg et al., 1996), *notch1b* (Westin and Lardelli, 1997), *notch3* (Westin and Lardelli, 1997), *ephrinB2a* (Durbin et al., 1998), *ephB4* (Cooke et al., 1997) were as previously described.

The probe for zebrafish *magi1* corresponded to nucleotides 3018 to 3530 of the cDNA sequence (GenBank accession number BC133867) (Wright et al., 2004) and for zebrafish *dll4* corresponded to nucleotides 510 to 989 of the cDNA sequence (GenBank accession number NM_001079835) (Leslie et al., 2007).

Plasmids containing the probe template were linearized with the appropriate restriction endonuclease and purified using the QIAquick PCR purification kit (Qiagen) according to the manufacturer's instructions. The purity and concentration of the linearized DNA was confirmed by agarose gel electrophoresis using a quantitative DNA ladder. Digoxigenin-11-UTP (DIG)- or fluorescein-labelled riboprobes were synthesized from 1 µg linearized DNA

using an RNA labelling kit (Roche) with the appropriate RNA polymerase for 2 hours at 37°C. The transcription reactions were then stopped by addition of EDTA (pH 8.0) to a final concentration of 20 mM. RNA was purified using mini Quick spin columns (Roche) according to the manufacturer's instructions. The purity and concentration of the RNA was determined by agarose gel electrophoresis and probes were stored at -20°C.

### 2.5.2.3 Hybridisation and washes

Embryos were pre-hybridised in hybridisation buffer (50% formamide, 5X SSC (20X SSC: 3 M NaCl, 0.3 M sodium citrate ($Na_3C_6H_5O_7 \cdot 2H_2O$; pH 7.0)), 2% blocking powder (Roche), 0.2% Triton X-100, 50 µg/ml Heparin (Sigma), 1 mg/ml torula yeast RNA (Sigma), 5 mM EDTA) for 1-2 hours at 65°C. Probes were diluted 1:200 in hybridisation buffer and denatured at 95°C for 5 minutes immediately prior to being added to the samples. Hybridisations were carried out overnight at 65°C. Embryos were washed as follows: 5 minutes in 50% hybridisation buffer/2X SSC at 65°C; 5 minutes in 2X SSC at 65°C; 20 minutes in 0.2X SSC, 0.1% Tween-20 at 65°C; twice for 20 minutes in 0.1X SSC, 0.1% Tween-20 at 65°C; and several changes over 2-4 hours in PBST at room temperature.

### 2.5.2.4 Antibody binding and colour development

Embryos were blocked in PBST containing 10% heat-inactivated sheep serum (sheep serum) for 1-3 hours at room temperature. Alkaline phosphatase-conjugated anti-DIG antibody (Roche) was diluted 1:5000 in PBST containing 1% sheep serum and was applied to the embryos overnight at 4°C. Embryos were washed with several changes of PBST over 2-4 hours at room temperature and then washed with several 5-minute changes of fresh colouration buffer (100 mM Tris-HCl (pH 9.5), 50 mM $MgCl_2$, 100 mM NaCl, 0.1% Tween-20). Embryos were incubated in the dark in colouration buffer (10 ml colouration buffer containing 45 µl of 75 mg/ml nitro-blue tetrazolium (NBT; Roche) in dimethylformamide (DMF) and 35 µl of 50 mg/ml 5-bromo-4-chloro-3-indolyl phosphate (BCIP; Roche) in DMF) until an appropriate level of staining was detectable. The reaction was stopped by rinsing the embryos several times in deionized water.

For experiments using only one probe, the embryos were washed for between a few hours to several days in PBST to reduce non-specific background staining and stored in 4% paraformaldehyde/PBS at 4°C. For double-labelling experiments, the embryos were incubated in 0.1 M glycine (pH 2.2) for 10 minutes and then washed in several changes of PBST over several hours at room temperature. Embryos were blocked as above and then incubated overnight at 4°C in PBST containing 1% sheep serum and a 1:20,000 dilution of alkaline phosphatase-conjugated anti-fluorescein antibody (Roche). Embryos were washed and equilibrated in colouration buffer as above, and colour development was carried out in the dark in colouration buffer containing 7.5 µl/ml of a solution (Roche) containing 33 mg/ml INT (2-[4-iodophenyl]-3-[4-nitrophenyl]-5-phenyltetrazolium chloride) and 33 mg/ml BCIP (5-bromo-4-chloro-3-indolyl phosphate, toluidine salt in DMSO) until a suitable level of staining was detectable. The reaction was stopped and the embryos were washed and stored as above.

### 2.5.2.5 Mounting, examination and photography

For whole mount histology, embryos were equilibrated in PBST and the yolks removed. Samples were allowed to equilibrate in 50% glycerol/PBS for an hour and mounted on a microscope slide in 95% glycerol/PBS. For sections, embryos were incubated overnight at 4°C in PBS containing 5% sucrose. The tissue was embedded in PBS containing 1.5% agar (Lennox LB agar) and 5% sucrose that was allowed to set into blocks which were then equilibrated to 30% sucrose overnight at 4°C. The tissue was cut into 15 µm cryosections. Samples were examined on a Leitz Diaplan microscope and photographed using a Leica DC500 digital camera using Leica FireCam software; images were processed using Adobe Photoshop.

For GFP detection, embryos were counterstained with rabbit anti-GFP antibody (Molecular Probes) as described below. Images were captured on a Zeiss LSM510 confocal microscope.

# Chapter 3: Delta proteins and MAGI proteins

## 3.1 Introduction

### 3.1.1 MAGI proteins form the backbone of signalling complexes

All signalling pathways possess a cast of molecules that act in concert to efficiently transduce signals; these include receptors, downstream effectors, proteolytic enzymes, cytoskeletal elements and motor proteins. To ensure that the process works efficiently, the localisation of these molecules within the cell is tightly controlled. One way that eukaryotic cells accomplish this is by gathering many of these molecules into large, multiprotein signalling complexes (Tsunoda et al., 1997). These complexes serve to bring many of the proteins involved in intracellular signalling pathways together, thereby enhancing their ability to interact. In multicellular organisms such complexes are often localized to specific subcellular domains, such as the apicolateral surface of polarized epithelial cells or the synaptic membrane of neurons (reviewed in (Dimitratos et al., 1999)), and may be precisely positioned at sites such as junctional complexes at points of cell-cell contact. Thus, signalling complexes containing receptor molecules in one cell can be held in direct contact with similar complexes containing ligands in neighbouring cells, greatly increasing the chance that they will interact (reviewed in (Matter and Balda, 2003; Perez-Moreno et al., 2003)).

At the core of many signalling complexes are intracellular scaffolds composed of proteins containing multiple protein-binding domains that serve to hold signalling components together. The proteins of the MAGUK (Membrane-associated Guanylate Kinase) family are a prime example. These contain multiple PDZ (Postsynaptic density/Discs large/Zona occludens-1) domains, an SH3 (Src Homology-3) domain and an enzymatically inactive guanylate kinase (GuK) domain (Dimitratos et al., 1999) that mediates

protein-protein interactions (Kim et al., 1997; Satoh et al., 1997; Takeuchi et al., 1997). MAGUKs can be grouped into several subfamilies on the basis of domain content and sequence similarity. Among these, the MAGI (Membrane-associated Guanylate Kinase with an inverted domain arrangement) subfamily is somewhat unusual for several reasons: (1) the domain structure is inverted compared to all other MAGUK proteins, (2) the SH3 domain is replaced by two WW domains (protein interaction domains characterised by two conserved tryptophan residues (Sudol et al., 1995)) and (3) the proteins contain six PDZ domains rather than the one or three found in all other MAGUKs (Dobrosotskaya et al., 1997) (see Appendix Fig. 1B). Mammals possess three MAGI homologs that have each been shown to interact with a vast number of signalling, junctional and cytoskeleton-associated proteins (Supplementary Data 1 of the Appendix).

Because Notch signalling occurs between cells that are in direct contact, one might predict that both ligand and receptor would be normally recruited to cell-cell junctions, thereby increasing the likelihood that they meet in trans, and that this recruitment might depend on binding to junctional scaffold proteins. There are good reasons to suppose that this is the case, perhaps the most compelling of which is the fact that all vertebrates possess a subset of Delta ligands that contain the carboxy-terminal (C-terminal) sequence ATEV*, a PDZ-binding motif (Kornau et al., 1995; Niethammer et al., 1996; Nourry et al., 2003; Songyang et al., 1997). Yet until recently, evidence linking Notch pathway components with multiprotein signalling complexes was lacking.

Using an in vitro binding assay, previous studies in our lab found that the C-terminal region of one of the ATEV*-containing Deltas (termed "ATEV-Deltas" from here on), human Delta-like 1 (Dll1), binds MAGI1, MAGI2 and MAGI3 of both human and mouse. This finding opens the possibility that Delta ligands may, in fact, reside in junctional complexes, and it raises several interesting questions regarding the functional significance of this recruitment. For example, one might think that the localization of ligand and receptor to junctional complexes is essential for efficient signalling. A reasonable prediction, therefore, would be that blocking that localization should result in a deficiency in Notch activation and a failure of Notch-

dependent developmental processes. (Since beginning this project, Six et al and Mizuhara et al have shown that this is, indeed, the case for Dll1 in the mouse (Mizuhara et al., 2005; Six et al., 2004).)

In order for DSL ligands to activate Notch, they must be targeted for endocytosis (Seugnet et al., 1997); might MAGI proteins somehow be involved? While we know that DSL ligands must be ubiquitinated by Mind bomb or Neuralized as part of this process (Itoh et al., 2003; Lai et al., 2005; Le Borgne et al., 2005; Wang and Struhl, 2005), exactly how a ligand's ubiquitination and internalization affect its ability to activate receptors on neighbouring cells largely remains a mystery. Perhaps MAGI proteins help ensure that these ubiquitin ligases find their DSL targets by bringing them in close proximity to one another. If so, blocking the interaction between DSL ligands and MAGI proteins might shed light on the functional significance of these steps.

Several studies have shown that Delta proteins lacking their intracellular domains block Notch activation in cis (Chitnis et al., 1995; Glittenberg et al., 2006; Haddon et al., 1998b; Henrique et al., 1997; Sun and Artavanis-Tsakonas, 1996). Might this reflect an undiscovered role for Delta in attenuating Notch activation in a cell-autonomous manner? If so, MAGI proteins, or other proteins in MAGI-containing complexes, could mediate this process.

Because signalling complexes appear to bring receptors and effectors from many different pathways together (Supplementary Data 1 of the Appendix), the recruitment of Delta to these complexes might somehow allow for direct cross-talk between the Notch pathway and other signalling pathways. Similarly, it is possible that the Notch pathway can have direct effects on other cellular processes, such as cell motility, and that the recruitment of Delta to signalling complexes is involved with this. Moreover, recent studies have shown that Notch ligands, like the receptor itself, are proteolytically cleaved to release an intracellular domain, which may have a role in transcriptional regulation (Kiyota and Kinoshita, 2004; LaVoie and Selkoe, 2003; Six et al., 2003). MAGI proteins could play a role in any of these processes.

Clearly, there are many unanswered questions regarding the molecular biology of Notch ligands. While we have clues about the importance of some of the processes in which they are involved, the details and the functional consequences of many of these are still poorly understood. When I began my graduate studies in the Vertebrate Development Laboratory I took over the Delta-MAGI project, which had been started several years earlier by a postdoctoral fellow who had left the lab, Gavin Wright. As mentioned above, Dr. Wright had used a biochemical screen to identify several possible Delta binding partners in mammals, and the MAGI family of scaffolding molecules were among them. He went on to characterise the interaction of MAGI proteins and Delta in the zebrafish and discovered that an unexpected brain malformation phenotype emerges when the interaction is blocked. When I started my research, his findings had been submitted for publication to Development. The manuscript was not accepted, but the authors were given the opportunity to resubmit provided they could adequately address the referees' comments. This is where my contribution to the project began. My findings took the project on a rather unexpected course, and a revised manuscript, on which I was an author, was accepted with few further revisions (Wright et al., 2004). I have included the published manuscript as an appendix to this thesis and will briefly summarize Dr. Wright's findings and my contributions to the manuscript in the following sections of this chapter's Introduction. In the Results section of this chapter, I will present experiments that I did to follow up our published findings.

## 3.1.2 The intracellular domain of Delta proteins

### 3.1.2.1 Reasons to believe that the intracellular domain of Delta is important

As outlined in the first chapter of this thesis, Notch signalling is initiated when the receptor on one cell encounters the ligand on another cell, resulting in a series of proteolytic cleavages that releases the activated, intracellular domain of Notch, $N^{ICD}$ (Selkoe and Kopan, 2003). Although the interaction between ligand and receptor occurs via their extracellular domains, there are strong

reasons to believe that the intracellular domain of the ligand also plays an important role in activating the Notch receptor in trans. For example, the intracellular domain of Delta contains sites for ubiquitination that are crucial for proper Delta function (Itoh et al., 2003; Lai et al., 2001; Pavlopoulos et al., 2001). Secondly, when the intracellular (C-terminal) domain of Delta is removed, the protein acquires a powerful dominant-negative effect, blocking Notch activation in cis (Chitnis et al., 1995; Glittenberg et al., 2006; Haddon et al., 1998b; Henrique et al., 1997; Sun and Artavanis-Tsakonas, 1996). Additionally, Notch ligands, like the Notch receptor itself, can be cleaved, releasing an intracellular fragment that may have a function in the nucleus as a transcriptional regulator (Ikeuchi and Sisodia, 2003; Kiyota and Kinoshita, 2004; LaVoie and Selkoe, 2003; Six et al., 2003).

Additional evidence for the importance of the intracellular domain of Delta comes from sequence conservation. Among often-conserved domains, we find in all vertebrates a subset of Delta proteins ending in the motif ATEV, a typical C-terminal PDZ ligand sequence (Nourry et al., 2003). This includes Delta-like1, Delta-like-2 and Delta-like 4 in mammals and DeltaA, DeltaC, DeltaD and Delta-like 4 in the zebrafish (Fig. 4.1). This evolutionary conservation suggests that this motif has some important function.

### 3.1.2.2 Characterisation of the C-terminal ATEV motif

To investigate what functions the ATEV motif might have, Dr. Wright performed in vitro binding assays in which he exposed a peptide corresponding to the C-terminus of human Delta-like 1 to lysates made from adult mouse brain or human neuroblastoma NB100 cells. He found that the C-terminus of Delta bound, among other proteins, the proteins of the MAGI family

To further investigate the role of the MAGI-Delta interaction, we turned to the zebrafish, using Magi1 as a representative of the MAGI family. *magi1* is widely expressed in the zebrafish embryo. Embryonic expression was seen by 6 hpf, a similar time to when the expression of *deltaC* and *deltaD* become detectable (Haddon et al., 1998b; Smithers et al., 2000). *magi1* is expressed ubiquitously through 24 hpf, after which time expression becomes restricted to the central nervous system (Appendix Fig. 2).

To verify that Magi1 can interact with ATEV-Deltas in the zebrafish, Dr. Wright performed in vitro binding assays using purified protein corresponding to each of the six PDZ domains of Magi1. These proteins were assayed for their ability to bind to the C-terminal 27 amino acids of DeltaC or DeltaD. As a negative control, the PDZ proteins were assayed against a second pair of DeltaC or DeltaD peptides in which the C-terminal valine residue was absent. He found that both DeltaC and DeltaD bound only to PDZ4 of Magi1, and that this interaction was completely lost when the terminal valine was removed (Appendix Fig. 3A).

These biochemical assays indicate that Delta proteins bind PDZ4 of MAGI, and that this interaction requires the ATEV motif to be intact. To confirm this interaction in a living system, I performed cotransfection experiments in HEK293T cells. Cells were cotransfected with plasmids coding for (1) a C-terminal GFP-tagged version of zebrafish Magi1 and (2) either full-length DeltaD or DeltaD lacking its C-terminal valine (DeltaD-TE*). Delta protein was detected with an anti-DeltaD antibody. In both cases, Delta protein was found on the cell surface (Appendix Fig. 3B,C). In cells expressing full-length DeltaD, Magi1 and DeltaD colocalised at the cell surface, an association that appeared to be enriched at sites of cell-cell contact (Appendix Fig 3B). In contrast, Magi1 was found only in the cytosol of cells expressing DeltaD-TE*; Magi and Delta co-localization was undetectable and there was no evidence of Magi protein enrichment at cell-cell junctions (Appendix Fig. 3C). Taken together, these data indicate that, at least in this system, DeltaD can recruit Magi1 to the cell membrane.

### 3.1.3 A splice-modifying morpholino can be used to block the DeltaD-Magi interaction

Both in vitro and in living cells, we have seen that the interaction between DeltaD and Magi1 requires the C-terminal valine: removal of this residue completely abrogates Delta-Magi binding. We should, therefore, be able to block this interaction in the living embryo by removing the C-terminal valine from endogenous DeltaD, providing us with the opportunity to examine the

function of this interaction in vivo. By good fortune, the C-terminal valine is encoded on a separate exon from the rest of the ATEV motif, thus providing a unique opportunity to disrupt the motif while still maintaining normal levels of DeltaD protein that is otherwise normal. We designed a splice-modifying morpholino (MO[dlD-V]) targeted to the 3' end of exon 11. RT-PCR analysis confirmed that in embryos injected with 5 ng of the morpholino, normal *deltaD* transcript is undetectable and the predominant form (expressed at normal levels) is a misspliced variant in which intron 11 has not been removed. In the resulting protein, the C-terminal valine is replaced by 34 amino acids ending in LVLN* (Appendix Fig. 4A,B).

To confirm that MO[dlD-V] injection does indeed block the DeltaD-Magi interaction in the living embryo, I performed an experiment in which I injected embryos with a plasmid coding EGFP-tagged Magi1 either alone or together with 5 ng MO[dlD-V] and looked for evidence of Magi1-DeltaD co-localisation. In embryos injected with only Magi1-EGFP, colocalisation was detectable in some tissues expressing high levels of DeltaD, for example in the somites (Appendix Fig. 3D). In contrast, cells in embryos receiving both the plasmid and the morpholino had no perceptible colocalisation of the two proteins (Appendix Fig. 3E). Thus, the morpholino, by destroying the C-terminal ATEV motif, blocks the ability of DeltaD to bind Magi in the living embryo. It is also likely that MO[dlD-V] blocks DeltaD's ability to bind other Magi homologues, although this is only a prediction that I have never tested directly.

### 3.1.4 The DeltaD-Magi interaction: mysterious results and a lesson in control experiments

To test the functional significance of the DeltaD-Magi1 interaction, we examined the phenotype of embryos injected with MO[dlD-V]. We began by examining MO[dlD-V]-injected embryos for defects in processes in which DeltaD is known to play an important role. As a positive control, we took advantage of the *after eight* ($aei^{AR33}$) mutant, which has a stop codon in the fifth EGF-like repeat of the extracellular domain of *deltaD*, leading to a

DeltaD loss-of-function phenotype (Holley et al., 2000). In homozygous *aei* embryos, somite segmentation is defective (Holley et al., 2002; Jiang et al., 2000; van Eeden et al., 1996a), primary neurons are produced in excessive numbers (Holley et al., 2000), and the numbers of hypochord (ventral midline) cells are reduced (Latimer et al., 2002). These defects all reflect DeltaD's function as a Notch ligand. If DeltaD's interaction with Magi proteins is important for its role as a Notch ligand, we would expect to see similar defects in MO[dlD-V]-injected embryos. Surprisingly, our prediction was wrong. Embryos injected with 5 ng of MO[dlD-V] were normal in the formation of somites and the hypochord (Appendix Fig. 5F-K), and the number of Rohon-Beard primary sensory neurons (as assayed by in situ hybridization for *islet1*) was unaffected (Appendix Fig. 6A,B,E).

We did, however, observe a rather striking morphological phenotype. MO[dlD-V]-injected embryos showed clear and reproducible abnormalities in the formation of the midbrain and hindbrain, such that by 24 hpf, the width of the roofplate and the lumen of the third and fourth brain ventricles were markedly reduced (Appendix Fig. 5A-C; Appendix Table 2). Injection of a 5 base-pair mismatch control morpholino did not produce this effect (data not shown), suggesting that it was a specific effect resulting from blockade of the DeltaD-Magi interaction. Morpholinos can have deleterious side-effects, however, and similar structural abnormalities have been documented as an effect of morpholino mistargeting (Ekker and Larson, 2001). A BLAST search for other targets of MO[dlD-V] revealed no obvious candidates, yet the brain ventricle phenotype observed is hard to explain in terms of known functions of DeltaD or Magi1. Spurred on by the doubts of a referee, I therefore performed one further, more decisive control.

Because the C-terminus is missing in *aei* mutants, these embryos should show a similar narrowed-ventricle phenotype to MO[dlD-V] morphants, in which only the C-terminus of the protein has been altered. In any case, injection of MO[dlD-V] into *aei* homozygous embryos should have no additional effect since these embryos do not contain the supposed target of the morpholino. Our prediction was wrong on both scores: the brain ventricles of *aei* embryos appeared completely normal, but injection of 5 ng of MO[dlD-V] into *aei* homozygotes produced an identical phenotype to genetically wild-

type morphants (Appendix Fig. 5D,E; Appendix Table 2). We conclude, therefore, that the narrowed-ventricle phenotype seen in MO[dlD-V] morphants is due to some non-specific toxic effect of the morpholino that were not detected with a mismatch control, thus underscoring the importance of rigorous controls in morpholino-based experiments, an issue that resurfaces in Chapter 5.

In our case, the scepticism of a referee (which we felt was somewhat undeserved) spurred us to perform an additional experiment. As it turned out, the unexpected results of that experiment radically changed the message of our paper, and we offered this story as a cautionary tale to others who rely on morpholino-mediated knock-down experiments (Wright et al., 2004).

### 3.1.5 The DeltaD-Magi interaction in vivo revisited: a result we can believe in.

As part of our studies into how the DeltaD-Magi interaction affects DeltaD's function as a Notch ligand, I investigated its role in primary neurogenesis. My hypothesis was that if the DeltaD-Magi interaction is important for DeltaD-Notch signalling, then I should observe an overproduction of Rohon-Beard primary sensory neurons, as is seen in *aei* mutants (Holley et al., 2000). This hypothesis was wrong, as discussed in the previous section. However, during the course of these experiments, I observed a rather unexpected phenotype. In normal embryos at 16 hpf, Rohon-Beard neurons lie in two longitudinal strips on either side of the dorsal midline, but not crossing a medial span of three or four cell diameters (Appendix Fig. 6A). In MO[dlD-V]-injected embryos, however, these cells were often mislocalised such that their cell bodies were often observed to cross the midline (Appendix Fig. 6B,F). This defect is not seen in homozygous *aei* embryos (Appendix Fig. 6C, F), indicating that it is not due to failed DeltaD function. Armed with this decisive *aei* control, I injected 5 ng of MO[dlD-V] into homozygous *aei* mutant embryos: both the number and the location Rohon-Beard neurons in morpholino-injected *aei* mutants were indistinguishable from uninjected *aei* siblings (Appendix Fig. 6D, F). Our interpretation is that when DeltaD is prevented from binding Magi

proteins, it acts as a gain-of-function mutation, implying that Magi proteins somehow restrain DeltaD function.

These data suggest that the DeltaD-Magi interaction could play some role in the migration or dispersal of Rohon-Beard neurons, and possibly other cells. In the following Results section, I describe experiments aimed at exploring this possibility. Mr. Jonathan Tobin, a summer student who I mentored in the lab, performed some of these experiments. Although they were not published in a peer-reviewed journal, Jon used his findings for his undergraduate Final Honours Project report at the University of Oxford (Tobin, 2005).

# 3.2 Results

## 3.2.1 Overexpression of DeltaD induces filopodia in cultured cells

My studies on the functional significance of the DeltaD-Magi interaction indicate that Delta proteins might affect motility in some cell types and that the C-terminal ATEV motif is important to regulate that activity. Others have shown similar findings in other systems. For example, Lowell and Watt (Lowell and Watt, 2001) found that mammalian keratinocytes show enhanced motility when expressing a form of Delta1 lacking the intracellular domain (including the ATEV motif), but expression of full-length Delta1 produces the opposite effect: a reduction in motility. Similarly, Six et al showed that expression of full-length Delta1 in NIH 3T3 cells reduces motility but that this effect is not seen if a version of Delta1 lacking its ATEV motif is substituted for the full-length protein (Six et al., 2004).

To see if zebrafish DeltaD could have a similar a effect on cell motility or morphology, we turned to a mammalian tissue culture assay in which we transfected mouse L-cells with *deltaD* or *deltaD-TE** (that is, encoding for a variant of DeltaD lacking its terminal valine). We found that both versions of Delta produced a dramatic change in cell morphology: untransfected cells have very few filopodia as determined by phalloidin staining, but cells

transfected with either form of DeltaD had numerous filopodia (Fig. 3.1A,B). This observation is reminiscent of the findings of De Joussineau and colleagues (De Joussineau et al., 2003), who showed that expression of Delta in *Drosophila* sense-organ precursor cells induces the formation and extension of filopodia. In contrast, cells that were transfected with a plasmid coding for Magi1-EGFP (Wright et al., 2004) were indistinguishable from non-transfected cells (compare Fig. 3.1C with arrow in Fig. 3.1A). Thus, it appears that in my system, Delta can induce filopodia formation in a similar way to what has been demonstrated in *Drosophila* (De Joussineau et al., 2003).

My observations on Rohon-Beard cell mislocalization suggest that MAGI restricts Delta's induction of cell motility. If that effect is at all related to Delta's effect on cell morphology, one might predict that the induction of filopodia seen in cultured cells expressing full-length DeltaD would be inhibited by the addition of Magi. To see if this is the case, we cotransfected L-cells with plasmids coding for Magi-EGFP and either full-length DeltaD or DeltaD-TE*. As expected, full-length DeltaD, but not DeltaD-TE*, recruited Magi-EGFP to the cell surface (Fig. 3.1D,E). However, we were surprised to see that Magi seemed to have no effect on Delta's induction of filopodia: cells that were double-positive for Magi1-EGFP and DeltaD were indistinguishable from cells expressing DeltaD alone (Fig. 3.1A,D).

This result would seem to argue against our hypothesis, but there are explanations that could account the discrepancy. For example, stoichiometry could be a major factor. These experiments were performed using transient transfections; consequently the absolute and relative levels of DeltaD and Magi1-EGFP could vary tremendously from cell to cell and from one experiment to another. To perform this experiment more rigorously, it would be preferable to generate stable cell lines expressing a constant level of either DeltaD. One could, then, transiently transfect these cells with varying levels of the Magi to determine if there would be a dose-response effect on Delta's ability to induce filopodia.

It is likely that the protein composition of L-cells, which is bound to be significantly different from that of zebrafish Rohon-Beard neurons, has a strong impact on the way that DeltaD and Magi affect cell morphology. For a more physiological test, it would be better to study more neuronal-like culture

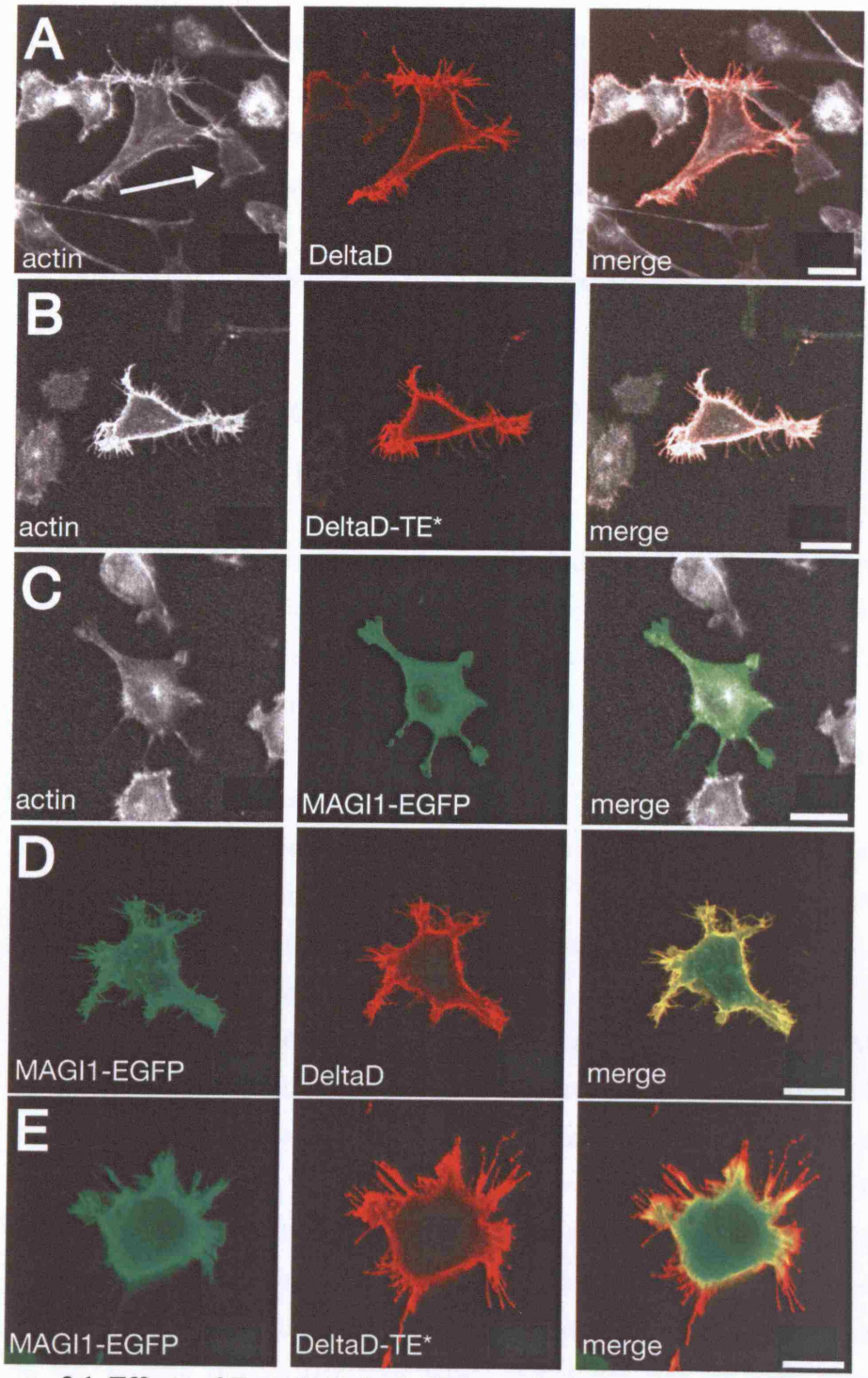


**Figure 3.1. Effects of DeltaD, DeltaD-TE* and Magi1 on L-cell morphology.** Confocal images of L-cells transfected with DeltaD (**A,D**), DeltaD-TE* (**B,E**) or Magi1-EGFP (**C-E**). Note the increase in filopodia in (A,B,D,E) versus an untransfected cell (arrow in A). Actin was detected with phalloidin in all samples in the far-red channel (633 nm laser) and pseudocoloured white in (A-C) and omitted from (D,E) for ease of visualisation. Scale bars: 20 μm.

cells, or to culture zebrafish cells. Although it would have been interesting to investigate this further, I felt that the time it would take to rigorously perform these experiments would be substantial. Because our lab has very little experience in cell culture, I felt that this line of investigation had a low chance of yielding informative results and was taking my research away from studies in development, a recurrent theme for this project.

### 3.2.2 Overexpression of DeltaD results in increased levels of Magi2

Using a cell culture assay system, we showed that DeltaD interacts with zebrafish Magi1 and that the two proteins colocalise via DeltaD's recruitment of Magi to the cell surface. We hypothesise that MAGI proteins hold ATEV-Deltas at multiprotein signalling complexes, and that these complexes may be focused in specific regions of the cell, yet the distribution of both proteins appeared to be uniform at the membrane. One possible explanation for this observation is that exogenous zebrafish Magi1 is unable to associate with such complexes in this mammalian cell. It is possible, however, that L-cells express endogenous Magi proteins and that these may interact with DeltaD.

To test this, we took advantage of commercial antibodies that recognise each of the rat Magi proteins. The epitopes for the anti-rat Magi antibodies are conserved in each of the mouse proteins, thus we predicted that they would detect endogenous Magi1, Magi2 and Magi3 in L-cells, if they were in fact expressed. We transfected L-cells with a plasmid coding for full-length DeltaD and examined the distribution of each of the endogenous Magi proteins. Magi1 was found in a punctate pattern at the cell surface and in DeltaD-induced filopodia (Fig. 3.2A). In contrast, Magi3 was found primarily in the nucleus (Fig. 3.2B). The levels and distribution of both proteins appeared to be unaffected by the presence of DeltaD (compare DeltaD-positive to DeltaD-negative cells in Fig. 3.2A,B), suggesting that any apparent colocalization might be simply due to the high levels of DeltaD protein at the surface rather than to any specific interaction between DeltaD and either Magi1 or Magi3.

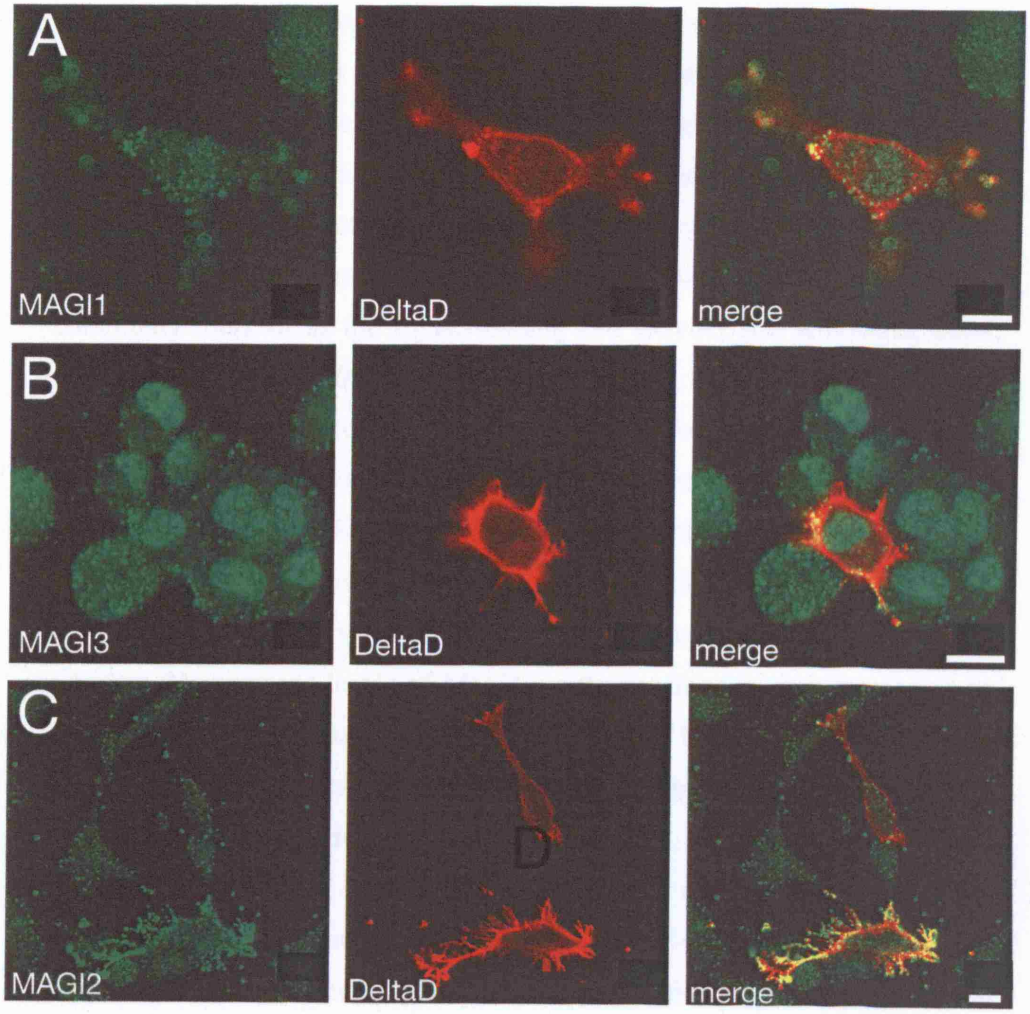


**Figure 3.2. Effects of DeltaD overexpression on endogenous Magi protein levels.** Confocal images of L-cells transfected with a plasmid coding for full-length DeltaD and immunostained for endogenous Magi proteins (green) with antibodies against rat Magi1 (**A**), Magi3 (**B**) or Magi2 (**C**). DeltaD (red) was detected with an anti-DeltaD antibody. Note that the levels of Magi2 (C) are greater in the cell strongly expressing DeltaD compared to untransfected or weakly-transfected neighbours. The same does not appear to be true for Magi1 (A) or Magi3 (B). Scale bars: 20 μm.

In contrast, expression of DeltaD had a dramatic effect on Magi2. Cells that had not been transfected with DeltaD had low levels of Magi2 with a punctate staining pattern at the cell surface (Fig. 3.2C). However, neighbouring, DeltaD-positive cells had a dramatic increase in the levels of Magi2, which was usually enriched in the filopodia (Fig. 3.2C). This unexpected observation indicates that DeltaD either stabilizes Magi2 at the cell surface or else somehow induces increased Magi2 synthesis. The fact that DeltaD appears to recruit Magi2 to filopodial extensions seems to support the former. However, biochemical studies have shown that the intracellular domains of Notch ligands may translocate to the nucleus of what we commonly think of as the signal-sending cell (Kiyota and Kinoshita, 2004; LaVoie and Selkoe, 2003; Six et al., 2003), raising the possibility that Notch ligands, like the receptor itself, may have some transcriptional regulatory role and may, thereby, provide a mechanism for bidirectional signalling (Kiyota and Kinoshita, 2004; Six et al., 2003). Perhaps the enrichment of Magi2 represents one such gene regulatory function of DeltaD.

Substituting DeltaD-TE* for full-length DeltaD might give clues as to whether the increased levels of Magi2 are the result of its stabilisation or an increase in its synthesis. Since DeltaD-TE* cannot bind to Magi2, we would expect that cells expressing DeltaD-TE* would be indistinguishable from normal control cells. However, it is possible that a different region of the intracellular domain of DeltaD could interact with other molecules, and that these associations might somehow stabilise Magi2-containing complexes. If that were the case, substituting DeltaD-TE* for the full-length molecule would have no effect on Magi2 levels.

### 3.2.3 In vitro analysis of the interaction between Delta, MAGI and Mind bomb

In order for Delta proteins to activate the Notch receptor in neighbouring cells, the intracellular domain of Delta must be ubiquitinated by the E3 ubiquitin ligases, Mind bomb (Chen and Casey Corliss, 2004; Itoh et al., 2003), Mind bomb2 (Koo et al., 2005; Zhang et al., 2007) or Neuralized (Lai et al., 2001; Pavlopoulos et al., 2001), which, in turn, triggers Delta internalization. Indeed,

in the zebrafish, Delta protein is found almost exclusively in intracellular vesicles rather than at the cell surface, indicating that the vast majority of Delta is rapidly internalized once it reaches the membrane (Itoh et al., 2003; Zhang et al., 2007). In the zebrafish loss-of-function *mind bomb* (*mib*) mutant, Delta internalisation fails and all Notch signalling is lost (Itoh et al., 2003). One might suppose, therefore, that MAGI proteins somehow mediate the interaction between Delta and Mind bomb. To investigate this possibility, we returned to a tissue culture assay system.

To confirm that Mind bomb induces the internalisation of DeltaD in this system, cells were co-transfected with plasmids coding for a myc-tagged Mind bomb and either full-length DeltaD or DeltaD-TE*. I found that Mind bomb does, indeed, trigger the internalisation of both forms of DeltaD (Fig. 3.3A,B and data not shown), as has been shown with other Delta proteins in other tissue culture assays (Itoh et al., 2003).

In triple-transfected cells containing plasmid coding for full-length DeltaD, myc-Mind bomb and Magi1-EGFP the internalisation of DeltaD was blocked in 50% of the cells (Fig. 3.3C), suggesting that MAGI proteins may interfere with Mind bomb-induced Delta internalisation, thus attenuating the ability of Delta to function as a Notch ligand. However, when DeltaD-TE* (which cannot bind Magi, Appendix Fig. 3C), was substituted for full-length DeltaD, its internalisation was also blocked by the addition of Magi1-EGFP in a similar proportion of cells (Fig. 3.3D). Since Magi cannot interact directly with DeltaD-TE*, I cannot explain this result. It is possible that, as with our other tissue culture-based assays, stoichiometry could be a factor. To control for that possibility would require very precise measurements of the levels of each of the proteins involved.

A problem that I consistently battled with in this and other tissue culture-based experiments was a tremendous variability, both within a given sample and from one experiment to the next. The data I have presented are my best efforts to accurately represent the effects I observed; yet without rigorous quantification, they are admittedly quite dubious. For example, in the above experiments, I found that the addition of Magi1 could block the Mind bomb-mediated internalisation in approximately 50% of the cells. Yet, in some neighbouring cells, Magi1 had absolutely no effect. In an effort to make sense

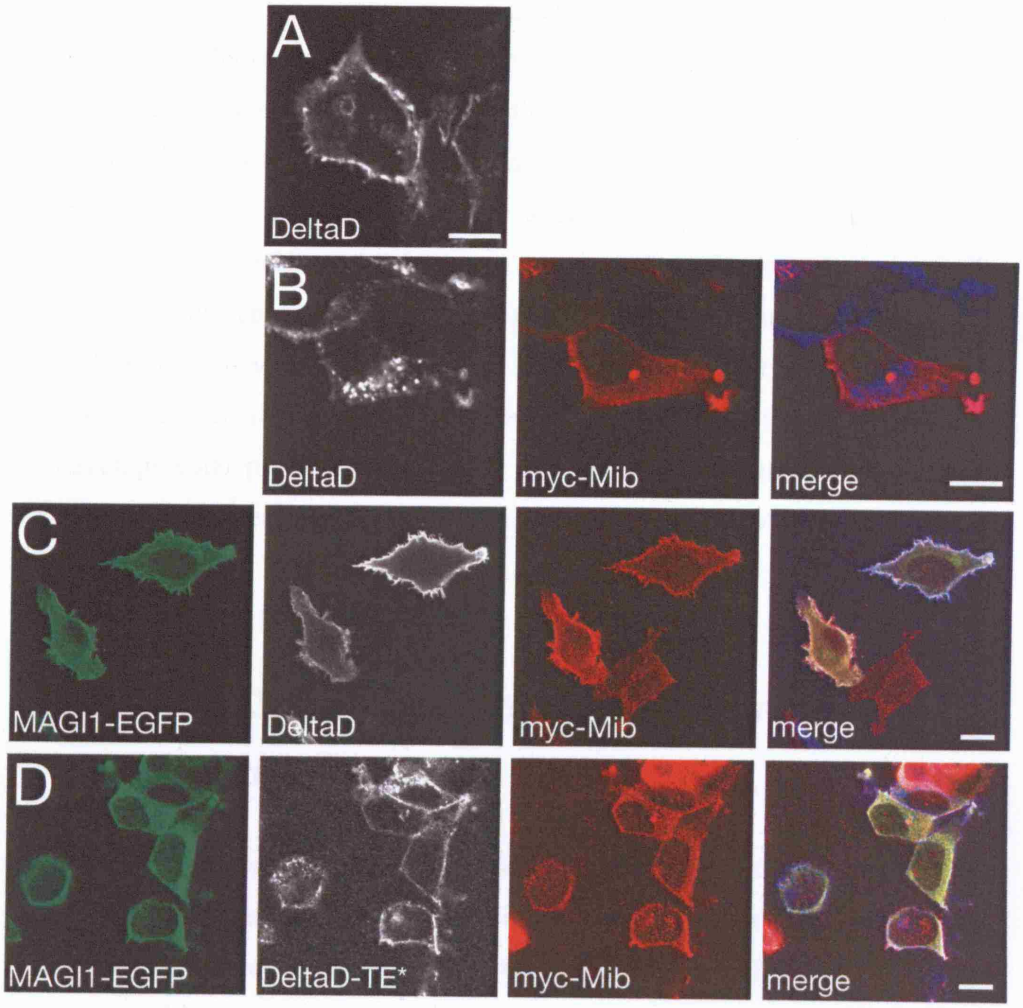


**Figure 3.3. Effects of Magi1 on Mindbomb-induced DeltaD internalization.** HEK 293T cells were transfected with plasmids coding for full-length DeltaD (**A**); DeltaD and myc-tagged Mind bomb (Mib; **B**); DeltaD, Mib and Magi1-EGFP (**C**) or DeltaD-TE*, Mib and Magi1-EGFP (**D**). Addition of Mib induces DeltaD internalization (B). This effect is blocked by the addition of Magi1 in 50% of cells (C). Magi1 appears to have the same effect on DeltaD-TE* internalization (D). Images for DeltaD and DeltaD-TE* were pseudocoloured white in the single channel pannels (for ease of visualization), but appear as blue in the merged image. DeltaD and DeltaD-TE* were detected with an anti-DeltaD antibody, Myc-Mib was detected with an anti-Myc antibody. Scale bars: 10 μm.

of this puzzling observation, I tried to quantify the effect by scoring cells for DeltaD internalisation. In doing this, I was careful to only consider cells that had similar levels of each of the three proteins, thereby normalising the sample set. Again, I found radically different effects from one cell to the next. (For example, in one triple transfection experiment I found DeltaD in vesicles in 9 out of 20 cells examined, with the remaining 11 cells having DeltaD only at the surface. If DeltaD-TE* was used, the trend was the same: I found vesicular staining in 14 out of 28 cells examined with the remaining cells expressing DeltaD exclusively at the surface.) In an effort to correct for the influence that neighbouring cells might have on one another, I performed a similar quantification considering only cells that were not in contact with any other cell. Sadly this was also to no avail: the results were just as variable. In the end, I felt that these studies were taking me away from the questions about developmental processes that I most wanted to investigate, so we chose to draw a line under our studies into the Delta/Mind bomb/MAGI interaction in vitro.

### 3.2.4 The DeltaD-Magi interaction is important for neurite formation

In zebrafish embryos in which the DeltaD-Magi interaction is blocked, Rohon-Beard primary sensory neurons stray into ectopic locations (Appendix Fig. 6). Might this defect be accompanied by alterations in cell morphology? To answer this, we examined Rohon-Beard axons in MO[dlD-V]-injected embryos using a neuron-specific antibody against HNK-1/NCAM. Rohon-Beard cells have two types of axons: longitudinal axons that project anteriorly and posteriorly along the body axis, and peripheral axons that extend ventrally near the lateral surface of the embryo. MO[dlD-V]-injected embryos or uninjected siblings were allowed to grow until 27 hpf and were stained with the HNK-1 antibody. In normal embryos, the peripheral axons form a dense arborised network (Fig. 3.4A). In contrast, the density of the axon network in morphant embryos was substantially reduced, with very few axons following a proper trajectory (Fig. 3.4B). The peripheral axons of *aei* mutant embryos,

while greater in number than wild-type embryos, were otherwise normal (Fig. 3.4C). This was unchanged in *aei* embryos which had been injected with MO[dlD-V] (Fig. 3.4D).

Morphant embryos also had defects in the projections of the longitudinal Rohon-Beard axons. In normal embryos, these axon projections are continuous, extending from the tail to the hindbrain, where they join the descending projections of the trigeminal ganglia (Fig. 3.5A). In MO[dlD-V]-injected embryos, this track of Rohon-Beard projections was discontinuous, with a gap often seen in a region just caudal to the hindbrain (Fig. 3.5B). This defect was not apparent in either uninjected or MO[dlD-V]-injected *aei* embryos (Fig. 3.5C,D), indicating that it is a result of failed DeltaD-Magi interaction. Whether these defects in Rohon-Beard morphology are linked to the mislocalisation of these cells, or vice versa, remains to be determined.

While this appears to be an interesting and important result, it should be noted that this particular observation was made by the aforementioned summer student in the lab, Jonathan Tobin, on a small number of cases. I have not reproduced the experiment myself. While I believe that Jonathan was very thorough in his experiments, I cannot personally vouch for the validity of this particular result. I include it here for the benefit of future people in the lab who may wish to pursue the Delta-MAGI project.

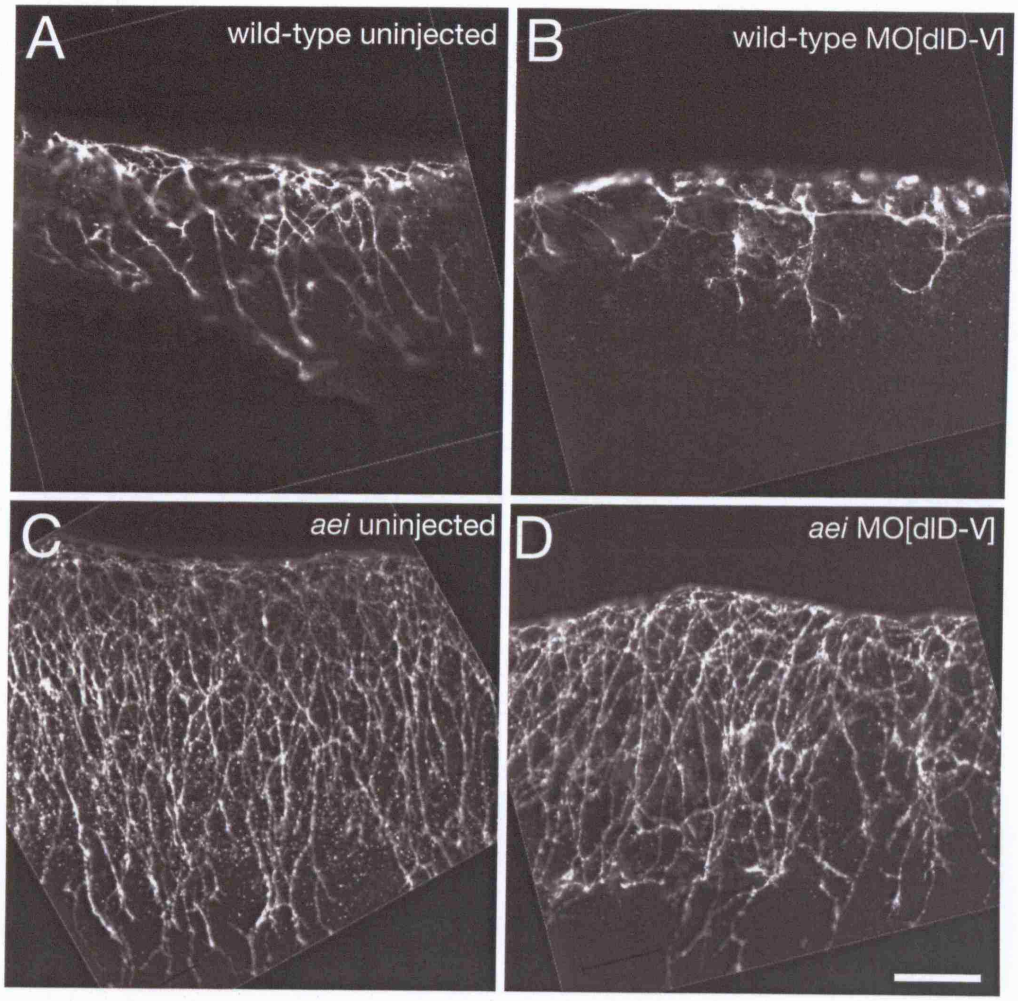


**Figure 3.4. Effects of MO[dlD-V] on Rohon-Beard peripheral axons in wild-type and *aei* embryos.** Lateral view of the mid-trunk of 27 hpf wild-type (**A,B**) or *aei* (**C,D**) embryos that were uninjected (**A,C**) or injected with 5 ng of MO[dlD-V] (**B,D**). Whole embryos were stained with an antibody against HNK-1/N-CAM to detect Rohon-Beard neurons. Note *aei* embryos are slightly more developed. This is due to the fact that they were injected and gathered on a separate day from the wild-type embryos and the two samples were not precisely stage-matched. Scale bar: 50 μm.

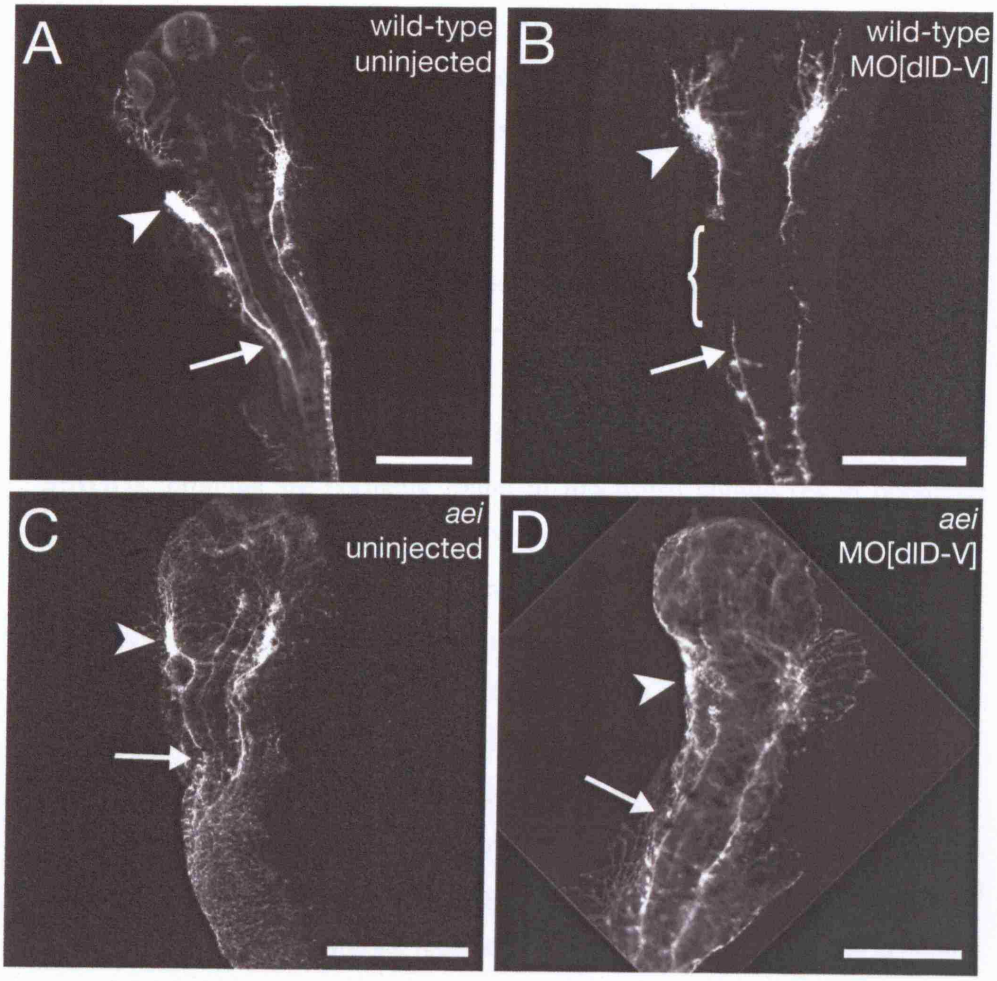


**Figure 3.5. Effects of MO[dlD-V] on Rohon-Beard connections to the trigeminal ganglia.** Dorsal view of 27 hpf wild-type (**A,B**) or *aei* (**C,D**) embryos that were uninjected (**A,C**) or injected with 5 ng MO[dlD-V] (**B,D**). Whole embryos were stained with an antibody against HNK-1/N-CAM to detect neurons. Arrowheads indicate the trigeminal ganglia and arrows indicate longitudinal Rohon-Beard axons. Note the gap between the axons of the trigeminal ganglia and the Rohon-Beard axons in the morphant embryos (bracket in B). Scale bars: 200 μm.

### 3.2.5 The formation of the lateral line organ is unaffected in MO[dlD-V] morphants

My studies on the interaction between Delta proteins and MAGI proteins had produced somewhat frustrating results. We had seen that the interaction appeared to be important for some aspects of Rohon-Beard primary sensory neuron behaviour in vivo, but our efforts to determine exactly how the interaction exerted its effects had been met with results that were difficult to interpret and often contradictory. The interaction between DeltaD and Magi proteins doesn't appear to be important for DeltaD's function as a Notch ligand, yet blocking the interaction does have some consequences which appear to involve a gain of DeltaD function (Wright et al., 2004). Because MAGUK proteins are normally found in junctional complexes in polarized cells (reviewed in (Funke et al., 2005)), one might think that they might function to recruit Delta proteins to specific subcellular domains, thereby spatially focusing Delta's availability for interaction with Notch. Indeed, similar findings have been reported for other MAGUK proteins (Mizuhara et al., 2005; Six et al., 2004). One might expect, therefore, that the loss of the DeltaD-Magi interaction could produce a phenotype in polarized tissues where Notch signalling is known to be important.

In fish, the lateral line system is comprised of numerous clusters of sensory organs, or neuromasts, located at the surface of the body and arranged around the head (anterior lateral line system) and along the length of the body trunk (posterior lateral line system). The posterior lateral line neuromasts are derived from a two primordia that migrate posteriorly, depositing prosensory clusters that differentiate into the cells of the neuromast (Stone, 1922; Stone, 1933). The first primordium begins migrating by 20 hpf and reaches the tail by 40 hpf, depositing seven to nine neuromasts along the way. The second, smaller primordium begins migrating along the same path shortly after 40 hpf and deposits a few smaller neuromasts in the more anterior region of the trunk. Because the DeltaD-Magi interaction appears to somehow affect cell motility, we reasoned that we might see defects in neuromast deposition in embryos where DeltaD cannot bind to Magi proteins. I, therefore, examined MO[dlD-

V]-injected zebrafish embryos at 6 dpf to look for defects in the number or placement of neuromasts in the posterior lateral line system. I found that the number of neuromasts was reduced in morphant embryos (uninjected: 11.3 neuromasts per each side of each embryo, n=4; MO[dlD-V]: 4.2 neuromasts per each side of each embryo, n=11; Fig. 3.6A,B).

Like the sensory epithelium of the ear, each neuromast consists of a mosaic pattern of mechanosensory hair cells and supporting cells. Unlike the inner ear, however, the hair cells within each neuromast are arranged with a precise planar polarity that is oriented in opposing directions in neighbouring cells. This is easily observed by the location of a single acetylated tubulin-positive kinocilium within each actin-positive hair bundle (for example, see (Lopez-Schier et al., 2004)). As in the ear, Delta-Notch signalling appears to play an important role in specifying hair cells and supporting cells in the neuromast (Itoh and Chitnis, 2001). I wondered, therefore, whether Magi might be involved in this process. Additionally, while we have no evidence indicating that the Notch pathway is involved in planar cell polarity in other systems, it is possible that an asymmetric distribution of Notch ligands might be involved in the establishment planar cell polarity of neuromasts, and that MAGI proteins might mediate a polar recruitment of ligands to junctional complexes. I examined posterior lateral line neuromasts in MO[dlD-V]-injected embryos to see if the planar polarity of the hair cells was affected. This was not the case: the planar polarity of the hair cells looked normal in the morphants (Fig. 3.6C,D).

It is interesting to note that the neuromasts in the morphant embryos were consistently smaller than those of uninjected control siblings (Fig. 3.6C,D). Thus, embryos in which the DeltaD-Magi interaction has been blocked have (1) a reduction in neuromast number, (2) a reduction in neuromast size and (3) a posterior lateral line that fails to migrate all the way to the tail. These observations could be explained if we consider that the neuromasts derived from the second lateral line primordium are fewer, smaller and restricted to the anterior half of the trunk (as discussed in (Lopez-Schier et al., 2004)). It is tempting to speculate that, in morphant embryos, the first posterior lateral line primordium fails to form, but that the second lateral line primordium develops and migrates normally. This could reflect a fundamental

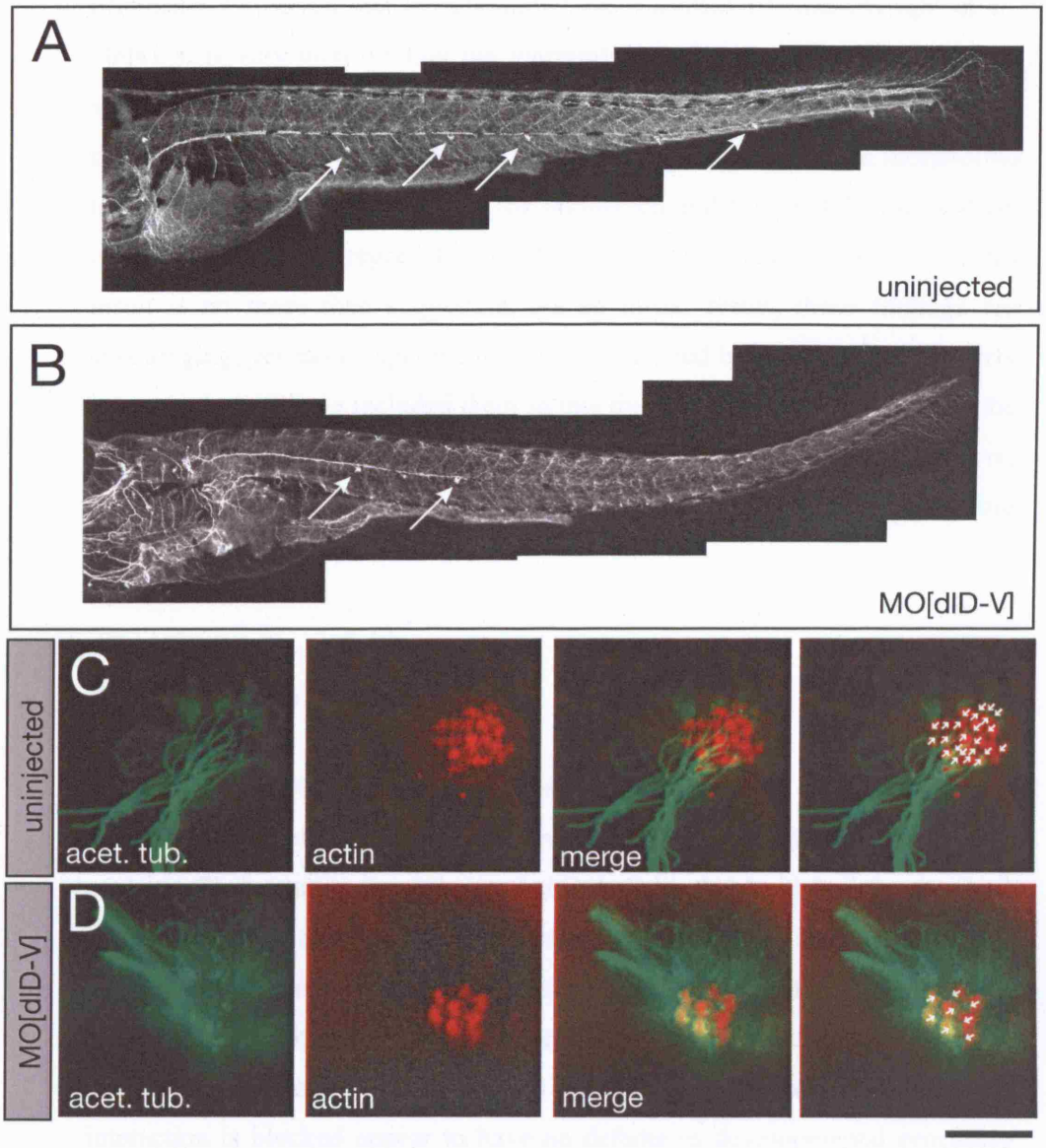


**Figure 3.6. Effects of MO[dlD-V] on lateral line formation and neuromast hair cell polarity.** (**A,B**) Lateral view of 6 dpf embryos that were uninjected (A) or injected with 5 ng of MO[dlD-V] (B) and stained for actin with phalloidin. Neuromasts are indicated with the arrows. Note fewer neuromasts in the morphant (B). (**C,D**) Hair cells of neuromasts in an uninjected (C) or morphant (D) embryo. Kinocilia (green) were detected with an antibody against acetylated tubulin and actin-rich hair cells bundles (red) were detected with phalloidin. The planar polarity of each hair cell (in which a determination was possible) is displayed with white arrows in the duplicate merged image on the far right. Scale bar: 200 μm in A,B; 25 μm in C,D.

difference in the mechanisms governing the formation of the two lateral line primordia. Or, given that morpholinos have a limited lifetime (Wright et al., 2004), it is very possible that the morpholino had degraded by the time the second primordium had formed and began to migrate. It is also possible that the defects I observed in the lateral line system simply result from morpholino toxicity. Without the inclusion of the uninjected and MO[dlD-V]-injected *aei* controls (which were regrettably omitted from this particular experiment), this result is no more than suggestive. As an initial result, these findings are encouraging, yet more experiments would be needed before we could properly interpret them. I have included them in this thesis for the sake of others in the lab who may wish one day to follow up on this project. For my part, however, I chose to focus my efforts on another project, as we will see in the following chapters.

## 3.3 Discussion

In this chapter I have described results from studies investigating the interaction between ATEV-Deltas and the MAGI family of scaffolding proteins. These studies have shown that DeltaD binds Magi1 both in vitro and in vivo, and that the interaction occurs between PDZ4 of Magi1 and the C-terminal ATEV motif of DeltaD. If we remove or replace the terminal valine residue, the interaction is abolished. Surprisingly, this interaction appears to be dispensible for DeltaD's function as a Notch ligand: zebrafish in which the interaction is blocked appear to have no defects in developmental processes that require DeltaD-Notch signalling. Yet the striking evolutionary conservation of this motif strongly suggests that it must be important for something. What, then, is its function?

### 3.3.1 The Delta-MAGI interaction may be important in the control of cell motility and morphology

My studies indicate that the DeltaD-Magi interaction might have a role in controlling cell motility. In embryos where the interaction is blocked, Rohon-Beard primary sensory neurons are mislocalised. Yet these cells are localised properly in embryos lacking DeltaD (Appendix Fig. 6). This suggests that in MO[dlD-V]-injected embryos, DeltaD somehow misbehaves, and that Magi proteins normally restrain this misbehaviour. It is interesting to note that the same cells are defective in their axonal projections: both peripheral and longitudinal axons fail to extend properly. The deposition of neuromast precursors from the migrating lateral line primordium also appears to be defective in MO[dlD-V]-injected embryos. However, both the mislocalisation of Rohon-Beard cells (which seem to migrate excessively) and the deficit of neuromasts (indicating a deficit in migration) are difficult to explain in terms of known functions of Delta proteins.

To investigate possible ways in which DeltaD and its interaction with Magi might affect cell motility, we turned to a tissue culture system. We found that the overexpression of DeltaD or DeltaD-TE* causes a dramatic change in cell morphology, inducing filopodia formation in L-cells (Fig. 3.1A,B). De Joussineau et al have reported similar findings in *Drosophila*: Delta overexpression in sense organ precursor cells induces a dramatic increase in the filopodial arbour (De Joussineau et al., 2003). The authors further demonstrate that these filopodia are important for long-range signalling between these cells and their neighbours. Might a similar phenomenon explain my observations on Rohon-Beard morphology and location? Given that Magi proteins are present in L-cells, and that similar effects are seen with normal DeltaD and with DeltaD-TE*, which cannot bind Magi proteins, these observations suggest that the induction of filopodia by DeltaD is independent of DeltaD-Magi interaction in L-cells. The possibility remains, however, that this action of DeltaD might be Magi-dependent in Rohon-Beard cells.

An obvious question that has yet to be answered is whether DeltaD is expressed in Rohon-Beard cells. If so, its effect on their location and morphology could reflect a cell-autonomous activity. One could suppose that within Rohon-Beard neurons, Magi proteins normally recruit DeltaD, or are recruited by DeltaD, to signalling complexes at the tips of filopodia and thereby somehow influence the direction or rate of extension of cell processes. Thus, in the Rohon-Beard cells of MO[dlD-V]-injected embryos, the proper signalling complexes may simply fail to form.

An alternative possibility is that the effect I observed in Rohon-Beard cells is a non-cell-autonomous consequence of mislocalized DeltaD in the neighbouring cells, for example in the cells of the neural tube. Magi proteins may be required to recruit DeltaD to specific subcellular regions of the neural tube, and blocking their interaction may prevent that from occurring properly. In this way, it may be important that DeltaD be recruited to places where it is available to interact with Notch in the Rohon-Beard cells. Alternatively, DeltaD might normally be kept in subcellular regions that are inaccessible to Rohon-Beard cells. In morphant embryos this would no longer be the case, thereby allowing DeltaD to ectopically activate Notch signalling in Rohon-Beard cells when it normally should not. This model is reminiscent of studies in mouse showing that Magi1 recruits Dll1 to apical junctional complexes in nascent neurons within the neural tube (Mizuhara et al., 2005). If the same were true in the zebrafish, then blocking the interaction might indeed allow DeltaD to become available to interact with Rohon-Beard neurons at the basal surface of the neural tube.

Six et al have shown that Dll1 recruits the MAGUK protein Discs large 1 (Dlg1) to points of cell-cell contact and that this interaction requires the C-terminal ATEV motif of Dll1 (Six et al., 2004). Additionally, the authors show that overexpressing Dll1 in NIH 3T3 cells cell-autonomously causes a reduction in cell motility, an effect that appears to be independent of Delta's function as a Notch ligand. Thus, mounting evidence supports the notion that Delta proteins may indeed have a cell-autonomous role in controlling cell motility. Whether these observations have physiological relevance in vivo remains to be determined.

### 3.3.2 Lessons from an abandoned project

To investigate the developmental functions of the DeltaD-Magi interaction, we exploited a morpholino that produced, at normal levels, an altered form of DeltaD that could no longer bind Magi proteins. We found that this morpholino produced a clear, reproducible phenotype, a narrowing of the brain ventricles. A BLAST search indicated that this morpholino should only bind to its intended target, and a commonly used form of control morpholino indicated that this defect was specific. Yet we were misled: only by controlling for MO[dlD-V]'s effects in a null mutant background did we discover that our findings were erroneous, a lesson that we hope will serve the scientific community well. We offered this cautionary tale so that it may serve as a warning of the risks of misinterpreting morpholino experiments. As a side-note, I should also mention that I performed this experiment only for the sake of appeasing a sceptical referee, who we admittedly felt was being somewhat unreasonable in his/her demands. Perhaps a good lesson to have learned from this experience is that the demands of a referee, while often frustrating, may indeed be more deserved than we, as authors, might like to think.

My studies provide evidence for an unexpected role of Delta proteins in controlling cell behaviour. Yet this project was somewhat plagued by results that are difficult to explain because of high variability, especially in the cell-culture experiments. During the course of these studies, I began working on a second project, which was aimed at investigating the role of a novel zebrafish ATEV-Delta, Delta-like 4 (Dll4). I carried on with both projects for some time, however the Dll4 project quickly began to produce encouraging results. My strong feeling was that my Delta-MAGI project had strayed quite far away from its intended purpose: to investigate the role of Delta-mediated Notch signalling in development. I, therefore, chose to put my efforts exclusively into the Dll4 project, which appears to have been a good choice. My studies on the role of Dll4 are covered in Chapters 4 and 5.

# Chapter 4: Delta-like 4, a novel zebrafish Notch ligand

## 4.1 Introduction

In comparing the genomes of higher vertebrates to those of simpler organisms, multiple gene homologues begin to appear. Such is the case with the genes encoding the members of the Notch pathway: the genome of the fruitfly *Drosophila melanogaster* has one *Notch* gene and one *Delta* gene in contrast to the genomes of mammals, which contain four *Notch* paralogues and three *Delta* paralogues. The zebrafish includes another level of complexity: a duplication event thought to have occurred after the divergence of the teleost and the mammalian lineages has left the zebrafish genome often possessing two paralogues for many mammalian genes (Amores et al., 1998; Kortschak et al., 2001; Taylor et al., 2003; Taylor et al., 2001). In some instances, these genes have overlapping or shared functions, while in other cases the function of a particular gene may have diverged substantially from its mammalian counterpart. Due to this duplication, as well as difficulties arising from a large number of repetitive elements and a high degree of polymorphism, the sequencing and annotation of the zebrafish genome has been a troublesome task. Yet, our understanding has improved immensely since the zebrafish genome sequencing project began in February 2001: novel genes and predicted transcripts are constantly being discovered. Sequence gazing, therefore, can often be a rewarding, albeit somewhat tedious, endeavour.

What began for me as a side project was the result of such a venture. Until recently, four zebrafish *deltas* had been known: *deltaA, deltaB, deltaC* and *deltaD* (Haddon et al., 1998b). Given that mammalian genomes contain three *Delta*s, it was reasonable to expect that the zebrafish may have additional, undiscovered *delta* genes. Searching the zebrafish genome database revealed such a gene in the form of an incomplete predicted transcript corresponding to a novel *delta* (Ensembl Gene ENSDARG00000053401). The protein encoded by this novel gene most-

closely resembled mammalian Delta-like 4 (Dll4), an endothelial-specific Notch ligand that has been linked with vascular remodelling and angiogenesis. Mice homozygous for a knockout mutation in *Dll4* die early, around E10, and heterozygotes show severe vascular abnormalities (Duarte et al., 2004; Gale et al., 2004; Krebs et al., 2004). Until recently, there was good reason to believe that *deltaC* was the zebrafish orthologue of *Dll4*: the expression of *deltaC*, like *Dll4* in mammals, is found in the endothelial cells of arteries but not of veins (Smithers et al., 2000). What, then, is the role of zebrafish Dll4, and how does its function overlap with DeltaC?

I have found that zebrafish *dll4*, like *deltaC* and mammalian *Dll4*, is expressed in the endothelial cells of arteries but not in those of veins, as well as in other tissues in the developing embryo. The amino acid sequence of human DLL4 shares 57% identity with zebrafish Dll4, but only 44% with DeltaC. Moreover, the genomic (exon/intron) structure of zebrafish *dll4* more closely resembles that of mammalian *Dll4* than does *deltaC*. We conclude that this novel gene is the true zebrafish orthologue of mammalian Dll4. What might the characterisation of the zebrafish orthologue tell us about this unique and essential Notch ligand, and what might we therefore learn about the role that Notch signalling plays in vascular patterning and angiogenesis?

# 4.2 Results

## 4.2.1 Identification of zebrafish Delta-like 4

In searching the Ensembl zebrafish genome database (http://www.ensembl.org/Danio_rerio/index.html), we identified a previously unknown predicted transcript (Ensembl Gene ENSDARG00000053401) on Chromosome 20 encoding a protein with strong sequence homology to the Delta family of Notch ligands, which we tentatively named *deltaE*. The predicted transcript lacked both a start and stop codon. I identified an EST clone (IMAGE 7418341) that included sequences 5' and 3' of the Ensembl gene, indicating that the first and last exons had not been identified in the predicted transcript. The Eponine Transcription Start Finder

(http://servlet.sanger.ac.uk:8080/eponine/) revealed just upstream from exon 1 a potential transcription initiation site 22 base pairs downstream of a TATA box (Fig. 4.1A). These elements, as well as much of exon 1 itself, are highly conserved between the zebrafish and the pufferfish *Tetraodon nigroviridis* and *Takifugu rubripes* (Fig. 4.1A). We also discovered an additional exon downstream of the predicted transcript, containing sequence coding for the terminal amino acid, stop codon and 3' untranslated region, thus giving *deltaE* a total of 11 exons (Fig. 4.1B). The DeltaE protein contains all of the hallmark domains of Delta proteins (see Introduction), with an extracellular domain that contains an MNNL domain, a DSL domain and a region containing several EGF-like repeats (Fig. 4.1C). It also contains a hydrophobic membrane-spanning region. In its intracellular domain we find the conserved ([E/D]$x_{2-4}$NN[L/I]) motif, which appears to be essential for the internalization of Notch ligands and the trans-activation of Notch receptors (Glittenberg et al., 2006) (see Introduction and Fig. 1.2B), and the motif ([D/E/R]$x_{3-5}$L[L/I]), which is involved with intracellular sorting and protein internalization (Bonifacino and Traub, 2003; Sandoval et al., 2000) (Introduction and Fig. 1.2B). It also possesses the highly conserved PDZ-binding motif ATEV* on its intracellular, carboxy terminus (Wright et al., 2004) (Fig. 4.1C).

We had identified a novel zebrafish Delta, but does it actually have a function? It's possible that the teleost genome duplication (Amores et al., 1998; Taylor et al., 2003; Taylor et al., 2001) has left some of the zebrafish's *delta* genes as degenerate genes; might this be the case for *deltaE*? If so, we would expect that over time its sequence, free of selective constraints, would have diverged considerably from those of the functional zebrafish *deltas* or their mammalian orthologues. We, therefore, performed a phylogenetic analysis using CLUSTAL W for sequence alignments (Thompson et al., 1994) and a standard neighbour-joining method (Saitou and Nei, 1987) to compare the amino acid sequences of known Deltas from the zebrafish, the pufferfish *Tetraodon nigroviridis* (also a teleost), mouse and human (Fig. 4.2). The resulting phylogenetic tree contains three major branches, corresponding to each of the three mammalian Deltas, with zebrafish DeltaA and DeltaD grouped with Dll1, DeltaB and DeltaC grouped with Dll3, and DeltaE as the lone counterpart to Dll4. (The sequence identities shared between DeltaE and

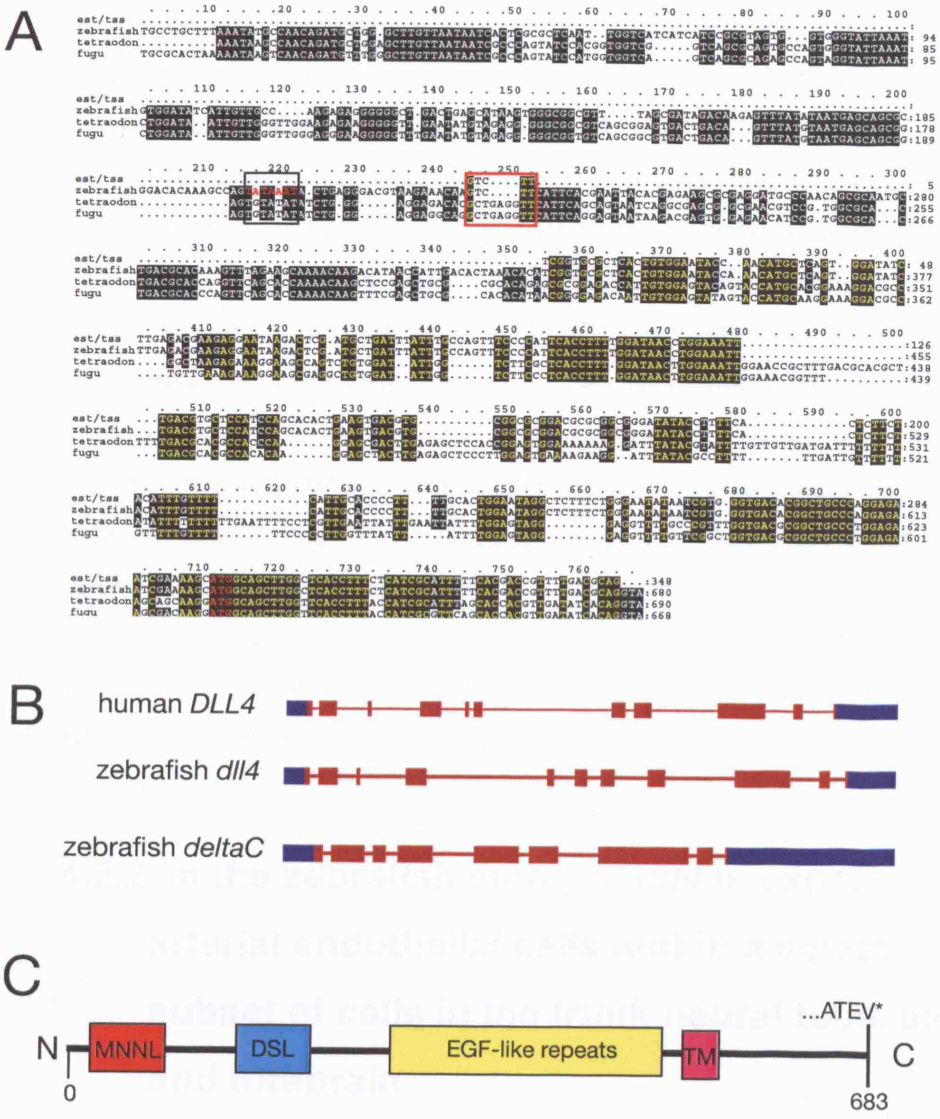


**Figure 4.1. A novel zebrafish *delta*.** (**A**) Sequence comparison of exon 1 (5' EST and the beginning of the coding sequence) and upstream regions of zebrafish *dll4* and putative orthologues in the pufferfish *Tetraodon nigroviridis* and *Takifugu rubripes* (fugu). The zebrafish sequence was derived from an EST clone (IMAGE 7418341; top line) and extended upstream based on genomic sequence data from the ENSEMBL zebrafish genome database. The predicted transcriptional start site (tss) is also listed in the top row and in the region demarcated by the red box. A putative TATA box is marked by the black box. The start codon is highlighted in red at position 295 of the zebrafish sequence. (**B**) Exon/intron structure of human *DLL4* (genbank accession number: NM_019074.2), zebrafish *dll4* (NM_001079835.1) and zebrafish *deltaC* (NM_130944). (**C**) Domain structure of zebrafish Dll4. TM: transmembrane region.

each of the human Deltas are: 57% for DLL4, 49% for DLL1 and 34% for both of the DLL3 isoforms.) Interestingly, two *Tetraodon* Deltas are found on the Dll4 branch; it is thus possible that the zebrafish, like the pufferfish, may have a second, unknown and heretofore unidentified *Dll4* orthologue.

In addition to sequence similarity, four other pieces of evidence link *deltaE* to *Dll4*: (1) both *deltaE* and *Dll4* have 11 exons, whereas *deltaC* has only 9 (Fig. 4.1B), (2) the sizes of the corresponding exons and the introns of *deltaE* and *Dll4* are similar (Fig. 4.1B), (3) the locations of the exon/intron boundaries are conserved between the two (data not shown) and (4) the regions upstream of both *deltaE* and *Dll4* contain the *vacuolar protein sorting 18* gene (data not shown), indicating synteny in this region of the chromosome between teleost and the mammalian genomes. The strong suggestion, therefore, is that *deltaE* is the zebrafish orthologue of mammalian *Dll4*; I refer to it as "*dll4*" from this point forward. (In keeping with the convention of zebrafish nomenclature, gene names begin with a lowercase letter, ie "*dll4*", whereas the first letter of the protein is capitalized, "Dll4".)

### 4.2.2 In the zebrafish embryo, *dll4* is expressed in arterial endothelial cells and in a select subset of cells in the trunk neural tube, ear and forebrain

My sequence analysis of the zebrafish *dll4* gene indicates its orthology to mammalian *Dll4*. Yet sequence similarity between two genes does not necessarily ensure that the protein products perform similar functions: while the two genes may have originated from the same ancestor, they may have evolved to take on substantially different roles. To investigate what role Dll4 plays in zebrafish development, I first examined the timing and location of its expression. RT-PCR analysis on whole zebrafish embryos revealed that *dll4* begins to be expressed by 8 hpf (75% epiboly), with levels increasing through to the third day of development (Fig. 4.3A).

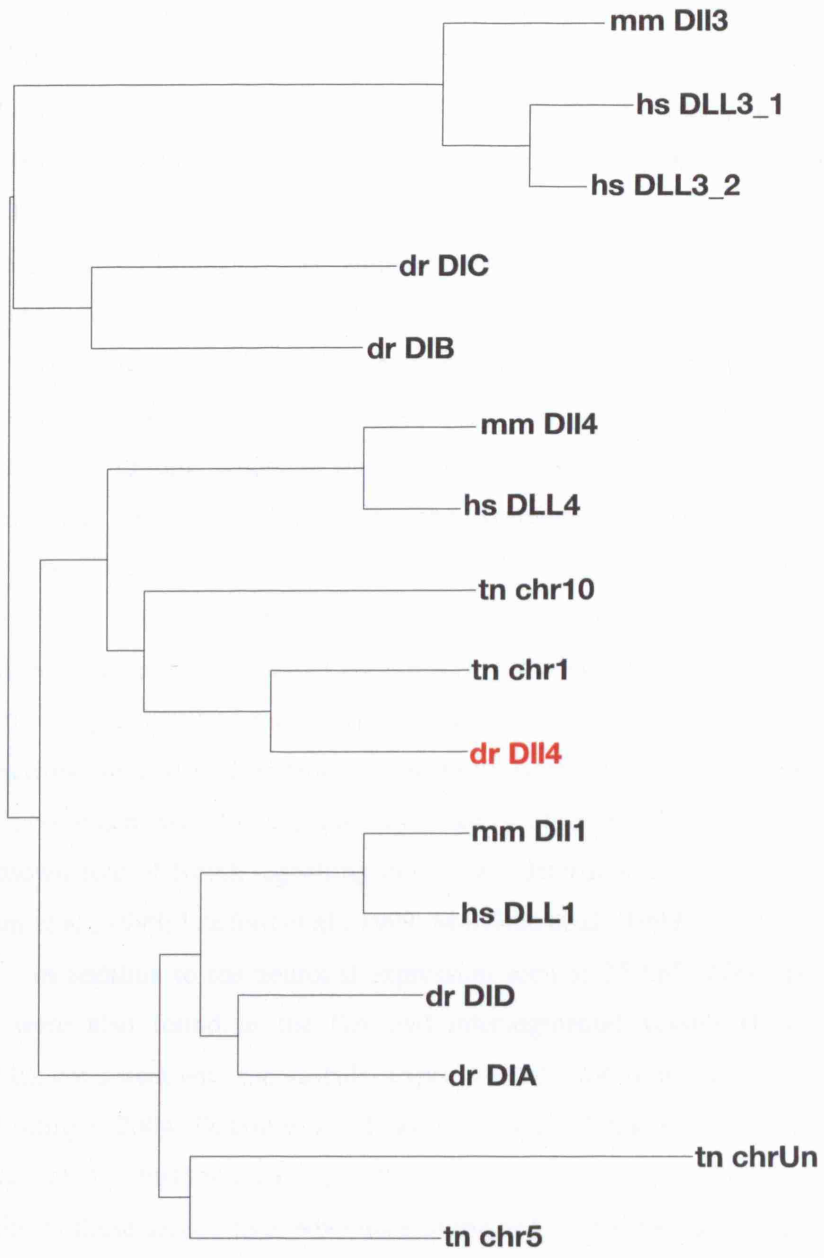


**Figure 4.2. Phylogenetic distribution of mammalian and teleost Deltas.** The amino acid sequences of the known mouse, human, zebrafish and pufferfish *Tetraodon nigroviridis* were compared. Note two predicted *Tetraodon* proteins, but only one known zebrafish protein, share a branch with the mammalian Dll4. The two human DLL3 branches correspond to the sequences of two isoforms of the gene. *Tetraodon* entries are listed according to the chromosome on which they lie. tn: *Tetraodon nigroviridis*, dr: *Danio rerio*, mm: *Mus musculus*, hs: *Homo sapiens*, chrUn: sequence on an unspecified chromosome.

In mammals, *Dll4* is expressed in the endothelial cells of developing arteries: studies in embryonic mice have shown that *Dll4* transcript can be found in the dorsal aorta (DA), umbilical artery and heart (Shutter et al., 2000; Villa et al., 2001) and that its expression is restricted to a subset of endothelial cells (Benedito and Duarte, 2005; Claxton and Fruttiger, 2004; Hellstrom et al., 2007; Krebs et al., 2000; Mailhos et al., 2001), suggesting that it may play a role in arterial branching and angiogenesis. *Dll4* expression has also been reported in the nervous system and the gut (Benedito and Duarte, 2005).

To determine which tissues express *dll4* in the zebrafish, I performed in situ hybridization on whole embryos (Fig. 4.3). *dll4* transcripts were first detectable at 13 hpf, where it was found in a select subset of cells in the ventro-lateral neural tube (Fig. 4.3B). The expression was confined to one or two pairs of cells per somite, becoming increasingly clear at 18 hpf (Fig. 4.3C). At 25 hpf, this expression pattern was still present, however it was restricted to the posterior 10 to 15 somites (Fig 4.3D,F). Additionally, a strong region of expression became clearly visible in the forebrain (data not shown). Transcripts were also detectable in the prosensory regions of the ear (Fig. 4.4A), consistent with the expression pattern of other Notch ligands and with the known role of Notch signalling in cell fate determination in the inner ear (Adam et al., 1998; Lanford et al., 1999; Morrison et al., 1999).

In addition to the neuronal expression seen at 25 hpf, *dll4*-expressing cells were also found in the DA and intersegmental vessels (ISVs; Fig. 4.3D,E), consistent with the vascular expression of *Dll4* in the mouse (Claxton and Fruttiger, 2004; Duarte et al., 2004; Gale et al., 2004; Krebs et al., 2000; Mailhos et al., 2001; Shutter et al., 2000; Villa et al., 2001). To determine the identity of these cells, I took advantage of the *fli1:EGFP* transgenic zebrafish, in which all endothelial cells are labelled with a cytosolic EGFP reporter (Lawson and Weinstein, 2002b). Combining *dll4* in situ hybridisation with EGFP immunohistochemistry revealed that the *dll4*-expressing cells were endothelial and that expression was artery-specific – no expression was detectable in the endothelium of veins (Fig. 4.3G-I).

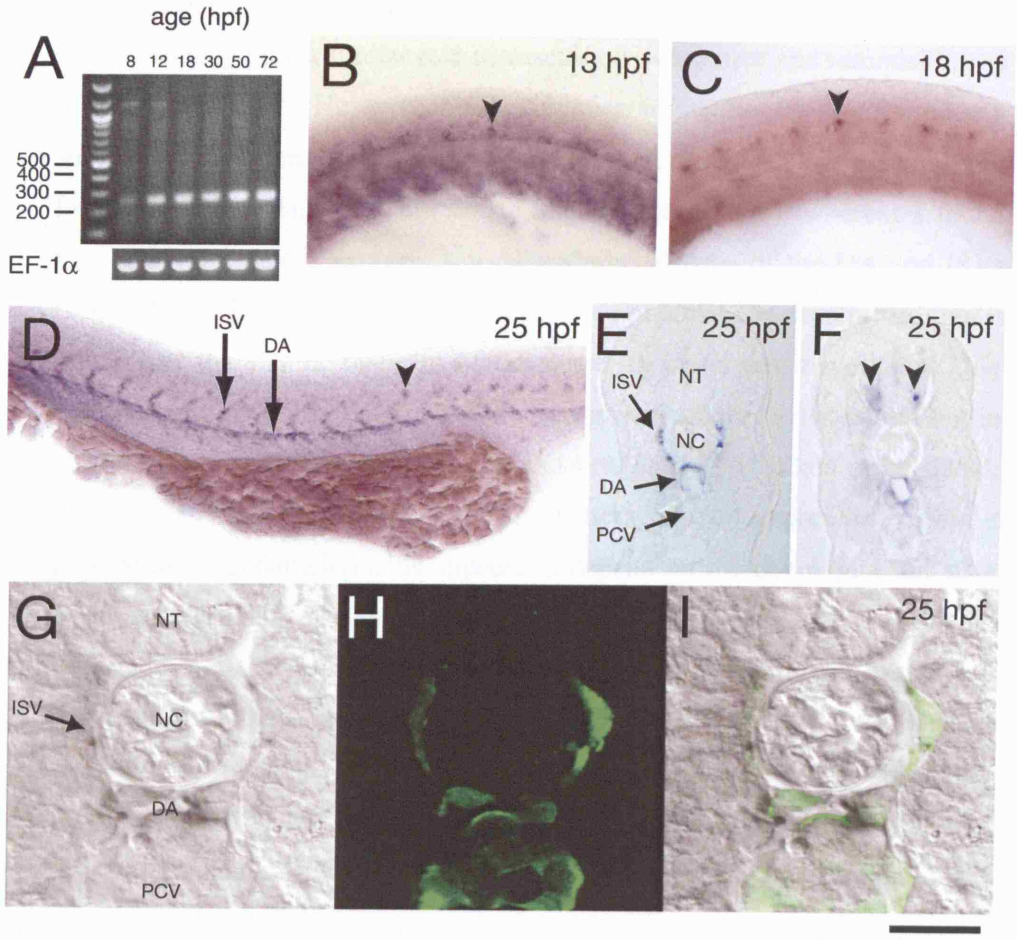


**Figure 4.3. Expression of zebrafish *dll4*.** (**A**) RT-PCR analysis of whole homogenized embryos showing weak *dll4* expression as early as 8 hpf, becoming steadily stronger thereafter. EF-1α was used as a normalization control. (**B-D**) Lateral view of mid-trunk region stained by situ hybridization for *dll4* expression at 13 hpf (B), 18 hpf (C) and 25 hpf (D). Expression is detectable in a subset of cells in the neural tube (NT) (arrowheads), however this domain becomes restricted to the posterior-most somites at 25 hpf, at which time endothelial expression in the intersegmental vessels (ISVs) and dorsal aorta (DA) is detectable (D). (**E**) Cross section of the trunk of a similar specimen showing *dll4* expression in the endothelial cells of DA and ISVs but not in those of the posterior cardinal vein (PCV). (**F**) Similar section at a slightly different level with respect to somite boundaries does not pass through any ISVs but reveals cells expressing *dll4* in the ventrolateral NT, as well as the DA. (**G-I**) The neighbourhood of the notochord (NC) in a 25 hpf *fli1:EGFP* transgenic embryos, comparing *dll4* expression (visible in the DA and ISVs by in situ hybridization; G,I) with the endothelium-specific expression of EGFP (green, visible by immunofluorescence in the DA, ISVs and PCV; H,I). Scale bar: 100 μm in B,C,E,F; 140 μm in D; 30 μm in G-I.

These findings mirror those for *Dll4* in the mouse, suggesting that Dll4 in the fish may play a similar role in vascular development and remodelling as it does in mammals. However, *Dll4* expression in the mouse is restricted to a subset of arterial endothelial cells (Benedito and Duarte, 2005; Claxton and Fruttiger, 2004; Mailhos et al., 2001; Shutter et al., 2000); whereas I found that at 25 hpf, *dll4* is expressed in *all* endothelial cells of the DA and ISVs (Fig. 4.3G-I). The reason for this discrepancy remains to be determined, but it seems that the size or maturity of the vessel is important: endothelial *Dll4* expression in mouse is found only in younger and smaller arteries and not in larger, more mature vessels (Claxton and Fruttiger, 2004; Gale et al., 2004; Mailhos et al., 2001). Additionally, the pattern of *Dll4* expression within a population of endothelial cells appears to depend on the developmental state of the vessel: in the vascular plexus of newly forming vessels, *Dll4* expression is found in all endothelial cells, but as the vessel anastomoses, expression becomes restricted to a subset of cells (Claxton and Fruttiger, 2004; Gale et al., 2004; Lobov et al., 2007; Suchting et al., 2007). In support of this are my findings that at 48 hpf *dll4* expression could only be detected in a subset of cells within the dorsal longitudinal anastomotic vessel (DLAV; see Fig. 5.12).

### 4.2.3 Notch signalling affects *dll4* expression differently in different tissues

The role of Delta-Notch signalling in tissue patterning depends critically on the way in which expression of the ligand is regulated by Notch activity (Lai, 2004; Lewis, 1998). In lateral inhibition, Notch activation inhibits Notch ligand expression, and this gives rise to a feedback loop that tends to create a mosaic pattern in which cells expressing the ligand alternate with cells that do not (Haddon et al., 1998b; Whitfield et al., 1997). In lateral induction, by contrast, Notch activation stimulates ligand expression, and the effect is to drive neighbouring cells into the same state, all expressing the ligand (de Celis and Bray, 1997; Eddison et al., 2000; Lewis, 1998; Ross and Kadesch, 2004). These different outcomes produce different patterns of cell differentiation, which is governed by the level of Notch activation in each cell.

In the zebrafish, the E3 ubiquitin ligase Mind bomb promotes the internalization of cell-surface Delta and is essential for Delta-mediated Notch activation in trans (Itoh et al., 2003). The loss-of-function mutant *mind bomb* (*mib*) is characterised by somite defects and neuronal hyperplasia, reflecting a failure in Delta-Notch signalling (Jiang et al., 1996). A consequence of this failure is an up-regulation of Notch ligands whose expression would normally be restrained by lateral inhibition (Haddon et al., 1999; Jiang et al., 1996). This is evident in the early inner ear and neural tube, where the Notch ligands *deltaA*, *deltaB*, *deltaD* and *jagged2* (formerly named *serrateB*) are expressed more intensely and in a greater number of cells in the *mib* mutant than in wild-type embryos. Similarly, the expressions of *deltaA*, *deltaB* and *deltaD* are increased in the neural plate of *mib* embryos (Haddon et al., 1998a). These findings support a lateral inhibition model in which Notch signalling delivered from a given cell represses the expression of Notch ligands in neighbouring, signal-receiving cells.

To determine how *dll4* is regulated, I examined its expression in $mib^{-/-}$ embryos and phenotypically wild-type sibling controls at 25 hpf. In the ear, *dll4* expression expanded from a few cells in the presumptive prosensory patches to include nearly all of the cells in the sensory patches (Fig. 4.4A,B). This observation is reminiscent of the expanded expression domains of *deltaA*, *deltaB*, *deltaD* and *jagged2* found in $mib^{-/-}$ embryos (Haddon et al., 1998a). In the trunk neural tube, *dll4* expression also increased in both intensity and cell number such that ectopic *dll4*-positive cells could be found at all medial to lateral positions in the ventral neural tube (Fig. 4.4C,D). These data imply that in the ear and neural tube, *dll4* expression is mediated by lateral inhibition.

In contrast to the increased neural *dll4* expression, vascular *dll4* expression was lost in $mib^{-/-}$ embryos (Fig. 4.4C,D). This observation is reminiscent of studies by Lawson and colleagues, who have shown that, within the endothelium, Notch signalling is responsible for establishing arterial identity and repressing venous character (Lawson et al., 2001; Lawson et al., 2002). The authors show that *mib* mutants have a deficit of artery-specific genes, including *notch3*, and ectopic expression of venous markers in the endothelium of arteries. Thus, *dll4* expression may be lost in *mib* simply

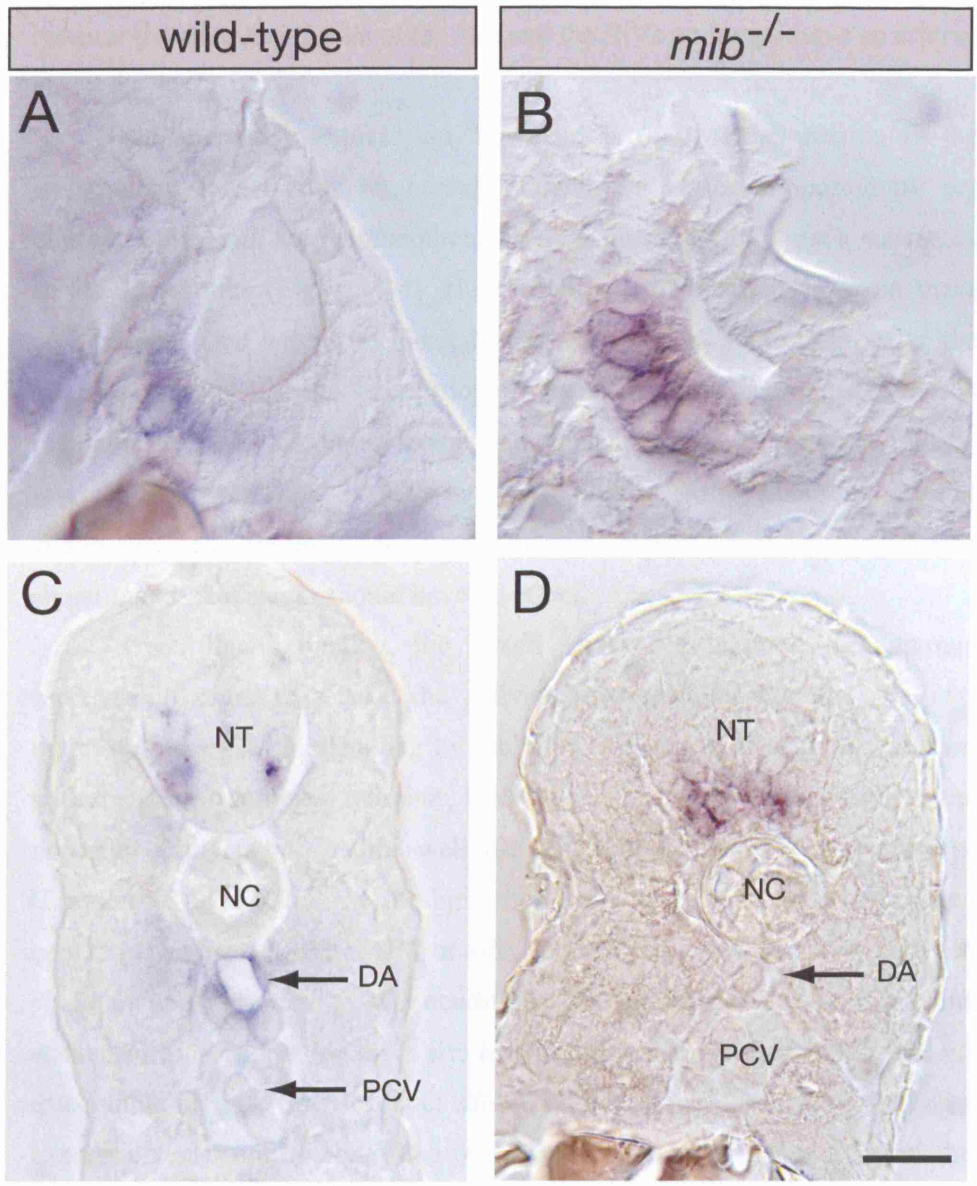


**Figure 4.4. *dll4* expression in wild-type and *mib*$^{-/-}$ mutant embryos.** (**A,B**) Section through the ear of 25 hpf wild-type (A) and mutant (B) embryos. Note the increased number of cells expressing *dll4* in the mutant (B). (**C,D**) Section through the mid-trunk of wild-type (C) and mutant (D) 25 hpf embryos. Note the *dll4* expression domain in (D) is expanded in the NT to include cells in the midline, but expression is absent from the DA. Image in (C) is identical to that in Figure 4.3F. Scale bar: 25 μm in A,B; 55 μm in C,D.

because the endothelial cells of the DA and the ISVs no longer have an arterial character.

An alternative explanation, however, is that *dll4* expression in the endothelium is regulated by lateral induction, a notion supported by my observation that *all* arterial endothelial cells express *dll4*, not just a subset, as in the neural tube (Fig. 4.3G-I). How might we differentiate between these possibilities? One way is to block Notch signalling at some point after the arterial endothelial cells have adopted their arterial character. If *dll4* is regulated by Notch-mediated lateral induction, then its expression should be lost. If, however, *dll4* is lost in *mib* embryos simply because arterial endothelial cells are unable to express arterial markers, then blocking Notch signalling at later stages should have no effect.

Upon ligand binding, the Notch receptor is cleaved by gamma-secretase in order to release the activated, intracellular domain. We can therefore block Notch signalling by inhibiting the action of gamma-secretase with the pharmacological inhibitor, DAPT. Embryos were allowed to develop normally until 30 hpf, a time well-after the expression of arterial markers (Lawson et al., 2001). At 30 hpf, they were placed in aquarium water containing either 100μM DAPT or vehicle (DMSO) alone and incubated for six hours under standard growth conditions. The embryos were then fixed and stained for *dll4* expression by in situ hybridisation. I found that DAPT had no discernable effect on the levels of *dll4* (data not shown), indicating that *dll4* expression may not be controlled by lateral induction. I cannot rule out the possibility that longer or earlier exposure to DAPT might have had a more dramatic effect. Six hours might be enough time for existing *dll4* mRNA to be degraded, but without knowing the lifetime of the transcript it is impossible to know. Consequently, it's possible that the *dll4* that was detected had simply been produced at earlier times, and that the DAPT did succeed in blocking production of nascent mRNA.

## 4.3 Discussion

I have described the identification of a novel zebrafish gene encoding a putative Notch ligand, Dll4. Like *Dll4* in the mouse, the zebrafish gene is expressed in arterial, but not venous endothelial cells as well as in a select subset of cells in the neural tube, ear and forebrain. Phylogenetic evidence and data from the zebrafish genome sequencing project indicate that *dll4* is the only known zebrafish *delta* orthologous to the mammalian gene, and the time and location of its expression suggest that it might have a similar role in embryonic development.

Studies in mouse have shown that the Notch pathway, and Dll4 in particular, are essential for proper vascular development (Carlson et al., 2005; Krebs et al., 2000; Leong et al., 2002; Uyttendaele et al., 2001; Xue et al., 1999): mice lacking one copy of the gene display severe vascular malformations and die before birth (Duarte et al., 2004; Gale et al., 2004; Krebs et al., 2004). But precisely how Dll4 exerts its effect in the vasculature has, until very recently, remained a mystery.

The zebrafish provides a powerful model system that could allow us to answer this question. The rapid development, ease of manipulation and optical transparency of the fish embryo enables us to observe its development over time. Additionally, zebrafish obtain oxygen through passive diffusion from the surrounding water for the first two weeks of life (Jacob et al., 2002), thereby enabling the embryo to survive for this time despite impaired circulation. In contrast, mouse embryos suffering from vascular malformations die from tissue hypoxia and starvation (Duarte et al., 2004; Gale et al., 2004; Krebs et al., 2004). Moreover, the *fli1:EGFP* transgenic (Lawson and Weinstein, 2002b), in which all endothelial cells are labelled with EGFP, provides us with a unique opportunity to observe the development of the vascular network and the behaviour of individual endothelial cells in the living embryo.

Angiogenesis has become an increasingly popular research topic in the last decade, with interest driven by both basic scientific curiosity as well as hopes of discovering potential therapeutic avenues in the fight against cancer. In this elegant process, the cells that make up the plumbing of the vertebrate

embryo are able to grow, divide, migrate, retract and self-assemble into tubes to form vascular circuits. This largely occurs in response to the oxygen requirements of the surrounding tissues, which via VEGF signalling trigger an angiogenic response in nearby endothelial cells. But a VEGF gradient alone cannot account for the precision required for efficient formation of a vascular network; in order for angiogenesis to occur properly, nearby endothelial cells must coordinate their behaviour with one another. For example, only a subset of endothelial cells is permitted to respond to VEGF while other, neighbouring cells are somehow maintained in an unresponsive state. How is this difference in responsiveness established from a group of seemingly equivalent cells? Signalling between cells must play an integral role.

Understanding the mechanisms underlying angiogenesis is currently one of the more active areas of research in the fight against cancer. Indeed, if we can understand how angiogenesis is controlled, then we may be able to block the neovascularisation of tumours and, thereby, inhibit their growth. For this reason, the Notch pathway has received a great deal of attention in recent years. It has been shown that tumour cells expressing Notch ligands are able to activate Notch receptors on endothelial cells (Zeng et al., 2005), yet our understanding of the pathway's role in tumour angiogenesis is clouded by seemingly contradictory findings (reviewed in (Rehman and Wang, 2006)). While some studies have shown that Notch activation promotes angiogenesis (Mailhos et al., 2001; Paris et al., 2005; Patel et al., 2005; Zeng et al., 2005), others have shown the opposite (Leong et al., 2002; MacKenzie et al., 2004; Noseda et al., 2004; Sainson et al., 2005; Taylor et al., 2002; Williams et al., 2006; Zimrin et al., 1996). It is important to note, however, that many of these studies were performed in culture; it would seem, therefore, that in vivo experimentation is required to properly understand the way in which the Notch signalling pathway affects endothelial cell behaviour. If Dll4 does, in fact, perform similar functions in the zebrafish as in the mouse, the zebrafish would be an ideal system in which to accomplish this. My functional studies of the role of Dll4 in angiogenesis are presented in Chapter 5.

# Chapter 5: Endothelial signalling by Delta-like 4 restricts angiogenesis

## 5.1 Introduction

Throughout development and in adult life, blood vessels undergo periods of growth, in which new vessels are formed in response to local oxygen requirements, and periods of quiescence, when vessels remain static as blood circulates through them. During times of growth, the normally quiescent endothelial cells that line a vessel switch their behaviour and begin to grow, divide, and migrate, thereby pioneering new sprouts from existing vessel walls. This change in behaviour does not happen in all the endothelial cells: only a select subset of cells, termed "tip" cells, are permitted to launch new sprouts while the others remain behind, maintaining the integrity of the parent vessel. As these exploratory cells invade the neighbouring tissue, other endothelial cells, the "stalk" cells, follow in their path to eventually form the walls of the new vessel. When two sprouts meet and, thus, complete a vascular circuit, the cells must stop migrating and form a vessel with a lumen. To create a vascular bed with the correct density of vessels, the behaviour of individual endothelial cells must be strictly controlled. How, then, is this control exerted, and what is the mechanism responsible for specifying a subset of cells as migratory from a seemingly equivalent population of quiescent cells?

The VEGF signalling pathway clearly plays a major role (reviewed in (Coultas et al., 2005)). Under hypoxic conditions, cells secrete VEGF, which in turn, stimulates proliferation and migration in nearby endothelial cells, and the cells get directional information from the direction of the VEGF gradient (Gerhardt et al., 2003; Ruhrberg et al., 2002). Thus, we can think of VEGF as the means by which hypoxic tissues tell endothelial cells when and where an oxygen demand exists. But Vegf is only one of many signals exchanged between endothelial cells and their surroundings, and between one endothelial cell and another. Other pathways that have also been implicated in the control

of angiogenesis, including the Angiopoietin/Tie2 receptor pathway, the platelet-derived growth factor (PDGF) pathway, the ephrin/Eph pathway, the transforming growth factor-β (TGF-β) pathway, and the fibroblast growth factor (FGF) pathway (reviewed in (Betsholtz et al., 2005; Coultas et al., 2005; Lebrin et al., 2005; Thurston, 2003)). Moreover, recent evidence indicates that many of the signalling molecules classically associated with axonal pathfinding also play a role in directing endothelial cell migration, such as the Roundabout4 (Robo4) (Bedell et al., 2005), UNC5b (Lu et al., 2004) and semaphorin and plexinD1 (Torres-Vazquez et al., 2004).

In recent years, the Notch signalling pathway has joined the list of important players in angiogenesis. Severe defects in vascular remodelling occur in *Notch1* mutant or *Notch1/Notch4* double mutant mouse embryos (Krebs et al., 2000). Overactivation of Notch4 in mice results in vascular patterning defects (Uyttendaele et al., 2001) and arteriovenous malformations (Carlson et al., 2005), and activated Notch4 has been shown to inhibit angiogenesis in cultured endothelial cells (Leong et al., 2002; MacKenzie et al., 2004). Downstream of the Notch receptor, loss of Hey2 causes lethal circulatory defects shortly after birth, and *Hey1/ Hey2* double mutant embryos die around E9.5 from vascular haemorrhage and failed vascular remodelling (Fischer et al., 2004; Kokubo et al., 2005). Additionally the Notch ligand Jagged1 has been shown to be essential for proper vascular development: embryos homozygous for a null mutation die early (E11.5) and exhibit severe defects in vascular remodelling (Xue et al., 1999).

Recently the Notch ligand Dll4 has become a focus of attention for vascular biologists. *Dll4* expression is seen in developing arteries (Shutter et al., 2000; Villa et al., 2001), where it is restricted to a subset of endothelial cells (Claxton and Fruttiger, 2004; Hellstrom et al., 2007; Krebs et al., 2000; Mailhos et al., 2001), suggesting a possible role in arterial branching and angiogenesis. Mice homozygous for a knockout mutation of *Dll4* die early, around E10, and even heterozygotes show severe vascular defects (Duarte et al., 2004; Gale et al., 2004; Krebs et al., 2004), yet the precise way in which these defects arise has been unclear. The gaps in our understanding have been largely due to the fact that live cell imaging in the mouse is very difficult. In contrast, the zebrafish provides excellent opportunities to directly observe

development in the living embryo. Moreover, the endothelial-specific reporter transgenic zebrafish line generated by Brant Weinstein and colleagues (Lawson and Weinstein, 2002b) makes it possible to observe all the fine detail of the vasculature as it develops in the living embryo. The discovery of *dll4* in the zebrafish, therefore, puts us in a strong position to analyze Dll4 function and the effects that loss of Dll4 may have in vascular remodelling.

As shown in Chapter 4, there is good reason to think that Dll4 might have a similar role in the fish as it does in mammals. I have found that zebrafish embryos lacking Dll4 exhibit vascular patterning defects reminiscent of those found in mice lacking Dll4. Using time-lapse confocal microscopy, I have developed a method to observe the behaviour of individual endothelial cells in the living embryo. Endothelial cells in embryos lacking Dll4 fail to cease their angiogenic behaviour at the appropriate times and places, resulting in excessive numbers of cells and continued cell motility which, in turn, results in the formation of ectopic vascular sprouts. Blocking Notch signalling with the gamma-secretase inhibitor DAPT has the same effect, while overactivation of the Notch pathway has opposite consequences. Blocking production of Notch1b, but not the other Notches, produces a similar phenotype, indicating that at least in this context, Dll4 signals through this receptor. The observed ectopic sprouting occurs in response to Vegf: inhibiting Vegf receptor function prevents the excessive endothelial sprouting. Thus, Dll4-Notch signalling functions as an angiogenic "off" switch, making endothelial cells deaf to VEGF gradients. Thus, in the presence of VEGF, endothelial cells communicate with one another, via Dll4-Notch signalling, to determine which cells respond to VEGF to produce an angiogenic sprout, and which cells do not. In this way, the VEGF signalling pathway gives endothelial cells information about oxygen demands in nearby tissues, while Dll4-Notch signalling enables cells to communicate with one another, thereby allowing them to coordinate their behaviour with their neighbours.

My findings have recently been published (Leslie et al., 2007), as have several other studies with similar conclusions: one examined the role of Dll4-Notch signalling in specifying tip cells in the zebrafish (Siekmann and Lawson, 2007), three investigated the role of Dll4-Notch signalling in angiogenesis in the mouse retina (Hellstrom et al., 2007; Lobov et al., 2007;

Suchting et al., 2007) and three disease model papers showed that Dll4-Notch signalling restricts angiogenesis and can be exploited for use in blocking tumour angiogenesis (Noguera-Troise et al., 2006; Ridgway et al., 2006; Scehnet et al., 2007). (For a review of these papers, see (Gridley, 2007)). Clearly, the role of Dll4-Notch signalling in angiogenesis is a very popular topic at the moment, largely because an understanding of how it controls endothelial cell behaviour opens many exciting possibilities for anti-angiogenic therapies for the treatment of solid-tumour cancers and other types of intervention in diseases involving the vasculature.

# 5.2 Results

## 5.2.1 A splice-blocking morpholino can be used to knock down Dll4 in vivo

No method has yet been found for targeted gene knock-out in the zebrafish, but two other techniques are available to study the effects of loss of a given gene function: one can screen for mutants, for example, by "tilling" (Sood et al., 2006; Wienholds et al., 2003), or one can target mRNA for knock-down using morpholino antisense oligonucleotides (Nasevicius and Ekker, 2000). I began my analysis of Dll4 function using the latter approach.

While some morpholino sequences work well and can knock down their targets to levels below the threshold of detection, others are only partially effective, completely ineffective, or can produce non-specific side effects, presumably due to cross-reactivity or chemical toxicity (see Chapter 3 and Appendix Fig. 5A-E) (Wright et al., 2004). When using morpholinos, therefore, it is critical to (1) assess their efficacy and (2) confirm that any observed effect is specific.

To block Dll4 function I designed three morpholinos: one targeted to the start codon to block translation (JLMO2), and two targeted to exon/intron boundaries (JLMO5 for the exon 3/intron 3 boundary and MO[Dll4] for the exon 6/intron 6 boundary) designed to produce mis-splicing of the primary transcript resulting in frame-shift mutations and protein loss-of-function. With

the translational-blocking morpholino, I had no reliable method to determine if levels of Dll4 protein were reduced in the embryo. However, the efficiency of the splice-blocking morpholinos could be determined by performing RT-PCR across the region intended for splice modification (Fig. 5.1), as I have shown with MO[Dll4] in Chapter 3 and the Appendix. For JLMO5, the morpholino was designed to anneal to a 25 bp sequence that includes the exon 3/intron 3 junction (FIg. 5.1A); if it is successful, splicing at this site will be prevented. One possible outcome is that the splicing machinery will use the next upstream splice donor site (at the exon 2/intron 2 boundary) to remove the entire region containing intron 2, exon 3 and intron 3 (Fig. 5.1B). Using primers located in exons 2 and 4, I can amplify a region spanning the potentially modified area. In this case, the normal transcript yields a PCR product 260 bp in length. If splicing has been modified as we predict, the PCR product will lack exon 3 and, therefore, be 50 bp shorter (Fig. 5.1B).

Using this method I found that JLMO5 partially reduced the levels of the normal transcript in a dose-dependent manner, however even a high dose (20 ng/embryo) was unable to completely abrogate normal Dll4 production (Fig. 5.1B). In contrast, 10 ng of MO[Dll4] was able to eliminate the normal transcript to levels below the threshold of detection. Therefore, I used MO[Dll4] for nearly all subsequent experiments (Fig. 5.1C).

### 5.2.2 Dll4 is not required to regulate arterial versus venous identity

On the macroscopic level, arteries and veins differ in many ways, such as in the direction and rate of the circulation they carry, in the haemodynamic pressure found within, in the amount of smooth muscle that surrounds the vessels and in the presence of specialized structures, such as valves (Gray, 1901). On the molecular level, a growing body of evidence indicates that the character of the endothelial cells that line these vessels is also different, and that this molecular identity is established early in the development of the vessel before the onset of circulation (Adams et al., 1999; Lawson et al., 2001; Lawson et al., 2002; Moyon et al., 2001; Wang et al., 1998). Studies in the

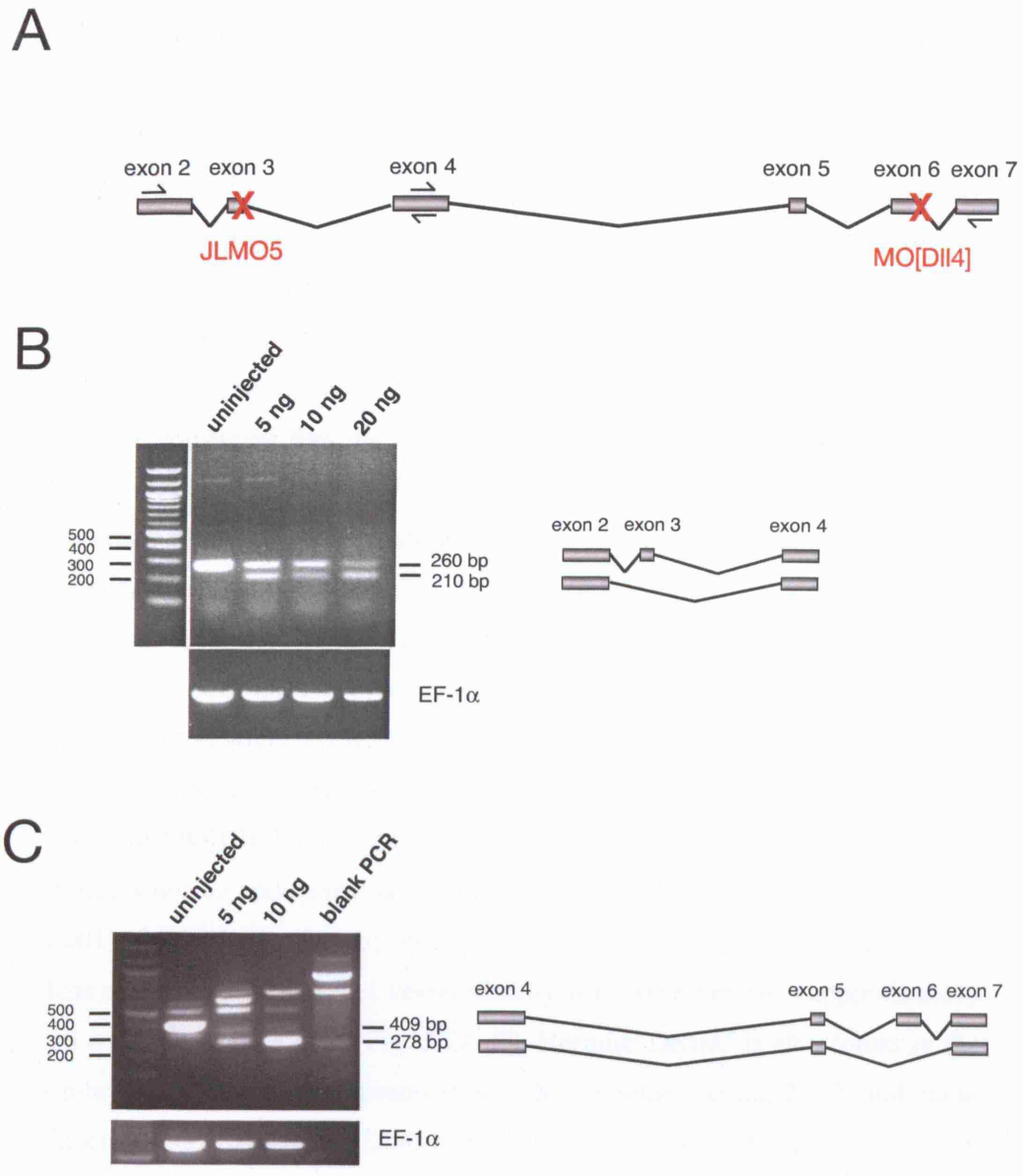


**Figure 5.1. Morpholino knock-down of zebrafish Dll4.** (**A**) Exon/intron structure of the *dll4* gene in the region targeted for morpholino knock-down. Approximate locations of PCR primers used in (B) and (C) are denoted with small arrow. (**B**,**C**) RT-PCR analysis of *dll4* splicing in 30 hpf embryos injected with JLMO5 (B) or MO[Dll4] (C) and schematics of the regions amplified and the predicted splice variants. EF-1α was used as a normalization control.

mouse and zebrafish have shown that the Notch signalling pathway functions in the control of this identity (Duarte et al., 2004; Krebs et al., 2004; Lawson et al., 2001; Lawson and Weinstein, 2002a) and lies downstream of the Sonic hedgehog (Shh) and Vegf signalling pathways (Lawson et al., 2002). Specifically, Notch signalling drives endothelial cells towards an arterial cell fate: blockade of the Notch pathway results in the loss of arterial marker expression and the ectopic expression of venous markers in arteries (Krebs et al., 2004; Lawson et al., 2001). Moreover, Antonio Duarte and colleagues have demonstrated that the arteries of *Dll4* mutant mice fail to express the artery-specific markers *EphrinB2* and *Connexin37* and ectopically express the venous marker *EphB4*, suggesting that these mice are unable to specify arterial identity in their endothelium (Duarte et al., 2004).

In the zebrafish, the receptor *notch3* is found in arteries but not veins (Lawson et al., 2001). Given that zebrafish *dll4* expression is also found specifically in arteries (Fig. 4.3), the question arises whether Dll4 could signal via Notch3 to drive arterial cell fate. To address this, I injected embryos with 10 ng of MO[Dll4] and examined at 25 hpf for the expression of the arterial markers *notch3* and *ephrinB2a* and the venous marker *ephB4a* (Lawson et al., 2001). Surprisingly, the expression of all three genes was unaffected by the loss of Dll4, indicating that vessel identity was preserved (n = approximately 10 embryos in each case; Fig. 5.2A-D). Because DeltaC is also found in the embryonic vasculature (Lawson et al., 2001; Smithers et al., 2000) and could function redundantly with Dll4, I repeated the Dll4 knock-down experiment in $dlc^{bea/bea}$ mutants, in which DeltaC is defective. Again, I found no effect on vessel identity (n = approximately 10 embryos in each case; Fig. 5.2E-F). These data suggest that some Notch ligand other than Dll4 is responsible for the control of vessel identity, although it is possible that the morpholino's effect was incomplete and allowed some residual, undetectable level of Dll4, which was sufficient to maintain arterial identity. Yet these findings suggest that in the zebrafish, expression of *dll4* is a consequence, not a cause, of the adoption of an arterial character. This may explain why *dll4* expression is undetectable in the vasculature of *mib* mutant embryos, in which arterial character is lost in the endothelial cells of the DA and ISVs (see Chapter 4, Section 2.3) (Lawson et al., 2001).

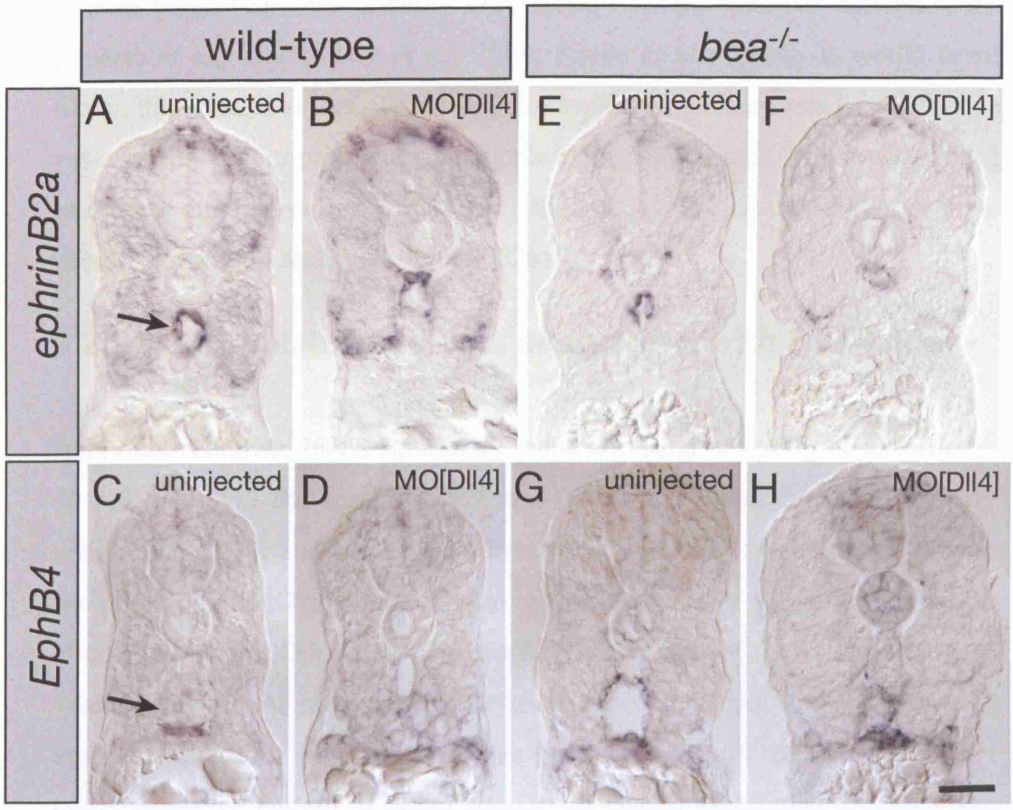


**Figure 5.2. Endothelial cells in embryos lacking Dll4 maintain their correct arterial-venous identity.** (**A-D**) 25 hpf wild-type embryos were uninjected (A,C) or injected with 10 ng MO[Dll4] (B,D) and stained by in situ hybridization for *ephrinB2a* to mark arterial endothelial cells (A,B) or *EphB4* to mark venous endothelial cells (C,D), for example in the dorsal aorta (arrow in A) or the posterior cardinal vein (arrow in C), respectively. Note that the pattern of expression of both markers is unchanged. (**E-H**) 25 hpf *bea*$^{-/-}$ embryos were uninjected (E,G) or injected with 10 ng MO[Dll4] (F,H) and stained by in situ hybridization for *ephrinB2a* (E,F) or *EphB4* (G,H) as in (A-D). Again, the pattern of expression is unaffected. Scale bar: 60 μm.

## 5.2.3 Loss of Dll4 causes circulatory defects and vascular patterning abnormalities

I have shown that zebrafish *dll4*, like *Dll4* in the mouse, is expressed in arteries (Fig. 4.3). Mice lacking Dll4 exhibit severe vascular abnormalities (Duarte et al., 2004; Gale et al., 2004; Krebs et al., 2004). It would seem likely, therefore, that loss of Dll4 in the zebrafish might also result in defective vascular function or patterning. Using morpholinos to block Dll4 production, I examined circulation and vessel formation using the *fli1:EGFP* transgenic zebrafish (Lawson and Weinstein, 2002b).

### 5.2.3.1 Circulatory defects associated with Dll4 knock-down

In normal zebrafish, blood flow in the trunk and head is readily observable by 30 hpf, and by 3 dpf the DA, PCV and ISVs carry circulation that is easily visible (Fig. 5.3A and Movie 5.1). Treatment with the translational blocking morpholino (JLMO2; 5 ng/embryo) produced only a slight reduction in circulation in the DA, ISVs and the ISVs: the rate of flow through these vessels was almost identical to that in uninjected control embryos (n = 22 embryos). Because this injection was performed on *fli1:EGFP* embryos, I could assess the pattern of blood vessels: all vessels developed normally and showed no signs of aberrant patterning through the third day of development. Similarly, 5 ng, 10 ng and 20 ng of JLMO5 (which targets the exon 3/intron 3 boundary with incomplete efficiency) also caused a reduction in circulation but no apparent defects in the pattern of blood vessel formation (for example, n = 26 embryos for 5 ng treatment). When 5 ng each of both morpholinos (JLMO2 and JLMO5) were injected together, the effect was the same as when each was injected alone. It is possible that the decreased circulation may indeed have been a consequence of reduced Dll4 levels, but it is also possible that it merely reflects a non-specific effect, i.e. a "sick fish". Indeed, oedema and reduced vascular functions are often associated with morpholino toxicity.

*deltaC* is also expressed in the vasculature (Lawson et al., 2001; Smithers et al., 2000), and $dlc^{bea/bea}$ mutants exhibit aberrant vascular

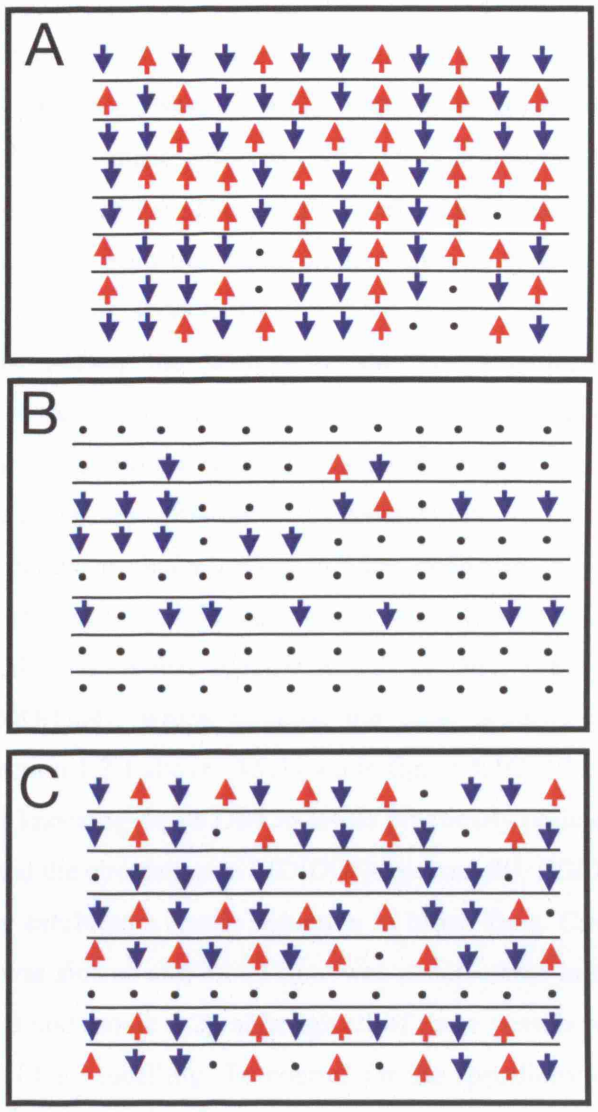


**Figure 5.3. Effects of Dll4 knock-down on trunk circulation.** Blood flow in intersegmental vessels (ISVs) of 3 dpf uninjected control sibling embryos (A) or embryos injected with 10 ng of MO[Dll4] (B) or a 5 bp mismatch control morpholino (C). Each horizontal row represents a set of ISVs on one side of one embryo, scored for direction of blood flow: upward arrows (red) denote flow from ventral to dorsal; downward arrows (blue) denote flow from dorsal to ventral; dots represent vessels carrying no flow.

patterning, presumably due to mis-formed somites (Shaw et al., 2006). It is plausible, therefore, that DeltaC and Dll4 may act redundantly and that a more severe phenotype may only become apparent when both molecules are removed. To test this, I injected each morpholino into *dlc*$^{bea/bea}$ mutant embryos. The pattern of blood vessels in these embryos was identical to uninjected *dlc*$^{bea/bea}$ mutant embryos, with ISVs following the boundaries between mis-formed somites. These embryos also had reduced circulation that was indistinguishable from the reduction seen in wild-type embryos injected with either JLMO2 or JLMO5 (n = 15 for JLMO2, n not available for JLMO5). Thus, neither the severity of the vessel patterning phenotype (characteristic of the *deltaC* mutation) nor the reduction in blood flow (as seen in wild-type embryos injected with either JLMO2 or JLMO5) was amplified, suggesting that DeltaC and Dll4 do not act redundantly.

In an attempt to obtain a more efficient reduction in Dll4 production and to clarify whether the subtle reduction in circulation seen in JLMO2- and JLMO5-injected embryos was specific to loss of Dll4, I designed a second morpholino, MO[Dll4], which targeted the exon 6/intron 6 junction, as explained in section 1.2.1 above. As shown in figure 5.1C, 10 ng of MO[Dll4] was capable of knocking-down Dll4 to levels practically undetectable by RT-PCR. I examined the circulation in MO[Dll4]-injected *fli1:EGFP* embryos and found that they exhibited a severe reduction in blood flow. Circulation in the DA and PCV was slowed and blood flow was undetectable in the majority of ISVs (Fig. 5.3B and movie 5.2), although all of these vessels were present as determined by EGFP labelling. To control for the specificity of the effect, I injected sibling embryos with 10 ng of a control morpholino in which five bases had been changed (see Materials and Methods for sequence): the circulation in these embryos was close to normal (Fig. 5.3C).

To quantitate this effect, I scored uninjected, MO[Dll4]-injected and control morpholino-injected embryos for reductions in blood flow through the ISVs on one side of the body. I set a threshold of two ISVs to lack circulation: any embryo lacking circulation in more than two ISVs per side was scored as positive for reduced circulation. In the uninjected sample, 0% of embryos had this defect (n = 8 embryos). In contrast, 100% of embryos injected with 10 ng of MO[Dll4] were positive (n = 16). 30% of the embryos injected with 10 ng

of the control morpholino had a positive score (n = 13). If I increased the threshold to three, however, none of the embryos injected with the control morpholino attained a positive score, whereas 100% of the MO[Dll4]-injected embryos remained positive. Figure 5.3 shows a representative data set from this experiment. It is interesting to note that in the few MO[Dll4] morphant ISVs that did carry circulation, the direction of flow was predominantly in the venous, or return, direction. For example, in Figure 5.3, all MO[Dll4]-injected embryos had one "artery" or less in the region examined. This was not the case in either the uninjected or control morpholino-injected groups, which had 0/8 and 2/8 embryos displaying this effect, respectively.

It is tempting to speculate that this might be explained by the fact that only arterial endothelial cells express *dll4*; endothelial cells derived from veins might, therefore, be immune to its loss. However, the endothelial cells that initially establish and constitute the ISVs and the dorsal longitudinal anastomotic vessel (DLAV) that connects them are all derived from the DA (Childs et al., 2002; Lawson and Weinstein, 2002b); it is only at later stages that PCV-derived endothelial cells connect into the ISVs that are already in place and therefore provide a circulatory outlet (Isogai et al., 2003). It seems unlikely, therefore, that this could account for the predominance of ventrally-directed circulation in the ISVs of MO[Dll4]-injected embryos.

#### 5.2.3.2 Embryos lacking Dll4 have ectopic endothelial sprouts and excessive numbers of endothelial cells

We have seen that embryos lacking Dll4 have a reduced circulation, and that non-specific side effects of the morpholino or the injection itself are not responsible for this effect. What, then, might be causing this defect? Because mice deficient in Dll4 show vascular patterning abnormalities, it seemed likely that the patterning of blood vessels in zebrafish lacking Dll4 might also be compromised. Yet on the gross level, the DA, PCV, ISVs and DLAV were present and seemed, at least initially, to form properly (data not shown). (It should be noted that all observations up to this point were made under low magnification using a dissecting microscope equipped with epifluorescent illumination.) To clarify this, I examined fixed specimens, allowing me to

observe the structure of the vessels and the morphology of individual endothelial cells in greater detail under higher magnification using either a conventional epifluorescent microscope or a laser scanning confocal microscope.

What I found was striking. At 2.5 dpf, the ISVs of normal embryos are continuous with the DLAV, forming well-ordered T-junctions (Childs et al., 2002; Lawson and Weinstein, 2002b) with endothelial cells clearly absent from the space between adjacent ISVs (Fig. 5.4A). In MO[Dll4]-injected embryos, the T-junctions were present, but endothelial cells were also found in the region between ISVs, creating a network of aberrant interconnected branches and sprouts (Fig. 5.4B), which became more profuse over the following few days (Fig. 5.4C,D). By increasing the brightness of the images I could detect numerous filopodia extending from the cells making up these ectopic sprouts as well as the cells of the ISVs and the DLAV; the cells making up the ISVs and the DLAV in normal embryos had very few of these projections (Fig. 5.4A',B'). This suggested that the endothelial cells in the morphant vessels were motile whereas the cells of normal embryos were relatively static. Thus, it appears that one function of Dll4 is to somehow restrict endothelial cell motility.

Although endothelial cells are very flat, they do bulge somewhat over the nucleus. Because cytosolic EGFP can cross the nuclear envelope and enter the nucleus, these bulges appear as brighter regions on the sides of vessels (confirmed as such by DAPI counterstaining). This allowed me to count the number of endothelial cells in each vessel (see arrows in Fig. 5.4A,B). I found that in addition to the presence of ectopic sprouts, the ISVs and the DLAV of morphants also contain a greater number of endothelial cells at 3 dpf, approximately a 40% increase over the vessels of uninjected siblings (Fig. 5.5). This suggests excessive proliferation of the endothelial cells in these vessels, although I cannot eliminate the possibility that the increase in cell number is the result of deficient apoptosis. Because the ISVs and the DLAV are composed of endothelial cells that emigrate from the DA, one could argue that this increase in cell number represents excessive endothelial cell migration from the DA rather than hyperproliferation. In this way, the extra cells would simply be misplaced endothelial cells that should normally have

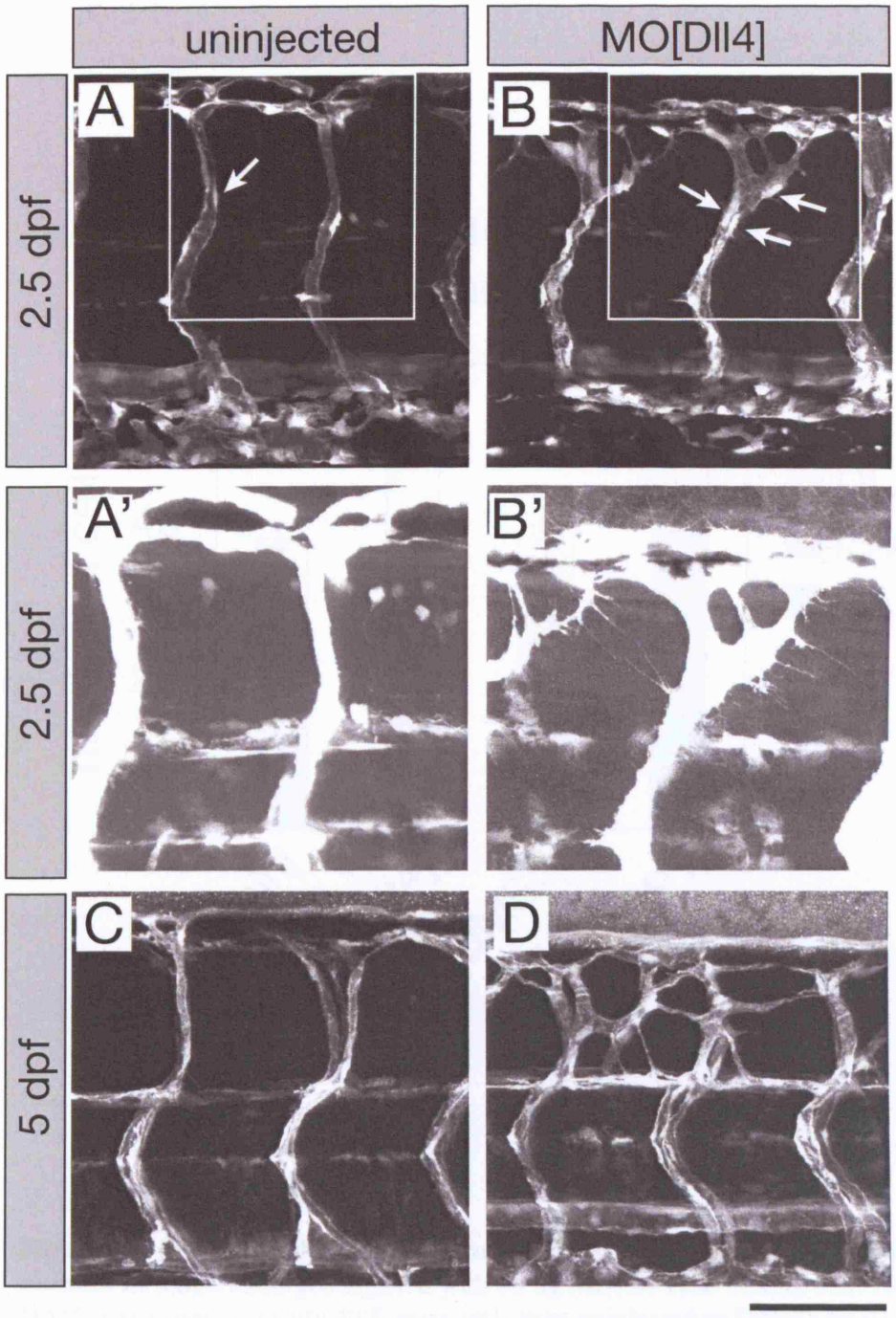


**Figure 5.4. Effects of Dll4 knock-down on vascular patterning.** *fli1:EGFP* embryos at 2.5 dpf (A,B) or 5 dpf (C,D) either uninjected (A,C) or injected with 10 ng of MO[Dll4] (B,D). (A') and (B') are details of the boxed regions of (A) and (B), respectively; the brightness has been increased in order to detect filopodia. White blobs (arrows in A,B) are endothelial cell nuclei, confirmed as such by DAPI counterstaining (not shown). Scale bar: 70 μm.

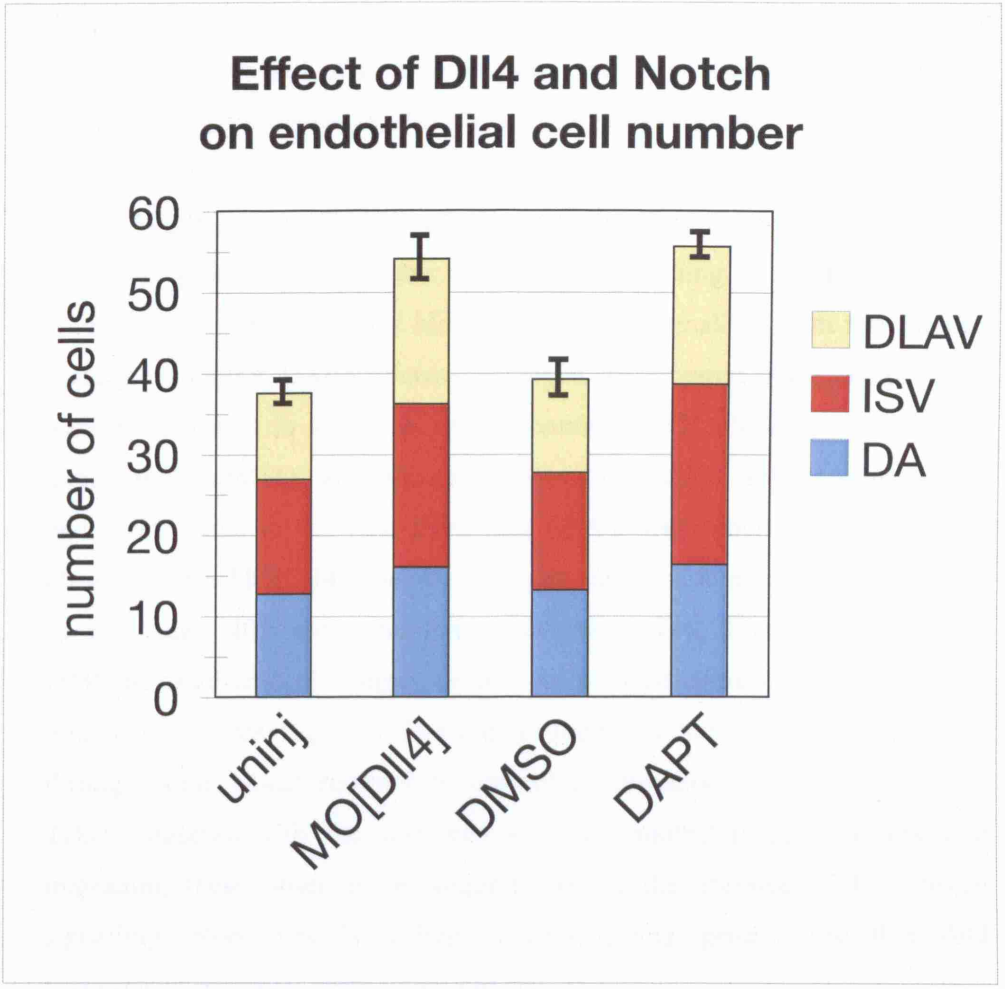


**Figure 5.5. Effects of Dll4 knock-down and Notch blockade on endothelial cell number at 3 dpf.** Embryos injected with 10 ng MO[Dll4] or treated with 100 μM DAPT have approximately 40% more cells than uninjected or DMSO-treated control siblings. (See text for experimental details.) Both effects are significant at the P=0.001 level (t-test; n≥6 specimens for each treatment; error bars represent s.e.m.). Values are: uninj = 37.6; MO[Dll4] = 54.0; DMSO = 39.2; DAPT = 55.6.

stayed behind in the DA. However, the fact that the DA also shows a 40% increase in cell number (Fig. 5.5) indicates that this is not the case and suggests that there is increased cell proliferation in all of these vessels. Given that all of the cells that make up the DLAV, ISVs and DA either express *dll4* or at least expressed *dll4* at some point (see Fig. 4.3G-I), these findings suggest that Dll4 somehow functions to negatively regulate endothelial cell proliferation.

While it seems likely that Dll4 exerts its effects by signalling through a Notch receptor, it is conceivable that it might be acting in a cell-autonomous way. To shed light on this, I blocked all Notch signalling with the gamma-secretase inhibitor DAPT. Normal embryos were reared until 33 hpf. They were then placed in aquarium water containing 100 μM DAPT or vehicle alone (0.2% DMSO) and allowed to develop until 3 dpf, at which point endothelial cells in the DA, ISVs and DLAV were counted as above. As observed with MO[Dll4]-injected embryos, embryos treated with DAPT had approximately 40% more endothelial cells in the DA, ISVs and DLAV than DMSO-treated control siblings (which were indistinguishable from normal, untreated embryos; Fig. 5.5). The strong suggestion, therefore, is that Dll4 acts through some Notch receptor to control proliferation in endothelial cells. Taken together with the observed ectopic endothelial cell motility and migration, these observations suggest that in the absence of Dll4-Notch signalling, blood vessels undergo excessive angiogenesis and that Dll4 functions to somehow restrict that process.

#### 5.2.3.3 Ectopic endothelial sprouting in embryos lacking Dll4 is not due to hypoxia or a lack of circulation

We have seen that embryos lacking Dll4 display hyperactive endothelial cell migration and proliferation, two hallmarks of angiogenesis. We have also seen that these embryos have a severe reduction in circulation. How might these two effects be related? More specifically, might one defect be caused by the other? In Dll4 morphant embryos, the vascular bed is mispatterned and potentially clogged with excessive numbers of endothelial cells, defects that could conceivably restrict blood flow. Conversely, the excessive angiogenesis

could be simply a normal physiological response to compromised circulation: if oxygen delivery to neighbouring tissues is compromised due to ineffective circulation, those tissues might become hypoxic and, consequently, produce higher levels of Vegf which would, in turn, elicit an angiogenic response in nearby vessels. In this way, this "hypoxia hypothesis" argues that the angiogenic phenotype observed could emerge merely as an indirect and not a direct result of failed Dll4-Notch signalling. Two lines of evidence argue against this scenario and, thus, indicate that the ectopic angiogenesis is indeed a direct result of failed Dll4-Notch signalling.

The first comes from studies that have shown that during the first two weeks of life, zebrafish obtain oxygen through passive diffusion from the surrounding water and not through convective oxygen transport (Jacob et al., 2002). While this argues against the hypoxia hypothesis, I felt it was important to address the issue more directly.

To do so, I blocked all trunk circulation by using a morpholino MO[cas] targeted to the *sox32* (*casanova*, *cas*) transcript, which is required for the development of a normal, beating heart (Sakaguchi et al., 2001). In normal zebrafish development, two populations of primordial cardiac cells converge near the midline to form the heart. In *cas* mutants, this does not happen properly and embryos display cardia bifida: two non-functional half-hearts (Chen et al., 1996). Thus, if the hypoxia hypothesis is correct, we should observe the same angiogenic phenotype in MO[cas]-injected embryos as we saw in Dll4 morphants. I injected 10 ng MO[cas] into *fli1:EGFP* embryos and found that, like in *cas* mutants, *cas* morphant embryos exhibit cardia bifida and a complete loss of circulation (approximately 95% of injected embryos had no circulation, n = 31). Although MO[cas]-treated embryos did show some dilations of their vessels (visible in 13% of embryos, n = 31), there was no sign of the ectopic sprouts observed in Dll4 morphants (compare Figs. 5.6 and 5.4B). I conclude, therefore, that the observed ISV branching phenotype is indeed a direct effect of Dll4 knockdown and not a secondary effect resulting from compromised circulation.

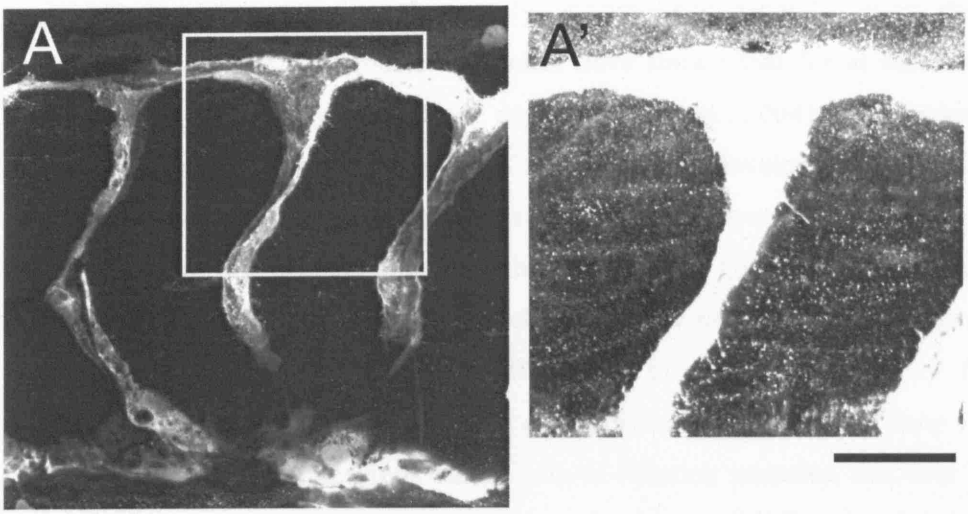


**Figure 5.6. Effects of blocking circulation on vascular patterning.** *fli1:EGFP* embryo at 2.5 dpf injected with 10 ng of a morpholino targeted against *casanova* (*sox32*) to block circulation in the trunk. (**A'**) Detail of the boxed region in A; the brightness has been increased in order to detect filopodia. Note that some of the ISVs appear to be discontinuous in their ventral regions: this is simply due to the fact that some regions of the vessels were out of the limits of the Z-series and therefore did not appear in the final projected image. Scale bar: 50 μm in A.

### 5.2.3.4 A *dll4* mutant also has a vascular phenotype

Morpholinos, when effective, provide a powerful means to knock down specific gene targets, yet significant caveats exist. As mentioned above, morpholinos can have undesirable side effects, often leaving the researcher with the difficult task of assessing subtle phenotypes over a high background of non-specific effects. Moreover, these non-specific effects often build up over time, resulting in fish that become sicker as development continues. Because morpholinos must be injected into each embryo individually, there can often be a great degree of variability in a given experiment, further complicating the analysis. Additionally, morpholinos generally exert their effect for a limited time (our own studies have shown that for at least one morpholino, this is only two or three days (Wright et al., 2004)), thus making it impossible to study the effects at later stages of development. Clearly, morpholinos have significant limitations compared to proper genetic mutants.

During the course of these studies we had the good fortune to come across a *dll4* mutant, *j16e1*, discovered by Stephen Johnson and colleagues (Washington University, St. Louis, MO, USA) in a genetic screen for fin morphology mutants. It was identified as a dominant suppressor of *long fin* (*lof*), a dominant, homozygous viable gain-of-function mutation that acts in arteries to cause fin overgrowth (Iovine and Johnson, 2000). Mapping and positional cloning revealed a glycine to serine (G270S) substitution at a conserved site in an EGF-like domain of the zebrafish *dll4* gene on LG20 (Stephen Johnson, personal communication; Fig. 5.7A); homozygous mutant embryos survive for up to two weeks.

On chromosome 20, *dll4* is located approximately 10 cM distal to the *c-kit* gene, which is defective in the mutant *sparse* (*spa*). *spa* homozygous mutants have a clearly visible defect in melanocyte migration and survival (Parichy et al., 1999). To facilitate the identification of *dll4* homozygous mutants, we carried the *j16e1* allele on a chromosome that also contained *spa*, thus, allowing us to identify *dll4* homozygous mutants by examining embryos for defects in pigmentation pattern (Stephen Johnson, personal communication). To determine if *dll4* mutants have a similar phenotype to Dll4 morphants, we crossed *j16e1* heterozygotes to *fli1:EGFP* transgenics and

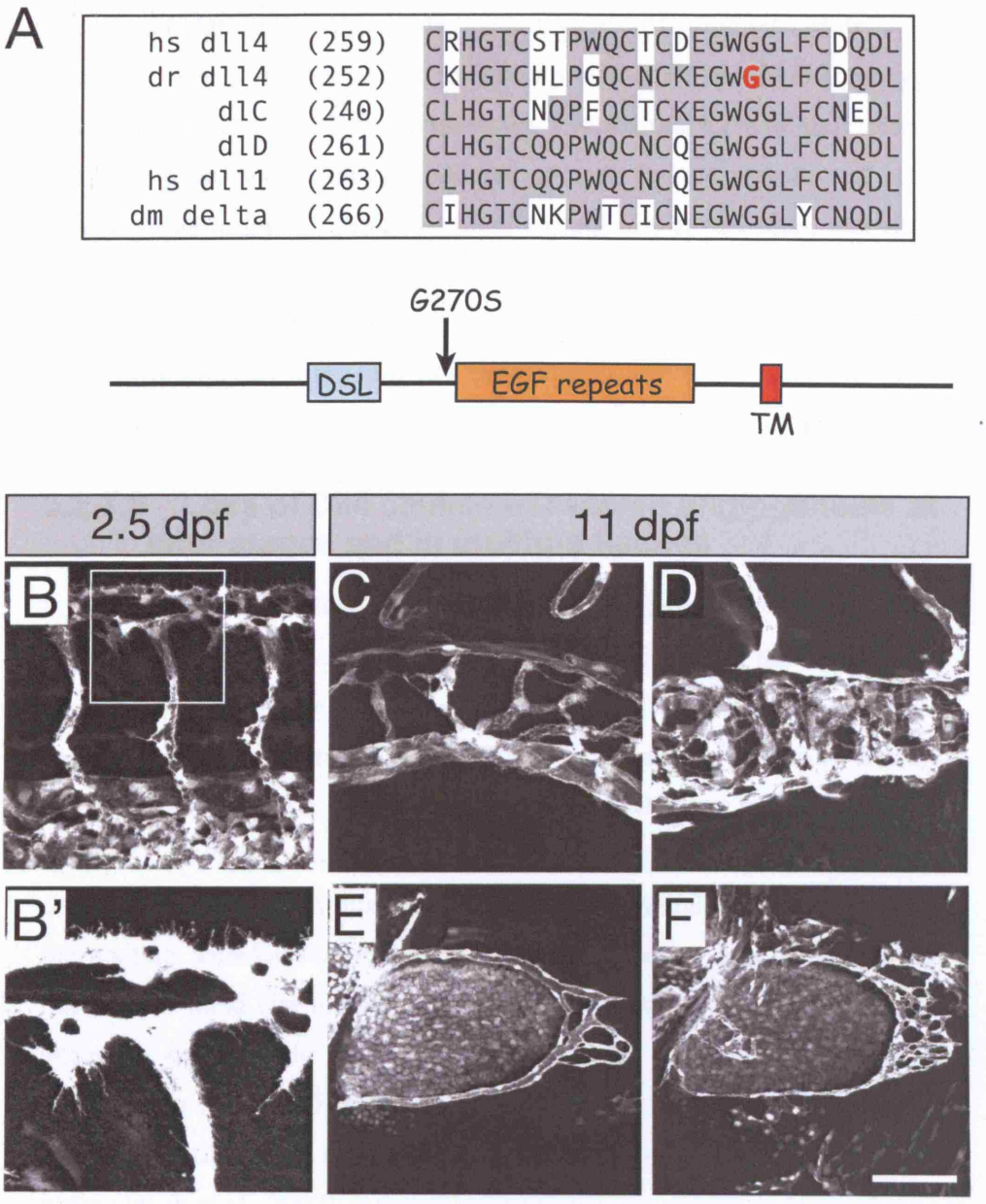


**Figure 5.7. Vascular patterning in the *dll4* mutant *j16e1*.** (**A**) Amino acid alignment of human DLL4, zebrafish Dll4, zebrafish DeltaC, zebrafish DeltaD, human DLL1 and *drosophila* Delta. The zebrafish *dll4* mutant *j16e1* has a glycine-to-serine substitution in its extracellular domain at residue 270, a highly-conserved amino acid. (**B**) ISVs and DLAV of 2.5 dpf homozygous mutant embryos carrying the *fli1:EGFP* transgene. (**B'**) Detail of the boxed region in (A); the brightness has been increased in order to visualize filopodia. Note the presence of ectopic vascular sprouts and numerous filopodia. (**C-F**) Vasculature in the region of the gut (C,D) or pectoral fin (E,F) of 11 dpf homozygous *j16e1* (D,F) or phenotypically wild-type sibling (C,E) larvae carrying the *fli1:EGFP* transgene. Note the increased vascular density in the mutant (D,F). Sale bar: 50 μm in B, 40 μm in C-F.

identified *fli1:EGFP*-positive *j16e1* heterozygote offspring (see Materials and Methods). These were then intercrossed to produce GFP-positive homozygous mutant progeny at Mendelian frequencies. I found that 83% of *spa*$^{-/-}$ embryos exhibited a vascular phenotype (scored as such by the presence of ectopic sprouts in more than 2 somites) similar to, but less severe than, that seen in Dll4 morphants (n = 6; Fig. 5.7B), further confirming our Dll4 knockdown results. The fact that the mutant phenotype is less severe than that of the morphants suggests that *j16e1* is a hypomorph and not a complete loss-of-function allele.

#### 5.2.3.5 Loss of Dll4 causes excessive angiogenesis at later stages and in multiple tissues

I have shown that when Dll4 is removed or defective, or when Notch signalling is blocked, we see excessive angiogenesis during the first few days of development in the ISVs and the DLAV. The strong implication is, therefore, that in endothelial cells, Dll4-Notch signalling somehow functions to restrict angiogenesis. Is this a general role of Dll4, or might it simply be specific for only this one particular region at this specific time of development? Although this would be difficult or impossible to address with morpholino knockdown, the *dll4* mutant provides a tool to answer this question. I found that mid-larval (11 dpf) *dll4* mutants also showed signs of excessive angiogenesis: the vessels of the gut and pectoral fin had excessive numbers of cells (Fig. 5.7C-F). Because Jacob et al have shown that zebrafish at this age still obtain oxygen passively via diffusion from the surrounding water (Jacob et al., 2002), is seems unlikely that this excessive angiogenesis is a response to tissue hypoxia. Thus, Dll4-Notch signalling is required to keep angiogenesis under proper control, not only in the embryo, but also at later stages and in multiple tissues.

### 5.2.4 Endothelial cells misbehave in embryos lacking Dll4

I have shown that blockade of Dll4-Notch signalling results in ectopic angiogenesis: endothelial cells appear to proliferate excessively and migrate into regions where they should normally not be found. How, then, might Dll4 affect the behaviour of individual endothelial cells in order to produce this effect?

To answer this question, it's important to first understand how the normal pattern of blood vessels develops in this system. In normal embryos, the ISVs originate as endothelial sprouts that migrate from the DA along somite boundaries (Fig. 5.8A). These sprouts are first seen around 20-24 hpf and grow dorsally and slightly anteriorly, following the chevron-shaped somite borders. When they reach the neural tube, the sprouts deviate from the intersomite space and project straight dorsally until they reach the top of the neural tube at approximately 30 hpf. At this point they bifurcate to form a T-shape, with the two branches extending longitudinally along the body axis. The branches of adjacent sprouts eventually link-up to form the DLAV by 48 hpf.

For ISVs to begin their development, a subset of the endothelial cells in the DA must become motile, while the remaining endothelial cells must remain static in order to maintain the integrity of the DA. As these cells move along their trajectory they possess numerous filopodia, a morphology indicative of active migration. As the ISV sprouts grow, filopodia can be seen not only in the leading cell, but also in the cells that follow. In the account given below, I shall refer to these as tip and stalk cells, following the nomenclature used in describing mouse retinal angiogenesis (Gerhardt and Betsholtz, 2005; Gerhardt et al., 2003). However, it should be borne in mind that the degree of similarity between the two angiogenic systems is questionable: there are substantial differences both in the architecture of the surrounding tissue, which appears to largely control the pattern of angiogenesis, and in the behaviour of the leading and following endothelial cells.

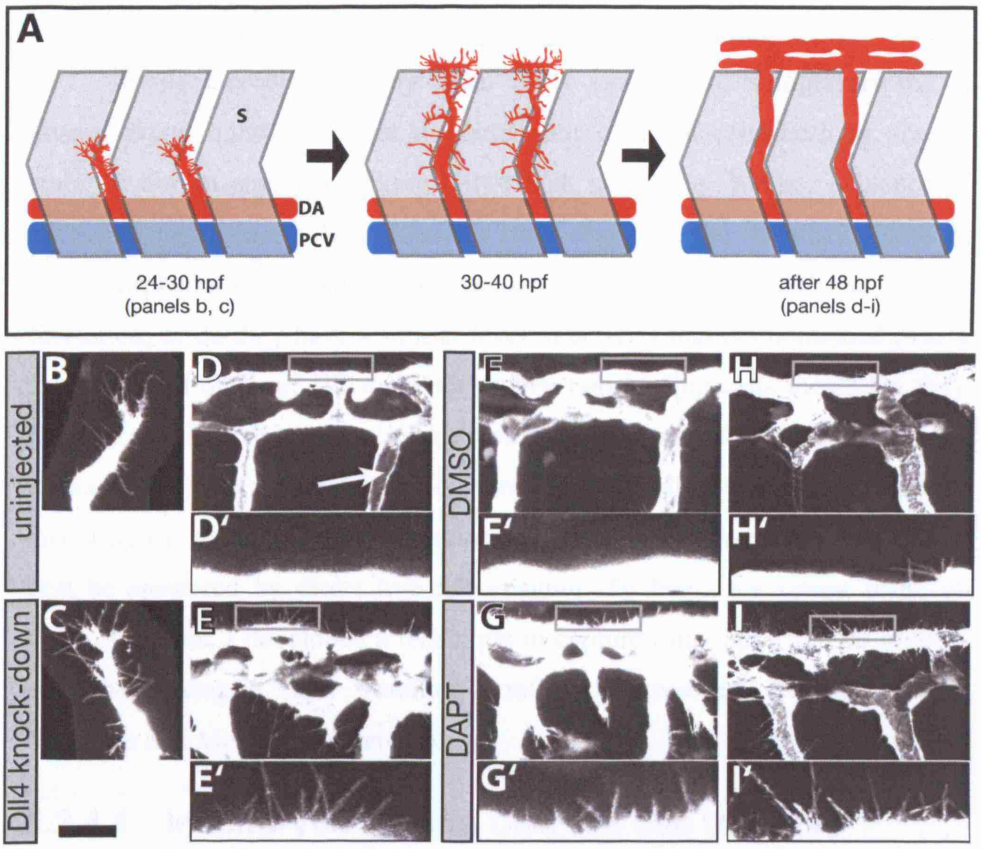


**Figure 5.8. Effects of Dll4 knock-down on endothelial cell behaviour.** (**A**) Schematic depiction of ISV and DLAV formation and the concomitant changes in endothelial cell morphology. (**B,C**) Leading cell of an ISV sprout at 30 hpf in a living uninjected embryo (B) or in a living embryos injected with 10 ng MO[Dll4] (C). (**D,E**) DLAV in the mid-trunk at 2.5 dpf in a living uninjected embryo (D) or in a living embryos injected with 10 ng MO[Dll4] (E). (**F-I**) Similar region at 2.5 dpf of living embryos treated with 100 µM DAPT (G,I) or control embryos treated with DMSO (F,H). Treatment with DAPT or DMSO began at either 33 hpf (F,G) or at 48 hpf (H,I) and continued through the course of the experiment. (**D'-I'**) Details of boxed regions in D-I. Arrow in D shows the lumen of a vessel. S, somite. Scale bar: 50 µm in B-I.

Some time after the leading cells of adjacent ISV sprouts connect, the motile behaviour in both the leading cells and the following "stalk" cells is switched off; they now set about creating a tube with a lumen (Fig. 5.8A). Indeed, after 48 hpf, the endothelial cells of the ISVs and the DLAV have few filopodia and the lumens become apparent in the EGFP-expressing endothelial cells as a fainter region between brighter edges (for example, see Fig. 5.4A).

While this process may seem fairly simple and straightforward, it raises several questions about the behaviour of these cells both in normal embryos and in embryos lacking Dll4-Notch signalling. We see evidence of excessive angiogenesis. How does this come about: do the endothelial cells in Dll4 morphants have hyperactive motility at all stages of ISV and DLAV formation, or do they have a similar level of activity that is maintained over a longer period of time? What happens when two leading cells meet? Do they turn off motility immediately, suggesting a mechanism for an immediate response, or does it take longer, opening the possibility that the response is mediated by transcriptional regulation of some sort? These questions might best be answered by direct live-cell imaging. To begin answering some of these questions, I developed a technique to capture time-lapse movies at high resolution using a laser scanning confocal microscope (see Chapter 2 Materials and Methods for details).

#### 5.2.4.1 In embryos lacking Dll4, the cue to cease migration is lost

To observe how loss of Dll4 affects the behaviour of endothelial cells, I made time-lapse movies at two stages: 30 hpf, when ISV sprouts are growing and extending dorsally, and 2.5 dpf, when the DLAV has formed, completing a vascular circuit via the ISVs. At 30 hpf, I could see that the exploratory cells at the tips of the ISVs rapidly extended and retracted filopodia; this behaviour was found in both uninjected and MO[Dll4]-injected embryos (Fig. 5.8B,C and Movie 5.3, 5.4). A typical stalk in an uninjected embryo, filmed in this way, had 37 filopodia averaging 15 μm in length, with a maximum length of 49 μm. A typical stalk in a MO[Dll4]-injected embryo had 46 filopodia averaging 14 μm in length with a maximum length of 61 μm. I measured the lifetime of these filopodia: on average, 5.6 minutes elapsed between the first

perceptible extension of a filopodium and its complete retraction in an uninjected embryo. This was reduced to 5.2 minutes in morphant embryos. Although these numbers indicate that the morphant embryos have more filopodia with shorter lifetimes, they are based on only one stalk in each treatment. Clearly I would have to make measurements on many more stalks in many more embryos before placing any significance on this result; I have included it here simply to give some indication of the scale of values. For the meantime, my qualitative impression is that the two samples are indistinguishable.

Later in development, however, differences became strikingly apparent. In normal embryos at 2.5 dpf, the endothelial cells of the DLAV and the ISVs had ceased their exploratory behaviour, and filopodia became few and far between (Fig. 5.8D and Movie 5.5). In contrast, the endothelial cells of morphant embryos continued to be active, extending and retracting filopodia and invading the areas between ISVs from which they normally would be excluded (Fig. 5.8E and Movie 5.6). Additionally, there was no evidence of a lumen in the vessels of morphant embryos, whereas a lumen was clearly visible in normal vessels (arrow in Fig. 5.8D). Clearly, the endothelial cells of morphant embryos were misbehaving, having failed to turn off their motility when the DLAV had formed. In this way, the cells continued to migrate, and presumably to divide, when they should have stopped. In short, angiogenesis had persisted when it should have been turned off. A similar effect was apparent in *dll4* mutant embryos (Movie 5.7, 5.8).

#### 5.2.4.2 Blockade of Notch signalling phenocopies the Dll4 phenotype

Evidently, Dll4 is required for endothelial cells to make the transition from exploratory behaviour to quiescence. As discussed earlier in the control of endothelial proliferation control, this could reflect a cell-autonomous function, or it could be due to cell-cell signalling via Notch. To test whether Notch receptor function mediated the effects of Dll4 on cell motility as well as the effects on proliferation, I blocked Notch signalling with the gamma-secretase inhibitor DAPT starting at 33 hpf (a time when the ISV sprouts are beginning to link up and when motility should normally be turned off) and examined the

embryos at 54 hpf. As in embryos lacking Dll4, the endothelial cells of DAPT-treated embryos continued to extend and retract filopodia (n = 8 embryos), whereas filopodia were essentially absent from the endothelial cells of DMSO-treated control siblings (n = 4 embryos; Fig. 5.8F,G and Movie 5.9,5.10).

These data indicate that Dll4 does indeed act via Notch to turn off angiogenesis. Could it also be that quiescent endothelial cells use Dll4-Notch signalling to maintain that quiescence? To test this, I performed a similar experiment, applying DAPT at 48 hpf (after the DLAV has formed and the exploratory behaviour is turned off) and examining endothelial cell behaviour at 54 hpf. Again, I observed increased filopodial activity; but I saw no sign that the cells were migrating into ectopic locations, and the lumens of the vessels remained apparently open ((n = 6 embryos for both DMSO and DAPT treatments; Fig. 5.8H,I and Movie 5.11,5.12). These data are only preliminary, and a more extensive time-course is needed, but they suggest that after migration has been turned off, something other than (or in addition to) Notch signalling keeps the endothelial cells from forming new vascular sprouts. This could be some other signalling pathway, or some cell-autonomous memory mechanism, or it could be some physical restriction from non-endothelial vascular cells such as mural cells. However, other recent studies in the mouse and zebrafish suggest that Notch signalling is required to maintain as well as initiate the quiescent state (Hellstrom et al., 2007; Lobov et al., 2007; Siekmann and Lawson, 2007; Suchting et al., 2007), and a full investigation remains as a task for the future.

### 5.2.4.3 Embryos lacking Notch1b have a similar vascular phenotype to Dll4 morphants

As a further check on the conclusion that Dll4 acts through the Notch pathway to exert its effect on endothelial cell behaviour, and to identify through which Notch receptor Dll4 acts, I performed morpholino knockdown on each of the four known zebrafish Notch receptors (Lorent et al., 2004; Milan et al., 2006). As described above, *notch3* is expressed in the arterial vasculature (Lawson et al., 2001); it seemed, therefore, to be the most likely candidate. Surprisingly,

the vasculature of Notch3 morphant fish looked completely normal through the third day of development, as did the vasculature of Notch2 morphants (data not shown). Embryos injected with the Notch1a morpholino showed ISV patterning defects, but these correlated with, and appeared to be secondary to, the disruptions in somite formation that result from loss of Notch1a, as in *notch1a* (*deadly seven*) mutants (Holley et al., 2002; van Eeden et al., 1996a).

Fish injected with the Notch1b morpholino, however, while showing no signs of somite defects, had dramatic vascular abnormalities. The development of the vasculature was retarded, such that by 30 hpf, no ISVs had formed (data not shown). Both the ISVs and the DLAV had formed by 50 hpf, but the pattern of the ISVs was irregular and very little blood flow could be detected throughout the trunk (data not shown). At 3 dpf, ectopic angiogenic sprouts had formed between the ISVs and the DLAV in much the same way as in Dll4 morphants or mutants (n = 13 out of 16 embryos examined; Fig. 5.9). I conclude, therefore, that Notch1b is the receptor responsible for Dll4's role in angiogenesis. While it is possible that the dosage of morpholino used for Notch1a, Notch2 and Notch3 was insufficient to effectively knock down their targets, this seems unlikely given that these are published reagents and were used at the concentrations reported in the literature (Lorent et al., 2004; Milan et al., 2006).

### 5.2.5 Overactivation of the Notch pathway blocks normal endothelial cell migration

My results indicate that Dll4-Notch1b signalling acts as a switch to turn off angiogenesis: if it fails, endothelial cells continue to migrate when they would normally stop. If that is true, then conversely, we should be able to stop motility in normally migrating endothelial cells by artificially imposing Notch signalling upon them. To test this, I used a GAL4-UAS system to drive the expression of the intracellular domain of Notch1a ($N^{ICD}$) under the control of a heat shock promoter (*hsp70:Gal4;UAS:*$N^{ICD}$) (Scheer et al., 2001). The $N^{ICD}$ transgene in this construct is fused to a *myc* tag, allowing detection of the

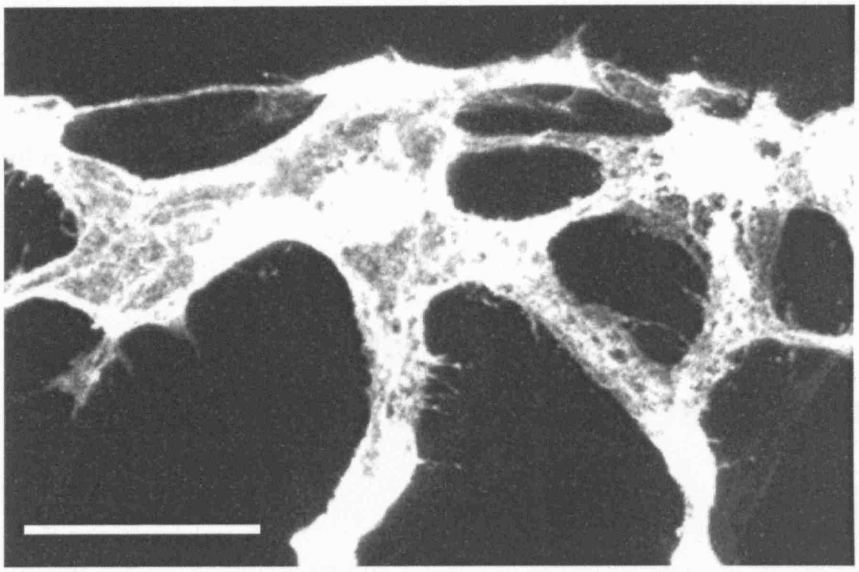

**Figure 5.9. Vascular patterning defects in an embryos lacking Notch1b.** DLAV and ISVs of a *fli1:EGFP* embryos injected with 7 ng of a morpholino targeted against Notch 1b. Note the irregular sprouts, numerous filopodia and absence of a lumen. Scale bar: 40 μm.

protein by immunostaining for Myc; and this enabled Scheer et al to show that a 30 minute heat shock is sufficient to drive expression of $N^{ICD}$-Myc protein beginning within 1 hour of the end of the heat shock and continuing for a further 24 hours. Accordingly, I applied a 37°C heat shock for 30 minutes early in ISV migration (24 hpf) and the fish were allowed to continue developing for 8 hours at the normal growth temperature (28°C). At this point (32 hpf), the embryos were fixed and processed for immunohistochemistry. I was able to identify triple transgenic $N^{ICD}$-expressing fish by Myc immunostaining. The ISVs of normal embryos had many filopodia, reflecting a high degree of motility (Fig. 5.10A). In contrast, the ISVs of double transgenic embryos had few detectable filopodia and were substantially shorter, indicating that they had been stopped in their migration shortly after the application of the heat shock (n = 12 out of 15 embryos examined; Fig 5.10B). Thus, while blockage of Dll4-Notch signalling allows for prolonged motility in endothelial cells, ectopic over-activation of the Notch pathway has a reciprocal effect.

### 5.2.6 The ectopic endothelial migration in embryos lacking Dll4 occurs in response to Vegf

It is well known that the VEGF signalling pathway plays a major role in vascular remodelling (reviewed in (Coultas et al., 2005)). In both normal angiogenesis and tumour angiogenesis, tissues secrete VEGF in response to hypoxic conditions, and the VEGF in turn forms a gradient that provides a directional cue indicating where blood vessels are needed. Nearby endothelial cells perceive extracellular VEGF through several VEGF receptors, and they respond by proliferating and migrating up the gradient towards the VEGF source (reviewed in (Gerhardt and Betsholtz, 2005)). Might the ectopic angiogenesis that we see in embryos lacking Dll4-Notch signalling be occurring in response to Vegf? To answer this, I took advantage of a pan-VEGF receptor inhibitor, SU5416, which has been shown to be effective in

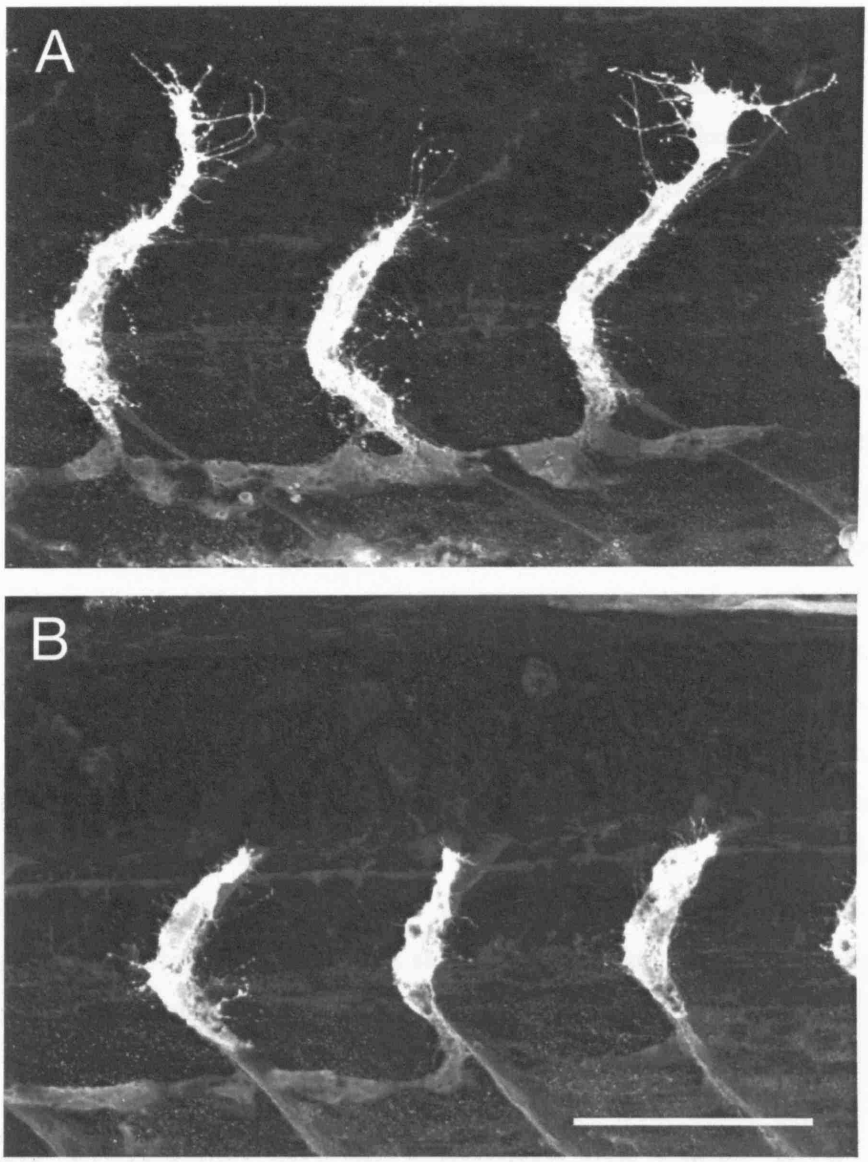


**Figure 5.10. Effects of Notch pathway overactivation on endothelial cell morphology.** Offspring of a cross between a *fli1:EGFP* transgenic and a *hsp70:Gal4;UAS:N$^{ICD}$* double transgenic at 30 hpf. ISV sprouts of a *fli1:EGFP*-positive normal sibling (**A**) and an embryo carrying all three transgenes (B; identified as such by positive Myc staining, not shown). The leading cells in the ISVs of normal embryos have numerous filopodia. In contrast, few filopodia are visible in the ISVs of N$^{ICD}$-positive embryos and the sprouts are retarded in their dorsal migration. A 30-minute heat-shock was applied at 24 hpf. Scale bar: 70 μm.

blocking angiogenesis in zebrafish (Covassin et al., 2006; Fong et al., 1999). *dll4* mutant or morphant embryos were allowed to develop until 48 hpf, the time when the ectopic vascular sprouts would normally start to emerge. The embryos were then placed in aquarium water containing either 2 μM SU5416 or vehicle alone and allowed to develop for 12 more hours. In control *dll4* mutant or morphant embryos, the ectopic sprouts were clearly detectable by 2.5 dpf (Fig. 5.11A and data not shown). In contrast, mutant or morphant embryos treated with SU5416 showed no signs of ectopic vascular sprouting (n = 14 out of 16 embryos examined for the *dll4* mutant, n = 6 out of 6 embryos examined for MO[Dll4]-injected embryos; Fig. 5.11B). It should be noted that embryos treated with SU5416 had GFP-positive spots in areas near the blood vessels, suggesting endothelial cell degenerative fragmentation (visible in Fig. 5.11B'). I suspect that these are fragments of endothelial cell filopodia that were left behind upon SU5416 treatment; time-lapse microscopy of living embryos at the time of SU5416 administration could confirm this.

These data tell us that (1) the excessive angiogenesis observed in embryos lacking Dll4-Notch signalling is conditional upon responsiveness to Vegf and (2) Vegf is normally present at a time and place when endothelial motility and proliferation are turned off - endothelial cells simply do not respond. Taken together, these data show that Dll4-Notch signalling restricts angiogenesis by making endothelial cells deaf to Vegf.

### 5.2.7 Molecular circuitry linking the VEGF and Notch pathways

My findings show that VEGF and Notch signalling are interwoven in the control of angiogenesis. In the continued presence of VEGF, angiogenesis may proceed or halt according to the level of activation of the Notch pathway. How, then, is this effect exerted? A number of studies in mammalian systems have demonstrated that the pathways cross-regulate one another (Hainaud et al., 2006; Liu et al., 2003; Lobov et al., 2007; Noguera-Troise et al., 2006; Patel et al., 2005; Suchting et al., 2007; Williams et al., 2006). To examine this possibility, I performed a series of experiments in which I examined the

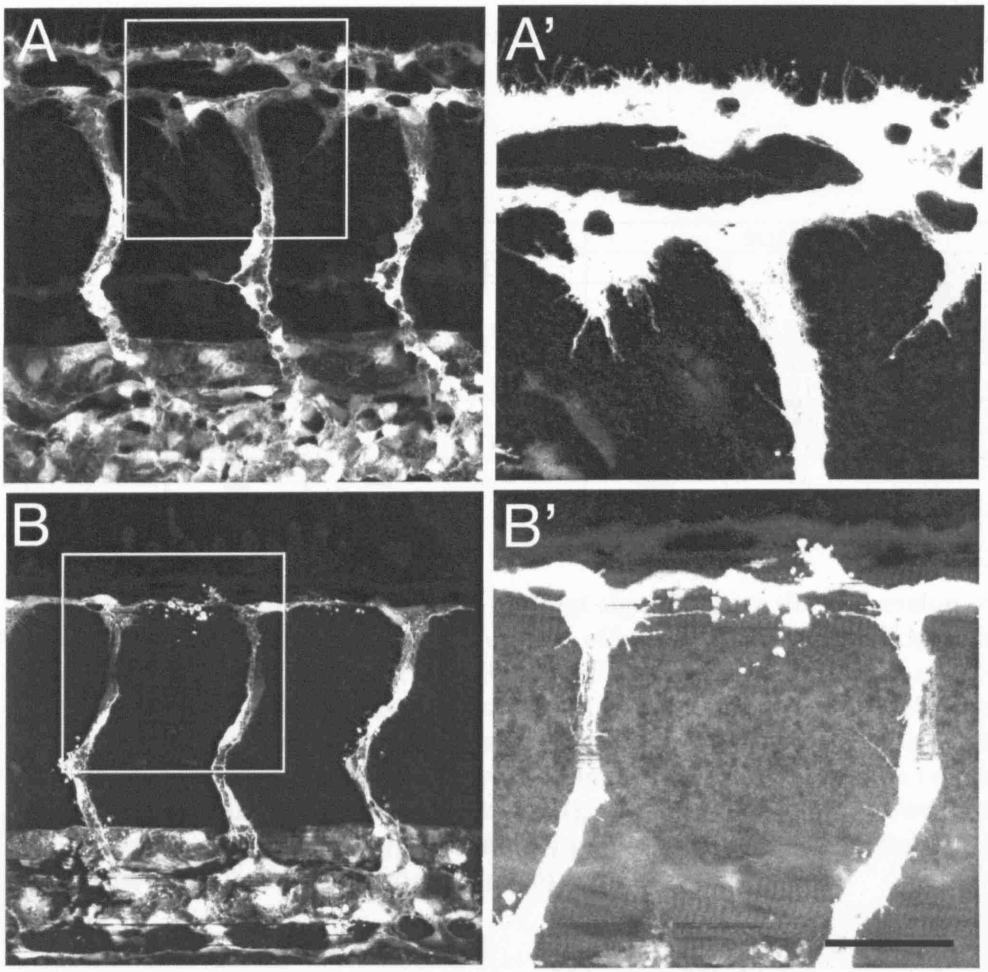


**Figure 5.11. Effects of VEGF receptor inhibition on the ectopic angiogenesis phenotype.** 2.5 dpf homozygous *dll4* mutant (*j16e1*) embryos treated with DMSO (**A**) or 2 μM SU5416 to block VEGF signalling (**B**). Treatment with DMSO or SU5416 began at 48 hpf and continued through the course of the experiment. (**A',B'**) Detail of boxed region in (A,B); the brightness has been increased in order to visualize filopodia. Note the ectopic sprouts and increased filopodia are largely absent in SU5416-treated mutants. (Images of DMSO-treated mutant (A,A') are identical to those in Figure 5.7B,B'.) Scale bar: 50 μm in A,B.

expression by whole mount in situ hybridisation of various pathway components in embryos in which either pathway was perturbed, and the embryos were then fixed and analyzed at 48 hpf (when the MO[Dll4]-induced ectopic angiogenesis begins). The results are summarized in Table 5.1, and described in detail below.

| | MO[Dll4] | | | SU5416 | | |
|---|---|---|---|---|---|---|
| | DA | ISV | DLAV | DA | ISV | DLAV |
| *dll4* | n/a | no change (5/5) | ↑ (5/5) | ↓ (18/19) | ↓ (18/19) | ↓↓↓ (18/19) |
| *vegfr3* | n/a | ↑↑ (10/13) | ↑↑ (12/13) | n/a | ↓↓ (14/14) | ↓ (13/14) |
| *vegfr2* | ↑↑↑ (12/14) | no change (14/14) | no change (14/14) | no change (17/17) | ↓↓↓ (16/17) | ↓↓↓ (16/17) |
| *nrp1b* | ↑↑ (5/7) | ↑↑ (5/7) | n/a | ↑↑↑ (19/19) | ↑↓ | n/a |

**Table 5.1. Effects of blocking Dll4 or Vegf signalling on the expression of pathway components.** Summary of the effects of Dll4 knock-down or SU5416 treatment on the expression of *dll4, vegfr3, vegfr2* and *nrp1b*, compared to the levels of expression in control embryos (Fig. 5.12-5.13). In all cases, the number of embryos displaying the reported effect is noted as a fraction of the total number of embryos examined. n/a: not applicable (when expression could not be reliably detected), ↑↓: some embryos showed an increase (n = 8 of 19 embryos examined) in expression and some showed a decrease (n = 10 of 19 embryos examined).

### 5.2.7.1 Dll4 expression is negatively regulated by Notch signalling and positively regulated by VEGF signalling

To understand the way in which Notch signalling affects cell fate decisions, one must consider feedback loops that control the expression of Notch ligands in neighbouring cells. In lateral inhibition, a Notch ligand in one cell will inhibit its own production in neighbouring cells. In this way, the signal-sending cell can maintain high levels of ligand while blocking expression in the signal-receiving cell (Haddon et al., 1998b; Lewis, 1998). The result is a mosaic of ligand-positive and ligand-negative cells. In contrast, lateral induction, in which ligand expression in one cell stimulates ligand expression in the neighbours, functions to drive all cells in a population towards a similar

fate. Examples of both types of Notch signalling are known (de Celis and Bray, 1997; Eddison et al., 2000; Lewis, 1998; Ross and Kadesch, 2004).

To determine the way in which Notch signalling regulates *dll4*, I examined *dll4* expression in MO[Dll4]-injected embryos. Embryos lacking Dll4 had increased levels of endothelial *dll4* mRNA (Table 5.1; Fig. 5.12A,B), suggesting that *dll4* is negatively regulated by Dll4-Notch signalling, as would be expected if it were controlled by lateral inhibition. In support of this, detailed examination of the newly formed DLAV in normal embryos revealed that *dll4* expression is discontinuous, indicating that within a vessel, neighbouring endothelial cells express different levels of *dll4* (Fig. 5.12A,C). It should be emphasized, however, that the number of embryos examined in this experiment was very small (n = 5). Additionally, it is possible that MO[Dll4], while blocking the production of functional Dll4 protein, might actually stabilize the misspliced transcript, causing increased levels of non-functional target mRNA and giving the false impression of increased expression.

Because one effect of Dll4 knock-down is an excessive number of endothelial cells, it is possible that the continuity of *dll4* mRNA expression seen in the DLAVs of morphant embryos is due to overcrowding (Fig. 5.12B). In normal embryos, by contrast, the endothelial cells may be more spread out. Thus, the gaps in *dll4* mRNA in normal embryos might simply be due to an absence of cells. The shape of the nuclei in the *dll4*-negative regions gives some indication: endothelial cell nuclei are distinctively elongated and can be visualized under high power Nomarski illumination. By examining the specimens in this way, I found that the *dll4*-negative regions of uninjected embryos contained such nuclei. It is possible, however, that these cells are not endothelial; indeed, mural cells can also have elongated nuclei (Holger Gerhardt, personal communication). In the future I will confirm the identity of these cells by performing a double label for *dll4* and *egfp* mRNAs in *fli1:EGFP* embryos.

In mammals, *Dll4* expression appears to be positively regulated by Vegf signalling (Hainaud et al., 2006; Liu et al., 2003; Lobov et al., 2007; Noguera-Troise et al., 2006; Patel et al., 2005; Suchting et al., 2007; Williams et al., 2006). To determine if the same is true in the zebrafish vasculature, I

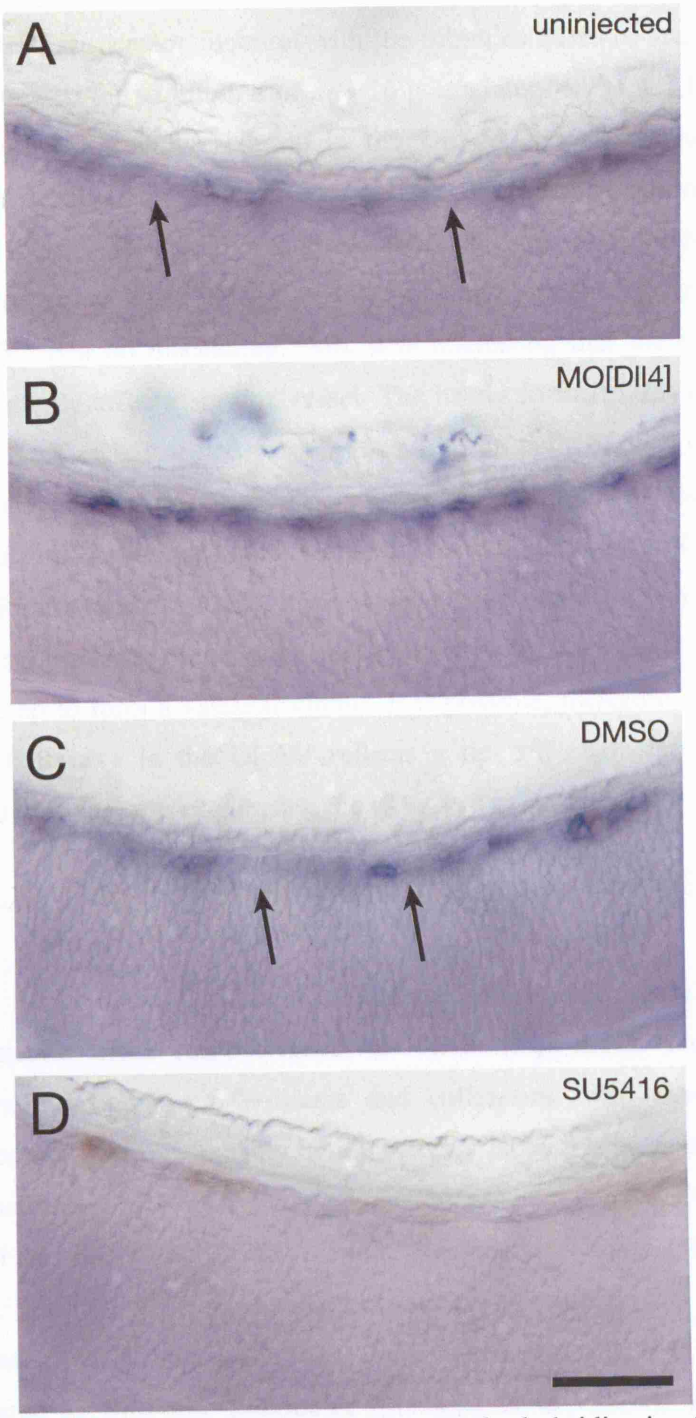


**Figure 5.12. The control of *dll4* expression.** In situ hybridization for *dll4* in the region of the DLAV of 48 hpf embryos that were uninjected (**A**), injected with 10 ng MO[Dll4] (**B**), treated with DMSO (**C**) or treated with 2 μM SU5416 (**D**). Treatment with DMSO or SU5416 began at 32 hpf and continued through the course of the experiment. Note the gaps in *dll4* expression along the DLAV (arrows in A,C), suggesting that only a subset of endothelial cells express *dll4*. Observation under high-powered Nomarski illumination revealed that these gaps contained elongated nuclei, indicating the presence of endothelial cells. The colour development reaction was allowed to proceed for a longer time in (C,D) than in (A,B) in order to better detect loss of *dll4* expression in (D). Scale bar: 50 μm.

blocked Vegf receptor function with the inhibitor SU5416 starting at 32 hpf and examined the expression of *dll4* 16 hours later (48 hpf). I found that *dll4* levels were drastically reduced in the DLAV and also reduced, but less severely, in the ISVs and the DA (n = 18 of 19 embryos examined; Table 5.1; Fig. 5.12C,D). It should be noted, however, that *dll4* mRNA levels are normally higher in the DLAV at this age, therefore the greater reduction in Table 5.1 is a bit misleading. Still, it is interesting that the expression was most strongly affected in this vessel. The newly formed DLAV is composed primarily of cells that had recently been the tip cells of ISV sprouts. In the mammalian retina, tip cells are initially singled-out by being more responsive to Vegf than their neighbours (Gerhardt and Betsholtz, 2005; Gerhardt et al., 2003; Ruhrberg et al., 2002). If the same is true in the zebrafish, it is plausible that they would continue to be more sensitive to Vegf for some time after linking up to form a vascular circuit. It is possible, therefore, that the strong effect I observe in the DLAV reflects a tip cell character in these cells compared to the cells comprising the ISVs.

#### 5.2.7.2 Notch signalling and the control of VEGF receptor expression

I have shown above that in endothelial cells, Dll4-Notch signalling functions to somehow block responsiveness to VEGF (Fig. 5.11). This observation mirrors the finding of Williams and colleagues, who have shown that mammalian Dll4, presumably acting through Notch, reduces endothelial cell responsiveness to VEGF by blocking the production of VEGF receptor 2 (VEGFR2, Flk1) and its co-receptor, Neuropilin1 (Nrp1) (Williams et al., 2006). Furthermore, a recent study of retinal angiogenesis has shown that the endothelial cells of *Dll4*$^{+/-}$ mice have elevated levels of *vegfr2* mRNA compared to wild-type littermates (Suchting et al., 2007). Taken together, these studies provide strong evidence that molecular cross-talk between the two pathways occurs on the level of gene regulation. It is important to note that these studies were focused on endothelial cell responsiveness to VEGF in the context of *initiation* of angiogenesis, whereas my observations describe effects on *cessation* of angiogenesis. Might the same molecular circuitry control both mechanisms?

To investigate *how* Dll4-Notch signalling affects responsiveness to Vegf in the zebrafish and whether the mechanism is the same as in the mouse, I examined the expression of *vegf receptor 3* (*vegfr3*, *flk4*), *vegfr2* and *nrp1b* in MO[Dll4]-injected embryos. I found that all three genes were up-regulated compared to uninjected siblings (Table 5.1; Fig. 5.13). These changes were not the same in the DA, ISVs and DLAV, indicating that the endothelial cells in each vessel may have distinct molecular mechanisms controlling their behaviour. For example, the levels of *vegfr2*, while strikingly increased in the DA, were unchanged in the ISVs and the DLAV (Table 5.1; Fig. 5.13G,H). In contrast, *vegfr3* was increased in the ISVs and the DLAV, but not in the DA (Table 5.1; Fig. 5.13A-D).

Embryos lacking Dll4 also had elevated levels of *nrp1b* mRNA (Fig. 5.13E,F). This increase was most easily seen in the ISVs and the DA; DLAV expression could not be reliably assessed because high levels of *nrp1b* expression in the neural tube mask the DLAV (Bovenkamp et al., 2004). NRP1 specifically binds the VEGF-165 isoform and acts both as a coreceptor for VEGFR2, enhancing its binding to VEGF-165 (Soker et al., 2002; Soker et al., 1998; Whitaker et al., 2001), and as a VEGFR2-independent receptor (Murga et al., 2005; Soker et al., 1996; Wang et al., 2003). Thus, increased NRP1b levels could account for, or contribute to, the failure of endothelial cells to turn off angiogenesis in embryos lacking Dll4.

Although these data do not directly prove that increased Vegf receptor levels account for the ectopic angiogenesis we see in embryos lacking Dll4, they do show that the expression of Vegf receptors and co-receptors in endothelial cells is negatively regulated by Dll4-Notch signalling. The strong implication, therefore, is that Dll4-Notch signalling makes endothelial cells unresponsive to VEGF by blocking the production of one or several VEGF receptors.

### 5.2.7.3 Molecular feedback in the VEGF signalling pathway

I have shown that VEGF positively regulates Notch signalling by inducing *dll4* expression and that Dll4 negatively regulates VEGF signalling by inhibiting the production of several VEGF receptors. One might predict,

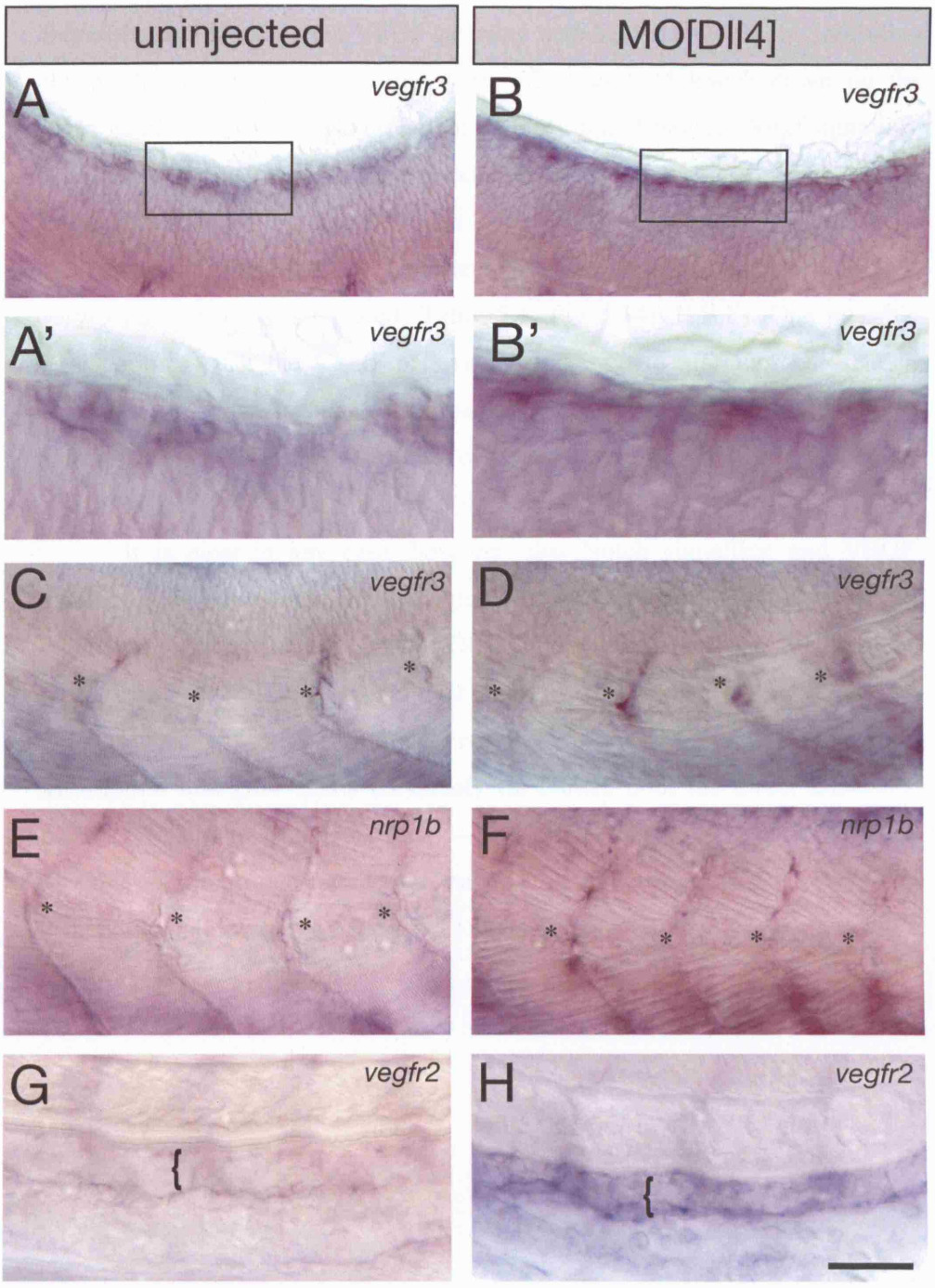


**Figure 5.13. The effects of Dll4 on *vegfr3*, *nrp1b* and *vegfr2* expression.** 48 hpf embryos stained by in situ hybridization for *vegfr3* (A-D), *nrp1b* (E,F) and *vegfr2* (G,H) in uninjected control embryos (A,C,E,G) or embryos injected with 10 ng MO[Dll4] (B,D,F,H). Control and experimental embryos in each case are siblings, processed identically and photographed under the same conditions. (**A',B'**) Detail of boxed regions in (A,B). Note increased expression of *vegfr3* in the DLAV (A,B) and the ISVs (asterisks in C,D), of *nrp1b* in the ISVs (asterisks in E,F) and of *vegfr2* in the DA (brackets in G,H). Scale bar: 50 μm.

therefore, that blocking the VEGF pathway with SU5416 would, by inhibiting the production of Dll4, have the same effect as Dll4 knock down on the expression of VEGF pathway members. To test this, I blocked Vegf signalling with SU5416 starting at 32 hpf and examined the expression of *vegfr2*, *vegfr3* and *nrp1b* at 48 hpf. As expected, the levels of *nrp1b* increased, at least in the DA (Table 5.1; Fig 5.14C,D). Unexpectedly, however, the expression of both *vegfr3* and *vegfr2* was reduced (Table 5.1: Fig 5.14A,B,E,F). One possible explanation is that the VEGF pathway, in addition to affecting Dll4-Notch signalling, may also positively feed back directly on itself. This could help to accentuate the difference between cells in which the VEGF pathway is activated and those in which it is not (see Figure 5.15A-D).

It is clear in any case, however, that Notch signalling and VEGF signalling are intertwined. VEGF signalling feeds into the Notch pathway by stimulating the production of Dll4. Dll4, in turn, can negatively regulate the VEGF pathway and can also feed back on itself by inhibiting the production of Dll4, suggesting some form of lateral inhibition. On the well-supported assumption that Dll4 exerts its effects via Notch, both the direct Dll4 —> Notch —| Dll4 loop and the Vegf —> VEGFR —> Dll4 —> Notch —| VEGFR loop represent interactions between neighbouring cells that have the effect of lateral inhibition (see Fig. 5.15), as discussed below.

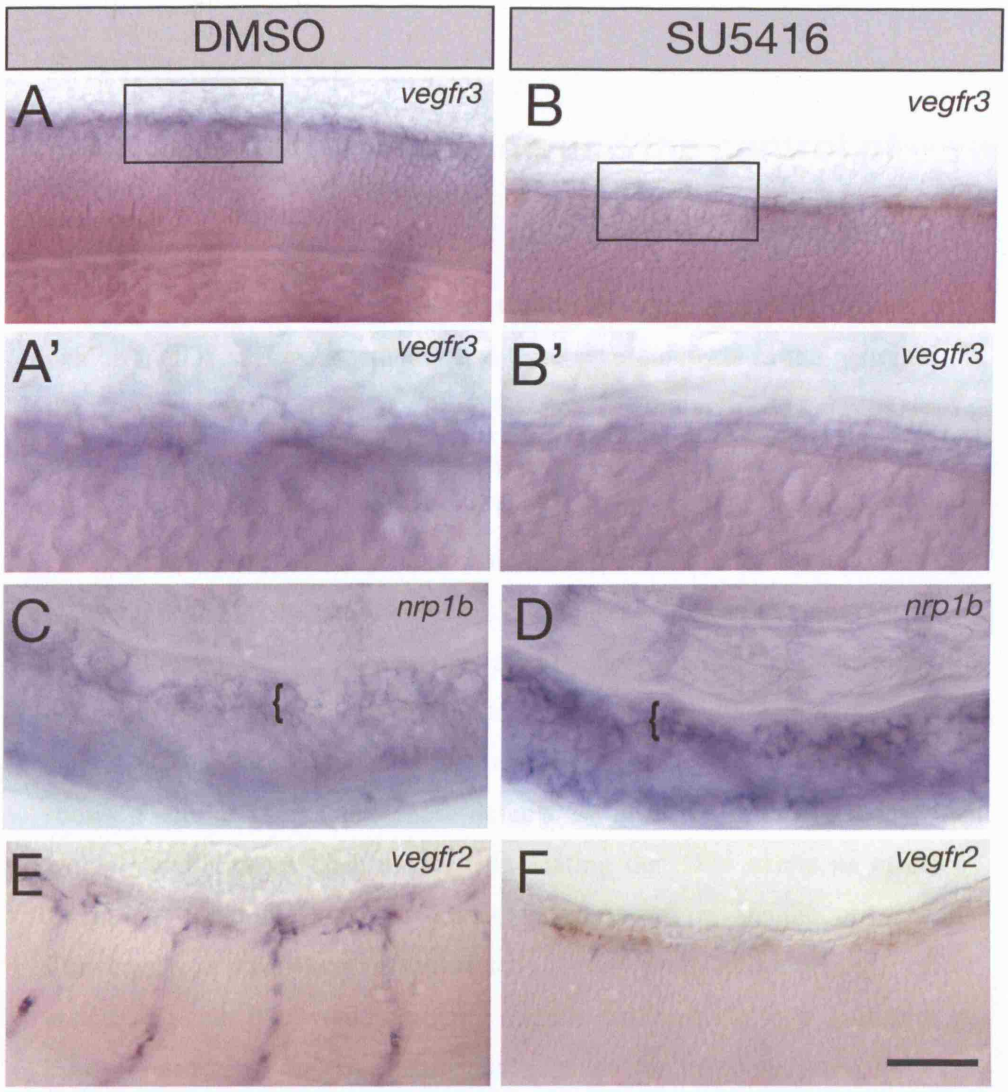


**Figure 5.14. The effects of Vegf signalling on *vegfr3*, *nrp1b* and *vegfr2* expression.** 48 hpf embryos stained by in situ hybridization for *vegfr3* (A,B), *nrp1b* (C,D) and *vegfr2* (E,F) in control embryos treated with DMSO (A,C,E) or embryos treated with 2 μM SU5416 to block Vegf signalling (B,D,F). Treatment with DMSO or SU5416 began at 32 hpf and continued through the course of the experiment. Images are of the DLAV (A,B), the DA (brackets in C,D) and the ISVs and DLAV (E,F). (**A',B'**) Detail of boxed region in (A,B). Scale bar: 50 μm.

## 5.3 Discussion

### 5.3.1 Dll4-Notch signalling and the control of angiogenesis

In mammals, Dll4 plays an essential role in vascular patterning: mutant mice exhibit haploinsufficient lethality and have severe defects in the patterning of the vascular bed (Duarte et al., 2004; Gale et al., 2004; Krebs et al., 2004). Yet what aspect of endothelial cell misbehaviour gives rise to these defects has remained, until recently, a mystery. Using a splice-modifying morpholino, I have been able to efficiently block production of Dll4 in the zebrafish embryo. I have found that zebrafish lacking Dll4 exhibit vascular patterning abnormalities resulting from ectopic angiogenesis, namely an overproduction of endothelial cells and excessive endothelial cell motility. A mutant zebrafish carrying a missense mutation in Dll4 at a highly conserved amino acid residue shows a similar phenotype. These defects are mirrored in embryos in which Notch signalling has been blocked, indicating that Dll4 exerts its effect by signalling through Notch receptors, presumably on neighbouring cells. Conversely, overactivation of the Notch pathway produces an opposite effect: endothelial cells that would normally migrate are forced to stop. Furthermore, I have found that this misbehaviour depends on responsiveness to Vegf, indicating that in a normal animal, Dll4-Notch limits angiogenesis by making cells unresponsive to Vegf stimulation.

My findings have recently been supported by a number of other studies, both in the zebrafish and in the mouse, published more or less simultaneously with our own paper (Hellstrom et al., 2007; Lobov et al., 2007; Noguera-Troise et al., 2006; Ridgway et al., 2006; Scehnet et al., 2007; Siekmann and Lawson, 2007; Suchting et al., 2007). Each of these studies has shown that Notch signalling limits angiogenic behaviour in endothelial cells and that loss of Dll4 results in excessive angiogenesis. Specifically, Suchting and colleagues, Hellström and colleagues, and Lobov and colleages have shown that Dll4-Notch signalling functions to regulate tip cell specification and vessel branching in the mouse retina: loss of Dll4 or blockade of Notch

signalling promotes increased numbers of tip cells (Hellstrom et al., 2007; Lobov et al., 2007; Suchting et al., 2007). Similarly, Siekmann and Lawson have shown in the zebrafish that Notch signalling functions to ensure that only a single tip cell is specified in each ISV. If Notch signalling is blocked, the number of cells at the tip of ISV sprouts is increased and endothelial cells proliferate excessively (Siekmann and Lawson, 2007).

I have observed that the circulation in embryos lacking Dll4 is severely deficient and that the vessels of these embryos appear to lack a properly formed lumen (compare Figs. 5.8D and E). In a similar way, in vitro studies using cultured endothelial cells have shown that blocking Dll4 function or Notch signalling inhibits the formation of endothelial networks (Liu et al., 2003; Patel et al., 2005; Williams et al., 2006). Perhaps most exciting, however, are several recent reports investigating angiogenesis in xenografted tumours in the mouse: blockade of Dll4 or Notch signalling results in excessive tumour angiogenesis, but the vessels that are formed lack lumens and fail to carry blood (Noguera-Troise et al., 2006; Ridgway et al., 2006; Scehnet et al., 2007). Consequently, tumour tissues become hypoxic and tumour growth is inhibited, raising possibilities for the use of Dll4-Notch signalling as a target for anti-tumour therapy.

How does Dll4-Notch signalling exert its effect? My results indicate that it somehow functions to block responsiveness to VEGF: when embryos lacking Dll4 are treated with the VEGF receptor inhibitor SU5416, the ectopic angiogenesis is impeded. Furthermore, I have shown that Dll4-Notch inhibits the expression of Vegf pathway components (Fig. 5.13) and may normally act by negatively regulating VEGF signalling in this way. These findings support other in vivo and in vitro studies that have shown that Notch activation down-regulates the VEGF receptors *vegfr2*, *vegfr3* or *nrp1* and thereby attenuates endothelial cell responsiveness to VEGF (Leong et al., 2002; MacKenzie et al., 2004; Patel et al., 2005; Ridgway et al., 2006; Siekmann and Lawson, 2007; Suchting et al., 2007; Taylor et al., 2002; Williams et al., 2006).

My observations are similar to the findings of Siekmann and Lawson, who showed (1) that the expression of *vegfr3* is normally restricted to the ISV tip cells, (2) that this is lost once the ISVs link up to form the DLAV and (3) that loss of Notch signalling results in expanded expression throughout the

ISV stalk (Siekmann and Lawson, 2007). The authors go on to demonstrate that ectopic angiogenesis observed upon blockade of Notch signalling can be prevented by knocking down Vegfr3. These observations would suggest that while Dll4-Notch signalling acts by blocking VEGFR2 production in mammals, the more important target in the zebrafish is Vegfr3. Yet the increased expression of *vegfr2* I observed in the DA was dramatic (Table 5.1; Fig. 5.13), suggesting that Dll4-Notch signalling must also have an important role in controlling Vegfr2 in this vessel. Perhaps Dll4-Notch signalling acts on Vegfr2 to limit the *initiation* of angiogenesis from the DA, but the *cessation* of angiogenesis in the DLAV occurs via Dll4-Notch-mediated repression of Vegfr3. More detailed examination of these processes will be required to dissect exactly how the different receptors affect angiogenesis, and what role Notch signalling plays in those processes.

Taken together these data indicate that Dll4-Notch signalling acts as an angiogenic "off" switch, and that this switch works by making the endothelial cells unresponsive to VEGF. In the case of ISV patterning in the zebrafish, activation of this switch appears to coincide with the interaction between leading cells of two adjacent vascular sprouts. Could the same molecular mechanism underlie the specification of tip cells from a population of seemingly equivalent endothelial cells during normal angiogenesis, for example in the developing mouse retina (Gerhardt and Betsholtz, 2005)? The fact that a response is permitted in a subset of cells but inhibited in their neighbours would suggest that some form of lateral inhibition is involved, a process for which Notch signalling is perhaps most well known (Lewis, 1998). How might Dll4-Notch signalling and lateral inhibition control the pattern of responsiveness of a set of endothelial cells to VEGF? To answer this question, we must first understand the molecular circuitry that links these two pathways.

### 5.3.2 Molecular cross-talk between VEGF and Notch signalling

Until very recently, most of what we knew about the molecular circuitry intertwining VEGF and Notch signalling had come from in vitro studies on

cultured endothelial cells. For example, several studies have shown that VEGF receptor activation drives *Dll4* expression (Liu et al., 2003; Patel et al., 2005; Williams et al., 2006), a finding that I have confirmed in the zebrafish embryo. This has been recently supported by other in vivo evidence: blocking Vegf signalling in the mouse retina or in tumour vessels causes a reduction in *Dll4* expression (Lobov et al., 2007; Noguera-Troise et al., 2006; Suchting et al., 2007), whereas stimulating the Vegf pathway leads to an increase in *Dll4* expression (Lobov et al., 2007). Thus, activation of the VEGF pathway in a given cell will tend to increase the levels of Dll4 in that cell, which will in turn increase the level of Notch activation in its neighbours.

Both my own results and those of the other groups show that Notch signalling in turn regulates reception of VEGF signals. Much of what we know on this score comes from in vitro studies that have shown that activation of the Notch pathway leads to a down-regulation of *VEGFR2* and attenuates endothelial cell responsiveness to VEGF (Leong et al., 2002; MacKenzie et al., 2004; Patel et al., 2005; Ridgway et al., 2006; Taylor et al., 2002). Similarly, both I and Siekmann and Lawson have found that when Notch signalling is blocked in the zebrafish embryo, the stalk cells of ISVs ectopically express *vegfr3* (Table 5.1; Fig. 5.13A-D; (Siekmann and Lawson, 2007)). Thus, Notch signalling appears to reduce the level of VEGF receptors in endothelial cells and, thereby, block their ability to respond to VEGF.

These data allow us to formulate a model to account for how neighbouring endothelial cells might affect one another's responsiveness to VEGF (Fig. 5.15). VEGF signalling in one cell would tend to increase the level of Dll4 in that cell and, in turn, increase the level of Notch activation delivered to the neighbouring cell. This increase in Notch signalling would, in turn, cause a decrease in the levels of VEGF receptor and, thus, dampen the neighbour's responsiveness to VEGF. In this way, the first cell would be allowed to respond to VEGF and would, at the same time, inhibit responsiveness in the neighbour. Consistent with this model are the findings of Williams and colleagues, who have demonstrated that overexpression of Dll4 in cultured human primary endothelial cells causes a down-regulation of *VEGFR2* and *Nrp1* and a concomitant reduction in their responsiveness to VEGF (Williams et al., 2006). This effect appears to be exerted in a non-cell-

autonomous manner, and the authors provide strong evidence that, in their system at least, Dll4 signals through a Notch receptor. These findings have recently been supported in vivo: retinas of *Dll4*$^{-/+}$ mice have increased levels of *vegfr2* and decreased levels of *vegf receptor 1* (*vegfr1, flt1*; a VEGF sink that competes with VEGFR2 to dampen VEGF signalling) compared to wild-type littermates (Suchting et al., 2007). Others, however, report contradictory findings: Dll4 blockade causes a reduction in *vegfr2* expression (Lobov et al., 2007). The reason for this discrepancy is unclear, but, in my system at least, Dll4-Notch signalling appears to block the expression of *vegfr3*, *vegfr2* and *nrp1b*.

### 5.3.3 Molecular cross-talk between VEGF and Notch could prune the angiogenic response in a population of endothelial cells

During angiogenesis, hypoxic tissues communicate with endothelial cells by secreting VEGF. VEGF forms an extracellular gradient that gives the endothelial cells directional information, guiding them towards the regions where new blood vessels are needed (reviewed in (Gerhardt and Betsholtz, 2005)). One can think of the VEGF gradient as an "analogue" signal, a notion put forth recently by Hellström and colleagues (Hellstrom et al., 2007). In response to this signal, some cells become tip cells while others do not – a "digital" response. Thus, one can think of the mechanism responsible for specifying tip cells as an analogue/digital converter: analogue information is somehow converted to an "all or nothing" response. Can our model, as it stands, account for this conversion?

I have argued that the VEGF and Notch pathways are cross-regulatory, and that neighbouring endothelial cells communicate with one another, via Dll4 and Notch, exerting lateral inhibition. If VEGF exposure varies from cell to cell, the effect of lateral inhibition will be to intensify the difference in behaviour between cells that experience the highest levels of exposure, and their immediate neighbours, exposed to somewhat lower levels. It is important

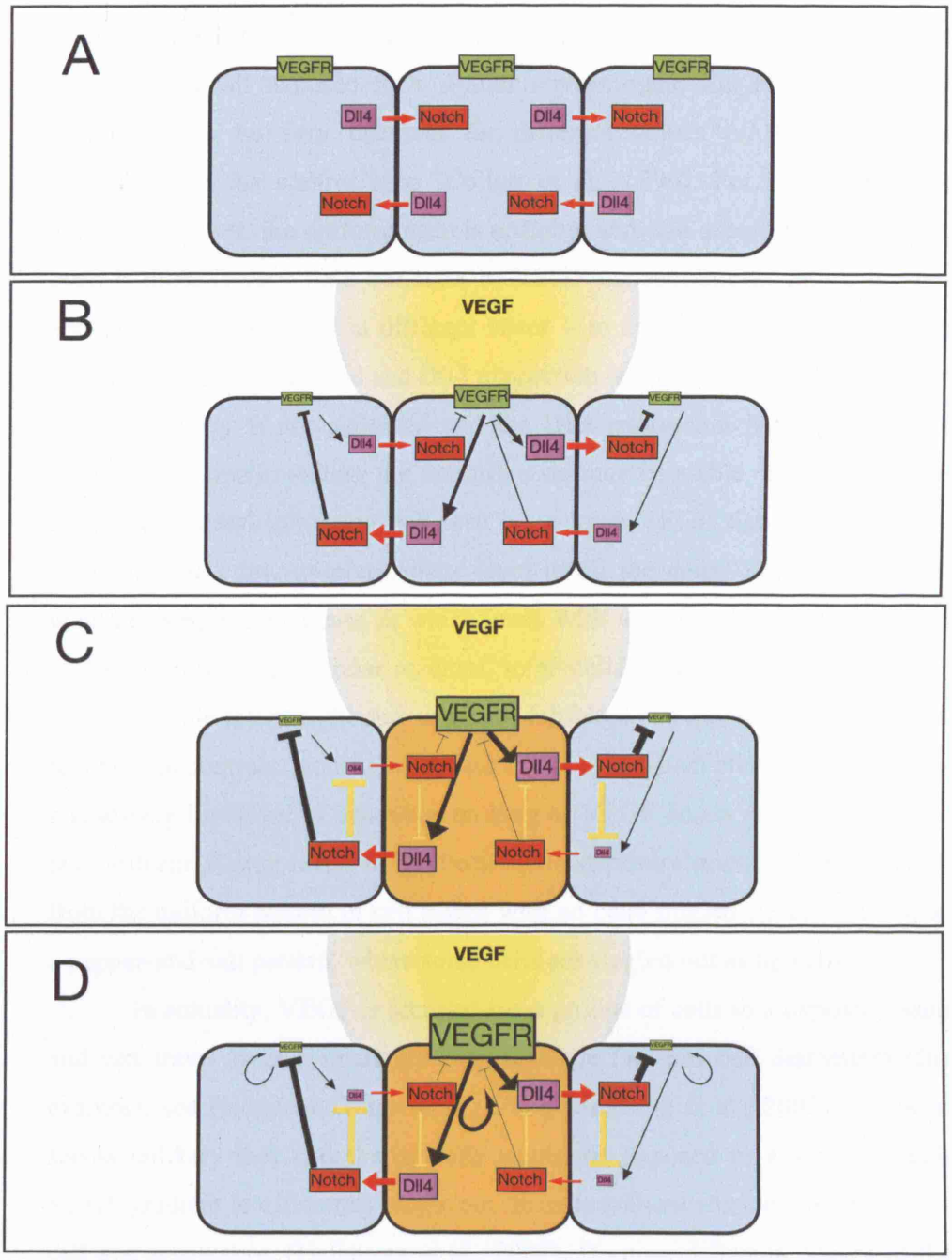


**Figure 5.15. A model for the control of angiogenesis by cross-talk between the VEGF and the Dll4-Notch pathways.** (**A**) In times of stasis, endothelial cells have basal levels of VEGF receptors (VEGFR), Dll4 and Notch. (**B**) Upon VEGF secretion by nearby tissues, one cell receiving more VEGF stimulation (middle) will deliver, via Dll4, more Notch activation to its neighbours than it receives, thereby repressing the level of VEGF receptor in those cells. (**C**) By adding a circuit repressing direct lateral inhibitory control over the levels of Dll4 (yellow bars), the changes in component expression and activity are exaggerated and the middle cell is favoured to become a tip cell (orange). (**D**) Adding a feedback loop (black curved arrows) in which VEGF activation stimulates its own expression will accentuate the difference between the highly activated cell and its neighbours. Different sizes of proteins and arrows represent different levels of expresssion and activity.

to appreciate, however, that in a system of cells that all start out in a similar state and are all exposed to a similar environment, the effects of lateral inhibition can be very different for different values of the quantitative parameters of the control loop (Collier et al., 1996). For some ranges of parameter values, the uniform state is unstable and will automatically resolve, even if there is very little variation in VEGF concentrations, into a pepper-and-salt mixture of cells in different states – in this case, cells in which the VEGF pathway is activated and Dll4 expression is high, and cells in which the VEGF pathway is not activated and the Dll4 expression is low. For other ranges of parameter values, the uniform state may be stable, and the effect of the mutual lateral inhibition will then be to keep VEGF signalling and Dll4 expression at a low-to-intermediate level in all the cells. The first scenario would correspond to a case in which, even with very little variation in levels of VEGF in the extracellular medium, some cells would be singled out to be tip cells, while their neighbours would be inhibited and quiescent. The second scenario, in contrast, would correspond to a case in which all cells would show a relatively low level of activation so long as VEGF levels remained more or less uniform. Rising levels of uniform VEGF exposure might trigger a switch from the uniform pattern of cell states, with no cells singled out as tip cells, to a pepper-and-salt pattern, where some cells are singled out as tip cells.

In actuality, VEGF is secreted from groups of cells in a hypoxic tissue and can travel over a relatively long distance (several cell diameters) (for example, see (Noguera-Troise et al., 2006; Ruhrberg et al., 2002)). Thus, it seems unlikely that endothelial cells would be exposed to a steep enough VEGF gradient to efficiently single out tip cells without some endothelial cell-cell communication (Hellstrom et al., 2007). Because diffusion occurs in the space between cells, one could imagine that non-uniform diffusion of VEGF could produce local gradients, which would, in turn, stimulate one cell more than another. Still, it seems hard to believe that this explanation can account for the dramatic differences in responsiveness seen between neighbouring endothelial cells. Lateral inhibition, based on Dll4-Notch signalling between adjacent endothelial cells, provides a simple solution to this problem.

My observations suggest that there may in fact be two mechanisms that reinforce one another to produce lateral inhibition in the endothelium, one

arising from direct regulation of Dll4 expression by Notch activity, the other less direct, based on the effect of Notch activation on VEGF signal reception. Thus, in embryos lacking Dll4, the expression of Dll4 is increased in endothelial cells as in classical models of lateral inhibition (Haddon et al., 1998b; Lewis, 1998). In this way, analogue information would be transduced into a digital response much more efficiently than if Dll4 expression was unaffected by Notch signalling (Fig. 5.15C).

The lateral inhibition circuitry provides a means by which very small differences in VEGF can efficiently single out tip cells from non-tip cells. While this may indeed be the way the system works in some situations, a mechanism that does not depend on VEGF gradients might be responsible in others. In more mature arteries, Dll4 expression is found in only a subset of endothelial cells, indicating that within a local population, endothelial cells have inherent differences (Benedito and Duarte, 2005; Claxton and Fruttiger, 2004; Mailhos et al., 2001). As explained above, these could arise through lateral inhibition even without a VEGF gradient, or by some other means. Detailed expression studies in the mouse retina have shown that Dll4 expression appears in an alternating pattern of Dll4-positive and Dll4-negative regions (Claxton and Fruttiger, 2004). In this way, a predetermined, Dll4-positive subset of endothelial cells might be primed to take on the role of tip cell, essentially lying in wait for angiogenic stimulation in the form of VEGF. Upon VEGF stimulation, a given Dll4-positive cell could, thus, immediately deliver more Notch activation than it would receive, thereby allowing it to escape lateral inhibition and pioneer a new vascular sprout. However these Dll4-positive regions correspond to groups of cells rather than individual cells, making it somewhat harder to account for the specification of *individual* tip cells (Claxton and Fruttiger, 2004).

### 5.3.4 The cessation of motility is related to tip cell specification

The majority of the recent interest in Dll4 focuses on its role in restricting tip cell specification: in the absence of Dll4-Notch signalling, an excessive

number of endothelial cells are allowed to behave as tip cells, suggesting that in the normal state, some form of lateral inhibition limits tip-cell specification. Put simply, tip cells use Dll4-Notch signalling to keep angiogenesis turned off in their neighbours. The model discussed above provides one possible mechanism that could drive this process. In my system, however, Dll4-Notch signalling appears to have a somewhat different function: to stop angiogenesis at the appropriate times and places. How might these two roles be related, and could the molecular circuitry linking the Notch and VEGF signalling pathways control both processes?

My model suggests that endothelial cells become tip cells by delivering more Dll4-Notch signalling than they receive (Fig. 5.15). In this way, an endothelial cell that has successfully escaped lateral inhibition and begun to pioneer a vascular sprout will express high levels of *Dll4*, as observed in the tip cells of retinal angiogenesis (Claxton and Fruttiger, 2004; Hellstrom et al., 2007; Lobov et al., 2007; Suchting et al., 2007). Likewise, the levels of Notch activation in that cell will be low, and according to my model, the levels of VEGF receptor will be high, thus maintaining high levels of Dll4 (Fig. 5.16A). If two such cells meet, as occurs when ISV sprouts link up to form the DLAV, each cell would deliver a strong Dll4-Notch signal to the other, thus causing a rapid increase in Notch activation and subsequent down-regulation of Dll4 and Vegf receptors (Fig. 5.16B). In this way, each tip cell successfully turns off the ability to respond to Vegf in the other.

This model provides a mechanism to control endothelial cell behaviour during angiogenesis, and thus ensures that the developing vasculature will have the correct density of blood vessels. VEGF gives the cells information about nearby oxygen demand and provides directional cues for their migration, while Dll4-Notch signalling is important for giving endothelial cells information about their position with respect to one another. The two pathways thus cooperate to ensure that the correct density of vessels is produced at the correct times and places.

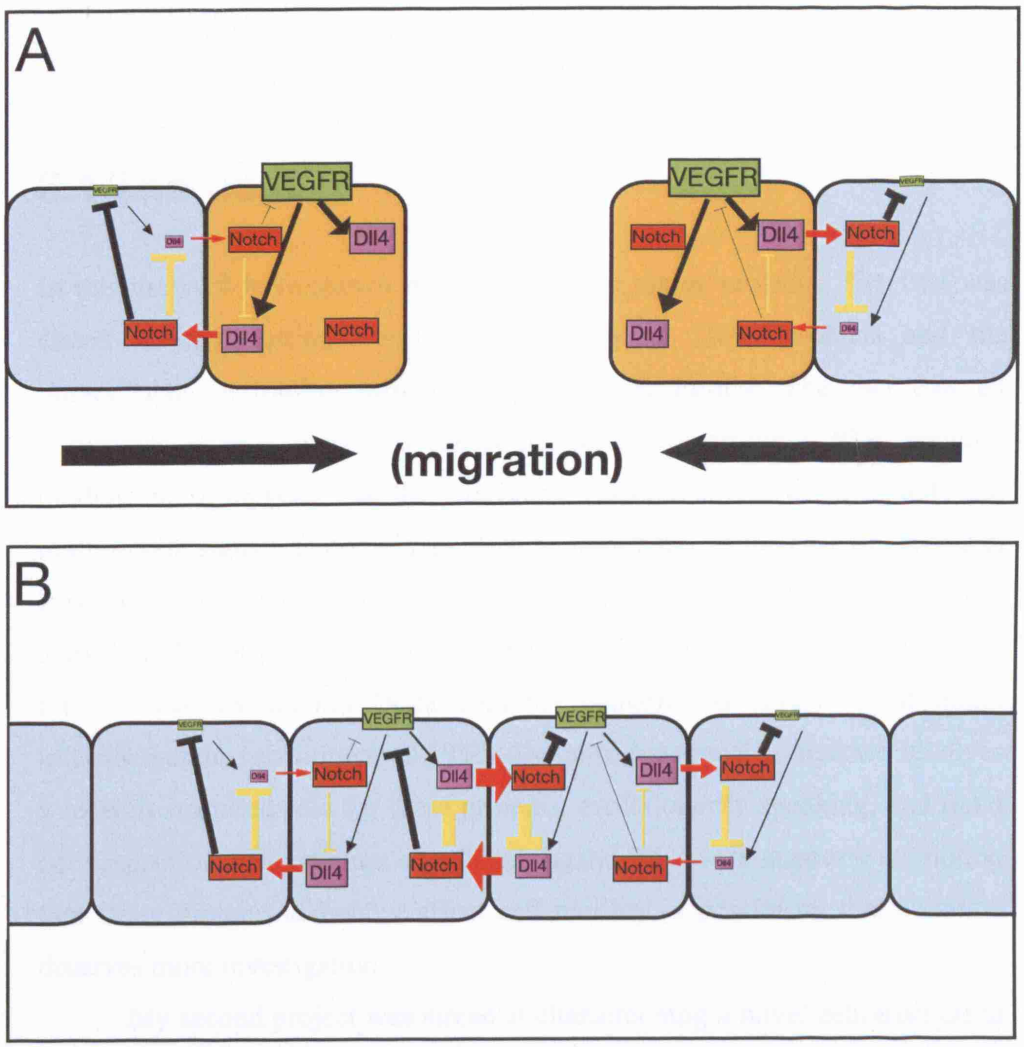


**Figure 5.16. A model for the cessation of angiogenesis by cross-talk between the VEGF and the Dll4-Notch pathways.** (**A**) As angiogenic sprouts migrate, the leading tip cells (orange) express high levels of Dll4 and VEGF receptor, but receive little Notch activation. (**B**) When two tip cells meet, high levels of Dll4 trigger high Notch activation in both tip cells, which leads to a down-regulation of VEGF receptors (black bars) and Dll4 (yellow bars).

# Chapter 6: Discussion

## 6.1 The past

In this thesis, I have shown my work on two major projects. The first was aimed at investigating the interaction between Delta proteins and the intracellular scaffolding proteins of the MAGI family. The fact that all vertebrates have a conserved subset of Deltas containing a PDZ domain-binding motif suggests that the interaction between these Notch ligands and multiprotein signalling complexes must be important. In the case of DeltaD at least, this interaction does not seem to be required for efficient Notch activation. Initially, this may seem to be a rather surprising finding. However, the fact that *Drosophila* Delta does not contain this ATEV motif might indicate that the recruitment of ATEV-Deltas to junctional complexes involves a recently acquired role for these proteins, evolutionarily speaking, and not a core aspect of their function as a Notch ligand. My work supports the notion that Delta proteins somehow affect cell motility, a possibility that certainly deserves more investigation.

My second project was aimed at characterising a novel zebrafish Delta protein, Dll4. This began initially as a side-project while I was immersed in the MAGI project, however it quickly yielded encouraging results and soon became a rather fruitful investigation into the role that Notch signalling plays in vascular remodelling. As we have seen, Dll4 is currently a very popular molecule; the role of Dll4-Notch signalling in angiogenesis has received a great deal of attention in the past year. This is underpinned by the fact that our research was one of several concomitant studies that, collectively, made a large step forward in our understanding of how endothelial cells communicate and control one another's behaviour during the initiation and termination of angiogenesis (Hellstrom et al., 2007; Leslie et al., 2007; Lobov et al., 2007; Noguera-Troise et al., 2006; Ridgway et al., 2006; Scehnet et al., 2007; Siekmann and Lawson, 2007; Suchting et al., 2007).

In Chapter 5, I also presented preliminary data from my most recent experiments in which I have tried to shed light on the specific way in which

Dll4 in one cell influences the ability of a neighbouring cell to respond to an angiogenic stimulus, namely VEGF. I have proposed a model that can account for this, both in the specification of tip cells and in the cessation of angiogenesis. However, these data and the model that they suggest are very preliminary and will require confirmation. Towards this end, I will continue with this project for the next year, as I have the good fortune to continue in the lab as a postdoctoral research fellow. I have outlined my plans for this year in the following section.

## 6.2 The future

My work has shown that the zebrafish offers the unique benefit of allowing us to observe the events of vascular remodelling in the living embryo. While my studies on Dll4 have shed light on one important step in this process, the cessation of endothelial motility, the underlying mechanisms driving this event are not completely understood. Indeed, as we learn more about angiogenesis, more questions emerge - questions that I may be poised to answer both with my own research and through collaborative efforts with the Vascular Biology Laboratory (Holger Gerhardt, London Research Institute), the Biomolecular Modelling Laboratory (Paul Bates, London Research Institute) and Katharine Lewis (Cambridge University).

My studies show that during angiogenesis, Dll4-Notch signalling restricts the movement and proliferation of endothelial cells by blocking their ability to respond to VEGF. My preliminary data indicate that the underlying mechanism responsible for this inhibition involves the transcriptional regulation of VEGF pathway components; however, a more direct effect of Notch activation on cell motility might also play a part. I will extend my current time-lapse studies to look carefully at the events that occur when tip cells meet. For example, does their motile behaviour cease immediately upon contact (suggesting that signalling cascade acts directly on the cell migration machinery) or does it take more time (implying that the effect occurs exclusively through the regulation of gene expression)?

My findings suggest that during angiogenesis, the cue to cease endothelial migration occurs when adjacent tip cells encounter one another, and that Dll4-Notch signalling is responsible for relaying this signal. This could occur through direct contact between endothelial cells, or it could happen indirectly by some mechanism involving instructions with other cell types, such as pericytes, that have an intimate relation with endothelial cells and help to form the vessel wall. In the mammalian retina, microglia are closely associated with the expanding angiogenic plexus, yet the precise role that they play is not well understood. Are non-endothelial cells involved in a similar way during angiogenesis in the zebrafish, and if so, might we be able to use the zebrafish to shed light on exactly how they affect angiogenesis and endothelial cell behaviour? I hope to pursue this question through a collaborative effort with Holger Gerhardt's laboratory at the London Research Institute.

The level of Notch activity affects a cell's behaviour cell-autonomously, yet activation of the Notch pathway in one cell can also have drastic effects on neighbouring cells through inhibitory or inductive feedback loops. In our system, my working hypothesis is that the cue to cease migration is exchanged between tip cells that meet. Yet tip cells are not the only migrating endothelial cells: the stalk cells that follow are also motile (with many filopodia), and this behaviour also ceases upon tip cell-tip cell encounter. How, then, does the instruction propagate through the length of the angiogenic sprout? The mechanism could be explained by a Notch-mediated signal passed in series from one cell to the next. Cell transplantation experiments will allow me to examine this directly. For example, if I were to graft a normal cell into an embryo lacking Dll4, that cell would deliver, but not receive, Notch activation. How would that cell behave, and how would it affect the behaviour of neighbouring cells? One would predict that it would continue to migrate while preventing motility in its immediate neighbours. In a similar way, this type of assay would allow me to more directly assess how Dll4 in one cell affects the levels of *vegfr2*, *vegfr3* and *dll4* in neighbouring cells. This would substantially contribute to my preliminary data in Chapter 5, which gave hints at the ways in which the VEGF and Notch pathways are intertwined.

In Chapter 3 I investigated the role of a C-terminal ATEV motif in DeltaD and found that it has an effect on cell motility. Dll4, like DeltaD, also contains this PDZ domain-binding sequence, and, as in DeltaD, it can be disrupted using a splice-blocking morpholino targeted to the last intron of the primary transcript. If the ATEV motif of Dll4 is required for proper formation of signalling complexes in migrating endothelial cells, disrupting the interaction might have dramatic effects on angiogenesis. I have tested a morpholino that disrupts the Dll4 ATEV motif in *fli1:EGFP* embryos and found that vascular patterning is severely disrupted (data not shown); however, the fish are very sick and the specificity of the effect is dubious at best. I would like to pursue this by performing the same injection into Dll4-defective embryos, thereby allowing me to distinguish Dll4-specific abnormalities from those arising simply from morpholino toxicity and cross-reactivity.

In Chapter 4 I showed that *dll4*, in addition to its endothelial expression, is also found in a select subset of cells within the ventrolateral neural tube, implying that it may play a role in controlling the differentiation of motorneurons or interneurons (see Fig. 4.3F). These cells have been extensively characterised in the zebrafish and molecular markers are readily available. We have recently established a collaboration with Dr. Katharine Lewis (Cambridge University) to investigate possible roles of Dll4 in the specification of these cells. Thus far, we have no preliminary data to offer, but the prospect that Dll4 is involved in the specification of neuronal cell types is an attractive one.

As a somewhat peripheral branch of my research, we have worked with Katie Bentley and Paul Bates (Biomolecular Modelling Laboratory, London Research Institute) to develop and test mathematical models for Dll4's role in controlling angiogenesis. These studies are still in their infancy, but open the possibility that we may be able to use mathematical predictions in conjunction with our live-cell imaging of endothelial cells to refine current models of how Notch signalling affects endothelial cell behaviour.

## 6.3 Clinical implications

The fact that Dll4 is essential for proper vascular development has been well documented; in most genetic backgrounds, mice lacking a single copy of the gene die of vascular defects well before birth (Duarte et al., 2004; Gale et al., 2004; Krebs et al., 2004). In addition to Dll4-mediated signalling, the Notch pathway has also been shown to have other roles in the development and maintenance of the vasculature; indeed, mutations in various other Notch pathway components are responsible for a number of distinct vascular disorders. For example, gain-of-function mutations in *NOTCH3* have been linked to the human disorder CADASIL (cerebral autosomal dominant arteriopathy with subcortical infarction and leukoencephalopathy) (Joutel et al., 1996), characterised by degeneration of vascular smooth muscle cells causing a variety of symptoms. Alagille syndrome, an autosomal dominant disorder characterised by various vascular abnormalities, is due to mutations in *JAGGED1* (Warthen et al., 2006) or, in some rare instances, *NOTCH2* (McDaniell et al., 2006). The heart defects associated with Alagille syndrome appear to be due to Notch's role in the differentiation of cardiac neural crest cells into smooth muscle cells (High et al., 2007). Additionally, another congenital cardiac disorder, bicuspid aortic valve, is caused by mutations in *NOTCH1* in both inherited (Garg et al., 2005) and sporadic (Mohamed et al., 2006) forms of the disease.

The Notch pathway also appears to play an important role in tumour angiogenesis, although somewhat contradictory findings have made it difficult to determine exactly how the pathway might be targeted for anti-tumour therapies. For example, blocking the Notch pathway with gamma-secretase inhibitors has been reported to both reduce (Paris et al., 2005) and induce (Hellstrom et al., 2007; Leslie et al., 2007; Suchting et al., 2007) endothelial cell proliferation and sprouting. Dll4, in particular, has received a great deal of attention recently as a possible therapeutic target, partly due to the fact that its expression is upregulated in tumour vasculature (Mailhos et al., 2001) and under hypoxic conditions (Patel et al., 2005). These findings would lead one to believe that Dll4 functions to *induce* angiogenesis. However, as we have seen

in the preceding chapters and in the multitude of recent papers, Dll4 actually has to opposite effect: that of *inhibiting* angiogenesis (Hellstrom et al., 2007; Leslie et al., 2007; Lobov et al., 2007; Noguera-Troise et al., 2006; Ridgway et al., 2006; Scehnet et al., 2007; Siekmann and Lawson, 2007; Suchting et al., 2007).

Since Dll4 inhibits angiogenesis, one might think that it loses appeal as a target for anti-angiogenic tumour therapy, yet quite the opposite appears to be the case. Paradoxically, blockade of Dll4 inhibits tumour growth, not by depriving the tumour of blood vessels, but by producing an *excess* of blood vessels that are non-productive in supporting circulation (Noguera-Troise et al., 2006; Ridgway et al., 2006; Scehnet et al., 2007). Blocking angiogenesis in tumours has become an attractive approach to inhibiting their growth; anti-VEGF strategies appear to be effective in many preclinical rodent tumour models (Ferrara and Kerbel, 2005; Jain et al., 2006) and an antibody directed aginst VEGF (bevacizumab/Avastin) has been approved for clinical use in the treatment of colorectal and some other cancers (Shih and Lindley, 2006). Yet these treatments are far from being completely curative, and some tumours are unresponsive to anti-VEGF treatment. Significantly, two of the above studies (Noguera-Troise et al., 2006; Ridgway et al., 2006) showed that blockade of Dll4 in experimental tumours successfully inhibited their growth, underscoring the attractiveness of Dll4-Notch signalling as a therapeutic target.

Thus, we are brought back to the central goal of Cancer Research UK, "...to improve our understanding of cancer and find out how to prevent, diagnose and treat different kinds of cancer." While I did not come to CRUK with the expectation that my research would have clinical implications, it is gratifying to think that my work has made at least some contribution towards of the charity's goals. Whether Dll4 will become a useful anti-cancer target remains to be determined, but the possibility is indeed an exciting one for those of us who are interested in understanding and fighting this disease.

# References


**Adam, J., Myat, A., Le Roux, I., Eddison, M., Henrique, D., Ish-Horowicz, D. and Lewis, J.** (1998). Cell fate choices and the expression of Notch, Delta and Serrate homologues in the chick inner ear: parallels with Drosophila sense-organ development. *Development* **125**, 4645-54.

**Adams, R. H., Wilkinson, G. A., Weiss, C., Diella, F., Gale, N. W., Deutsch, U., Risau, W. and Klein, R.** (1999). Roles of ephrinB ligands and EphB receptors in cardiovascular development: demarcation of arterial/venous domains, vascular morphogenesis, and sprouting angiogenesis. *Genes Dev.* **13**, 295-306.

**Ahmad, I., Zaqouras, P. and Artavanis-Tsakonas, S.** (1995). Involvement of Notch-1 in mammalian retinal neurogenesis: association of Notch-1 activity with both immature and terminally differentiated cells. *Mech Dev* **53**, 73-85.

**Amores, A., Force, A., Yan, Y. L., Joly, L., Amemiya, C., Fritz, A., Ho, R. K., Langeland, J., Prince, V., Wang, Y. L. et al.** (1998). Zebrafish hox clusters and vertebrate genome evolution. *Science* **282**, 1711-4.

**Ariza-McNaughton, L. and Krumlauf, R.** (2002). Non-radioactive in situ hybridization: simplified procedures for use in whole-mounts of mouse and chick embryos. *Int Rev Neurobiol* **47**, 239-50.

**Artavanis-Tsakonas, S., Rand, M. D. and Lake, R. J.** (1999). Notch signaling: cell fate control and signal integration in development. *Science* **284**, 770-6.

**Aster, J. C., Xu, L., Karnell, F. G., Patriub, V., Pui, J. C. and Pear, W. S.** (2000). Essential roles for ankyrin repeat and transactivation domains in induction of T-cell leukemia by notch1. *Mol Cell Biol* **20**, 7505-15.

**Bash, J., Zong, W. X., Banga, S., Rivera, A., Ballard, D. W., Ron, Y. and Gelinas, C.** (1999). Rel/NF-kappaB can trigger the Notch signaling pathway by inducing the expression of Jagged1, a ligand for Notch receptors. *Embo J* **18**, 2803-11.

**Bedell, V. M., Yeo, S. Y., Park, K. W., Chung, J., Seth, P., Shivalingappa, V., Zhao, J., Obara, T., Sukhatme, V. P., Drummond, I. A. et al.** (2005). roundabout4 is essential for angiogenesis in vivo. *Proc Natl Acad Sci U S A* **102**, 6373-8.

**Benedito, R. and Duarte, A.** (2005). Expression of Dll4 during mouse embryogenesis suggests multiple developmental roles. *Gene Expr. Patterns* **5**, 750-5.

**Berezovska, O., McLean, P., Knowles, R., Frosh, M., Lu, F. M., Lux, S. E. and Hyman, B. T.** (1999). Notch1 inhibits neurite outgrowth in postmitotic primary neurons. *Neuroscience* **93**, 433-9.

**Betsholtz, C., Lindblom, P. and Gerhardt, H.** (2005). Role of pericytes in vascular morphogenesis. *Exs*, 115-25.

**Blaumueller, C. M., Qi, H., Zagouras, P. and Artavanis-Tsakonas, S.** (1997). Intracellular cleavage of Notch leads to a heterodimeric receptor on the plasma membrane. *Cell* **90**, 281-91.

**Bonifacino, J. S. and Traub, L. M.** (2003). Signals for sorting of transmembrane proteins to endosomes and lysosomes. *Annu Rev Biochem* **72**, 395-447.

**Bovenkamp, D. E., Goishi, K., Bahary, N., Davidson, A. J., Zhou, Y., Becker, T., Becker, C. G., Zon, L. I. and Klagsbrun, M.** (2004). Expression and mapping of duplicate neuropilin-1 and neuropilin-2 genes in developing zebrafish. *Gene Expr Patterns* **4**, 361-70.
**Bray, S.** (1998). Notch signalling in Drosophila: three ways to use a pathway. *Semin Cell Dev Biol* **9**, 591-7.
**Brou, C., Logeat, F., Gupta, N., Bessia, C., LeBail, O., Doedens, J. R., Cumano, A., Roux, P., Black, R. A. and Israel, A.** (2000). A novel proteolytic cleavage involved in Notch signaling: the role of the disintegrin-metalloprotease TACE. *Mol Cell* **5**, 207-16.
**Busseau, I., Diederich, R. J., Xu, T. and Artavanis-Tsakonas, S.** (1994). A member of the Notch group of interacting loci, deltex encodes a cytoplasmic basic protein. *Genetics* **136**, 585-96.
**Carlson, T. R., Yan, Y., Wu, X., Lam, M. T., Tang, G. L., Beverly, L. J., Messina, L. M., Capobianco, A. J., Werb, Z. and Wang, R.** (2005). Endothelial expression of constitutively active Notch4 elicits reversible arteriovenous malformations in adult mice. *Proc. Natl. Acad. Sci. U. S. A.* **102**, 9884-9.
**Chastagner, P., Israel, A. and Brou, C.** (2006). Itch/AIP4 mediates Deltex degradation through the formation of K29-linked polyubiquitin chains. *EMBO Rep* **7**, 1147-53.
**Chen, J., Moloney, D. J. and Stanley, P.** (2001). Fringe modulation of Jagged1-induced Notch signaling requires the action of beta 4galactosyltransferase-1. *Proc Natl Acad Sci U S A* **98**, 13716-21.
**Chen, J. N., Haffter, P., Odenthal, J., Vogelsang, E., Brand, M., van Eeden, F. J., Furutani-Seiki, M., Granato, M., Hammerschmidt, M., Heisenberg, C. P. et al.** (1996). Mutations affecting the cardiovascular system and other internal organs in zebrafish. *Development* **123**, 293-302.
**Chen, W. and Casey Corliss, D.** (2004). Three modules of zebrafish Mind bomb work cooperatively to promote Delta ubiquitination and endocytosis. *Dev Biol* **267**, 361-73.
**Childs, S., Chen, J. N., Garrity, D. M. and Fishman, M. C.** (2002). Patterning of angiogenesis in the zebrafish embryo. *Development* **129**, 973-82.
**Chitnis, A., Henrique, D., Lewis, J., Ish-Horowicz, D. and Kintner, C.** (1995). Primary neurogenesis in Xenopus embryos regulated by a homologue of the Drosophila neurogenic gene Delta [see comments]. *Nature* **375**, 761-6.
**Claxton, S. and Fruttiger, M.** (2004). Periodic Delta-like 4 expression in developing retinal arteries. *Gene Expr. Patterns* **5**, 123-7.
**Collier, J. R., Monk, N. A., Maini, P. K. and Lewis, J. H.** (1996). Pattern formation by lateral inhibition with feedback: a mathematical model of delta-notch intercellular signalling. *J Theor Biol* **183**, 429-46.
**Conlon, R. A., Reaume, A. G. and Rossant, J.** (1995). Notch1 is required for the coordinate segmentation of somites. *Development* **121**, 1533-45.
**Cooke, J. E., Xu, Q. L., Wilson, S. W. and Holder, N.** (1997). Characterisation of five novel zebrafish Eph-related receptor tyrosine kinases suggests roles in patterning the neural plate. *Dev. Genes Evol.* **206**, 515-531.
**Cornell, M., Evans, D. A., Mann, R., Fostier, M., Flasza, M., Monthatong, M., Artavanis-Tsakonas, S. and Baron, M.** (1999). The Drosophila melanogaster Suppressor of deltex gene, a regulator of the Notch receptor signaling pathway, is an E3 class ubiquitin ligase. *Genetics* **152**, 567-76.

**Coultas, L., Chawengsaksophak, K. and Rossant, J.** (2005). Endothelial cells and VEGF in vascular development. *Nature* **438**, 937-45.
**Covassin, L. D., Villefranc, J. A., Kacergis, M. C., Weinstein, B. M. and Lawson, N. D.** (2006). Distinct genetic interactions between multiple Vegf receptors are required for development of different blood vessel types in zebrafish. *Proc Natl Acad Sci U S A* **103**, 6554-9.
**De Bellard, M. E., Ching, W., Gossler, A. and Bronner-Fraser, M.** (2002). Disruption of segmental neural crest migration and ephrin expression in delta-1 null mice. *Dev Biol* **249**, 121-30.
**de Celis, J. F. and Bray, S.** (1997). Feed-back mechanisms affecting Notch activation at the dorsoventral boundary in the Drosophila wing. *Development* **124**, 3241-51.
**de Celis, J. F., Garcia-Bellido, A. and Bray, S. J.** (1996). Activation and function of Notch at the dorsal-ventral boundary of the wing imaginal disc. *Development* **122**, 359-69.
**de Celis, J. F., Tyler, D. M., de Celis, J. and Bray, S. J.** (1998). Notch signalling mediates segmentation of the Drosophila leg. *Development* **125**, 4617-26.
**De Joussineau, C., Soule, J., Martin, M., Anguille, C., Montcourrier, P. and Alexandre, D.** (2003). Delta-promoted filopodia mediate long-range lateral inhibition in Drosophila. *Nature* **426**, 555-9.
**De Strooper, B., Annaert, W., Cupers, P., Saftig, P., Craessaerts, K., Mumm, J. S., Schroeter, E. H., Schrijvers, V., Wolfe, M. S., Ray, W. J. et al.** (1999). A presenilin-1-dependent gamma-secretase-like protease mediates release of Notch intracellular domain. *Nature* **398**, 518-22.
**Diederich, R. J., Matsuno, K., Hing, H. and Artavanis-Tsakonas, S.** (1994). Cytosolic interaction between deltex and Notch ankyrin repeats implicates deltex in the Notch signaling pathway. *Development* **120**, 473-81.
**Dimitratos, S. D., Woods, D. F., Stathakis, D. G. and Bryant, P. J.** (1999). Signaling pathways are focused at specialized regions of the plasma membrane by scaffolding proteins of the MAGUK family. *Bioessays* **21**, 912-21.
**Dobrosotskaya, I., Guy, R. K. and James, G. L.** (1997). MAGI-1, a membrane-associated guanylate kinase with a unique arrangement of protein-protein interaction domains. *J Biol Chem* **272**, 31589-97.
**Doherty, D., Feger, G., Younger-Shepherd, S., Jan, L. Y. and Jan, Y. N.** (1996). Delta is a ventral to dorsal signal complementary to Serrate, another Notch ligand, in Drosophila wing formation. *Genes Dev* **10**, 421-34.
**Driever, W., Solnica-Krezel, L., Schier, A. F., Neuhauss, S. C., Malicki, J., Stemple, D. L., Stainier, D. Y., Zwartkruis, F., Abdelilah, S., Rangini, Z. et al.** (1996). A genetic screen for mutations affecting embryogenesis in zebrafish. *Development* **123**, 37-46.
**Duarte, A., Hirashima, M., Benedito, R., Trindade, A., Diniz, P., Bekman, E., Costa, L., Henrique, D. and Rossant, J.** (2004). Dosage-sensitive requirement for mouse Dll4 in artery development. *Genes Dev.* **18**, 2474-8.
**Dunwoodie, S. L., Henrique, D., Harrison, S. M. and Beddington, R. S.** (1997). Mouse Dll3: a novel divergent Delta gene which may complement the function of other Delta homologues during early pattern formation in the mouse embryo. *Development* **124**, 3065-76.

**Durbin, L., Brennan, C., Shiomi, K., Cooke, J., Barrios, A., Shanmugalingam, S., Guthrie, B., Lindberg, R. and Holder, N.** (1998). Eph signaling is required for segmentation and differentiation of the somites. *Genes Dev* **12**, 3096-109.
**Eddison, M., Le Roux, I. and Lewis, J.** (2000). Notch signaling in the development of the inner ear: lessons from Drosophila. *Proc Natl Acad Sci U S A* **97**, 11692-9.
**Edenfeld, G., Altenhein, B., Zierau, A., Cleppien, D., Krukkert, K., Technau, G. and Klambt, C.** (2007). Notch and Numb are required for normal migration of peripheral glia in Drosophila. *Dev Biol* **301**, 27-37.
**Ekker, S. C. and Larson, J. D.** (2001). Morphant technology in model developmental systems. *Genesis* **30**, 89-93.
**Ellisen, L. W., Bird, J., West, D. C., Soreng, A. L., Reynolds, T. C., Smith, S. D. and Sklar, J.** (1991). TAN-1, the human homolog of the Drosophila notch gene, is broken by chromosomal translocations in T lymphoblastic neoplasms. *Cell* **66**, 649-61.
**Emery, G., Hutterer, A., Berdnik, D., Mayer, B., Wirtz-Peitz, F., Gaitan, M. G. and Knoblich, J. A.** (2005). Asymmetric Rab 11 endosomes regulate delta recycling and specify cell fate in the Drosophila nervous system. *Cell* **122**, 763-73.
**Espinosa, L., Ingles-Esteve, J., Robert-Moreno, A. and Bigas, A.** (2003). IkappaBalpha and p65 regulate the cytoplasmic shuttling of nuclear corepressors: cross-talk between Notch and NFkappaB pathways. *Mol Biol Cell* **14**, 491-502.
**Evrard, Y. A., Lun, Y., Aulehla, A., Gan, L. and Johnson, R. L.** (1998). lunatic fringe is an essential mediator of somite segmentation and patterning. *Nature* **394**, 377-81.
**Ferrara, N. and Kerbel, R. S.** (2005). Angiogenesis as a therapeutic target. *Nature* **438**, 967-74.
**Fischer, A., Schumacher, N., Maier, M., Sendtner, M. and Gessler, M.** (2004). The Notch target genes Hey1 and Hey2 are required for embryonic vascular development. *Genes Dev* **18**, 901-11.
**Fleming, R. J.** (1998). Structural conservation of Notch receptors and ligands. *Semin Cell Dev Biol* **9**, 599-607.
**Fleming, R. J., Gu, Y. and Hukriede, N. A.** (1997). Serrate-mediated activation of Notch is specifically blocked by the product of the gene fringe in the dorsal compartment of the Drosophila wing imaginal disc. *Development* **124**, 2973-81.
**Fong, T. A., Shawver, L. K., Sun, L., Tang, C., App, H., Powell, T. J., Kim, Y. H., Schreck, R., Wang, X., Risau, W. et al.** (1999). SU5416 is a potent and selective inhibitor of the vascular endothelial growth factor receptor (Flk-1/KDR) that inhibits tyrosine kinase catalysis, tumor vascularization, and growth of multiple tumor types. *Cancer Res* **59**, 99-106.
**Fortini, M. E. and Artavanis-Tsakonas, S.** (1994). The suppressor of hairless protein participates in notch receptor signaling. *Cell* **79**, 273-82.
**Fostier, M., Evans, D. A., Artavanis-Tsakonas, S. and Baron, M.** (1998). Genetic characterization of the Drosophila melanogaster Suppressor of deltex gene: A regulator of notch signaling. *Genetics* **150**, 1477-85.
**Franklin, J. L., Berechid, B. E., Cutting, F. B., Presente, A., Chambers, C. B., Foltz, D. R., Ferreira, A. and Nye, J. S.** (1999). Autonomous and non-

autonomous regulation of mammalian neurite development by Notch1 and Delta1. *Curr Biol* **9**, 1448-57.
**Frise, E., Knoblich, J. A., Younger-Shepherd, S., Jan, L. Y. and Jan, Y. N.** (1996). The Drosophila Numb protein inhibits signaling of the Notch receptor during cell-cell interaction in sensory organ lineage. *Proc Natl Acad Sci U S A* **93**, 11925-32.
**Fryer, C. J., Lamar, E., Turbachova, I., Kintner, C. and Jones, K. A.** (2002). Mastermind mediates chromatin-specific transcription and turnover of the Notch enhancer complex. *Genes Dev* **16**, 1397-411.
**Fryer, C. J., White, J. B. and Jones, K. A.** (2004). Mastermind recruits CycC:CDK8 to phosphorylate the Notch ICD and coordinate activation with turnover. *Mol Cell* **16**, 509-20.
**Funke, L., Dakoji, S. and Bredt, D. S.** (2005). Membrane-associated guanylate kinases regulate adhesion and plasticity at cell junctions. *Annu Rev Biochem* **74**, 219-45.
**Fuss, B., Josten, F., Feix, M. and Hoch, M.** (2004). Cell movements controlled by the Notch signalling cascade during foregut development in Drosophila. *Development* **131**, 1587-95.
**Gale, N. W., Dominguez, M. G., Noguera, I., Pan, L., Hughes, V., Valenzuela, D. M., Murphy, A. J., Adams, N. C., Lin, H. C., Holash, J. et al.** (2004). Haploinsufficiency of delta-like 4 ligand results in embryonic lethality due to major defects in arterial and vascular development. *Proc. Natl. Acad. Sci. U. S. A.* **101**, 15949-54.
**Garg, V., Muth, A. N., Ransom, J. F., Schluterman, M. K., Barnes, R., King, I. N., Grossfeld, P. D. and Srivastava, D.** (2005). Mutations in NOTCH1 cause aortic valve disease. *Nature* **437**, 270-4.
**Gerhardt, H. and Betsholtz, C.** (2005). How do endothelial cells orientate? *Exs*, 3-15.
**Gerhardt, H., Golding, M., Fruttiger, M., Ruhrberg, C., Lundkvist, A., Abramsson, A., Jeltsch, M., Mitchell, C., Alitalo, K., Shima, D. et al.** (2003). VEGF guides angiogenic sprouting utilizing endothelial tip cell filopodia. *J Cell Biol* **161**, 1163-77.
**Glittenberg, M., Pitsouli, C., Garvey, C., Delidakis, C. and Bray, S.** (2006). Role of conserved intracellular motifs in Serrate signalling, cis-inhibition and endocytosis. *Embo J* **25**, 4697-706.
**Gray, H.** (1901). Gray's Anatomy. Philadelphia: Running Press.
**Greenwald, I. and Seydoux, G.** (1990). Analysis of gain-of-function mutations of the lin-12 gene of Caenorhabditis elegans. *Nature* **346**, 197-9.
**Gridley, T.** (2007). Vascular biology: vessel guidance. *Nature* **445**, 722-3.
**Guan, E., Wang, J., Laborda, J., Norcross, M., Baeuerle, P. A. and Hoffman, T.** (1996). T cell leukemia-associated human Notch/translocation-associated Notch homologue has I kappa B-like activity and physically interacts with nuclear factor-kappa B proteins in T cells. *J Exp Med* **183**, 2025-32.
**Guo, M., Jan, L. Y. and Jan, Y. N.** (1996). Control of daughter cell fates during asymmetric division: interaction of Numb and Notch. *Neuron* **17**, 27-41.
**Gupta-Rossi, N., Six, E., LeBail, O., Logeat, F., Chastagner, P., Olry, A., Israel, A. and Brou, C.** (2004). Monoubiquitination and endocytosis direct gamma-secretase cleavage of activated Notch receptor. *J Cell Biol* **166**, 73-83.

**Haddon, C., Jiang, Y. J., Smithers, L. and Lewis, J.** (1998a). Delta-Notch signalling and the patterning of sensory cell differentiation in the zebrafish ear: evidence from the mind bomb mutant. *Development* **125**, 4637-44.
**Haddon, C., Mowbray, C., Whitfield, T., Jones, D., Gschmeissner, S. and Lewis, J.** (1999). Hair cells without supporting cells: further studies in the ear of the zebrafish mind bomb mutant. *J Neurocytol* **28**, 837-50.
**Haddon, C., Smithers, L., Schneider-Maunoury, S., Coche, T., Henrique, D. and Lewis, J.** (1998b). Multiple delta genes and lateral inhibition in zebrafish primary neurogenesis. *Development* **125**, 359-70.
**Hainaud, P., Contreres, J. O., Villemain, A., Liu, L. X., Plouet, J., Tobelem, G. and Dupuy, E.** (2006). The Role of the Vascular Endothelial Growth Factor-Delta-like 4 Ligand/Notch4-Ephrin B2 Cascade in Tumor Vessel Remodeling and Endothelial Cell Functions. *Cancer Res* **66**, 8501-10.
**Hartenstein, V. and Posakony, J. W.** (1989). Development of adult sensilla on the wing and notum of Drosophila melanogaster. *Development* **107**, 389-405.
**Hartenstein, V. and Posakony, J. W.** (1990). A dual function of the Notch gene in Drosophila sensillum development. *Dev Biol* **142**, 13-30.
**Hellstrom, M., Phng, L. K., Hofmann, J. J., Wallgard, E., Coultas, L., Lindblom, P., Alva, J., Nilsson, A. K., Karlsson, L., Gaiano, N. et al.** (2007). Dll4 signalling through Notch1 regulates formation of tip cells during angiogenesis. *Nature* **445**, 776-80.
**Henrique, D., Hirsinger, E., Adam, J., Le Roux, I., Pourquié, O., Ish-Horowicz, D. and Lewis, J.** (1997). Maintenance of neuroepithelial progenitor cells by Delta-Notch signaling in the embryonic chick retina. *Curr. Biol.* 7, 661-670.
**Hicks, C., Johnston, S. H., diSibio, G., Collazo, A., Vogt, T. F. and Weinmaster, G.** (2000). Fringe differentially modulates Jagged1 and Delta1 signalling through Notch1 and Notch2. *Nat Cell Biol* **2**, 515-20.
**High, F. A., Zhang, M., Proweller, A., Tu, L., Parmacek, M. S., Pear, W. S. and Epstein, J. A.** (2007). An essential role for Notch in neural crest during cardiovascular development and smooth muscle differentiation. *J Clin Invest* **117**, 353-63.
**Holley, S. A., Geisler, R. and Nusslein-Volhard, C.** (2000). Control of her1 expression during zebrafish somitogenesis by a delta-dependent oscillator and an independent wave-front activity. *Genes Dev.* **14**, 1678-90.
**Holley, S. A., Julich, D., Rauch, G. J., Geisler, R. and Nusslein-Volhard, C.** (2002). her1 and the notch pathway function within the oscillator mechanism that regulates zebrafish somitogenesis. *Development* **129**, 1175-83.
**Hori, K., Fostier, M., Ito, M., Fuwa, T. J., Go, M. J., Okano, H., Baron, M. and Matsuno, K.** (2004). Drosophila deltex mediates suppressor of Hairless-independent and late-endosomal activation of Notch signaling. *Development* **131**, 5527-37.
**Hsieh, J. J., Zhou, S., Chen, L., Young, D. B. and Hayward, S. D.** (1999). CIR, a corepressor linking the DNA binding factor CBF1 to the histone deacetylase complex. *Proc Natl Acad Sci U S A* **96**, 23-8.
**Hubbard, E. J., Wu, G., Kitajewski, J. and Greenwald, I.** (1997). sel-10, a negative regulator of lin-12 activity in Caenorhabditis elegans, encodes a member of the CDC4 family of proteins. *Genes Dev* **11**, 3182-93.

**Hukriede, N. A. and Fleming, R. J.** (1997). Beaded of Goldschmidt, an antimorphic allele of Serrate, encodes a protein lacking transmembrane and intracellular domains. *Genetics* **145**, 359-74.
**Hukriede, N. A., Gu, Y. and Fleming, R. J.** (1997). A dominant-negative form of Serrate acts as a general antagonist of Notch activation. *Development* **124**, 3427-37.
**Ikeuchi, T. and Sisodia, S. S.** (2003). The Notch ligands, Delta1 and Jagged2, are substrates for presenilin-dependent "gamma-secretase" cleavage. *J Biol Chem* **278**, 7751-4.
**Inoue, A., Takahashi, M., Hatta, K., Hotta, Y. and Okamoto, H.** (1994). Developmental regulation of islet-1 mRNA expression during neuronal differentiation in embryonic zebrafish. *Dev Dyn* **199**, 1-11.
**Iovine, M. K. and Johnson, S. L.** (2000). Genetic analysis of isometric growth control mechanisms in the zebrafish caudal Fin. *Genetics* **155**, 1321-9.
**Irvine, K. D.** (1999). Fringe, Notch, and making developmental boundaries. *Curr Opin Genet Dev* **9**, 434-41.
**Isogai, S., Lawson, N. D., Torrealday, S., Horiguchi, M. and Weinstein, B. M.** (2003). Angiogenic network formation in the developing vertebrate trunk. *Development* **130**, 5281-90.
**Itoh, M. and Chitnis, A. B.** (2001). Expression of proneural and neurogenic genes in the zebrafish lateral line primordium correlates with selection of hair cell fate in neuromasts. *Mech Dev* **102**, 263-6.
**Itoh, M., Kim, C. H., Palardy, G., Oda, T., Jiang, Y. J., Maust, D., Yeo, S. Y., Lorick, K., Wright, G. J., Ariza-McNaughton, L. et al.** (2003). Mind bomb is a ubiquitin ligase that is essential for efficient activation of Notch signaling by Delta. *Dev. Cell* **4**, 67-82.
**Jacob, E., Drexel, M., Schwerte, T. and Pelster, B.** (2002). Influence of hypoxia and of hypoxemia on the development of cardiac activity in zebrafish larvae. *Am J Physiol Regul Integr Comp Physiol* **283**, R911-7.
**Jafar-Nejad, H., Andrews, H. K., Acar, M., Bayat, V., Wirtz-Peitz, F., Mehta, S. Q., Knoblich, J. A. and Bellen, H. J.** (2005). Sec15, a component of the exocyst, promotes notch signaling during the asymmetric division of Drosophila sensory organ precursors. *Dev Cell* **9**, 351-63.
**Jain, R. K., Duda, D. G., Clark, J. W. and Loeffler, J. S.** (2006). Lessons from phase III clinical trials on anti-VEGF therapy for cancer. *Nat Clin Pract Oncol* **3**, 24-40.
**Jarriault, S., Brou, C., Logeat, F., Schroeter, E. H., Kopan, R. and Israel, A.** (1995). Signalling downstream of activated mammalian Notch. *Nature* **377**, 355-8.
**Jeffries, S., Robbins, D. J. and Capobianco, A. J.** (2002). Characterization of a high-molecular-weight Notch complex in the nucleus of Notch(ic)-transformed RKE cells and in a human T-cell leukemia cell line. *Mol Cell Biol* **22**, 3927-41.
**Jen, W. C., Wettstein, D., Turner, D., Chitnis, A. and Kintner, C.** (1997). The Notch ligand, X-Delta-2, mediates segmentation of the paraxial mesoderm in Xenopus embryos. *Development* **124**, 1169-78.
**Jiang, Y. J., Aerne, B. L., Smithers, L., Haddon, C., Ish-Horowicz, D. and Lewis, J.** (2000). Notch signalling and the synchronization of the somite segmentation clock. *Nature* **408**, 475-9.

**Jiang, Y. J., Brand, M., Heisenberg, C. P., Beuchle, D., Furutani-Seiki, M., Kelsh, R. N., Warga, R. M., Granato, M., Haffter, P., Hammerschmidt, M. et al.** (1996). Mutations affecting neurogenesis and brain morphology in the zebrafish, Danio rerio. *Development* **123**, 205-16.
**Joutel, A., Corpechot, C., Ducros, A., Vahedi, K., Chabriat, H., Mouton, P., Alamowitch, S., Domenga, V., Cecillion, M., Marechal, E. et al.** (1996). Notch3 mutations in CADASIL, a hereditary adult-onset condition causing stroke and dementia. *Nature* **383**, 707-10.
**Kao, H. Y., Ordentlich, P., Koyano-Nakagawa, N., Tang, Z., Downes, M., Kintner, C. R., Evans, R. M. and Kadesch, T.** (1998). A histone deacetylase corepressor complex regulates the Notch signal transduction pathway. *Genes Dev* **12**, 2269-77.
**Kato, H., Taniguchi, Y., Kurooka, H., Minoguchi, S., Sakai, T., Nomura-Okazaki, S., Tamura, K. and Honjo, T.** (1997). Involvement of RBP-J in biological functions of mouse Notch1 and its derivatives. *Development* **124**, 4133-41.
**Kim, E., Naisbitt, S., Hsueh, Y. P., Rao, A., Rothschild, A., Craig, A. M. and Sheng, M.** (1997). GKAP, a novel synaptic protein that interacts with the guanylate kinase-like domain of the PSD-95/SAP90 family of channel clustering molecules. *J Cell Biol* **136**, 669-78.
**Kim, J., Irvine, K. D. and Carroll, S. B.** (1995). Cell recognition, signal induction, and symmetrical gene activation at the dorsal-ventral boundary of the developing Drosophila wing. *Cell* **82**, 795-802.
**Kimmel, C. B., Ballard, W. W., Kimmel, S. R., Ullmann, B. and Schilling, T. F.** (1995). Stages of embryonic development of the zebrafish. *Dev Dyn* **203**, 253-310.
**Kitagawa, M., Oyama, T., Kawashima, T., Yedvobnick, B., Kumar, A., Matsuno, K. and Harigaya, K.** (2001). A human protein with sequence similarity to Drosophila mastermind coordinates the nuclear form of notch and a CSL protein to build a transcriptional activator complex on target promoters. *Mol Cell Biol* **21**, 4337-46.
**Kiyota, T. and Kinoshita, T.** (2002). Cysteine-rich region of X-Serrate-1 is required for activation of Notch signaling in Xenopus primary neurogenesis. *Int J Dev Biol* **46**, 1057-60.
**Kiyota, T. and Kinoshita, T.** (2004). The intracellular domain of X-Serrate-1 is cleaved and suppresses primary neurogenesis in Xenopus laevis. *Mech Dev* **121**, 573-85.
**Klein, T. and Arias, A. M.** (1998). Interactions among Delta, Serrate and Fringe modulate Notch activity during Drosophila wing development. *Development* **125**, 2951-62.
**Klein, T., Brennan, K. and Arias, A. M.** (1997). An intrinsic dominant negative activity of serrate that is modulated during wing development in Drosophila. *Dev Biol* **189**, 123-34.
**Kodoyianni, V., Maine, E. M. and Kimble, J.** (1992). Molecular basis of loss-of-function mutations in the glp-1 gene of Caenorhabditis elegans. *Mol Biol Cell* **3**, 1199-213.
**Kokubo, H., Miyagawa-Tomita, S., Nakazawa, M., Saga, Y. and Johnson, R. L.** (2005). Mouse hesr1 and hesr2 genes are redundantly required to mediate Notch signaling in the developing cardiovascular system. *Dev Biol* **278**, 301-9.

**Koo, B. K., Yoon, K. J., Yoo, K. W., Lim, H. S., Song, R., So, J. H., Kim, C. H. and Kong, Y. Y.** (2005). Mind bomb-2 is an E3 ligase for Notch ligand. *J Biol Chem* **280**, 22335-42.
**Kopan, R., Nye, J. S. and Weintraub, H.** (1994). The intracellular domain of mouse Notch: a constitutively activated repressor of myogenesis directed at the basic helix-loop-helix region of MyoD. *Development* **120**, 2385-96.
**Kornau, H. C., Schenker, L. T., Kennedy, M. B. and Seeburg, P. H.** (1995). Domain interaction between NMDA receptor subunits and the postsynaptic density protein PSD-95. *Science* **269**, 1737-40.
**Kortschak, R. D., Tamme, R. and Lardelli, M.** (2001). Evolutionary analysis of vertebrate Notch genes. *Dev Genes Evol* **211**, 350-4.
**Krebs, L. T., Shutter, J. R., Tanigaki, K., Honjo, T., Stark, K. L. and Gridley, T.** (2004). Haploinsufficient lethality and formation of arteriovenous malformations in Notch pathway mutants. *Genes Dev.* **18**, 2469-73.
**Krebs, L. T., Xue, Y., Norton, C. R., Shutter, J. R., Maguire, M., Sundberg, J. P., Gallahan, D., Closson, V., Kitajewski, J., Callahan, R. et al.** (2000). Notch signaling is essential for vascular morphogenesis in mice. *Genes Dev.* **14**, 1343-52.
**Kurooka, H. and Honjo, T.** (2000). Functional interaction between the mouse notch1 intracellular region and histone acetyltransferases PCAF and GCN5. *J Biol Chem* **275**, 17211-20.
**Kusumi, K., Sun, E. S., Kerrebrock, A. W., Bronson, R. T., Chi, D. C., Bulotsky, M. S., Spencer, J. B., Birren, B. W., Frankel, W. N. and Lander, E. S.** (1998). The mouse pudgy mutation disrupts Delta homologue Dll3 and initiation of early somite boundaries. *Nat Genet* **19**, 274-8.
**Lai, E. C.** (2004). Notch signaling: control of cell communication and cell fate. *Development* **131**, 965-73.
**Lai, E. C., Deblandre, G. A., Kintner, C. and Rubin, G. M.** (2001). Drosophila neuralized is a ubiquitin ligase that promotes the internalization and degradation of delta. *Dev Cell* **1**, 783-94.
**Lai, E. C., Roegiers, F., Qin, X., Jan, Y. N. and Rubin, G. M.** (2005). The ubiquitin ligase Drosophila Mind bomb promotes Notch signaling by regulating the localization and activity of Serrate and Delta. *Development* **132**, 2319-32.
**Lanford, P. J., Lan, Y., Jiang, R., Lindsell, C., Weinmaster, G., Gridley, T. and Kelley, M. W.** (1999). Notch signalling pathway mediates hair cell development in mammalian cochlea. *Nat Genet* **21**, 289-92.
**Latimer, A. J., Dong, X., Markov, Y. and Appel, B.** (2002). Delta-Notch signaling induces hypochord development in zebrafish. *Development* **129**, 2555-63.
**Laufer, E., Dahn, R., Orozco, O. E., Yeo, C. Y., Pisenti, J., Henrique, D., Abbott, U. K., Fallon, J. F. and Tabin, C.** (1997). Expression of Radical fringe in limb-bud ectoderm regulates apical ectodermal ridge formation. *Nature* **386**, 366-73.
**LaVoie, M. J. and Selkoe, D. J.** (2003). The Notch ligands, Jagged and Delta, are sequentially processed by alpha-secretase and presenilin/gamma-secretase and release signaling fragments. *J. Biol. Chem.* **278**, 34427-37.
**Lawson, N. D., Scheer, N., Pham, V. N., Kim, C. H., Chitnis, A. B., Campos-Ortega, J. A. and Weinstein, B. M.** (2001). Notch signaling is

required for arterial-venous differentiation during embryonic vascular development. *Development* **128**, 3675-83.
**Lawson, N. D., Vogel, A. M. and Weinstein, B. M.** (2002). sonic hedgehog and vascular endothelial growth factor act upstream of the Notch pathway during arterial endothelial differentiation. *Dev. Cell* **3**, 127-36.
**Lawson, N. D. and Weinstein, B. M.** (2002a). Arteries and veins: making a difference with zebrafish. *Nat Rev Genet* **3**, 674-82.
**Lawson, N. D. and Weinstein, B. M.** (2002b). In vivo imaging of embryonic vascular development using transgenic zebrafish. *Dev. Biol.* **248**, 307-18.
**Le Borgne, R., Remaud, S., Hamel, S. and Schweisguth, F.** (2005). Two distinct E3 ubiquitin ligases have complementary functions in the regulation of delta and serrate signaling in Drosophila. *PLoS Biol* **3**, e96.
**Le Borgne, R. and Schweisguth, F.** (2003). Unequal segregation of Neuralized biases Notch activation during asymmetric cell division. *Dev Cell* **5**, 139-48.
**Lebrin, F., Deckers, M., Bertolino, P. and Ten Dijke, P.** (2005). TGF-beta receptor function in the endothelium. *Cardiovasc Res* **65**, 599-608.
**Leong, K. G., Hu, X., Li, L., Noseda, M., Larrivee, B., Hull, C., Hood, L., Wong, F. and Karsan, A.** (2002). Activated Notch4 inhibits angiogenesis: role of beta 1-integrin activation. *Mol. Cell Biol.* **22**, 2830-41.
**Leslie, J. D., Ariza-McNaughton, L., Bermange, A. L., McAdow, R., Johnson, S. L. and Lewis, J.** (2007). Endothelial signalling by the Notch ligand Delta-like 4 restricts angiogenesis. *Development* **134**, 839-44.
**Levy, O. A., Lah, J. J. and Levey, A. I.** (2002). Notch signaling inhibits PC12 cell neurite outgrowth via RBP-J-dependent and -independent mechanisms. *Dev Neurosci* **24**, 79-88.
**Lewis, J.** (1996). Neurogenic genes and vertebrate neurogenesis. *Curr Opin Neurobiol* **6**, 3-10.
**Lewis, J.** (1998). Notch signalling and the control of cell fate choices in vertebrates. *Semin. Cell Dev. Biol.* **9**, 583-9.
**Li, Y. and Baker, N. E.** (2004). The roles of cis-inactivation by Notch ligands and of neuralized during eye and bristle patterning in Drosophila. *BMC Dev Biol* **4**, 5.
**Liu, Z. J., Shirakawa, T., Li, Y., Soma, A., Oka, M., Dotto, G. P., Fairman, R. M., Velazquez, O. C. and Herlyn, M.** (2003). Regulation of Notch1 and Dll4 by vascular endothelial growth factor in arterial endothelial cells: implications for modulating arteriogenesis and angiogenesis. *Mol. Cell Biol.* **23**, 14-25.
**Lobov, I. B., Renard, R. A., Papadopoulos, N., Gale, N. W., Thurston, G., Yancopoulos, G. D. and Wiegand, S. J.** (2007). Delta-like ligand 4 (Dll4) is induced by VEGF as a negative regulator of angiogenic sprouting. *Proc Natl Acad Sci U S A* **104**, 3219-24.
**Logeat, F., Bessia, C., Brou, C., LeBail, O., Jarriault, S., Seidah, N. G. and Israel, A.** (1998). The Notch1 receptor is cleaved constitutively by a furin-like convertase. *Proc Natl Acad Sci U S A* **95**, 8108-12.
**Lopez-Schier, H., Starr, C. J., Kappler, J. A., Kollmar, R. and Hudspeth, A. J.** (2004). Directional cell migration establishes the axes of planar polarity in the posterior lateral-line organ of the zebrafish. *Dev Cell* **7**, 401-12.
**Lorent, K., Yeo, S. Y., Oda, T., Chandrasekharappa, S., Chitnis, A., Matthews, R. P. and Pack, M.** (2004). Inhibition of Jagged-mediated Notch

signaling disrupts zebrafish biliary development and generates multi-organ defects compatible with an Alagille syndrome phenocopy. *Development* **131**, 5753-66.
**Lowell, S. and Watt, F. M.** (2001). Delta regulates keratinocyte spreading and motility independently of differentiation. *Mech. Dev.* **107**, 133-40.
**Lu, X., Le Noble, F., Yuan, L., Jiang, Q., De Lafarge, B., Sugiyama, D., Breant, C., Claes, F., De Smet, F., Thomas, J. L. et al.** (2004). The netrin receptor UNC5B mediates guidance events controlling morphogenesis of the vascular system. *Nature* **432**, 179-86.
**Lubman, O. Y., Korolev, S. V. and Kopan, R.** (2004). Anchoring notch genetics and biochemistry; structural analysis of the ankyrin domain sheds light on existing data. *Mol Cell* **13**, 619-26.
**MacKenzie, F., Duriez, P., Larrivee, B., Chang, L., Pollet, I., Wong, F., Yip, C. and Karsan, A.** (2004). Notch4-induced inhibition of endothelial sprouting requires the ankyrin repeats and involves signaling through RBP-Jkappa. *Blood* **104**, 1760-8.
**Mailhos, C., Modlich, U., Lewis, J., Harris, A., Bicknell, R. and Ish-Horowicz, D.** (2001). Delta4, an endothelial specific Notch ligand expressed at sites of physiological and tumor angiogenesis. *Differentiation* **69**, 135-44.
**Malecki, M. J., Sanchez-Irizarry, C., Mitchell, J. L., Histen, G., Xu, M. L., Aster, J. C. and Blacklow, S. C.** (2006). Leukemia-associated mutations within the NOTCH1 heterodimerization domain fall into at least two distinct mechanistic classes. *Mol Cell Biol* **26**, 4642-51.
**Marchler-Bauer, A., Anderson, J. B., Derbyshire, M. K., DeWeese-Scott, C., Gonzales, N. R., Gwadz, M., Hao, L., He, S., Hurwitz, D. I., Jackson, J. D. et al.** (2007). CDD: a conserved domain database for interactive domain family analysis. *Nucleic Acids Res* **35**, D237-40.
**Matsuno, K., Diederich, R. J., Go, M. J., Blaumueller, C. M. and Artavanis-Tsakonas, S.** (1995). Deltex acts as a positive regulator of Notch signaling through interactions with the Notch ankyrin repeats. *Development* **121**, 2633-44.
**Matsuno, K., Go, M. J., Sun, X., Eastman, D. S. and Artavanis-Tsakonas, S.** (1997). Suppressor of Hairless-independent events in Notch signaling imply novel pathway elements. *Development* **124**, 4265-73.
**Matter, K. and Balda, M. S.** (2003). Signalling to and from tight junctions. *Nat Rev Mol Cell Biol* **4**, 225-36.
**McDaniell, R., Warthen, D. M., Sanchez-Lara, P. A., Pai, A., Krantz, I. D., Piccoli, D. A. and Spinner, N. B.** (2006). NOTCH2 mutations cause Alagille syndrome, a heterogeneous disorder of the notch signaling pathway. *Am J Hum Genet* **79**, 169-73.
**McGrew, M. J., Dale, J. K., Fraboulet, S. and Pourquie, O.** (1998). The lunatic fringe gene is a target of the molecular clock linked to somite segmentation in avian embryos. *Curr Biol* **8**, 979-82.
**Micchelli, C. A., Rulifson, E. J. and Blair, S. S.** (1997). The function and regulation of cut expression on the wing margin of Drosophila: Notch, Wingless and a dominant negative role for Delta and Serrate. *Development* **124**, 1485-95.
**Milan, D. J., Giokas, A. C., Serluca, F. C., Peterson, R. T. and MacRae, C. A.** (2006). Notch1b and neuregulin are required for specification of central cardiac conduction tissue. *Development* **133**, 1125-32.

**Mizuhara, E., Nakatani, T., Minaki, Y., Sakamoto, Y., Ono, Y. and Takai, Y.** (2005). MAGI1 recruits Dll1 to cadherin-based adherens junctions and stabilizes it on the cell surface. *J Biol Chem* **280**, 26499-507.
**Mohamed, S. A., Aherrahrou, Z., Liptau, H., Erasmi, A. W., Hagemann, C., Wrobel, S., Borzym, K., Schunkert, H., Sievers, H. H. and Erdmann, J.** (2006). Novel missense mutations (p.T596M and p.P1797H) in NOTCH1 in patients with bicuspid aortic valve. *Biochem Biophys Res Commun* **345**, 1460-5.
**Moloney, D. J., Panin, V. M., Johnston, S. H., Chen, J., Shao, L., Wilson, R., Wang, Y., Stanley, P., Irvine, K. D., Haltiwanger, R. S. et al.** (2000a). Fringe is a glycosyltransferase that modifies Notch. *Nature* **406**, 369-75.
**Moloney, D. J., Shair, L. H., Lu, F. M., Xia, J., Locke, R., Matta, K. L. and Haltiwanger, R. S.** (2000b). Mammalian Notch1 is modified with two unusual forms of O-linked glycosylation found on epidermal growth factor-like modules. *J Biol Chem* **275**, 9604-11.
**Morimoto, M., Takahashi, Y., Endo, M. and Saga, Y.** (2005). The Mesp2 transcription factor establishes segmental borders by suppressing Notch activity. *Nature* **435**, 354-9.
**Morrison, A., Hodgetts, C., Gossler, A., Hrabe de Angelis, M. and Lewis, J.** (1999). Expression of Delta1 and Serrate1 (Jagged1) in the mouse inner ear. *Mech Dev* **84**, 169-72.
**Moyon, D., Pardanaud, L., Yuan, L., Breant, C. and Eichmann, A.** (2001). Plasticity of endothelial cells during arterial-venous differentiation in the avian embryo. *Development* **128**, 3359-70.
**Mumm, J. S., Schroeter, E. H., Saxena, M. T., Griesemer, A., Tian, X., Pan, D. J., Ray, W. J. and Kopan, R.** (2000). A ligand-induced extracellular cleavage regulates gamma-secretase-like proteolytic activation of Notch1. *Mol Cell* **5**, 197-206.
**Murga, M., Fernandez-Capetillo, O. and Tosato, G.** (2005). Neuropilin-1 regulates attachment in human endothelial cells independently of vascular endothelial growth factor receptor-2. *Blood* **105**, 1992-9.
**Muskavitch, M. A.** (1994). Delta-notch signaling and Drosophila cell fate choice. *Dev Biol* **166**, 415-30.
**Nasevicius, A. and Ekker, S. C.** (2000). Effective targeted gene 'knockdown' in zebrafish. *Nat Genet* **26**, 216-20.
**Nichols, J. T., Miyamoto, A., Olsen, S. L., D'Souza, B., Yao, C. and Weinmaster, G.** (2007). DSL ligand endocytosis physically dissociates Notch1 heterodimers before activating proteolysis can occur. *J Cell Biol* **176**, 445-58.
**Niethammer, M., Kim, E. and Sheng, M.** (1996). Interaction between the C terminus of NMDA receptor subunits and multiple members of the PSD-95 family of membrane-associated guanylate kinases. *J Neurosci* **16**, 2157-63.
**Noguera-Troise, I., Daly, C., Papadopoulos, N. J., Coetzee, S., Boland, P., Gale, N. W., Lin, H. C., Yancopoulos, G. D. and Thurston, G.** (2006). Blockade of Dll4 inhibits tumour growth by promoting non-productive angiogenesis. *Nature* **444**, 1032-7.
**Noseda, M., Chang, L., McLean, G., Grim, J. E., Clurman, B. E., Smith, L. L. and Karsan, A.** (2004). Notch activation induces endothelial cell cycle arrest and participates in contact inhibition: role of p21Cip1 repression. *Mol Cell Biol* **24**, 8813-22.

**Nourry, C., Grant, S. G. and Borg, J. P.** (2003). PDZ domain proteins: plug and play! *Sci STKE* **2003**, RE7.
**Okajima, T. and Irvine, K. D.** (2002). Regulation of notch signaling by o-linked fucose. *Cell* **111**, 893-904.
**Okajima, T., Xu, A. and Irvine, K. D.** (2003). Modulation of notch-ligand binding by protein O-fucosyltransferase 1 and fringe. *J Biol Chem* **278**, 42340-5.
**Oswald, F., Kostezka, U., Astrahantseff, K., Bourteele, S., Dillinger, K., Zechner, U., Ludwig, L., Wilda, M., Hameister, H., Knochel, W. et al.** (2002). SHARP is a novel component of the Notch/RBP-Jkappa signalling pathway. *Embo J* **21**, 5417-26.
**Oswald, F., Liptay, S., Adler, G. and Schmid, R. M.** (1998). NF-kappaB2 is a putative target gene of activated Notch-1 via RBP-Jkappa. *Mol Cell Biol* **18**, 2077-88.
**Oswald, F., Tauber, B., Dobner, T., Bourteele, S., Kostezka, U., Adler, G., Liptay, S. and Schmid, R. M.** (2001). p300 acts as a transcriptional coactivator for mammalian Notch-1. *Mol Cell Biol* **21**, 7761-74.
**Overstreet, E., Fitch, E. and Fischer, J. A.** (2004). Fat facets and Liquid facets promote Delta endocytosis and Delta signaling in the signaling cells. *Development* **131**, 5355-66.
**Palmeirim, I., Henrique, D., Ish-Horowicz, D. and Pourquie, O.** (1997). Avian hairy gene expression identifies a molecular clock linked to vertebrate segmentation and somitogenesis. *Cell* **91**, 639-48.
**Panin, V. M., Papayannopoulos, V., Wilson, R. and Irvine, K. D.** (1997). Fringe modulates Notch-ligand interactions. *Nature* **387**, 908-12.
**Papayannopoulos, V., Tomlinson, A., Panin, V. M., Rauskolb, C. and Irvine, K. D.** (1998). Dorsal-ventral signaling in the Drosophila eye. *Science* **281**, 2031-4.
**Parichy, D. M., Rawls, J. F., Pratt, S. J., Whitfield, T. T. and Johnson, S. L.** (1999). Zebrafish sparse corresponds to an orthologue of c-kit and is required for the morphogenesis of a subpopulation of melanocytes, but is not essential for hematopoiesis or primordial germ cell development. *Development* **126**, 3425-36.
**Paris, D., Quadros, A., Patel, N., DelleDonne, A., Humphrey, J. and Mullan, M.** (2005). Inhibition of angiogenesis and tumor growth by beta and gamma-secretase inhibitors. *Eur. J. Pharmacol.* **514**, 1-15.
**Parks, A. L., Klueg, K. M., Stout, J. R. and Muskavitch, M. A.** (2000). Ligand endocytosis drives receptor dissociation and activation in the Notch pathway. *Development* **127**, 1373-85.
**Parodi, A. J.** (2000). Role of N-oligosaccharide endoplasmic reticulum processing reactions in glycoprotein folding and degradation. *Biochem J* **348 Pt 1**, 1-13.
**Patel, N. S., Li, J. L., Generali, D., Poulsom, R., Cranston, D. W. and Harris, A. L.** (2005). Up-regulation of delta-like 4 ligand in human tumor vasculature and the role of basal expression in endothelial cell function. *Cancer Res.* **65**, 8690-7.
**Pavlopoulos, E., Pitsouli, C., Klueg, K. M., Muskavitch, M. A., Moschonas, N. K. and Delidakis, C.** (2001). neuralized Encodes a peripheral membrane protein involved in delta signaling and endocytosis. *Dev Cell* **1**, 807-16.

**Pear, W. S., Aster, J. C., Scott, M. L., Hasserjian, R. P., Soffer, B., Sklar, J. and Baltimore, D.** (1996). Exclusive development of T cell neoplasms in mice transplanted with bone marrow expressing activated Notch alleles. *J Exp Med* **183**, 2283-91.
**Perez-Moreno, M., Jamora, C. and Fuchs, E.** (2003). Sticky business: orchestrating cellular signals at adherens junctions. *Cell* **112**, 535-48.
**Rand, M. D., Grimm, L. M., Artavanis-Tsakonas, S., Patriub, V., Blacklow, S. C., Sklar, J. and Aster, J. C.** (2000). Calcium depletion dissociates and activates heterodimeric notch receptors. *Mol Cell Biol* **20**, 1825-35.
**Ray, W. J., Yao, M., Mumm, J., Schroeter, E. H., Saftig, P., Wolfe, M., Selkoe, D. J., Kopan, R. and Goate, A. M.** (1999). Cell surface presenilin-1 participates in the gamma-secretase-like proteolysis of Notch. *J Biol Chem* **274**, 36801-7.
**Rebay, I., Fleming, R. J., Fehon, R. G., Cherbas, L., Cherbas, P. and Artavanis-Tsakonas, S.** (1991). Specific EGF repeats of Notch mediate interactions with Delta and Serrate: implications for Notch as a multifunctional receptor. *Cell* **67**, 687-99.
**Rechsteiner, M.** (1988). Regulation of enzyme levels by proteolysis: the role of pest regions. *Adv Enzyme Regul* **27**, 135-51.
**Rehman, A. O. and Wang, C. Y.** (2006). Notch signaling in the regulation of tumor angiogenesis. *Trends Cell Biol* **16**, 293-300.
**Rhyu, M. S., Jan, L. Y. and Jan, Y. N.** (1994). Asymmetric distribution of numb protein during division of the sensory organ precursor cell confers distinct fates to daughter cells. *Cell* **76**, 477-91.
**Ridgway, J., Zhang, G., Wu, Y., Stawicki, S., Liang, W. C., Chanthery, Y., Kowalski, J., Watts, R. J., Callahan, C., Kasman, I. et al.** (2006). Inhibition of Dll4 signalling inhibits tumour growth by deregulating angiogenesis. *Nature* **444**, 1083-7.
**Rodriguez-Esteban, C., Schwabe, J. W., De La Pena, J., Foys, B., Eshelman, B. and Belmonte, J. C.** (1997). Radical fringe positions the apical ectodermal ridge at the dorsoventral boundary of the vertebrate limb. *Nature* **386**, 360-6.
**Ross, D. A. and Kadesch, T.** (2004). Consequences of Notch-mediated induction of Jagged1. *Exp Cell Res* **296**, 173-82.
**Ruhrberg, C., Gerhardt, H., Golding, M., Watson, R., Ioannidou, S., Fujisawa, H., Betsholtz, C. and Shima, D. T.** (2002). Spatially restricted patterning cues provided by heparin-binding VEGF-A control blood vessel branching morphogenesis. *Genes Dev* **16**, 2684-98.
**Sainson, R. C., Aoto, J., Nakatsu, M. N., Holderfield, M., Conn, E., Koller, E. and Hughes, C. C.** (2005). Cell-autonomous notch signaling regulates endothelial cell branching and proliferation during vascular tubulogenesis. *FASEB J.* **19**, 1027-9.
**Saitou, N. and Nei, M.** (1987). The neighbor-joining method: a new method for reconstructing phylogenetic trees. *Mol Biol Evol* **4**, 406-25.
**Sakaguchi, T., Kuroiwa, A. and Takeda, H.** (2001). A novel sox gene, 226D7, acts downstream of Nodal signaling to specify endoderm precursors in zebrafish. *Mech. Dev.* **107**, 25-38.

**Sakamoto, K., Ohara, O., Takagi, M., Takeda, S. and Katsube, K.** (2002). Intracellular cell-autonomous association of Notch and its ligands: a novel mechanism of Notch signal modification. *Dev Biol* **241**, 313-26.
**Sakata, T., Sakaguchi, H., Tsuda, L., Higashitani, A., Aigaki, T., Matsuno, K. and Hayashi, S.** (2004). Drosophila Nedd4 regulates endocytosis of notch and suppresses its ligand-independent activation. *Curr Biol* **14**, 2228-36.
**Sandoval, I. V., Martinez-Arca, S., Valdueza, J., Palacios, S. and Holman, G. D.** (2000). Distinct reading of different structural determinants modulates the dileucine-mediated transport steps of the lysosomal membrane protein LIMPII and the insulin-sensitive glucose transporter GLUT4. *J Biol Chem* **275**, 39874-85.
**Sasamura, T., Sasaki, N., Miyashita, F., Nakao, S., Ishikawa, H. O., Ito, M., Kitagawa, M., Harigaya, K., Spana, E., Bilder, D. et al.** (2003). neurotic, a novel maternal neurogenic gene, encodes an O-fucosyltransferase that is essential for Notch-Delta interactions. *Development* **130**, 4785-95.
**Satoh, K., Yanai, H., Senda, T., Kohu, K., Nakamura, T., Okumura, N., Matsumine, A., Kobayashi, S., Toyoshima, K. and Akiyama, T.** (1997). DAP-1, a novel protein that interacts with the guanylate kinase-like domains of hDLG and PSD-95. *Genes Cells* **2**, 415-24.
**Scehnet, J. S., Jiang, W., Kumar, S. R., Krasnoperov, V., Trindade, A., Benedito, R., Djokovic, D., Borges, C., Ley, E. J., Duarte, A. et al.** (2007). Inhibition of Dll4 mediated signaling induces proliferation of immature vessels and results in poor tissue perfusion. *Blood.*
**Scheer, N., Groth, A., Hans, S. and Campos-Ortega, J. A.** (2001). An instructive function for Notch in promoting gliogenesis in the zebrafish retina. *Development* **128**, 1099-107.
**Schweisguth, F.** (1999). Dominant-negative mutation in the beta2 and beta6 proteasome subunit genes affect alternative cell fate decisions in the Drosophila sense organ lineage. *Proc Natl Acad Sci U S A* **96**, 11382-6.
**Selkoe, D. and Kopan, R.** (2003). Notch and Presenilin: regulated intramembrane proteolysis links development and degeneration. *Annu. Rev. Neurosci.*
**Seugnet, L., Simpson, P. and Haenlin, M.** (1997). Requirement for dynamin during Notch signaling in Drosophila neurogenesis. *Dev Biol* **192**, 585-98.
**Shaw, K. M., Castranova, D. A., Pham, V. N., Kamei, M., Kidd, K. R., Lo, B. D., Torres-Vasquez, J., Ruby, A. and Weinstein, B. M.** (2006). fused-somites-like mutants exhibit defects in trunk vessel patterning. *Dev Dyn* **235**, 1753-60.
**Shi, S. and Stanley, P.** (2003). Protein O-fucosyltransferase 1 is an essential component of Notch signaling pathways. *Proc Natl Acad Sci U S A* **100**, 5234-9.
**Shih, T. and Lindley, C.** (2006). Bevacizumab: an angiogenesis inhibitor for the treatment of solid malignancies. *Clin Ther* **28**, 1779-802.
**Shimizu, K., Chiba, S., Saito, T., Kumano, K., Takahashi, T. and Hirai, H.** (2001). Manic fringe and lunatic fringe modify different sites of the Notch2 extracellular region, resulting in different signaling modulation. *J Biol Chem* **276**, 25753-8.

**Shutter, J. R., Scully, S., Fan, W., Richards, W. G., Kitajewski, J., Deblandre, G. A., Kintner, C. R. and Stark, K. L.** (2000). Dll4, a novel Notch ligand expressed in arterial endothelium. *Genes Dev.* **14**, 1313-8.
**Siekmann, A. F. and Lawson, N. D.** (2007). Notch signalling limits angiogenic cell behaviour in developing zebrafish arteries. *Nature* **445**, 781-4.
**Six, E., Ndiaye, D., Laabi, Y., Brou, C., Gupta-Rossi, N., Israel, A. and Logeat, F.** (2003). The Notch ligand Delta1 is sequentially cleaved by an ADAM protease and gamma-secretase. *Proc Natl Acad Sci U S A* **100**, 7638-43.
**Six, E. M., Ndiaye, D., Sauer, G., Laabi, Y., Athman, R., Cumano, A., Brou, C., Israel, A. and Logeat, F.** (2004). The notch ligand Delta1 recruits Dlg1 at cell-cell contacts and regulates cell migration. *J Biol Chem* **279**, 55818-26.
**Smithers, L., Haddon, C., Jiang, Y. J. and Lewis, J.** (2000). Sequence and embryonic expression of deltaC in the zebrafish. *Mech. Dev.* **90**, 119-23.
**Soker, S., Fidder, H., Neufeld, G. and Klagsbrun, M.** (1996). Characterization of novel vascular endothelial growth factor (VEGF) receptors on tumor cells that bind VEGF165 via its exon 7-encoded domain. *J Biol Chem* **271**, 5761-7.
**Soker, S., Miao, H. Q., Nomi, M., Takashima, S. and Klagsbrun, M.** (2002). VEGF165 mediates formation of complexes containing VEGFR-2 and neuropilin-1 that enhance VEGF165-receptor binding. *J Cell Biochem* **85**, 357-68.
**Soker, S., Takashima, S., Miao, H. Q., Neufeld, G. and Klagsbrun, M.** (1998). Neuropilin-1 is expressed by endothelial and tumor cells as an isoform-specific receptor for vascular endothelial growth factor. *Cell* **92**, 735-45.
**Song, W., Nadeau, P., Yuan, M., Yang, X., Shen, J. and Yankner, B. A.** (1999). Proteolytic release and nuclear translocation of Notch-1 are induced by presenilin-1 and impaired by pathogenic presenilin-1 mutations. *Proc Natl Acad Sci U S A* **96**, 6959-63.
**Songyang, Z., Fanning, A. S., Fu, C., Xu, J., Marfatia, S. M., Chishti, A. H., Crompton, A., Chan, A. C., Anderson, J. M. and Cantley, L. C.** (1997). Recognition of unique carboxyl-terminal motifs by distinct PDZ domains. *Science* **275**, 73-7.
**Sood, R., English, M. A., Jones, M., Mullikin, J., Wang, D. M., Anderson, M., Wu, D., Chandrasekharappa, S. C., Yu, J., Zhang, J. et al.** (2006). Methods for reverse genetic screening in zebrafish by resequencing and TILLING. *Methods* **39**, 220-7.
**Spana, E. P. and Doe, C. Q.** (1996). Numb antagonizes Notch signaling to specify sibling neuron cell fates. *Neuron* **17**, 21-6.
**Spana, E. P., Kopczynski, C., Goodman, C. S. and Doe, C. Q.** (1995). Asymmetric localization of numb autonomously determines sibling neuron identity in the Drosophila CNS. *Development* **121**, 3489-94.
**Stone, L. S.** (1922). Experiments on the development of the lateral line sense organs in *Amblystomea punctatum*. *J. Exp. Zool.* **35**, 421--496.
**Stone, L. S.** (1933). The development of lateral-line sense organs in amphibians observed in living and vital-stained preparations. *J. Comp. Neurol.* **57**, 507-540.

**Struhl, G. and Adachi, A.** (1998). Nuclear access and action of notch in vivo. *Cell* **93**, 649-60.
**Struhl, G. and Greenwald, I.** (1999). Presenilin is required for activity and nuclear access of Notch in Drosophila. *Nature* **398**, 522-5.
**Suchting, S., Freitas, C., le Noble, F., Benedito, R., Breant, C., Duarte, A. and Eichmann, A.** (2007). The Notch ligand Delta-like 4 negatively regulates endothelial tip cell formation and vessel branching. *Proc Natl Acad Sci U S A* **104**, 3225-30.
**Sudol, M., Chen, H. I., Bougeret, C., Einbond, A. and Bork, P.** (1995). Characterization of a novel protein-binding module--the WW domain. *FEBS Lett* **369**, 67-71.
**Sun, X. and Artavanis-Tsakonas, S.** (1996). The intracellular deletions of Delta and Serrate define dominant negative forms of the Drosophila Notch ligands. *Development* **122**, 2465-74.
**Sun, X. and Artavanis-Tsakonas, S.** (1997). Secreted forms of DELTA and SERRATE define antagonists of Notch signaling in Drosophila. *Development* **124**, 3439-48.
**Takahashi, Y.** (2005). Common mechanisms for boundary formation in somitogenesis and brain development: shaping the 'chic' chick. *Int J Dev Biol* **49**, 221-30.
**Takahashi, Y., Koizumi, K., Takagi, A., Kitajima, S., Inoue, T., Koseki, H. and Saga, Y.** (2000). Mesp2 initiates somite segmentation through the Notch signalling pathway. *Nat Genet* **25**, 390-6.
**Takeuchi, M., Hata, Y., Hirao, K., Toyoda, A., Irie, M. and Takai, Y.** (1997). SAPAPs. A family of PSD-95/SAP90-associated proteins localized at postsynaptic density. *J Biol Chem* **272**, 11943-51.
**Tamura, K., Taniguchi, Y., Minoguchi, S., Sakai, T., Tun, T., Furukawa, T. and Honjo, T.** (1995). Physical interaction between a novel domain of the receptor Notch and the transcription factor RBP-J kappa/Su(H). *Curr Biol* **5**, 1416-23.
**Tani, S., Kurooka, H., Aoki, T., Hashimoto, N. and Honjo, T.** (2001). The N- and C-terminal regions of RBP-J interact with the ankyrin repeats of Notch1 RAMIC to activate transcription. *Nucleic Acids Res* **29**, 1373-80.
**Taniguchi, Y., Furukawa, T., Tun, T., Han, H. and Honjo, T.** (1998). LIM protein KyoT2 negatively regulates transcription by association with the RBP-J DNA-binding protein. *Mol Cell Biol* **18**, 644-54.
**Taylor, J. S., Braasch, I., Frickey, T., Meyer, A. and Van de Peer, Y.** (2003). Genome duplication, a trait shared by 22000 species of ray-finned fish. *Genome Res* **13**, 382-90.
**Taylor, J. S., Van de Peer, Y., Braasch, I. and Meyer, A.** (2001). Comparative genomics provides evidence for an ancient genome duplication event in fish. *Philos Trans R Soc Lond B Biol Sci* **356**, 1661-79.
**Taylor, K. L., Henderson, A. M. and Hughes, C. C.** (2002). Notch activation during endothelial cell network formation in vitro targets the basic HLH transcription factor HESR-1 and downregulates VEGFR-2/KDR expression. *Microvasc Res* **64**, 372-83.
**Thompson, J. D., Higgins, D. G. and Gibson, T. J.** (1994). CLUSTAL W: improving the sensitivity of progressive multiple sequence alignment through sequence weighting, position-specific gap penalties and weight matrix choice. *Nucleic Acids Res* **22**, 4673-80.

**Thurston, G.** (2003). Role of Angiopoietins and Tie receptor tyrosine kinases in angiogenesis and lymphangiogenesis. *Cell Tissue Res* **314**, 61-8.
**Tian, X., Hansen, D., Schedl, T. and Skeath, J. B.** (2004). Epsin potentiates Notch pathway activity in Drosophila and C. elegans. *Development* **131**, 5807-15.
**Tobin, J.** (2005). Characterising the Significance of the Interaction Between Delta and MAGI proteins in Zebrafish Neural Development. In *Biological Science*, (ed. Oxford: University of Oxford.
**Torres-Vazquez, J., Gitler, A. D., Fraser, S. D., Berk, J. D., Pham, V. N., Fishman, M. C., Childs, S., Epstein, J. A. and Weinstein, B. M.** (2004). Semaphorin-plexin signaling guides patterning of the developing vasculature. *Dev Cell* **7**, 117-23.
**Tsunoda, S., Sierralta, J., Sun, Y., Bodner, R., Suzuki, E., Becker, A., Socolich, M. and Zuker, C. S.** (1997). A multivalent PDZ-domain protein assembles signalling complexes in a G-protein-coupled cascade. *Nature* **388**, 243-9.
**Turner, D. L. and Weintraub, H.** (1994). Expression of achaete-scute homolog 3 in Xenopus embryos converts ectodermal cells to a neural fate. *Genes Dev* **8**, 1434-47.
**Uyttendaele, H., Ho, J., Rossant, J. and Kitajewski, J.** (2001). Vascular patterning defects associated with expression of activated Notch4 in embryonic endothelium. *Proc. Natl. Acad. Sci. U. S. A.* **98**, 5643-8.
**van Eeden, F. J., Granato, M., Schach, U., Brand, M., Furutani-Seiki, M., Haffter, P., Hammerschmidt, M., Heisenberg, C. P., Jiang, Y. J., Kane, D. A. et al.** (1996a). Mutations affecting somite formation and patterning in the zebrafish, Danio rerio. *Development* **123**, 153-64.
**van Eeden, F. J., Granato, M., Schach, U., Brand, M., Furutani-Seiki, M., Haffter, P., Hammerschmidt, M., Heisenberg, C. P., Jiang, Y. J., Kane, D. A. et al.** (1996b). Genetic analysis of fin formation in the zebrafish, Danio rerio. *Development* **123**, 255-62.
**Villa, N., Walker, L., Lindsell, C. E., Gasson, J., Iruela-Arispe, M. L. and Weinmaster, G.** (2001). Vascular expression of Notch pathway receptors and ligands is restricted to arterial vessels. *Mech Dev* **108**, 161-4.
**Wallberg, A. E., Pedersen, K., Lendahl, U. and Roeder, R. G.** (2002). p300 and PCAF act cooperatively to mediate transcriptional activation from chromatin templates by notch intracellular domains in vitro. *Mol Cell Biol* **22**, 7812-9.
**Wang, H. U., Chen, Z. F. and Anderson, D. J.** (1998). Molecular distinction and angiogenic interaction between embryonic arteries and veins revealed by ephrin-B2 and its receptor Eph-B4. *Cell* **93**, 741-53.
**Wang, J., Shelly, L., Miele, L., Boykins, R., Norcross, M. A. and Guan, E.** (2001). Human Notch-1 inhibits NF-kappa B activity in the nucleus through a direct interaction involving a novel domain. *J Immunol* **167**, 289-95.
**Wang, L., Zeng, H., Wang, P., Soker, S. and Mukhopadhyay, D.** (2003). Neuropilin-1-mediated vascular permeability factor/vascular endothelial growth factor-dependent endothelial cell migration. *J Biol Chem* **278**, 48848-60.
**Wang, W. and Struhl, G.** (2004). Drosophila Epsin mediates a select endocytic pathway that DSL ligands must enter to activate Notch. *Development* **131**, 5367-80.

**Wang, W. and Struhl, G.** (2005). Distinct roles for Mind bomb, Neuralized and Epsin in mediating DSL endocytosis and signaling in Drosophila. *Development* **132**, 2883-94.
**Wang, X., Adam, J. C. and Montell, D.** (2007). Spatially localized Kuzbanian required for specific activation of Notch during border cell migration. *Dev Biol* **301**, 532-40.
**Warthen, D. M., Moore, E. C., Kamath, B. M., Morrissette, J. J., Sanchez, P., Piccoli, D. A., Krantz, I. D. and Spinner, N. B.** (2006). Jagged1 (JAG1) mutations in Alagille syndrome: increasing the mutation detection rate. *Hum Mutat* **27**, 436-43.
**Weinberg, E. S., Allende, M. L., Kelly, C. S., Abdelhamid, A., Murakami, T., Andermann, P., Doerre, O. G., Grunwald, D. J. and Riggleman, B.** (1996). Developmental regulation of zebrafish MyoD in wild-type, no tail and spadetail embryos. *Development* **122**, 271-80.
**Weng, A. P., Ferrando, A. A., Lee, W., Morris, J. P. t., Silverman, L. B., Sanchez-Irizarry, C., Blacklow, S. C., Look, A. T. and Aster, J. C.** (2004). Activating mutations of NOTCH1 in human T cell acute lymphoblastic leukemia. *Science* **306**, 269-71.
**Westerfield, M.** (2000). The zebrafish book. A guide for the laboratory use of zebrafish (Danio rerio). Eugene, OR: Univ. of Oregon Press.
**Westin, J. and Lardelli, M.** (1997). Three novel Notch genes in zebrafish: implications for vertebrate Notch gene evolution and function. *Dev. Genes Evol.* **207**, 51-63.
**Wharton, K. A., Johansen, K. M., Xu, T. and Artavanis-Tsakonas, S.** (1985). Nucleotide sequence from the neurogenic locus notch implies a gene product that shares homology with proteins containing EGF-like repeats. *Cell* **43**, 567-81.
**Whitaker, G. B., Limberg, B. J. and Rosenbaum, J. S.** (2001). Vascular endothelial growth factor receptor-2 and neuropilin-1 form a receptor complex that is responsible for the differential signaling potency of VEGF(165) and VEGF(121). *J Biol Chem* **276**, 25520-31.
**Whitfield, T., Haddon, C. and Lewis, J.** (1997). Intercellular signals and cell-fate choices in the developing inner ear: origins of global and of fine-grained pattern. *Semin Cell Dev Biol* **8**, 239-247.
**Wienholds, E., van Eeden, F., Kosters, M., Mudde, J., Plasterk, R. H. and Cuppen, E.** (2003). Efficient target-selected mutagenesis in zebrafish. *Genome Res* **13**, 2700-7.
**Wilkin, M. B., Carbery, A. M., Fostier, M., Aslam, H., Mazaleyrat, S. L., Higgs, J., Myat, A., Evans, D. A., Cornell, M. and Baron, M.** (2004). Regulation of notch endosomal sorting and signaling by Drosophila Nedd4 family proteins. *Curr Biol* **14**, 2237-44.
**Williams, C. K., Li, J. L., Murga, M., Harris, A. L. and Tosato, G.** (2006). Up-regulation of the Notch ligand Delta-like 4 inhibits VEGF-induced endothelial cell function. *Blood* **107**, 931-9.
**Wright, G. J., Leslie, J. D., Ariza-McNaughton, L. and Lewis, J.** (2004). Delta proteins and MAGI proteins: an interaction of Notch ligands with intracellular scaffolding molecules and its significance for zebrafish development. *Development* **131**, 5659-69.
**Wu, L., Aster, J. C., Blacklow, S. C., Lake, R., Artavanis-Tsakonas, S. and Griffin, J. D.** (2000). MAML1, a human homologue of Drosophila

mastermind, is a transcriptional co-activator for NOTCH receptors. *Nat Genet* **26**, 484-9.
**Xu, A., Lei, L. and Irvine, K. D.** (2005). Regions of Drosophila Notch that contribute to ligand binding and the modulatory influence of Fringe. *J Biol Chem* **280**, 30158-65.
**Xu, T. and Artavanis-Tsakonas, S.** (1990). deltex, a locus interacting with the neurogenic genes, Notch, Delta and mastermind in Drosophila melanogaster. *Genetics* **126**, 665-77.
**Xue, Y., Gao, X., Lindsell, C. E., Norton, C. R., Chang, B., Hicks, C., Gendron-Maguire, M., Rand, E. B., Weinmaster, G. and Gridley, T.** (1999). Embryonic lethality and vascular defects in mice lacking the Notch ligand Jagged1. *Hum. Mol. Genet.* **8**, 723-30.
**Yan, Y. L., Hatta, K., Riggleman, B. and Postlethwait, J. H.** (1995). Expression of a type II collagen gene in the zebrafish embryonic axis. *Dev Dyn* **203**, 363-76.
**Ye, Y., Lukinova, N. and Fortini, M. E.** (1999). Neurogenic phenotypes and altered Notch processing in Drosophila Presenilin mutants. *Nature* **398**, 525-9.
**Yeh, E., Dermer, M., Commisso, C., Zhou, L., McGlade, C. J. and Boulianne, G. L.** (2001). Neuralized functions as an E3 ubiquitin ligase during Drosophila development. *Curr Biol* **11**, 1675-9.
**Zecchini, V., Brennan, K. and Martinez-Arias, A.** (1999). An activity of Notch regulates JNK signalling and affects dorsal closure in Drosophila. *Curr Biol* **9**, 460-9.
**Zeng, Q., Li, S., Chepeha, D. B., Giordano, T. J., Li, J., Zhang, H., Polverini, P. J., Nor, J., Kitajewski, J. and Wang, C. Y.** (2005). Crosstalk between tumor and endothelial cells promotes tumor angiogenesis by MAPK activation of Notch signaling. *Cancer Cell* **8**, 13-23.
**Zhang, C., Li, Q. and Jiang, Y. J.** (2007). Zebrafish Mib and Mib2 are mutual E3 ubiquitin ligases with common and specific delta substrates. *J Mol Biol* **366**, 1115-28.
**Zhang, N. and Gridley, T.** (1998). Defects in somite formation in lunatic fringe-deficient mice. *Nature* **394**, 374-7.
**Zhou, S., Fujimuro, M., Hsieh, J. J., Chen, L. and Hayward, S. D.** (2000a). A role for SKIP in EBNA2 activation of CBF1-repressed promoters. *J Virol* **74**, 1939-47.
**Zhou, S., Fujimuro, M., Hsieh, J. J., Chen, L., Miyamoto, A., Weinmaster, G. and Hayward, S. D.** (2000b). SKIP, a CBF1-associated protein, interacts with the ankyrin repeat domain of NotchIC To facilitate NotchIC function. *Mol Cell Biol* **20**, 2400-10.
**Zimrin, A. B., Pepper, M. S., McMahon, G. A., Nguyen, F., Montesano, R. and Maciag, T.** (1996). An antisense oligonucleotide to the notch ligand jagged enhances fibroblast growth factor-induced angiogenesis in vitro. *J Biol Chem* **271**, 32499-502.

# Appendix

# Delta proteins and MAGI proteins: an interaction of Notch ligands with intracellular scaffolding molecules and its significance for zebrafish development

**Gavin J. Wright[1,2,*], Jonathan D. Leslie[1,*], Linda Ariza-McNaughton[1] and Julian Lewis[1,†]**

[1]Vertebrate Development Laboratory, Cancer Research UK London Research Institute, 44 Lincoln's Inn Fields, London WC2A 3PX, UK
[2]Vertebrate Functional Proteomics Laboratory, Wellcome Trust Sanger Institute, Cambridge CB10 1SA, UK
*These authors contributed equally to this work
†Author for correspondence (e-mail: julian.lewis@cancer.org.uk)

*Accepted 23 August 2004*

Development 131, 5659-5669
Published by The Company of Biologists 2004
doi:10.1242/dev.01417

## Summary

**Delta proteins activate Notch through a binding reaction that depends on their extracellular domains; but the intracellular (C-terminal) domains of the Deltas also have significant functions. All classes of vertebrates possess a subset of Delta proteins with a conserved ATEV* motif at their C termini. These ATEV Deltas include Delta1 and Delta4 in mammals and DeltaD and DeltaC in the zebrafish. We show that these Deltas associate with the membrane-associated scaffolding proteins MAGI1, MAGI2 and MAGI3, through a direct interaction between the C termini of the Deltas and a specific PDZ domain (PDZ4) of the MAGIs. In cultured cells and in subsets of cells in the intact zebrafish embryo, DeltaD and MAGI1 are co-localized at the plasma membrane. The interaction and the co-localization can be abolished by injection of a morpholino that blocks the mRNA splicing reaction that gives DeltaD its terminal valine, on which the interaction depends. Embryos treated in this way appear normal with respect to some known functions of DeltaD as a Notch ligand, including the control of somite segmentation, neurogenesis, and hypochord formation. They do, however, show an anomalous distribution of Rohon-Beard neurons in the dorsal neural tube, suggesting that the Delta-MAGI interaction may play some part in the control of neuron migration.**

Key words: DeltaD, DeltaC, MAGI proteins, Notch, PDZ domains, Zebrafish, Morpholino, Rohon-Beard neurons

## Introduction

The Notch cell-to-cell signalling pathway has a central role in animal development, controlling cell diversification and many other processes in a great variety of tissues (Artavanis-Tsakonas et al., 1999; Lewis, 1998). At its core lie the Notch family of receptors and their ligands, the proteins of the Delta/Serrate family. Both the receptors and the ligands are single-pass type I transmembrane glycoproteins, which are thought to interact at sites of cell-cell contact. Signalling is initiated when the extracellular domain of the ligand interacts with that of the receptor, resulting in a proteolytic cleavage that releases an intracellular fragment of Notch, $N^{ICD}$, which translocates to the cell nucleus and regulates transcription of various target genes (Selkoe and Kopan, 2003).

From this perspective, it might seem that the only part of the ligand that really matters is the part that binds to Notch. There are, however, strong grounds for believing that the intracellular domains of Notch ligands are functionally important. The Delta subfamily has attracted most attention in this respect and is our concern in this paper. There are four main lines of evidence, to which the present study adds a fifth.

First, when the intracellular (C-terminal) domain of Delta is truncated, the protein acquires a powerful dominant-negative effect, blocking Notch signalling in cis (Chitnis et al., 1995; Haddon et al., 1998; Henrique et al., 1997; Sun and Artavanis-Tsakonas, 1996). The cell expressing the truncated Delta protein is thereby made insensitive to Notch-activating signals from its neighbours (Henrique et al., 1997; Sakamoto et al., 2002). It is not clear how the intracellular domain of Delta influences this effect.

Second, the intracellular domain of Delta contains sites for ubiquitination, and this is crucial for Delta function (Itoh et al., 2003; Lai et al., 2001; Pavlopoulos et al., 2001; Yeh et al., 2000). The ubiquitination promotes internalization of Delta, targets Delta for degradation in proteasomes, and, most importantly, is required in order to enable Delta to activate Notch. The effect operates in trans, affecting the ability of the cell to deliver a signal to its neighbours, and it is distinct from the dominant-negative cis effect described above, which is independent of ubiquitination (Itoh et al., 2003).

Third, recent work has shown that the Notch ligands, like Notch itself, are cleaved, releasing an intracellular fragment. This may have a function in the nucleus as a transcriptional regulator (Ikeuchi and Sisodia, 2003; LaVoie and Selkoe, 2003; Six et al., 2003).

The fourth line of evidence for importance of the intracellular domain of Delta comes from sequence

comparisons among the vertebrates: within this group, it is highly conserved (although it shows no detectable conservation between vertebrates and insects). For example, the Delta1 (DLL1) protein of humans has an intracellular domain that is 67% identical to that of chick Delta1, 61% identical to that of *Xenopus* X-Delta1 and 56% identical to that of zebrafish DeltaD. In all vertebrates, and in at least one echinoderm (Sweet et al., 2002), we find a subset of Delta proteins that share a conserved motif – ATEV* – at their C terminus. This motif fits the consensus for a PDZ-domain-binding protein (Nourry et al., 2003; Songyang et al., 1997). The ATEV subset of Delta proteins includes Delta1 and Delta4 in mammals and birds, Delta1 and Delta2 in *Xenopus*, and DeltaC and DeltaD in zebrafish. From their expression patterns, it seems that the ATEV Deltas have some functions in common that set them apart from other vertebrate Deltas that lack this motif. They are expressed in endothelial cells of blood vessels (Beckers et al., 1999; Mailhos et al., 2001; Shutter et al., 2000; Smithers et al., 2000), in the gut epithelium (Schroder and Gossler, 2002) (M. Skipper, G.J.W., L.A.-M. and C. Crosnier, unpublished), and in the presomitic mesoderm, where they play an essential part in the oscillator mechanism that controls somite segmentation (Davis et al., 2001; Holley et al., 2002; Hrabé de Angelis et al., 1997; Jen et al., 1997; Jiang et al., 2000).

On the other hand, the ATEV motif is not required for the core function of Delta proteins in the central nervous system (CNS) as mediators of lateral inhibition during neurogenesis: all members of the vertebrate Delta family seem to share this activity (e.g. Haddon et al., 1998), regardless of whether or not they possess a terminal ATEV. Moreover, removal of the ATEV is not sufficient to confer dominant-negative activity: in the chick retina, a version of Delta1 with a mild C-terminal truncation, removing the ATEV motif along with 96 adjacent amino acids, still showed normal function, activating Notch and delivering lateral inhibition; only with a more severe truncation, eliminating all but 13 amino acids of the intracellular domain, was a dominant-negative effect seen (Henrique et al., 1997).

What then is the function of the ATEV motif? In this paper we show that it mediates binding to MAGI proteins (MAGUK proteins with inverted domain arrangement) – a subset of the MAGUK (membrane-associated guanylate kinase homolog) protein family – through a specific one of the six PDZ domains that these contain. A similar conclusion has recently been reached independently by another group (Pfister et al., 2003), who have shown that the mouse Delta1 protein binds through its C terminus to Acvrinp-1, also known as MAGI2. Our data demonstrate that in fact all three members of the MAGI protein family can bind ATEV Delta proteins in this way. We show that MAGI1 is widely expressed in the developing zebrafish embryo, and that it co-localizes with DeltaD at a subcellular level if and only if the ATEV motif is intact. We find, furthermore, that disruption of the DeltaD-MAGI interaction leaves Delta-Notch signalling practically unaffected; but it appears to alter the migratory behaviour of some neurons in the embryonic neural tube.

## Materials and methods

### Animals

Zebrafish were maintained at 27.5°C on a 14/10 hour light/dark cycle and embryos collected from spontaneous spawnings. Staging was according to Kimmel at al. (Kimmel et al., 1995).

### Isolation of binding partners of Delta proteins

We used a modification of the protocol of Hutchings et al. (Hutchings et al., 2003). A peptide corresponding to the C-terminal 27 residues of human Delta1 was chemically synthesized containing an N-terminal biotin and aliphatic spacer. Peptide-saturated streptavidin-coated paramagnetic beads (Dynabeads® M-280, DYNAL®) were added to an adult mouse brain lysate [0.1 g wet weight per ml of WOP-40 buffer (Wright et al., 2000)]. The brains were crudely chopped in buffer and solubilized using a dounce homogenizer at 4°C. Insoluble material was removed by centrifugation at 400 *g* and the supernatant filtered. The beads were recovered with a magnet after an overnight rotating incubation at 4°C, and washed; associated proteins were eluted by boiling in SDS loading buffer.

### Mass spectrometry

Samples were resolved on 4-12% Bis-Tris NuPAGE™ precast gels and stained using SYPRO Orange dye (BIO-RAD) and scanned on a STORM 860 phosphoimager (Molecular Dynamics). Gels were then Coomassie stained and bands excised with a scalpel. Gel slices were destained and digested with 100-200 ng of trypsin for 4 hours at 37°C. Peptides were extracted and analysed by MALDI on a Tof Spec 2E (Micromass).

### Morpholino and mRNA injections

Injected reagents were diluted in Danieau buffer (Nasevicius and Ekker, 2000) containing 0.2% phenol red and 2-4 nl were injected into the yolk of 1- to 4-cell stage embryos. Morpholino sequences (GeneTools) are: for Delta splicing (MO[dlD-V]): GGTTTTGGACTTACCTCGGTTGCAA, with mismatch control GcTTTTcGACTTAgCTCGcTTcCAA; and for MAGI1 translation blocking (MO[MAGI1]): CACAGAAACAGGTGGCTCCGCTGAC (FITC-labelled). The MAGI-GFP fusion was made in pEGFP-N1 (Clontech) with the introduction of a linker (the protein product contains the sequences VFTP-GGVPRARDPPVAT-MVSK, where the first four and last four amino acids correspond to the C terminus of MAGI1 and N-terminus of EGFP respectively). The coding regions were then subcloned into the pCS2+ vector and mRNA was made using the mMessage mMachine kit (Ambion). For immunohistochemistry, embryos were dechorionated, fixed and stained with zdd2 anti-DeltaD monoclonal antibody and Alexa594-conjugated secondary antibody (Molecular Probes) as previously described (Itoh et al., 2003). MAGI1-EGFP was detected with Alexa488-conjugated rabbit anti-GFP antibody (Molecular Probes). Stained embryos were flat-mounted on slides in Citifluor mounting medium (Citifluor) and examined with a Zeiss LSM510 confocal microscope.

For analysis of phenotypes in the living state, embryos were anaesthetized, mounted in 3% methyl cellulose, and photographed on a Leitz Diaplan microscope.

### PDZ domain binding biochemistry

Sequences (available on request) corresponding to the six individual PDZ domains of zebrafish MAGI1 were amplified and cloned in-frame with a C-terminal 6 histidine tag in pET-23b and expressed in the *E. coli* strain BL21(DE3)pLysS. Proteins were purified using Nickel-NTA Agarose (Qiagen) using minor modifications to the manufacturer's protocols and stored at –70°C.

Biotinylated peptides corresponding to the C-terminal 27 or 26 amino acids of zebrafish DeltaC and D were synthesized as above, both with, and without, the C-terminal valine residue. 200 μl of streptavidin-coated Sepharose (Amersham Biosciences) was saturated with peptides corresponding to zebrafish DeltaC or D and divided equally into six aliquots; 12 μg of purified zfMAGI1 PDZ domains were added per tube and incubated with rotation at 4°C for 2 hours,

washed and eluted by adding SDS-PAGE loading buffer and heating to 50°C for 10 minutes. Eluates were resolved by SDS-PAGE on 4-12% NuPAGE gels using MES running buffer. Gels were stained with SYPRO orange as above.

### In situ hybridization

Wholemount in situ hybridization followed the protocol of Thisse (Westerfield, 2000) or of Ariza-McNaughton and Krumlauf (Ariza-McNaughton and Krumlauf, 2002). DIG-labelled antisense probes for zebrafish MAGI corresponded to nucleotides 3018 to 3530 of the *magi1* cDNA sequence. Probes for *islet1* (Inoue et al., 1994), *col2a1* (Yan et al., 1995) and *myoD* (Weinberg et al., 1996) were as previously described.

### PCR and cloning procedures

Total RNA was extracted from embryos using Trizol (GIBCO-BRL) according to the manufacturer's instructions and cDNA made according to Wright et al. (Wright et al., 2000). The primers used to detect the splicing forms of zebrafish *deltaD* were AGCTGAAG-CAGGAGGACTTG (sense) and CTTCAGTTGAGAACCAGCT-CATT (antisense), usually for 30 PCR cycles. The altered splice forms were characterized by cloning and sequencing.

The full-length zebrafish *magi1* cDNA was cloned by both 5′ and 3′ RACE using SMART RACE kit (Clontech) following the manufacturer's protocols using 24 hour zebrafish cDNA and oligonucleotides based on the zebrafish EST sequence number AW078333. The full-length zebrafish *magi1* cDNA has been submitted to GenBank (Accession number AY465352).

### Cell culture, transfection, and immunocytochemistry

HEK293T cells grown on coverslips were transiently transfected with 1 μg of plasmid DNA per well in a 24-well plate using Superfect Transfection Reagent (Qiagen). Twenty-four hours after transfection, cells were rinsed in PBS and fixed in 4% formaldehyde in PBS for 15 minutes at room temperature. Fixed cells were permeabilized in 0.2% Triton X-100 in PBS for 15 minutes at room temperature, rinsed in PBS, and incubated in blocking solution (1% BSA in PBS) for 30 minutes at room temperature. Cells were then stained with zdd2 antibody, essentially as in Itoh et al. (Itoh et al., 2003). Coverslips were mounted on slides in Citifluor (Citifluor) and examined with a Zeiss LSM510 confocal microscope.

## Results

### The C terminus of Delta1 binds MAGI proteins

To identify proteins that might interact with the intracellular domain of Delta in vertebrates, we used a biochemical purification strategy. A synthetic 27-amino-acid peptide corresponding to the C terminus of human Delta1 was used to purify Delta-binding proteins from lysates of either adult mouse brain or the human neuroblastoma cell line NB100, as described in Materials and methods. Bound proteins were resolved by SDS-PAGE and identified by tryptic peptide mass spectrometry. The mouse brain lysate gave the largest number of clearly identifiable bands (Fig. 1A). The most prominent and most reproducible of these corresponded to MAGI2 (MAGI paralog 2); bands corresponding to the closely related proteins MAGI1 and MAGI3 were also present. Other bands in the mouse brain preparation were identified as MPDZ/MUPP1 (multi PDZ protein), meprin A, and a putative zinc-finger protein. MAGI1 was also identified in the NB100 lysate, where it gave the most prominent band.

We have chosen to focus on the interaction with the MAGI proteins. This protein family, corresponding (in mammals) to

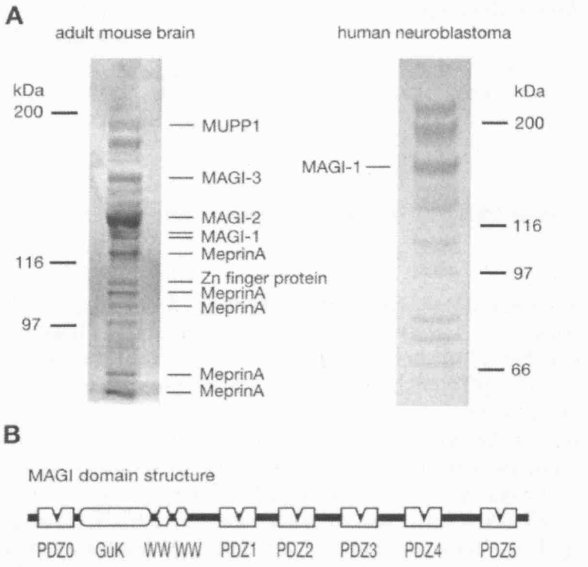


**Fig. 1.** Biochemical purification and identification of proteins that interact with a peptide corresponding to the C terminus of an –ATEV Delta. (A) Proteins purified using a C-terminal peptide of human Delta1 from lysates prepared from either an adult mouse whole brain (left panel) or the human neuroblastoma NB100 cell line (right panel) were resolved by SDS-PAGE under reducing conditions and identified by tryptic peptide mass spectrometry. Proteins that could be confidently identified have been labelled. (B) Domain structure of the MAGI family of proteins.

three distinct genes, is widely expressed; MAGI2 is especially plentiful in the adult central nervous system. This may account for its prominence in our purification assay using mouse brain. The domain structure of the MAGI proteins is shown in Fig. 1B: it includes a non-catalytic guanylate kinase homology region, two WW (protein interaction) domains, and six PDZ domains, numbered from 0 to 5, typical of scaffold proteins that hold the multiple components of signalling complexes by their C-terminal tails and keep them together at the plasma membrane. Because of their many interactions, the MAGI proteins have been given many different names (see Data S1 in supplementary material). In particular, the human MAGI1 protein is also known as BAIAP1 (BAI1-associated protein), because it binds BAI1 (brain angiogenesis inhibitor 1). BAI1, like Delta1, is a transmembrane protein with an intracellular C terminus ending in TEV. This strongly suggests that MAGI1, and perhaps the other MAGI proteins, contain a PDZ domain that specifically recognizes proteins with a terminal TEV and is thus responsible for the binding of Delta1.

Regarding the other Delta-binding proteins we identified, MUPP1, like the MAGI proteins, is a membrane-associated scaffold protein, containing no less than 13 PDZ domains; it too may recognize the C-terminal ATEV of Delta1. Meprin A is more puzzling: meprins are transmembrane or secreted proteins that normally act extracellularly as metallopeptidases. In our assay, they may have been detected because they bound to the Delta1 C-terminal peptide as a (non-physiological) substrate, or because they were attached to it indirectly via some scaffold protein such as MAGI1/2/3 or MUPP1. The zinc

**Table 1. Homology relationships between zebrafish and human MAGI proteins, as reflected in the percentage amino-acid sequence identity for PDZ domain 4**

| | zf MAGI1 PDZ4 (ENSDARG00000003169) | zf MAGI2A PDZ4 (ENSDARG00000010164) | zf MAGI2B PDZ4 (ENSDARG00000018908) | zf MAGI3 PDZ4 (ENSDARG00000004394) |
|---|---|---|---|---|
| Hs MAGI1 PDZ4 (BAIAP1) | 99 | 66 | 67 | 61 |
| Hs MAGI2 PDZ4 (AIP1) | 61 | 84 | 86 | 63 |
| Hs MAGI3 PDZ4 | 56 | 67 | 63 | 78 |

These data are from BLAST alignment of human MAGI sequences with transcribed sequences from the Ensembl zebrafish database. The ENSDARG numbers are Ensembl gene ID numbers.

finger protein we detected is one for which no function is yet known.

## The MAGI protein family is highly conserved between fish and mammals

For further analysis of the interactions of Delta proteins with MAGI proteins, we have used the zebrafish. A BLAST search for counterparts of human *MAGI1*, *-2* and *-3* in the Ensembl zebrafish cDNA database reveals one *MAGI1* ortholog, two *MAGI2* orthologs, and one *MAGI3* ortholog. We shall call the corresponding four zebrafish genes *magi1*, *magi2a*, *magi2b*, and *magi3*. The orthology relationships can be inferred from the percent amino-acid identity when corresponding domains are compared; Table 1 shows values based on PDZ domain 4 (PDZ4). From the sequence comparisons, it seems that the ancestral *MAGI1*, *-2* and *-3* genes must have diverged from one another before the divergence of the fish and tetrapod lineages, while divergence of the zebrafish *magi2a* and *magi2b* genes may have occurred after this.

Having identified a part of the *magi1* coding sequence in the zebrafish EST database, we were able to clone the entire cDNA sequence. The length of the corresponding MAGI1 protein (1247 amino acids) is similar to that of human MAGI1 (1256 amino acids), and the two proteins are 71% identical in sequence overall, with the same domain structure. The degree of conservation of individual domains is remarkably high: for example, the PDZ4 domains of human and zebrafish MAGI1 are identical in 101 out of 102 amino acids. We have used *magi1* as representative of the MAGI family for further analysis of Delta-MAGI interactions.

## *magi1* is widely expressed in the developing zebrafish, becoming most plentiful in the CNS

As a first step towards analysis of the Delta-MAGI interaction in vivo, we examined the expression of *magi1*, to see whether it overlaps with that of *deltaC* and *deltaD*. We used RT-PCR to assess the time course of early expression of *magi1* (Fig. 2A). The message is present already in the egg at 0 hours post-fertilization (hpf), has largely disappeared by 3 hpf, but is plentiful again by 6 hpf. This presumably reflects degradation of maternal message followed by a delay of a few hours before zygotic transcripts accumulate. Since the primary transcript is very long (>160 kb), there will presumably be an interval of 2 hours or more (assuming transcription at 1.2 kb/minute) from the initiation of zygotic transcription at 2.5-3 hpf until mature mRNA reaches the cytoplasm. Transcription of *deltaC* and *deltaD* begins to be seen by in situ hybridization at 5-6 hpf (Haddon et al., 1998; Smithers et al., 2000). Thus MAGI1 becomes available to interact with the Delta proteins at about the time of their first appearance.

Judged by in situ hybridization (Fig. 2B), *magi1* seems to be expressed ubiquitously up to 24 hpf. By 48 hpf, expression is seen more in the CNS than elsewhere, and by 72 hpf this heightened expression in the CNS is striking (Fig. 2D,E). Expression in the CNS is, however, evident even at early embryonic stages, while the neural tube is forming and the first neurons are being born – in other words, at the time when *delta* genes are being expressed and playing their part in regulating neurogenesis. Expression is seen also in other sites where Delta genes are expressed, such as the hair cells of the inner ear (Fig. 2E). Our further experiments imply that interaction between Delta and MAGI proteins indeed occurs and is functionally important.

## The C termini of DeltaC and DeltaD bind directly and specifically to PDZ4 of MAGI1

Previous studies (see Data S1 in supplementary material) have shown that the different PDZ (and other) domains in MAGI proteins selectively bind different partners. To understand the place that DeltaC and DeltaD might have in protein complexes

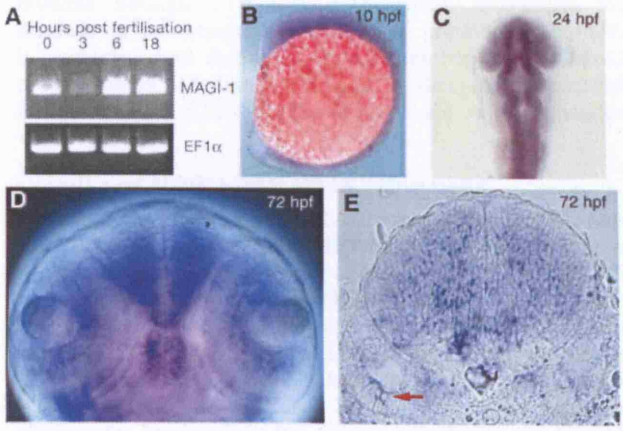


**Fig. 2.** Expression pattern of *magi1* in the zebrafish embryo. (A) Early stages analysed by RT-PCR (data replicated in three separate experiments). Maternal mRNA present in the 0 hpf egg has largely disappeared by 3 hpf, with fresh (zygotically synthesized) transcripts appearing by 6 hpf. EF1α was used as a positive control. (B-E) In situ hybridization patterns. (B) Lateral view at bud stage (10 hpf), showing diffuse expression. (C) Dorsal view at 24 hpf, showing expression still diffuse but strongest in the neural tube. (D) Dorsal view of the head of a whole mount at 72 hpf, showing expression in the retinae and, most strongly, in the diencephalon and telencephalon. (E) Transverse section of embryo stained as a whole mount at 72 hpf, showing expression in the hindbrain and in sensory hair cells in the ear (red arrow).

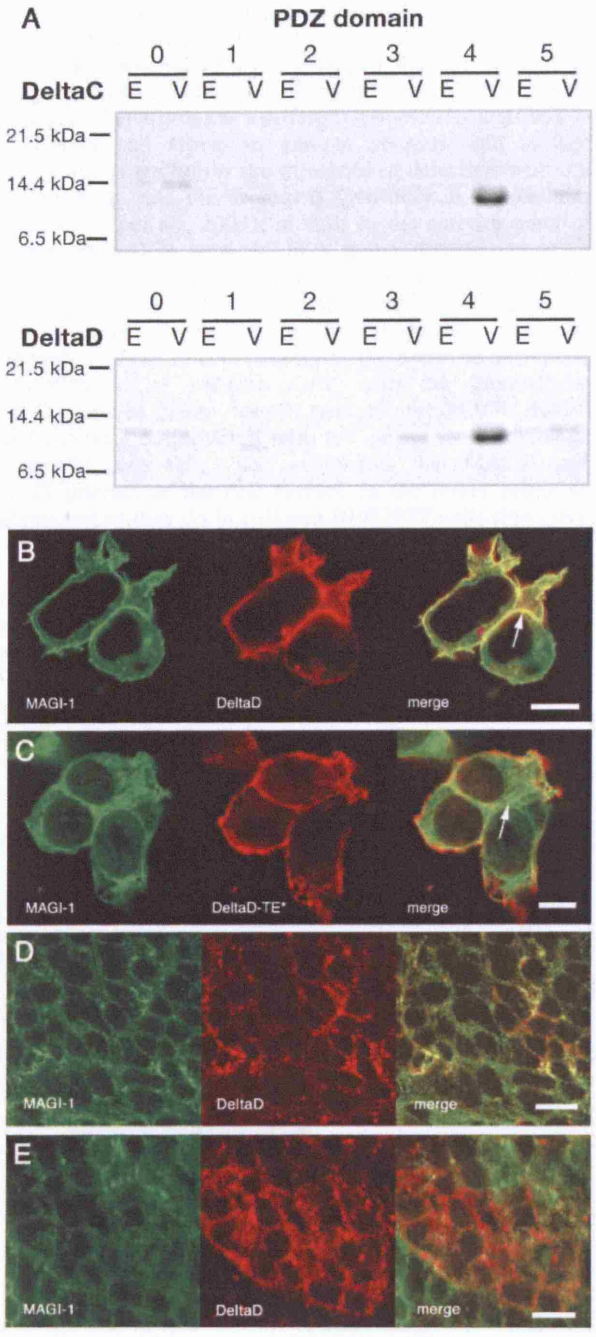


**Fig. 3.** Zebrafish MAGI1 binds directly and specifically to zebrafish DeltaC and DeltaD. (A) Beads were coated with peptides corresponding to the C-terminal 27 or 26 amino acids of DeltaC (top panel) or DeltaD (bottom panel) either with the terminal valine (V) or without (E). The beads were then incubated with purified proteins corresponding to each of the six individual PDZ domains of zebrafish MAGI1 (0 to 5). Beads were then washed and bound proteins eluted and resolved by SDS-PAGE under reducing conditions. Both DeltaC and DeltaD peptides that terminated in the ATEV motif interacted directly and selectively with the PDZ4 domain alone, while control peptides that lacked the terminal valine (ending –ATE) showed no binding to any PDZ domain. (B,C) HEK293T cells cotransfected with plasmids coding for MAGI1-EGFP (green) and either full-length DeltaD (red in B) or DeltaD lacking its terminal valine (DeltaD-TE*; red in C). Both forms of DeltaD were detected with zdd2 anti-DeltaD monoclonal antibody. DeltaD, but not DeltaD-TE*, recruits MAGI1 to the plasma membrane [compare regions indicated by arrows in (B) and (C)]. 56 out of 59 cells transfected with DeltaD showed MAGI1 membrane recruitment, but only 1 out of 37 transfected with DeltaD-TE* did so. (D,E) Confocal sections of somite cells in 10-14 somite stage zebrafish embryos injected with 20 pg mRNA encoding for MAGI1-EGFP at the two- to four-cell stage, either (D) alone or (E) with coinjection of 5 ng MO[dlD-V]. MAGI1-EGFP was detected with an anti-GFP antibody and endogenous DeltaD was detected with zdd2. Note co-localization of DeltaD and MAGI1 in (D) but not (E). Scale bars: 10 μm.

held together by MAGI1, and to test whether the Delta proteins indeed bind to MAGI1 directly, we examined the binding of artificially synthesized fragments of the proteins in vitro. Peptides corresponding to the C-terminal 26 or 27 amino acids of DeltaC and DeltaD were synthesized chemically. We prepared two variants of each – one with and the other, as a control, without the terminal valine. We also prepared individual His-tagged proteins corresponding to each of the six PDZ domains (~100 amino acids) of zebrafish MAGI1. The Delta peptides, as before, were prepared with an N-terminal biotin to allow coupling to streptavidin-coated beads, and the individual PDZ domains were then assayed for their ability to bind to these. As shown in Fig. 3A, the C termini of DeltaC and DeltaD both bind selectively to PDZ4, with only a faint trace of binding to other PDZ domains. No binding is seen when the Delta peptides lack their terminal valine. We conclude that PDZ4 selectively and directly binds the Delta proteins through a typical PDZ-domain interaction that depends on the terminal valines of these proteins. Since PDZ4 is conserved and distinctive in all members of the MAGI protein family, it is likely that in all of them it is responsible for binding the ATEV Deltas in the same valine-dependent way.

## DeltaD and MAGI1 interact in living cells

For a further test of the Delta-MAGI interaction, we performed cotransfection experiments in HEK293T cells. We constructed expression plasmids containing cDNA coding (1) for MAGI1, tagged at its C terminus with EGFP, (2) for full-length DeltaD, and (3) for DeltaD lacking the C-terminal valine residue (DeltaD-TE*). Both forms of DeltaD are recognized by our zdd2 monoclonal antibody against DeltaD (Itoh et al., 2003). Both full-length DeltaD and DeltaD-TE* when expressed alone were localized to the plasma membrane. In contrast, MAGI1-EGFP when expressed alone appeared cytosolic with scarcely perceptible membrane localization. However, in cells transfected with the full-length DeltaD and MAGI1-EGFP plasmids together, we observed a dramatic increase in the concentration of MAGI1-EFGP at the plasma membrane, where it was co-localized with the full-length DeltaD (Fig. 3B). This localization pattern was not observed when DeltaD-TE* was substituted for full-length DeltaD (Fig. 3C). These data support our in vitro findings as to the specificity of the interaction and imply that Delta proteins can recruit MAGI proteins to the cell surface.

To see whether DeltaD and MAGI1 proteins interact in the

living embryo, we injected mRNA coding for MAGI1-EGFP into 2- to 4-cell-stage zebrafish embryos and compared the subcellular localization of the tagged MAGI1 to that of endogenous DeltaD at the 10-14 somite stage. DeltaD protein in uninjected embryos has a different intracellular distribution in different cell types: in nascent neurons, cell surface concentrations are below the threshold of detection with our zdd2 antibody, and the protein is seen only in intracellular granules (Itoh et al., 2003); in cells in the anterior parts of somites, DeltaD is detected in a spotty distribution at or near the cell surface (L.A.-M. and François Giudicelli, unpublished). This DeltaD pattern was maintained in embryos injected with the MAGI1-EGFP construct. Although, in these injected embryos, there was no detectable co-localization of MAGI1-EGFP with the intracellular DeltaD granules of the nascent neurons, the MAGI1-EGFP was frequently co-localized with the cell-surface DeltaD of the somite cells (Fig. 3D), suggesting that MAGI1 and DeltaD interact at the cell surface in the intact zebrafish embryo just as they do in cultured HEK293T cells (Fig. 3B). It should be noted that spots of DeltaD without MAGI1 and of MAGI1 without DeltaD were also seen, presumably reflecting the fact that DeltaD is only one of many MAGI1-binding partners (Fig. 1, see Data S1 in supplementary material) and that the levels of MAGI1 protein generated upon mRNA injection may be much higher than endogenous levels.

### A splice-blocking morpholino can be used to deprive DeltaD of its terminal valine in vivo

We have shown that the terminal valine of DeltaC and DeltaD is required for binding to MAGI1. Removal of this valine should therefore provide a way to test the functional importance of the Delta-MAGI interaction while causing minimal disruption of other processes. By good fortune, the terminal valine of the ATEV Delta proteins is encoded on a separate exon. We were thus able to remove it in vivo by blocking the splicing reaction that links this exon to the rest. For this, we used a morpholino, which we shall call MO[dlD-V], complementary to the exon/intron junction on the 5′ side of the intron preceding the exon that encodes the terminal valine (Fig. 4A). A BLAST search of the zebrafish genome database indicated that this was the only target site for the morpholino. We injected varying doses of MO[dlD-V] into fertilized eggs at the one-cell stage, left them to develop as far as 6, 24, 48 or 72 hpf, and used RT-PCR to discover what splice variants of *deltaD* mRNA were present. As shown in Fig. 4B, 0.5 ng of MO[dlD-V] was sufficient to give a marked reduction in the amount of the normally spliced mRNA, and with 5 ng or more, this form was undetectable, implying that no DeltaD was being produced with a terminal valine. The block was still fully effective as late as 72 hpf (Fig. 4C). The predominant mRNA instead was a mis-spliced variant with the subterminal intron retained, so as to code for a protein whose terminal valine was replaced by a sequence of 34 amino acids ending in LVLN*.

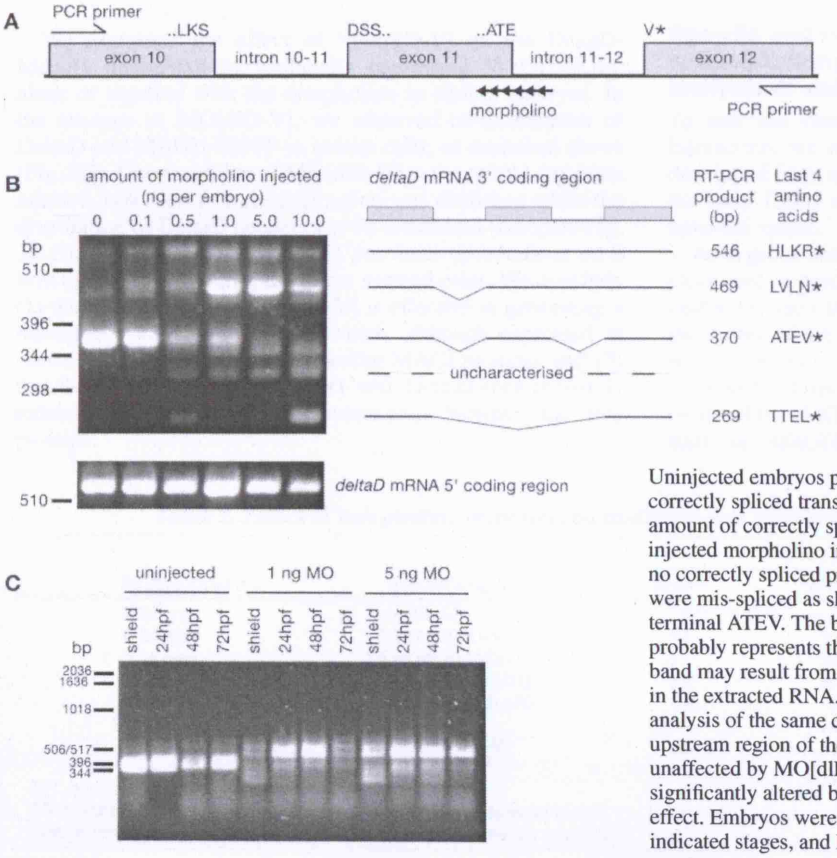


**Fig. 4.** A morpholino, MO[dlD-V], targeted to the intron-exon boundary responsible for the addition of the DeltaD terminal valine residue disrupts splicing and selectively removes the PDZ domain binding site for up to 72 hours of development. (A) The genomic structure of the zebrafish DeltaD gene surrounding the PDZ domain binding site, indicating the amino acids at the boundaries of each exon, the MO[dlD-V] morpholino annealing site, and primer binding sites used to monitor the effects on splicing by RT-PCR in (B). (B) Effects on *deltaD* mRNA splicing, monitored by RT-PCR, in embryos injected with MO[dlD-V] at the one-cell stage and left to develop until the shield stage (6 hpf). Total RNA was extracted from 20 embryos for each dose, reverse transcribed and amplified by PCR. PCR products were cloned and fully sequenced. Uninjected embryos produced a 370 bp band that corresponds to the correctly spliced transcript, coding for a protein that ends –ATEV. The amount of correctly spliced product decreases as the amount of injected morpholino increases; at a dose of 5 ng or more per embryo, no correctly spliced product is observable. Products at 469 and 269 bp were mis-spliced as shown and correspond to proteins lacking the terminal ATEV. The band at ~330 bp was not characterized but probably represents the use of a cryptic splice donor site. The 546 bp band may result from small amounts of contaminating genomic DNA in the extracted RNA. The separate small panel below shows RT-PCR analysis of the same cDNA using oligonucleotides targeted to an upstream region of the *deltaD* transcript (nucleotides 389-923) that is unaffected by MO[dlD-V]. The total quantity of *deltaD* mRNA is not significantly altered by the MO injections. (C) Time course of the effect. Embryos were injected and allowed to develop until the indicated stages, and RT-PCR was performed as in B.

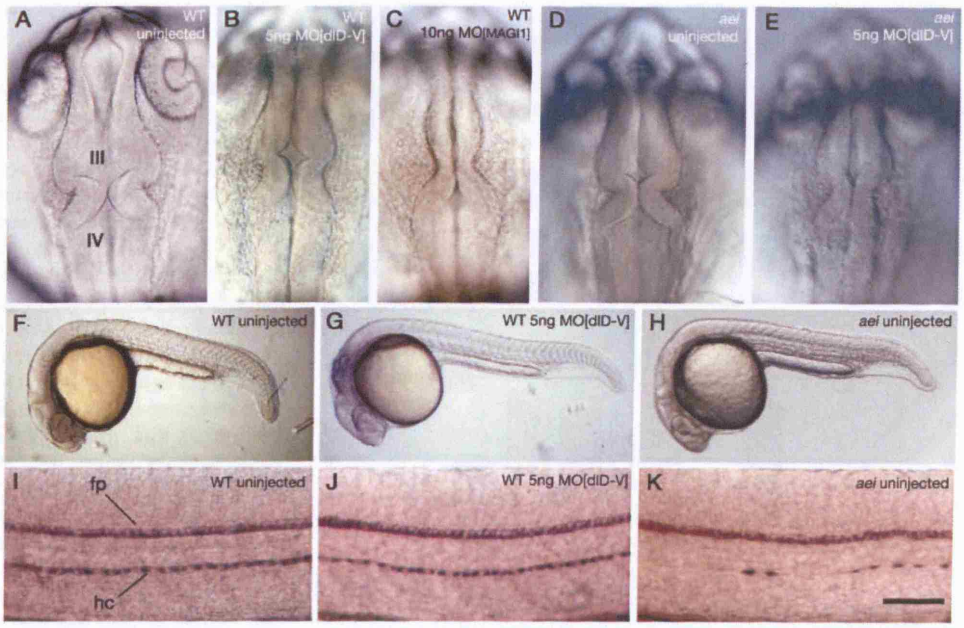


**Fig. 5.** Effects of morpholino injections that block the interaction of DeltaD with MAGI1. (A-E) Dorsal views of the midbrain-hindbrain region in live embryos at 24 hpf. (A) Uninjected wild-type control. (B) Wild-type embryo injected with 5 ng of MO[dlD-V]; note narrowed third (III) and fourth (IV) ventricles and irregular texture due to dying cells in the walls of the hindbrain. (C) Similar phenotype produced by injection of 10 ng of MO[MAGI1]. (D) *after eight* (*aei*) uninjected embryo; note normal morphology. (E) *aei* embryo injected with 5 ng of MO[dlD-V]; note phenotype similar to that seen in (B) and (C). (F-H) Lateral views of live embryos at 24 hpf showing somite segmentation. Somite boundaries are disorganized below the eighth somite in *aei* (H), but are unaffected by MO[dlD-V] treatment (G). (I-K) Lateral views, anterior towards the left, of embryos at 26 hpf analysed by *in situ* hybridization for *col2a1* expression to mark floor-plate (fp) and hypochord (hc). *aei* embryos exhibit a reduction in hypochord cell number. This effect is not observed upon MO[dlD-V] treatment (J). Scale bar: 50 μm for I,J,K.

We examined the effect of MO[dlD-V] on the DeltaD-MAGI1 interaction by artificially expressing MAGI1-EGFP alone or together with the morpholino in sibling embryos. In the absence of MO[dlD-V], we observed co-localization of DeltaD and MAGI1-EGFP in somite cells, as described above (Fig. 3D). Upon addition of MO[dlD-V] to the mRNA injection mixture, however, this co-localization was abolished while the distribution of DeltaD appeared to be unaffected (compare Fig. 3D,E). Although it is difficult to put these observations on a firm quantitative footing, the effect seemed clear. We conclude (1) that treatment with MO[dlD-V] is effective in generating a mis-spliced variant of DeltaD which, although expressed at normal levels, is incapable of binding MAGI proteins; and (2) that the co-localization of MAGI1 with DeltaD seen in vivo is indeed dependent on direct interaction between the two proteins.

## Specific and non-specific effects of the DeltaD splice-blocking morpholino can be distinguished by analysis of *aei/deltaD* mutants

To test the functional significance of the DeltaD-MAGI1 interaction, we examined the phenotype of the embryos that developed from eggs injected with 5 ng of MO[dlD-V], so that the only forms of DeltaD produced would be lacking their terminal valine.

At a gross anatomical level, the injected embryos showed clear and reproducible abnormalities in the hindbrain and midbrain, such that at 24 hpf, the width of the roofplate and the lumen of the third and fourth ventricles of the neural tube were markedly reduced (Fig. 5A,B, Table 2). A similar narrowed-ventricle effect was seen when we injected a morpholino (MO[MAGI1]) targeted against the translational start of *MAGI1* (Fig. 5C), whereas injection of other

**Table 2. Effect of morpholino injections on midbrain and hindbrain structure, scored at 24 hpf**

| Embryo genotype | Injected reagent: | Phenotype (%): Severe | Mild | WT | Embryos scored *n* |
|---|---|---|---|---|---|
| Wild type | uninjected | 1 | 3 | 96 | 99 |
| Wild type | 5 ng MO[dlD-V] | 52 | 30 | 18 | 98 |
| Wild type | 5 ng MO[MAGI1] | 17 | 38 | 45 | 53 |
| Wild type | 10 ng MO[MAGI1] | 53 | 39 | 8 | 49 |
| Wild type | 5 ng mis-match MO | 3 | 6 | 91 | 35 |
| $aei^{AR33}$ | uninjected | 6 | 14 | 81 | 101 |
| $aei^{AR33}$ | 5 ng MO[dlD-V] | 33 | 51 | 16 | 67 |

WT, brain ventricles very similar to uninjected.
Mild, brain ventricles have formed but are misshapen and reduced in size.
Severe, ventricles absent or severely reduced in size and severely misshapen.

morpholinos, including a five base-pair mismatch control for MO[dlD-V], did not produce this phenotype (data not shown, Table 2). These findings strongly suggested that the anatomical abnormality was a specific effect of disrupting the DeltaD-MAGI1 interaction. Similar structural abnormalities have, however, been seen as an effect of morpholino mistargeting (Ekker and Larson, 2001), and they are not easily explainable in terms of known functions of DeltaD or MAGI1. Spurred on by the doubts of a referee, we therefore performed a further, and more decisive, control experiment.

For this, we took advantage of the *aei*$^{AR33}$ mutant, which has a stop codon in the fifth EGF repeat of the extracellular domain of *deltaD*, leading to a DeltaD loss-of-function phenotype (Holley et al., 2000). Since the C terminus of DeltaD is already missing in *aei*$^{AR33}$ homozygotes, we might perhaps expect that they would show the narrowed-ventricle phenotype even without any morpholino injection; and in any case their phenotype should certainly show no further change when MO[dlD-V] is injected, if the only effect of this morpholino is to block the DeltaD-MAGI1 interaction. As it turned out, our expectations were confounded on both scores. The uninjected *aei*$^{AR33}$ homozygotes did not show a narrowed-ventricle phenotype, but when they were injected with MO[dlD-V] they did show it (Fig. 5D,E, Table 2). We can only conclude that the narrowed-ventricle phenotype resulting from MO[dlD-V] is due to a non-specific toxic effect of the morpholino.

## Disruption of the DeltaD-MAGI interaction does not significanly affect the known functions of DeltaD as a Notch ligand

The *aei*$^{AR33}$ mutant is useful not only as a negative but also as a positive control, displaying defects that result from loss of DeltaD: somite segmentation is disrupted (Holley et al., 2002; Jiang et al., 2000; van Eeden et al., 1996); primary neurons are produced in excessive numbers in the embryonic CNS (Holley et al., 2000); and the numbers of hypochord (ventral midline) cells are reduced (Latimer et al., 2002). These abnormalities have been well documented and reflect the functions of DeltaD as a Notch ligand. To see whether the DeltaD-MAGI interaction is important for these functions, we compared wild-type and *aei*$^{AR33}$ mutant embryos with genetically normal embryos that were injected with MO[dlD-V].

First of all, somite patterning appeared normal in the MO[dlD-V] injected embryos, with no sign of the disruption of somite segmentation that is seen in *aei* and in other Notch pathway loss-of-function mutants (Fig. 5F-H) (Holley et al., 2002; Jiang et al., 2000; van Eeden et al., 1996).

Our findings with regard to hypochord formation were similar. Defects in hypochord formation are readily observed in *aei/deltaD* mutants as well as *deltaA* loss-of-function mutants and morpholino-induced DeltaC knock-down embryos (Appel et al., 1999; Latimer et al., 2002); the phenotype can be seen by in situ hybridization with a probe for *alpha-1 collagen type II* (*col2a1*) which labels the floor plate and hypocord (Yan et al., 1995). Using this method, we saw a reduction in hypochord cell number in *aei*$^{AR33}$ embryos, as expected. However, we detected only a slight increase in hypochord defects in wild-type embryos treated with MO[dlD-V] (Fig. 5I-K). Moreover, we observed no effect of MO[dlD-V] treatment on expression of *her4* or *ntl* (data not shown); these genes are both regulated – *her4* positively and *ntl* negatively – by Delta-Notch signalling during normal hypochord development (Latimer et al., 2002). These findings indicate that the DeltaD-MAGI1 interaction is not important for the function of DeltaD as a Notch ligand in specification of the hypochord.

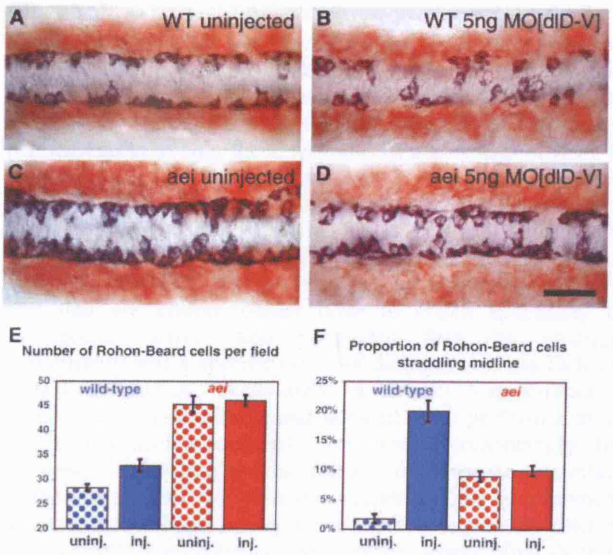


**Fig. 6.** Disruption of the DeltaD-MAGI interaction causes mislocalization of Rohon-Beard neurons. (A-D) Dorsal views of embryos at 16 hpf stained by *in situ* hybridization for *islet1* (black) to mark Rohon-Beard neurons (as well as other primary neurons below the plane of focus). *myoD* (brown) expression serves as a reference for somite number and position. *aei* embryos (C,D) show a 1.6-fold increase in the number of Rohon-Beard cells compared to wild-type embryos (A), whereas the number of these cells is only slightly increased in wild-type embryos injected with MO[dlD-V] (B). The MO[dlD-V] embryos are abnormal, however, in that many of the Rohon-Beard cells stray into the midline region. The proportion of such mislocalized cells is not affected by the morpholino in *aei* embryos, where DeltaD is missing (C,D). (E,F) Cell counts. The distribution of the neurons was quantified for a region corresponding approximately to somites 5 to 10; 10-13 embryos were analysed for each condition. Error bars represent s.e.m. Scale bar: 50 mm for A-D.

Lastly, Delta-Notch signalling, mediating lateral inhibition, is well known to regulate the proportion of cells committed to differentiate as neurons (Appel and Eisen, 1998; Chitnis et al., 1995; Haddon et al., 1998), and this is reflected in the phenotype of *aei/deltaD* mutants, which produce neurons in excess (Holley et al., 2000). If interaction with MAGI1 is important for DeltaD's function in lateral inhibition, we would expect to see alterations in neurogenesis when the interaction is blocked. We therefore counted neurons, at the 12-16 somite stage, in genetically wild-type embryos injected with MO[dlD-V] and in uninjected controls, using *in situ* hybridization for *islet1* as a neuronal marker (Haddon et al., 1998; Korzh et al., 1993). We found that the MO[dlD-V] injection produced little or no change in the number of *islet1*-positive cells. In contrast, *aei*$^{AR33}$ mutants showed a 1.6-fold increase (Fig. 6A-E). Specifically, in the dorsal neural tube, in the region corresponding to the middle five somites, we counted 28.3±0.6 (mean±s.e.m., $n$=10) *islet1*-positive neurons per wild-type

embryo, 32.8±1.3 ($n$=13) per MO[dlD-V]-injected wild-type embryo, 45.3±1.7 ($n$=10) per *aei*$^{AR33}$ embryo, and 46.2±1.1 ($n$=13) per *aei*$^{AR33}$ embryo injected with MO[dlD-V]. We conclude that the DeltaD-MAGI interaction has very little influence on the function of DeltaD in the regulation of neuronal commitment.

### When the DeltaD-MAGI interaction is disrupted, Rohon-Beard neurons are mislocalized

In the course of the above experiment, we noticed that Rohon-Beard neurons (primary sensory neurons in the dorsal part of the fish neural tube), although normal in numbers, were consistently mislocalized in the MO[dlD-V]-injected embryos. In wild-type and *aei*$^{AR33}$ mutant embryos at the 12-16 somite stage, the cell bodies of these *islet1*-positive neurons are located in two paraxial strips lying 3-4 cell diameters apart. In MO[dlD-V]-treated wild-type embryos, by contrast, the corresponding cells were often located more medially, between these strips (Fig. 6A-C,F). This effect was not observed when *aei*$^{AR33}$ mutants were injected with the morpholino, demonstrating that it is indeed a DeltaD-dependent effect and not a nonspecific artefact (Fig. 6D,F). For a quantitative estimate of the abnormality, we counted the proportion of the dorsal *islet1*-positive cells that spanned the midline. These amounted to 1.8±0.9% (mean±s.e.m., $n$=10) of the population in wild-type embryos, 20.0±1.8% ($n$=13) in MO[dlD-V]-injected wild-type embryos, 9.0±0.9% ($n$=10) in *aei*$^{AR33}$ mutants, and 10.0±0.9% ($n$=13) in MO[dlD-V]-injected *aei*$^{AR33}$ mutants (Fig. 6A-D,F). This suggests that the DeltaD-MAGI interaction could play some part in regulating migration or dispersal of the Rohon-Beard cells – and conceivably of other neurons – within the neural tube. Since relatively little mislocalization is seen in *aei*$^{AR33}$ mutants, which lack functional DeltaD, an implication would be that the suggested aberrant migratory behaviour depends on DeltaD and is normally restrained by the interaction of DeltaD with MAGI proteins (see Discussion). The slight degree of mislocalization seen in *aei*$^{AR33}$ mutants may reflect production of slightly ectopic neurons as a result of loss of lateral inhibition.

## Discussion

All vertebrates, apparently, and some invertebrates such as echinoderms, possess at least one Delta family member with a conserved ATEV motif at its intracellular terminus. We have found by in vitro studies that this terminus of the ATEV Deltas binds selectively to members of the MAGI family of PDZ-containing scaffold proteins. We have shown, moreover, that the binding is direct, is to all three MAGIs, and is specifically to their PDZ4 domain. The interaction is demonstrable in cultured cells, where it enables Delta protein to recruit MAGI protein to the plasma membrane. Using the zebrafish as a model system, we have observed that *magi1* is widely expressed and is present in particular in many, if not all, of the cells that express the ATEV Deltas. Additionally, in at least some cell types in the intact embryo, we have seen co-localization of DeltaD and MAGI1 at the plasma membrane and given evidence that the co-localization depends on the ATEV motif. All this amounts to a strong argument that the Delta-MAGI interaction is a real physiological phenomenon and is in some way functionally important.

### Morpholino experiments require stringent controls

To discover what the function of the interaction might be, we exploited a morpholino, MO[dlD-V], which, when injected into the early zebrafish embryo, specifically blocks the interaction by interfering with the splicing of the *deltaD* message so as to alter the C terminus of the DeltaD protein. In any morpholino experiment, however, there is a possibility that non-specific side-effects may also be produced. In our system, we were indeed initially misled. We saw a marked narrowing of the third and fourth ventricles of the neural tube in embryos injected with MO[dlD-V], performed several controls of the sort that are conventionally done to check specificity of morpholino action, and concluded that the ventricle abnormality was a specific effect of disruption of the DeltaD-MAGI interaction. Fortunately, a *deltaD* loss-of-function mutant, *aei*, was available and allowed us to perform a more stringent control experiment. This showed convincingly that the ventricle abnormality was after all a non-specific side-effect of the morpholino. We offer this cautionary tale as a footnote to our other findings: it may serve as a warning of the risks of misinterpreting morpholino experiments, where often there is no mutant available to provide a stringent test for non-specific side-effects.

### Delta-Notch signalling appears to be independent of the Delta-MAGI interaction

DeltaD has several well-characterized roles in Notch signaling, clearly revealed in the *deltaD* loss-of-function mutant *aei*, where disorders are seen in somitogenesis, hypochord formation, and neurogenesis (Holley et al., 2000; Jiang et al., 2000; Latimer et al., 2002; van Eeden et al., 1996). Upon disruption of the DeltaD-MAGI interaction, however, these processes are largely unaffected. The fact that this treatment does not phenocopy *aei* indicates that the interaction of DeltaD with MAGI proteins is not important for the function of DeltaD as an activating ligand for Notch, at least in these processes. This finding is perhaps not surprising given that, as explained in the Introduction, several forms of Delta protein lacking the MAGI-binding motif are already known to be effective Notch ligands.

### The Delta-MAGI interaction may be important in the control of neuron migration

In assaying neurogenesis in embryos injected with MO[dlD-V] to block DeltaD-MAGI interaction, we observed a mislocalization of Rohon-Beard sensory neurons, which frequently strayed into the dorsal midline of the neural tube – a phenomenon rarely seen in wild-type or *aei* embryos. This effect needs further investigation, but it suggests that the DeltaD-MAGI interaction is important in some way either in determining the site of production of the neurons, or in governing their migratory behaviour as they move away from their birthplace.

We are attracted by the latter possibility, since other studies have reported effects of Delta protein on cell motility: in particular, De Joussineau et al. (De Joussineau et al., 2003) found that Delta in *Drosophila* sense-organ precursor cells promoted extension of filopodia, while Lowell and Watt (Lowell and Watt, 2001) found that mammalian keratinocytes showed enhanced motility when they expressed a truncated form of Delta1 lacking most of the intracellular domain

(including the ATEV motif), but showed reduced motility when they expressed full-length Delta1. This latter pair of observations is consistent with what we saw in the zebrafish embryo: the mis-localization of the Rohon-Beard neurons suggests that they became abnormally motile when their DeltaD protein was deprived of the C-terminal motif that mediates binding to MAGI proteins. If this interpretation is correct, the implication would be that free Delta protein favours motility, and that this action of Delta is inhibited by the binding of Delta to MAGI.

The above account supposes that Delta and MAGI influence motility directly (cell-autonomously) in the cells that express them. An alternative possibility is that these proteins influence the ability of cells to serve as a substratum for the movement of other cells: it could be that cells expressing DeltaD that is not bound to MAGI encourage the Rohon-Beard neurons to move over them, while cells expressing DeltaD that binds to MAGI protein do not. This suggestion has an echo in the *nagie oko* (*nok*) zebrafish, where there is a mutation in a MAGUK scaffolding protein – that is, a protein related to the MAGI family. In this mutant, the polarity of the retinal epithelium is disrupted and the migrations of neurons within it are disordered, apparently in consequence of the neuroepithelial polarity defect (Wei and Malicki, 2002). Gray et al. (Gray et al., 2001) have also reported similar phenomena: they find that mutation of *des/notch1a* alters the migration of neural crest cells and has a non-cell-autonomous effect on axon outgrowth.

Whichever of these interpretations is correct, there are many possibilities for the detailed molecular mechanism. Delta and Delta-MAGI complexes could have direct effects on the adhesive or locomotor properties of the cell surface or actin cortex (Lowell and Watt, 2001); they could influence motility by binding (or failing to bind) to Notch on neighbouring cells (Franklin et al., 1999); or they could regulate gene expression cell-autonomously to exert their effects. This last possibility is suggested by recent studies (Ikeuchi and Sisodia, 2003; LaVoie and Selkoe, 2003; Six et al., 2003) showing that, like Notch, Delta itself can be cleaved to release an intracellular fragment that can enter the nucleus and act as a gene-regulatory protein. MAGI proteins could influence such a reverse signalling activity of ATEV Deltas by regulating their cleavage or their translocation to the nucleus.

## Conclusion

As Notch ligands, the Delta proteins play a central part in the development and maintenance of a great variety of tissues in the vertebrate body. We have established that a conserved subset of the Delta family – the ATEV Deltas – interact through their intracellular tails with the MAGI family of scaffolding proteins, not only in vitro but also in the living embryo. The interaction does not appear to be critical for Delta-Notch signalling, and yet its evolutionary conservation implies that it must have an important physiological function. The challenge is to discover what that function is. The MAGI proteins, with their multiple PDZ and other protein-recognition domains, have an extraordinary variety of binding partners, as listed in Data S1 (see supplementary material), and could mediate cross-talk between the Delta-Notch pathway and many other pieces of intracellular or extracellular machinery. MAGI may exert important effects on cell behaviour by influencing the location of Delta, or Delta may do so by influencing the location of MAGI. In this paper we have excluded some possible roles of the Delta-MAGI interaction and found preliminary evidence for an effect on cell positioning; further experiments will be needed to explore its functional significance fully.

We are indebted to Nicola O'Reilly, Tobias Simmonds, Hans Hansen, the late Maureen Harrison, Susan Kirkland, Phil Taylor, and Jenny Corrigan for peptide synthesis, protein purification, mass spectrometry, cultured cells, fish care, and cryosectioning. We thank Jonathan Tobin for help with cell counts, Steve Wilson and David Ish-Horowicz for discussions, and Derek Stemple, Katrin Layer and members of the Vertebrate Development Laboratory for comments on the manuscript. The work was supported by Cancer Research UK.

### Supplementary material

Supplementary material for this article is available at
http://dev.biologists.org/cgi/content/full/131/22/5659/DC1

## References

**Appel, B. and Eisen, J. S.** (1998). Regulation of neuronal specification in the zebrafish spinal cord by Delta function. *Development* **125**, 371-380.

**Appel, B., Fritz, A., Westerfield, M., Grunwald, D. J., Eisen, J. S. and Riley, B. B.** (1999). Delta-mediated specification of midline cell fates in zebrafish embryos. *Curr. Biol.* **9**, 247-256.

**Ariza-McNaughton, L. and Krumlauf, R.** (2002). Non-radioactive in situ hybridization: simplified procedures for use in whole-mounts of mouse and chick embryos. *Int. Rev. Neurobiol.* **47**, 239-250.

**Artavanis-Tsakonas, S., Rand, M. D. and Lake, R. J.** (1999). Notch signaling: cell fate control and signal integration in development. *Science* **284**, 770-776.

**Beckers, J., Clark, A., Wunsch, K., Hrabe De Angelis, M. and Gossler, A.** (1999). Expression of the mouse Delta1 gene during organogenesis and fetal development. *Mech. Dev.* **84**, 165-168.

**Chitnis, A., Henrique, D., Lewis, J., Ish-Horowicz, D. and Kintner, C.** (1995). Primary neurogenesis in *Xenopus* embryos regulated by a homologue of the Drosophila neurogenic gene Delta [see comments]. *Nature* **375**, 761-766.

**Davis, R. L., Turner, D. L., Evans, L. M. and Kirschner, M. W.** (2001). Molecular targets of vertebrate segmentation: two mechanisms control segmental expression of Xenopus hairy2 during somite formation. *Dev. Cell* **1**, 553-565.

**De Joussineau, C., Soule, J., Martin, M., Anguille, C., Montcourrier, P. and Alexandre, D.** (2003). Delta-promoted filopodia mediate long-range lateral inhibition in Drosophila. *Nature* **426**, 555-559.

**Ekker, S. C. and Larson, J. D.** (2001). Morphant technology in model developmental systems. *Genesis* **30**, 89-93.

**Franklin, J. L., Berechid, B. E., Cutting, F. B., Presente, A., Chambers, C. B., Foltz, D. R., Ferreira, A. and Nye, J. S.** (1999). Autonomous and non-autonomous regulation of mammalian neurite development by Notch1 and Delta1. *Curr. Biol.* **9**, 1448-1457.

**Gray, M., Moens, C. B., Amacher, S. L., Eisen, J. S. and Beattie, C. E.** (2001). Zebrafish deadly seven functions in neurogenesis. *Dev. Biol.* **237**, 306-323.

**Haddon, C., Smithers, L., Schneider-Maunoury, S., Coche, T., Henrique, D. and Lewis, J.** (1998). Multiple *delta* genes and lateral inhibition in zebrafish primary neurogenesis. *Development* **125**, 359-370.

**Henrique, D., Hirsinger, E., Adam, J., Le Roux, I., Pourquié, O., Ish-Horowicz, D. and Lewis, J.** (1997). Maintenance of neuroepithelial progenitor cells by Delta-Notch signaling in the embryonic chick retina. *Curr. Biol.* **7**, 661-670.

**Holley, S. A., Geisler, R. and Nusslein-Volhard, C.** (2000). Control of her1 expression during zebrafish somitogenesis by a delta-dependent oscillator and an independent wave-front activity. *Genes Dev.* **14**, 1678-1690.

**Holley, S. A., Julich, D., Rauch, G. J., Geisler, R. and Nusslein-Volhard, C.** (2002). her1 and the notch pathway function within the oscillator mechanism that regulates zebrafish somitogenesis. *Development* **129**, 1175-1183.

**Hrabé de Angelis, M., McIntyre, J. and Gossler, A.** (1997). Maintenance of

somite borders in mice requires the *Delta* homologue *Dll1*. *Nature* **386**, 717-721.

**Hruska-Hageman, A. M., Benson, C. J., Leonard, A. S., Price, M. P. and Welsh, M. J.** (2004). PSD-95 and Lin-7b interact with ASIC3 and have opposite effects on H+-gated current. *J. Biol. Chem.* (in press).

**Hutchings, N. J., Clarkson, N., Chalkley, R., Barclay, A. N. and Brown, M. H.** (2003). Linking the T cell surface protein CD2 to the actin-capping protein CAPZ via CMS and CIN85. *J. Biol. Chem.* **278**, 22396-22403.

**Ikeuchi, T. and Sisodia, S. S.** (2003). The Notch ligands, Delta1 and Jagged2, are substrates for presenilin-dependent "gamma-secretase" cleavage. *J. Biol. Chem.* **278**, 7751-7754.

**Inoue, A., Takahashi, M., Hatta, K., Hotta, Y. and Okamoto, H.** (1994). Developmental regulation of islet-1 mRNA expression during neuronal differentiation in embryonic zebrafish. *Dev. Dyn.* **199**, 1-11.

**Itoh, M., Kim, C. H., Palardy, G., Oda, T., Jiang, Y. J., Maust, D., Yeo, S. Y., Lorick, K., Wright, G. J., Ariza-McNaughton, L. et al.** (2003). Mind bomb Is a ubiquitin ligase that Is essential for efficient activation of Notch signaling by Delta. *Dev. Cell* **4**, 67-82.

**Jen, W. C., Wettstein, D., Turner, D., Chitnis, A. and Kintner, C.** (1997). The Notch ligand, X-Delta-2, mediates segmentation of the paraxial mesoderm in *Xenopus* embryos. *Development* **124**, 1169-1178.

**Jiang, Y. J., Aerne, B. L., Smithers, L., Haddon, C., Ish-Horowicz, D. and Lewis, J.** (2000). Notch signalling and the synchronization of the somite segmentation clock. *Nature* **408**, 475-479.

**Kimmel, C. B., Ballard, W. W., Kimmel, S. R., Ullmann, B. and Schilling, T. F.** (1995). Stages of embryonic development of the zebrafish. *Dev. Dyn.* **203**, 253-310.

**Korzh, V., Edlund, T. and Thor, S.** (1993). Zebrafish primary neurons initiate expression of the LIM homeodomain protein Isl-1 at the end of gastrulation. *Development* **118**, 417-425.

**Lai, E. C., Deblandre, G. A., Kintner, C. and Rubin, G. M.** (2001). Drosophila neuralized is a ubiquitin ligase that promotes the internalization and degradation of delta. *Dev. Cell* **1**, 783-794.

**Latimer, A. J., Dong, X., Markov, Y. and Appel, B.** (2002). Delta-Notch signaling induces hypochord development in zebrafish. *Development* **129**, 2555-2563.

**LaVoie, M. J. and Selkoe, D. J.** (2003). The Notch ligands, Jagged and Delta, are sequentially processed by alpha-secretase and presenilin/gamma-secretase and release signaling fragments. *J. Biol. Chem.* **278**, 34427-34437.

**Lewis, J.** (1998). Notch signalling and the control of cell fate choices in vertebrates. *Semin. Cell Dev. Biol.* **9**, 583-589.

**Lowell, S. and Watt, F. M.** (2001). Delta regulates keratinocyte spreading and motility independently of differentiation. *Mech. Dev.* **107**, 133-140.

**Mailhos, C., Modlich, U., Lewis, J., Harris, A., Bicknell, R. and Ish-Horowicz, D.** (2001). Delta4, an endothelial specific Notch ligand expressed at sites of physiological and tumor angiogenesis. *Differentiation* **69**, 135-144.

**Nasevicius, A. and Ekker, S. C.** (2000). Effective targeted gene 'knockdown' in zebrafish. *Nat. Genet.* **26**, 216-220.

**Pavlopoulos, E., Pitsouli, C., Klueg, K. M., Muskavitch, M. A., Moschonas, N. K. and Delidakis, C.** (2001). neuralized Encodes a peripheral membrane protein involved in delta signaling and endocytosis. *Dev. Cell* **1**, 807-816.

**Pfister, S., Przemeck, G. K., Gerber, J. K., Beckers, J., Adamski, J. and de Angelis, M. H.** (2003). Interaction of the MAGUK Family Member Acvrinp1 and the Cytoplasmic Domain of the Notch Ligand Delta1. *J. Mol. Biol.* **333**, 229-235.

**Sakamoto, K., Ohara, O., Takagi, M., Takeda, S. and Katsube, K.** (2002). Intracellular cell-autonomous association of Notch and its ligands: a novel mechanism of Notch signal modification. *Dev. Biol.* **241**, 313-326.

**Schroder, N. and Gossler, A.** (2002). Expression of Notch pathway components in fetal and adult mouse small intestine. *Gene Expr. Patterns* **2**, 247-250.

**Selkoe, D. and Kopan, R.** (2003). Notch and Presenilin: regulated intramembrane proteolysis links development and degeneration. *Annu. Rev. Neurosci.* **26**, 565-599.

**Shiratsuchi, T., Futamura, M., Oda, K., Nishimori, H., Nakamura, Y. and Tokino, T.** (1998). Cloning and characterization of BAI-associated protein 1: a PDZ domain-containing protein that interacts with BAI1. *Biochem. Biophys. Res. Commun.* **247**, 597-604.

**Shutter, J. R., Scully, S., Fan, W., Richards, W. G., Kitajewski, J., Deblandre, G. A., Kintner, C. R. and Stark, K. L.** (2000). Dll4, a novel Notch ligand expressed in arterial endothelium. *Genes Dev.* **14**, 1313-1318.

**Six, E., Ndiaye, D., Laabi, Y., Brou, C., Gupta-Rossi, N., Israel, A. and Logeat, F.** (2003). The Notch ligand Delta1 is sequentially cleaved by an ADAM protease and gamma-secretase. *Proc. Natl. Acad. Sci. USA* **100**, 7638-7643.

**Smithers, L., Haddon, C., Jiang, Y. and Lewis, J.** (2000). Sequence and embryonic expression of *deltaC* in the zebrafish. *Mech. Dev.* **90**, 119-123.

**Songyang, Z., Fanning, A. S., Fu, C., Xu, J., Marfatia, S. M., Chishti, A. H., Crompton, A., Chan, A. C., Anderson, J. M. and Cantley, L. C.** (1997). Recognition of unique carboxyl-terminal motifs by distinct PDZ domains. *Science* **275**, 73-77.

**Sun, X. and Artavanis-Tsakonas, S.** (1996). The intracellular deletions of Delta and Serrate define dominant negative forms of the Drosophila Notch ligands. *Development* **122**, 2465-2474.

**Sweet, H. C., Gehring, M. and Ettensohn, C. A.** (2002). LvDelta is a mesoderm-inducing signal in the sea urchin embryo and can endow blastomeres with organizer-like properties. *Development* **129**, 1945-1955.

**van Eeden, F. J., Granato, M., Schach, U., Brand, M., Furutani-Seiki, M., Haffter, P., Hammerschmidt, M., Heisenberg, C. P., Jiang, Y. J., Kane, D. A. et al.** (1996). Mutations affecting somite formation and patterning in the zebrafish, Danio rerio. *Development* **123**, 153-164.

**Wei, X. and Malicki, J.** (2002). nagie oko, encoding a MAGUK-family protein, is essential for cellular patterning of the retina. *Nat. Genet.* **31**, 150-157.

**Weinberg, E. S., Allende, M. L., Kelly, C. S., Abdelhamid, A., Murakami, T., Andermann, P., Doerre, O. G., Grunwald, D. J. and Riggleman, B.** (1996). Developmental regulation of zebrafish MyoD in wild-type, no tail and spadetail embryos. *Development* **122**, 271-280.

**Westerfield, M.** (2000). *The Zebrafish Book*. Eugene: University of Oregon Press.

**Wright, G. J., Puklavec, M. J., Willis, A. C., Hoek, R. M., Sedgwick, J. D., Brown, M. H. and Barclay, A. N.** (2000). Lymphoid/neuronal cell surface OX2 glycoprotein recognizes a novel receptor on macrophages implicated in the control of their function. *Immunity* **13**, 233-242.

**Yan, Y. L., Hatta, K., Riggleman, B. and Postlethwait, J. H.** (1995). Expression of a type II collagen gene in the zebrafish embryonic axis. *Dev. Dyn.* **203**, 363-376.

**Yeh, E., Zhou, L., Rudzik, N. and Boulianne, G. L.** (2000). Neuralized functions cell autonomously to regulate Drosophila sense organ development. *EMBO J.* **19**, 4827-4837.

**Data S1. MAGI proteins and their binding partners.** All three MAGI family members have the same domain structure, shown in the yellow column on the left. The boxes to the right of this show, for each of the MAGIs, which proteins bind to which of the MAGI domains. Boxes spanning more than one domain correspond to proteins whose binding site in MAGI has not been determined precisely but is known to lie somewhere within the indicated region.

| Domain | MAGI-1 (synonyms BAIAP1, BAP1, AIP3, WWP3, TNRC19) Binding partner(s) | | | MAGI-2 (synonyms AIP1, ACVRIP1, Acvrinp-1, ARIP1, S-SCAM) | | | MAGI-3 (synonym SLIPR) | |
|---|---|---|---|---|---|---|---|---|
| PDZ0 | | RapGEP [1] | | | | | | |
| GuK | | | | SAPAP [2] | | | | |
| WW1 | atrophin-1 [3] | | | atrophin-1 [3] | | | | |
| WW2 | synaptopodin [4] | | | SMAD3 [5] | | | | |
| PDZ1 | ß1-adrenergic receptor [6] mNET-1 [7] HPV16/18 E6 protein [8, 9], adenovirus-9 E4 protein [10] JAM4 [11] | | MuSK [12] ASIC3 [13] | ß1-adrenergic receptor [6] neuroligin [2] GDP-GTP exchange factor nRAP-GEP [14] HPV16/18 E6 protein [8] | KIF1Bα [15] | | HPV16/18 E6 protein [8] Ltap [16] Frizzled-4 [16] Frizzled-7 [16] | |
| PDZ2 | | | | PTEN [17-20] | | RPTPß [21] | PTEN [22] | RPTPß [21] |
| PDZ3 | adenovirus-9 E4 protein [10] | | | | | | | |
| PDZ4 | BAI-1 [23] JAM4 [11] Delta1/DeltaD/DeltaC [this paper] | | | Delta1 [32] Delta1/DeltaD/DeltaC [this paper] | | | Delta1/DeltaD/DeltaC [this paper] BAI-1 [22] | |
| PDZ5 | alpha-actinin-4 [4], megalin [25], ß-catenin [26] | | | delta2 glutamate receptor [27] activin receptor IIA [5] tamalin [28] NMDA receptors [2, 29] ß-catenin [30] delta-catenin/NPRAP [31] | MAGUIN-1 [24] | | NMDA receptor 2B [22] | |

[1] Mino et al. (2000).
[2] Hirao et al. (1998).
[3] Wood et al. (1998).
[4] Patrie et al. (2002).
[5] Shoji et al. (2000).
[6] Xu et al. (2001).
[7] Dobrosotskaya (2001).
[8] Thomas et al. (2002).
[9] Thomas et al. (2001).
[10] Glaunsinger et al. (2000).
[11] Hirabayashi et al. (2003).
[12] Strochlic et al. (2001).
[13] Hruska-Hageman et al. (2004).
[14] Ohtsuka et al. (1999).
[15] Mok et al. (2002).
[16] Yao et al. (2004).
[17] Wu et al. (2000a).
[18] Vazquez et al. (2001).
[19] Torres et al. (2003).
[20] Tolkacheva et al. (2001).
[21] Adamsky et al. (2003).
[22] Wu et al. (2000b).
[23] Shiratsuchi et al. (1998).
[24] Yao et al. (1999).
[25] Patrie et al. (2001).
[26] Dobrosotskaya and James (2000).
[27] Yap et al. (2003).
[28] Kitano et al. (2003).
[29] Hirao et al. (2000a; 2000b).
[30] Nishimura et al. (2002).
[31] Ide et al. (1999).
[32] Pfister et al. (2003)

## References


**Adamsky, K., Arnold, K., Sabanay, H. and Peles, E.** (2003). Junctional protein MAGI-3 interacts with receptor tyrosine phosphatase beta (RPTPbeta) and tyrosine-phosphorylated proteins. *J. Cell Sci.* **116**, 1279-1289.

**Dobrosotskaya, I. Y.** (2001). Identification of mNET1 as a candidate ligand for the first PDZ domain of MAGI-1. *Biochem. Biophys. Res. Commun.* **283**, 969-975.

**Dobrosotskaya, I. Y. and James, G. L.** (2000). MAGI-1 interacts with beta-catenin and is associated with cell-cell adhesion structures. *Biochem. Biophys. Res. Commun.* **270**, 903-909.

**Glaunsinger, B. A., Lee, S. S., Thomas, M., Banks, L. and Javier, R.** (2000). Interactions of the PDZ-protein MAGI-1 with adenovirus E4-ORF1 and high-risk papillomavirus E6 oncoproteins. *Oncogene* **19**, 5270-5280.

**Hirabayashi, S., Tajima, M., Yao, I., Nishimura, W., Mori, H. and Hata, Y.** (2003). JAM4, a junctional cell adhesion molecule interacting with a tight junction protein, MAGI-1. *Mol. Cell. Biol.* **23**, 4267-4282.

**Hirao, K., Hata, Y., Deguchi, M., Yao, I., Ogura, M., Rokukawa, C., Kawabe, H., Mizoguchi, A. and Takai, Y.** (2000a). Association of synapse-associated protein 90/ postsynaptic density-95-associated protein (SAPAP) with neurofilaments. *Genes Cells* **5**, 203-210.

**Hirao, K., Hata, Y., Ide, N., Takeuchi, M., Irie, M., Yao, I., Deguchi, M., Toyoda, A., Sudhof, T. C. and Takai, Y.** (1998). A novel multiple PDZ domain-containing molecule interacting with N-methyl-D-aspartate receptors and neuronal cell adhesion proteins. *J. Biol. Chem.* **273**, 21105-21110.

**Hirao, K., Hata, Y., Yao, I., Deguchi, M., Kawabe, H., Mizoguchi, A. and Takai, Y.** (2000b). Three isoforms of synaptic scaffolding molecule and their characterization. Multimerization between the isoforms and their interaction with N-methyl-D-aspartate receptors and SAP90/PSD-95-associated protein. *J. Biol. Chem.* **275**, 2966-2972.

**Hruska-Hageman, A. M., Benson, C. J., Leonard, A. S., Price, M. P. and Welsh, M. J.** (2004). PSD-95 and Lin-7b interact with ASIC3 and have opposite effects on H+-gated current. *J. Biol. Chem.* (in press).

**Ide, N., Hata, Y., Deguchi, M., Hirao, K., Yao, I. and Takai, Y.** (1999). Interaction of S-SCAM with neural plakophilin-related Armadillo-repeat protein/delta-catenin. *Biochem. Biophys. Res. Commun.* **256**, 456-461.

**Kitano, J., Yamazaki, Y., Kimura, K., Masukado, T., Nakajima, Y. and Nakanishi, S.** (2003). Tamalin is a scaffold protein that interacts with multiple neuronal proteins in distinct modes of protein-protein association. *J. Biol. Chem.* **278**, 14762-14768.

**Mino, A., Ohtsuka, T., Inoue, E. and Takai, Y.** (2000). Membrane-associated guanylate kinase with inverted orientation (MAGI)-1/brain angiogenesis inhibitor 1-associated protein (BAP1) as a scaffolding molecule for Rap small G protein GDP/GTP exchange protein at tight junctions. *Genes Cells* **5**, 1009-1016.

**Mok, H., Shin, H., Kim, S., Lee, J. R., Yoon, J. and Kim, E.** (2002). Association of the kinesin superfamily motor protein KIF1Balpha with postsynaptic density-95 (PSD-95), synapse-associated protein-97, and synaptic scaffolding molecule PSD-95/discs large/zona occludens-1 proteins. *J. Neurosci.* **22**, 5253-5258.

**Nishimura, W., Yao, I., Iida, J., Tanaka, N. and Hata, Y.** (2002). Interaction of synaptic scaffolding molecule and Beta - catenin. *J. Neurosci.* **22**, 757-765.

**Ohtsuka, T., Hata, Y., Ide, N., Yasuda, T., Inoue, E., Inoue, T., Mizoguchi, A. and Takai, Y.** (1999). nRap GEP: a novel neural GDP/GTP exchange protein for rap1 small G protein that interacts with synaptic scaffolding molecule (S-SCAM). *Biochem. Biophys. Res. Commun.* **265**, 38-44.

**Patrie, K. M., Drescher, A. J., Goyal, M., Wiggins, R. C. and Margolis, B.** (2001). The membrane-associated guanylate kinase protein MAGI-1 binds megalin and is present in glomerular podocytes. *J. Am. Soc. Nephrol.* **12**, 667-677.

**Patrie, K. M., Drescher, A. J., Welihinda, A., Mundel, P. and Margolis, B.** (2002). Interaction of two actin-binding proteins, synaptopodin and alpha-actinin-4, with the tight junction protein MAGI-1. *J. Biol. Chem.* **277**, 30183-30190.

**Pfister, S., Przemeck, G. K., Gerber, J. K., Beckers, J., Adamski, J. and de Angelis, M. H.** (2003). Interaction of the MAGUK family member Acvrinp1 and the cytoplasmic domain of the Notch ligand Delta1. *J. Mol. Biol.* **333**, 229-235.

**Shiratsuchi, T., Futamura, M., Oda, K., Nishimori, H., Nakamura, Y. and Tokino, T.** (1998). Cloning and characterization of BAI-associated protein 1: a PDZ domain-containing protein that interacts with BAI1. *Biochem. Biophys. Res. Commun.* **247**, 597-604.

**Shoji, H., Tsuchida, K., Kishi, H., Yamakawa, N., Matsuzaki, T., Liu, Z., Nakamura, T. and Sugino, H.** (2000). Identification and characterization of a PDZ protein that interacts with activin type II receptors. *J. Biol. Chem.* **275**, 5485-5492.

**Strochlic, L., Cartaud, A., Labas, V., Hoch, W., Rossier, J. and Cartaud, J.** (2001). MAGI-1c: a synaptic MAGUK interacting with muSK at the vertebrate neuromuscular junction. *J. Cell Biol.* **153**, 1127-1132.

**Thomas, M., Glaunsinger, B., Pim, D., Javier, R. and Banks, L.** (2001). HPV E6 and MAGUK protein interactions: determination of the molecular basis for specific protein recognition and degradation. *Oncogene* **20**, 5431-5439.

**Thomas, M., Laura, R., Hepner, K., Guccione, E., Sawyers, C., Lasky, L. and Banks, L.** (2002). Oncogenic human papillomavirus E6 proteins target the MAGI-2 and MAGI-3 proteins for degradation. *Oncogene* **21**, 5088-5096.

**Tolkacheva, T., Boddapati, M., Sanfiz, A., Tsuchida, K., Kimmelman, A. C. and Chan, A. M.** (2001). Regulation of PTEN binding to MAGI-2 by two putative phosphorylation sites at threonine 382 and 383. *Cancer Res.* **61**, 4985-4989.

**Torres, J., Rodriguez, J., Myers, M. P., Valiente, M., Graves, J. D., Tonks, N. K. and Pulido, R.** (2003). Phosphorylation-regulated cleavage of the tumor suppressor PTEN by caspase-3: implications for the control of protein stability and PTEN-protein interactions. *J. Biol. Chem.*

**Vazquez, F., Grossman, S. R., Takahashi, Y., Rokas, M. V., Nakamura, N. and Sellers, W. R.** (2001). Phosphorylation of the PTEN tail acts as an inhibitory switch by preventing its recruitment into a protein complex. *J. Biol. Chem.* **276**, 48627-48630.

**Wood, J. D., Yuan, J., Margolis, R. L., Colomer, V., Duan, K., Kushi, J., Kaminsky, Z., Kleiderlein, J. J., Sharp, A. H. and Ross, C. A.** (1998). Atrophin-1, the DRPLA gene product, interacts with two families of WW domain-containing proteins. *Mol. Cell. Neurosci.* **11**, 149-160.

**Wu, X., Hepner, K., Castelino-Prabhu, S., Do, D., Kaye, M. B., Yuan, X. J., Wood, J., Ross, C., Sawyers, C. L. and Whang, Y. E.** (2000a). Evidence for regulation of the PTEN tumor suppressor by a membrane-localized multi-PDZ domain containing scaffold protein MAGI-2. *Proc. Natl. Acad. Sci. USA* **97**, 4233-4238.

**Wu, Y., Dowbenko, D., Spencer, S., Laura, R., Lee, J., Gu, Q. and Lasky, L. A.** (2000b). Interaction of the tumor suppressor PTEN/MMAC with a PDZ domain of MAGI3, a novel membrane-associated guanylate kinase. *J. Biol. Chem.* **275**, 21477-21485.

**Xu, J., Paquet, M., Lau, A. G., Wood, J. D., Ross, C. A. and Hall, R. A.** (2001). beta 1-adrenergic receptor association with the synaptic scaffolding protein membrane-associated guanylate kinase inverted-2 (MAGI-2). Differential regulation of receptor internalization by MAGI-2 and PSD-95. *J. Biol. Chem.* **276**, 41310-41317.

**Yao, I., Hata, Y., Ide, N., Hirao, K., Deguchi, M., Nishioka, H., Mizoguchi, A. and Takai, Y.** (1999). MAGUIN, a novel neuronal membrane-associated guanylate kinase-interacting protein. *J. Biol. Chem.* **274**, 11889-11896.

**Yao, R., Natsume, Y. and Noda, T.** (2004). MAGI-3 is involved in the regulation of the JNK signaling pathway as a scaffold protein for frizzled and Ltap. *Oncogene* **23**, 6023-6030.

**Yap, C. C., Muto, Y., Kishida, H., Hashikawa, T. and Yano, R.** (2003). PKC regulates the delta2 glutamate receptor interaction with S-SCAM/MAGI-2 protein. *Biochem. Biophys. Res. Commun.* **301**, 1122-1128.